Université de Strasbourg

2012

Ecole doctorale des Sciences de la Vie et de la Santé

THÈSE

présentée pour l'obtention du grade de

DOCTEUR DE L'UNIVERSITE DE STRASBOURG

Discipline : Sciences du Vivant

Domaine : Aspects moléculaires et cellulaires de la biologie

par

SCHIRTZ Tom

Etude du mécanisme de translocation de l'ARNt$^{Lys(CUU)}$ dans les mitochondries de *Saccharomyces cerevisiae*

Soutenue le 12 octobre 2012 devant le jury de thèse composé comme suit :

Professeur Robert N. LIGHTOWLERS	**Rapporteur externe**
Professeur Johannes HERRMANN	**Rapporteur externe**
Dr Laurence MARECHAL-DROUARD	**Examinateur interne**
Dr Ivan TARASSOV	**Directeur de thèse**

UMR N°7156 UdS-CNRS
"Génétique Moléculaire, Génomique et Microbiologie"

TABLE OF CONTENTS

ACKNOWLEDGEMENTS

In a first place, I would like to thank Dr Laurence Maréchal-Drouard, Professor Robert Neil Lightowlers and Professor Johannes Herrmann for having the kindness to evaluate and to criticize my PhD work.

With a great pleasure, I express my thanks to my supervisor Dr Ivan Tarassov and to Dr Robert Martin for having accepted me as a member of their team and for giving me the opportunity to develop myself in a free and very stimulating environment. I would also express my gratitude to you Vania for helping me so much with administrative questions and especially for your support in more precarious situations, as the grant formulation for my 4th PhD year. I also want to express my thanks for all your great and kind scientific assistance and for the nice moments passed at your garden-parties.

I would like to thank Dr Nina Entelis for all her assistance and her advices she gave me during my PhD work and for her great help in interpreting my experimental results.

I also want to address many thanks to Dr Olga Kolesnikova who was my first mentor during my Master training. Thank you very much Olga for introducing me into the world of research work, for your great technical help and assistance and for your patience you brought to me during the time we worked together. I will also never forget the nice evening spent at your flat with the opportunity to taste a lot of Russian specialties.

I also want to express my deepest thanks to Dr Mikhail Vysokikh, who was my mentor during the last three years of my PhD work. Mike you really were an invaluable help and I want to thank you for all the scientific knowledge you taught me, for your brilliant assistance in every situation and for our close and fruitful cooperation. I wish you all the best for your restart in Moscow.

I would also like to address my thanks to Dr Olga Karicheva for her great help and assistance during my Master training.

Also many thanks to all the other members of our “Mito” team, to Dr Alexandre “Sacha” Smirnov, Anne-Marie Heckel, Yann Tonin, Dr Caroline Comte, Ali Gowher and Ilya

for all their help and their nice company during my stay in the lab. Yann ne je vais jamais oublier notre séjour fabouleux en Ukraine!

I also want to thank all our members of the UMR7156 for the great and very stimulating working atmosphere and for their kind help and discussions. I felt very happy among you during the past four years and I really enjoyed all our nice parties and evenings we spent together!!

Auch dir Matthias vielen dank für deine tolle Gesellschaft und für all die sehr lustigen Abende in den Straßburger Bars und bei dir zuhause. Ich sag nur Bouneschlupp!! Ich wünsche dir noch alles Gute und viel Erfolg für dein Postdoc in Stockholm.

Och dir Serge soen ech villmols merci fier deng Companie am Labo an eis flott Owenter hannert der Kachmaschine bei enger gudder Fläsch Wäin. Et war deck gudd een “Landsmann” op der Aarbecht ze hun mat deem een och ald mol e Wuert Lëtzebuergesch konnt schwetzen. Op jidwerfall wënschen ech der alles Guddes an dats däin Wuel fënns.

I also express my feelings toward my friends at home who supported me during all the last years.

My deepest thanks to my family, my mother Claudine, my father Romain and my brother Manou that were always there for me and encouraged me all along my studies here in Strasbourg.

Last but not least, the most thanks would even not be enough for you Steffi! Merci Stippi dats de all déi Zäit hei bei mier bliwen bass zu Stroosbuerg an dats de emmer fier mech do wars, och an denen bessen mei verzweifelten Situatiounen! Daat huet mer onendlech vill bedeit an ech blecken mat voller Erwaardung an eis Zukunft déi mer eis doheem wärten opbauen!!

ABBREVIATIONS

5-BrU	5-bromouridine
aaRS	aminoacyl-tRNA-synthetase
ANT	adenine nucleotide translocator
ADP	adenosine diphosphate
ATP	adenosine triphosphate
BB	breakage buffer
BrU-tRK1	tRK1 transcript synthesized in presence of 5-BrU
CLIP	crosslinking combined to immunoprecipitation
CK	creatine kinase
Cyt *c*	cytochrome *c*
Cyt*b2*-DHFR	fusion protein between cytochrome *b2* and dihydrofolate reductase
DEPC	diethylpyrocarbonate
DIDS	4,4'-diisothiocyano-2,2'-stilbenedisulfonic acid
DTNB	5,5'-dithiobis-(2-nitrobenzoic acid) or Ellman's reagent
DTT	dithiothreitol
E.coli	*Escherichia coli*
EDTA	ethylenediaminetetraacetic acid
EGTA	ethyleneglycoltetraacetic acid
Eno-2	enolase-2
EtOH	ethanol
FCCP	carbonyl cyanide-4-(trifluoromethoxy)phenylhydrazone
FRET	Förster resonance energy transfer
HB	hypotonic buffer
HEPES	4-(2-hydroxyethyl)-1-piperazineethanesulfonic acid
HK	hexokinase
Hsp	heat-shock protein
IM	inner membrane
IMS	intermembrane space
IP	immunoprecipitation
IPTG	isopropyl ß-D-1-thiogalactopyranoside
KRS	*Saccharomyces cerevisiae* cytosolic lysyl-tRNA-synthetase
mtHsp	mitochondrial heat-shock protein

MBS	3-maleimidobenzoic acid *N*-hydroxysuccinimide ester
MELAS	mitochondrial encephalomyopathy, lactic acidosis, stroke-like episodes
MERFF	myoclonic epilepsy with ragged red fibers
MIA	mitochondrial intermembrane space import and assembly
MOPS	3-(*N*-morpholino)propanesulfonic acid
MRP	mitochondrial ribosomal protein
NADH	nicotinamide adenine dinucleotide
OD	optical density
OM	outer membrane
OMVs	outer membrane vesicles
PAGE	polyacrylamide gel electrophoresis
PAM	presequence translocase-associated motor
PCR	polymerase chain reaction
PMSF	phenylmethylsulfonyl fluoride
preMSK	precursor form of *Saccharomyces cerevisiae* mitochondrial lysyl-tRNA-synthetase
Q	quinone
S.cerevisiae	*Saccharomyces cerevsisae*
SAM	sorting and assembly machinery
SDS	sodium dodecylsulfate
SSC	saline sodium citrate buffer
SUVs	small unilamellar vesicles
TE	Tris-EDTA buffer
TOM	translocase of the outer membrane
TIM	translocase of the inner membrane
Tris	tris(hydroxymethyl)aminomethane
tRK1	*Saccharomyces cerevisiae* cytosolic $tRNA^{Lys(CUU)}$
tRK2	*Saccharomyces cerevisiae* cytosolic $tRNA^{Lys(UUU)}$
tRK3	*Saccharomyces cerevisiae* mitochondrial $tRNA^{Lys(UUU)}$
VDAC	Voltage Dependent Anion Channel
$\Delta\Psi$	electrochemical membrane potential

INTRODUCTION

I) INTRODUCTION

1. GENERAL FUNCTIONS AND ORIGIN OF MITOCHONDRIA

One of the key events in the evolution of the eukaryotic cell and complex organisms was the acquisition of an organelle, termed mitochondrion, which guarantees cellular homeostasis by completing a wide range of important tasks. One of the most understood is the coupling of energy by ATP synthesis. In addition, mitochondria also trigger signalling cascades of the programmed cell death, the apoptosis, and are involved in numerous metabolic processes, such as the synthesis and oxidation of fatty acids, the synthesis of essential amino acids and steroids, the assembly and maturation of hemes and iron-sulphur clusters and the regulation of the intracellular calcium pool in concert with the endoplasmic reticulum (Scheffler, 2001b, 2001a; Lill, 2009; Payne and Hales, 2004; Pinton et al., 2008).

Mitochondria are organized in highly complex and dynamic networks throughout the cell undergoing permanent fission and fusion events (Chan, 2006). The movement of mitochondria through the cell is ensured by interactions of mitochondrial surface proteins with components of the cytoskeleton, such as actin filaments, microtubules and intermediary filaments (Hermann and Shaw, 1998). Structurally, mitochondria are composed of an outer membrane that separates the cytosol from the intermembrane space and an inner membrane delimiting the intermembrane space from the matrix compartment. The topology of the mitochondrial inner membrane can be divided into two distinct domains (Perkins et al., 1997); an inner boundary membrane closely juxtaposed to the outer membrane, a topology favourable to formation of contact sites *e.g.* during pre-protein import (Harner et al., 2011), and an organization into tubular and lamellar structures, called *cristae*, connected to the inner boundary membrane *via cristae* junctions. A recently identified protein complex, termed mitochondrial inner-membrane organizing system (MINOS), connects this two subdomains of the mitochondrial inner membrane and plays an essential role in the mitochondrial membrane architecture **(Fig.1)** (van der Laan et al., 2012).

The inner membrane embeds the respiratory chain that is composed of five protein complexes: NADH:coenyzme Q oxidoreductase (Complex I), succinate dehydrogenase (Complex II), ubiquinol:cytochrome *c* oxidoreductase (Complex III), cytochrome *c* oxidase (Complex IV) and the ATP synthase (F_1/F_0 complex). The respiratory chain carries out the oxidative phosphorylation, a process consisting in a sequence of enzymatic reactions in the

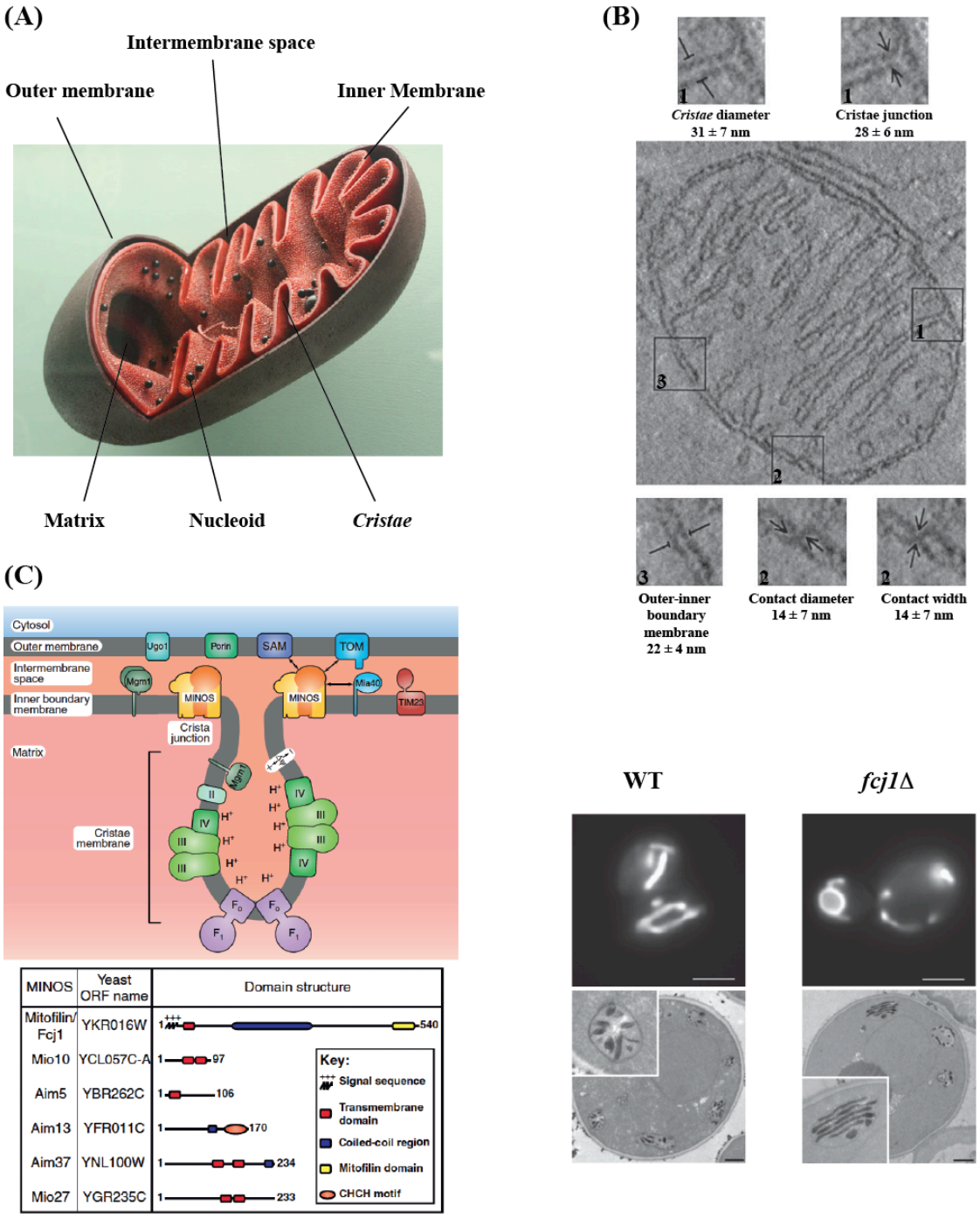

Fig.1 : **Structure of mitochondria.** **(A)** Schematic illustration of a mitochondrion (source : www.biotechnologie.de). **(B)** Electron microscopy picture of a mitochondrion highlightening *cristae* stuctures and *cristae* junctions (1), contact sites (2) and the inner boundary membrane juxtaposed to the outer membrane (3) (Perkins et *al*., 1997). **(C)** Architecture of mitochondrial membranes. left panel : the mitochondrial inner membrane organizing system (MINOS). Components of protein import machineries, like the TIM23 complex and Mia40, are enriched in the inner boundary membrane, whereas the *cristae* membranes house complexes of the respiratory chain. The proximity of *cristae* junctions is enriched by the MINOS complex interacting with the TOM and SAM complexes, the VDAC protein and the fusion component Ugo1 of the outer membrane. The fusion protein Mgm1 is differentially distributed in the inner boundary and *cristae* membranes. The protein compostition of the MINOS complex with systematic names, corresponding ORFs and domain structures is depicted in the small box (van der Laan et *al*., 2012). right panel : mitochondrial morphology (upper panels) and mitochondrial ultrastructure (lower panels) of wild type and *fcj1*Δ mitochondria. Deletion of the MINOS core component Fcj1 causes mitochondrial fragmentation and a loss of inner membrane *cristae* organization (Zerbes et *al*., 2012).

matrix leading to an electron transport through the different respiratory chain complexes with oxygen as a final electron acceptor. The energy released during this process is used to pump protons from the matrix to the intermembrane space, yielding the so-called proton-motive force, used for the generation of ATP by the ATP synthase (F_1/F_0 complex) **(Fig.2)**. Function and subunit composition of these respiratory chain complexes can vary between species, *e.g.* in the yeast *Saccharomyces cerevisiae* that is devoid of a rotenone sensitive NADH:coenzyme Q oxidoreductase (Complex I). Instead, they possess two NADH:coenzyme Q oxidoreductases, one at the external face and one at the matrix face of the inner membrane, that are not coupled to the generation of the proton-motive force (Rosenfeld and Beauvoit, 2003).

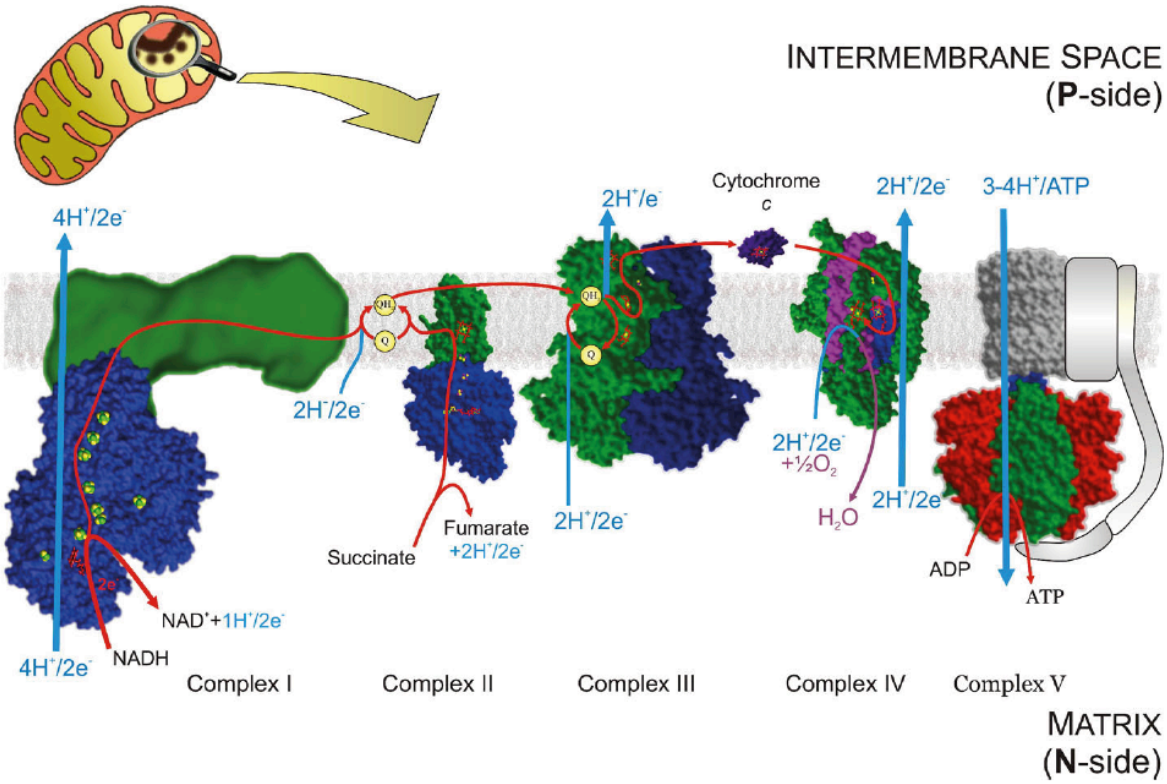

Fig.2 : **Schematic representation illustrating the respiratory chain embedded in the mitochondrial inner membrane** (adopted from Ilya Belevich 2007).

Mitochondria play a central role in the extrinsic and intrinsic induced apoptotic pathways (Kroemer et al., 2007). The extrinsic pathway is triggered by a ligand-induced activation of death receptors at the surface of the plasma membrane (*e.g.* TNF) causing the assembly of the death-induced-signalling-complex (DISC) that promotes activation of caspase-8. Latter cleaves and activates the effector caspase-3, -6, and -7 initiating the apoptosis process but it also activates the pro-apoptotic factor Bid responsible for mitochondrial outer membrane permeabilization and release of pro-apoptotic factors *e.g.* cytochrome *c*. In this way, Bid represents a functional link between the extrinsic and the intrinsic pathway, which is activated by intracellular signals, like DNA damage or endoplasmic reticulum stress also leading to mitochondrial membrane permeabilization and cytochrome *c* release into the cytosol. Here cytochrome *c* promotes formation of the "apoptosome", a platform for pro-caspase 9 and apoptosis inducing factors, maturating and activating caspase-9 that itself cleaves and activates effector caspase-3, -6, and -7. Both, the extrinsic and the intrinsic pathways lead to cell shrinkage, chromatin condensation, nuclear and DNA fragmentation, formation of vesicles (blebbing) and exposure of phophatidylserine on the plasma membrane, a degradation signal for macrophages.

Today it is commonly assumed that mitochondria emerged from an endosymbiotic event between an amitochondriae eukaryote that fused with an α-proteobacterium considered as the ancestor of mitochondria (Gray, 1999). Genomic studies of the α-proteobacterial group, *e.g.* the species *Rickettsia prowazekii*, an obligatory intracellular parasite, showed that they fulfil the best criteria to be the closest eubacterial relatives of todays mitochondria (Andersson et al., 1998; Yang et al., 1985). This fact illustrates another interesting feature of mitochondria, the presence of their own mitochondrial DNA (mtDNA) in the matrix compartment, owning a proper genetic code. During evolution a loss of redundant genes occurred and a considerable part of genes was transferred to the nuclear DNA. This process of mtDNA evolution within different life kingdoms was strikingly different and lead to a high diversity in conformation and size; mtDNAs being mostly circular, or rarely linear, with sizes ranging from <6kb in *Plasmodium falciparum* up to 367kb in *Arabidopsis thaliana*. But also gene content as well as genetic arrangement and expression display an important divergence, with human mtDNA being densely packed with coding sequences, whereas mtDNA of *Arabidopsis thaliana* comprises a high proportion (~80%) of noncoding sequences.

Despite the important participation of the mtDNA in mitochondrial functions and biogenesis, most part of genes encoding proteins of the respiratory chain or proteins involved in mitochondrial genome maintenance and expression are located in the nuclear genome.

Therefore the vast majority of mitochondrial proteins, but also many small noncoding RNAs, has to be imported from the cytosol.

2. MOLECULAR TRANSPORT INTO MITOCHONDRIA

The possibility of communication between mitochondria and the other cellular compartments probably goes hand in hand with transport of molecules in and out of mitochondria, processes requiring selective and regulated channels embedded in the two mitochondrial membranes.

2.1 Transport of Metabolites

Among the smallest chemical compounds transported in and out of mitochondria are ions (*e.g.* K^+, Na^+, Ca^{2+} or Cl^-) and metabolites like pyruvate, phosphate, amino acids, NADH and other nucleotides. The passage through the mitochondrial outer membrane happens *via* the Voltage-Dependant Anion Channel (VDAC) (Benz, 1994), to reach the intermembrane space where these molecules fulfil their activity or are further transported into the matrix. The transport of metabolites through the mitochondrial inner membrane is catalysed by specific proteins known as the mitochondrial carrier family, usually small proteins of 30kDa-35kDa encoded by the nuclear DNA (Palmieri et al., 2011). Most part of these carriers are antiporters and generally they are formed by three successively repeated homologous domains where each domain contains two hydrophobic membrane embedded α-helices and a characteristic amino acid motif PX[D/E]XX[K/R]X[K/R] (20-30 residues) [D/E]GXXXX[W/Y/F][K/R]G. Roughly, the mitochondrial carrier family can be divided into four subfamilies transporting nucleotides/dinucleotides, di-/tri-carboxylates and keto acids, amino acids and other substrates. A more detailed list is presented in **(Table 1)**.

Since in this thesis project the VDAC protein occupies a major role (see results and discussion), I would like to dedicate the following chapter to this protein.

Subfamily	Carrier	Main substrates
Nucleotides and dinucleotides	ADP/ATP carrier	ADP, ATP
	CoenzymeA/adenosine 3',5'-diphosphate (PAP) carrier	CoA, PAP, dephospho-CoA, AXP
	ATP-Mg/Pi carrier	ATP-Mg, Pi, AXP
	Thiamine pyrophosphate carrier	ThPP,ThMP, (d)NDP, (d)NTP
	Pyrimidine nucleotide carrier	pyrimidine (desoxy)nucleotides
	FAD carrier	folates, FAD
	Adenine nucleotide carrier	ATP, ADP, AMP
	NAD^+ carrier	NAD^+, (d)AMP, (d)GMP
	GDP/GTP carrier	(d)GTP, (d)GDP, ITP, IDP
di-/tri-carboxylates and keto acids	Dicarboxylate carrier	malate, succinate, phosphate, sulfate, thiosulfate
	Oxoglutarate carrier	oxoglutarate, malate
	Di-/tri-carboxylate carrier	oxoglutarate, citrate
	Succinate/fumarate carrier	succinate, fumarate
	Citrate carrier	citrate, malate, isocitrate, *cis*-aconitate, phosphoenolpyruvate
	Oxaloacetate/sulfate carrier	oxaloacetate, sulfate, thiosulfate, α-isopropylmalate
Amino acids	Glutamate carrier	glutamate

	Aspartate/glutamate carrier	aspartate, glutamate, cysteinesulfinate
	Ornithine carrier	ornithine, lysine, citrulline, arginine, histidine
	Carnitine carrier	carnitine, acylcarnitines
	S-adenosylmethionine carrier	S-adenosylmethionine, S-adenosylhomocysteine
Other substrates	Phosphate carrier	phosphate
	Uncoupling proteins (UCP1-UCP5 in humans)	H^+

Table 1: Summary of main mitochondrial inner membrane carrier families and their substrates (CoA: coenzymeA; AXP: adenin X=mono-, di-, tri-phosphate; FAD: flavin adenine dinucleotide; ITP: inosine triphosphate; IDP: inosine diphosphate; ThPP: thiamine pyrophosphate; ThMP: thiamine monophosphate)

2.1.1 The Voltage Dependent Anion Channel (VDAC)

VDAC, also called mitochondrial porin in analogy to its similarity to the bacterial porin family (Duy et al., 2007), was the first mitochondrial channel to be characterized more than 30 years ago (Schein et al., 1976) and represents one of the most abundant proteins of the mitochondrial outer membrane (Gonçalves et al., 2007). In this way, VDAC constitutes a main interface of communication between mitochondria and other cellular compartments.

2.1.1.1 General Functions of VDAC

In addition to the function as metabolite transporter across the mitochondrial outer membrane, VDAC is also believed to play a considerable role in the regulation of the cellular energy metabolism. Studies in mice using different VDAC knockout models showed a considerable impact on embryotic development, fertility and generation of diseases (Raghavan et al., 2011).

It has been shown that phosphorylation of VDAC regulates its interaction with hexokinase (HK) (Pastorino and Hoek, 2008), an enzyme of the glycolytic pathway catalysing the transformation of glucose to glucose-6-phosphate by hydrolysing ATP to ADP. Furthermore, it is known that the adenine nucleotide transporter (ANT) is able to form a complex with VDAC, an interaction facilitated if ANT adopts a cytoplasmic orientated conformation (c-ANT) (Vyssokikh and Brdiczka, 2003). Tetrameric hexokinase binds to VDAC at the cytosolic surface of the mitochondrial outer membrane to form the trimeric heterocomplex HK-VDAC-cANT that favours translocation of HK produced ADP through ANT to the matrix where it stimulates oxidative phosphorylation. This process is favoured by the interaction of HK with VDAC that closes VDAC like a cap thereby avoiding release of produced ADP to the cytosol. This energy metabolism is negatively regulated by the production of glucose-6-phosphate that inhibits the interaction of hexokinase with VDAC (Wilson and Chung, 1989; Azoulay-Zohar et al., 2004). In the same studies, another type of complex between VDAC and ANT was reported where both proteins are indirectly linked by an octamer of creatine kinase (CK) localized in the mitochondrial intermembrane space (Guzun et al., 2011). This trimeric complex VDAC-CK-ANT forms a microcompartment working in metabolite channelling. The synthesis of ATP by oxidative phosphorylation and its export *via* ANT are tightly coupled to CK stimulated trans-phosphorylation of ATP to phosphocreatine, exported by VDAC to the cytosol where it represents an important energy buffer for the cell. ANT translocates the yielded ADP back to the matrix where it stimulates oxidative phosphorylation, thereby closing the cycle.

The VDAC protein is also proposed to act in mitochondrial induced apoptosis by occupying a central role in the release of cytochrome *c* (cyt *c*) into the cytosol (Rostovtseva et al., 2005). A first mechanism, widely regarded, as being responsible for membrane permeabilization and release of cyt *c*, is the opening of the permeability transition pore (PTP), a putative unspecific channel increasing the inner mitochondrial membrane permeability. The precise molecular nature of this channel still remains elusive; various models have been proposed implicating VDAC and ANT, VDAC alone, misfolded inner membrane proteins or the pre-protein import machinery (Vyssokikh and Brdiczka, 2003; Kokoszka et al., 2004; He and Lemasters, 2002; Zoratti et al., 2005). Two major models exist that associate VDAC with the Bcl-2 protein family, also known as pro-apoptotic (*e.g.* Bax, Bak, Bid) and anti-apoptotic (*e.g.* Bcl-2, Bcl-X_L) protein factors. A first possibility was that the direct interaction of Bax, Bak and Bim with VDAC modulates its channel activity and leads to creation of channels large enough to promote cyt *c* permeation through the mitochondrial outer membrane and

depletion of the electrochemical membrane potential ΔΨ (Shimizu et al., 1999; Shimizu and Tsujimoto, 2000), while Bcl-X_L was shown to block this processes (Shimizu et al., 2000). The same group also showed that Bid, or its cleaved active form tBid, was not able to induce conformational changes of VDAC to favour cyt *c* release (Sugiyama et al., 2002). In a complete disagreement with hypotheses mentioned above, another theory maintained that Bax is not able to bind to VDAC and change its gating activity, whereas tBid was proposed to modulate channel activity of VDAC and prevent metabolite exchange leading to mitochondrial dysfunction (Rostovtseva et al., 2004). A more recent study proved that induction of apoptosis strongly upregulates VDAC oligomerization, leading to formation of megachannels potentially large enough to permit passage of cyt *c* into the cytosol (Keinan et al., 2010).

2.1.1.2 Genetic Organization of VDAC

VDAC is a highly conserved protein among eukaryotes, yet displaying a primary amino acid sequence homology often below 30%, with different isoforms ranging from one to five depending on the species. The yeast *Saccharomyces cerevisiae* has two isoforms, YVDAC1 and YVDAC2, on two single copy genes, *POR1* and *POR2* respectively, having 49% of amino acid identity. In mammals, three isoforms of VDAC have been characterized: VDAC1, VDAC2 and VDAC3 with approximately 70% of amino acid identity. VDAC1 and VDAC2 are differentially expressed in heart, skeletal muscles and brain, whereas VDAC3 is mainly expressed in testes, ovary, lung, spleen and kidney. However, in liver all three isoforms are expressed (Raghavan et al., 2011). In the plant *Arabidopsis thaliana*, four VDAC isoforms (AtVDAC1-4) are expressed and localized in mitochondria, whereas AtVDAC1-3 are also present in the plasma membrane (Robert et al., 2012). In mammals, the existence of a plasmalemmal splice variant of VDAC1, implicated in ATP traffic through the plasma membrane, was also reported (Okada et al., 2004), but still remains a subject of debate (Sabirov et al., 2006).

2.1.1.3 Channel Properties and Structure of VDAC

In the yeast *Saccharomyces cerevisiae* it is commonly accepted that YVDAC1 is the channel forming protein responsible for metabolite transport across the mitochondrial outer membrane. Deletion of this gene causes a temperature-sensitive growth defect on non-

fermentable carbon sources. Overexpression of the YVDAC2 isoform is able to functionally complement the growth deficiency, despite its reported inability to form channels in planar lipid bilayers reconstituted with mitochondrial outer membranes containing YVDAC1 and/or YVDAC2 (Blachly-Dyson et al., 1997). Expression of the mouse VDAC1 and VDAC2 isoforms in YVDAC1 deleted *S.cerevisiae* also rescued temperature-sensitive growth and both mouse isoforms expressed and isolated from *S.cerevisiae* (as well as human VDAC1 and VDAC2) displayed comparable channel activity as YVDAC1 (Sampson et al., 1997; Blachly-Dyson et al., 1993; Xu et al., 1999). These facts illustrate a functional conservation of different VDAC isoforms within and between species.

The term Voltage Dependant Anion Channel implicates that this channel is sensitive to potential generation at the mitochondrial outer membrane, a process yet poorly understood. Possible models considered the Donnan potential and the steady-state flux of charged metabolites as sources of outer membrane potential (Liu and Colombini, 1992; Zizi et al., 1994; Lemeshko and Lemeshko, 2000).

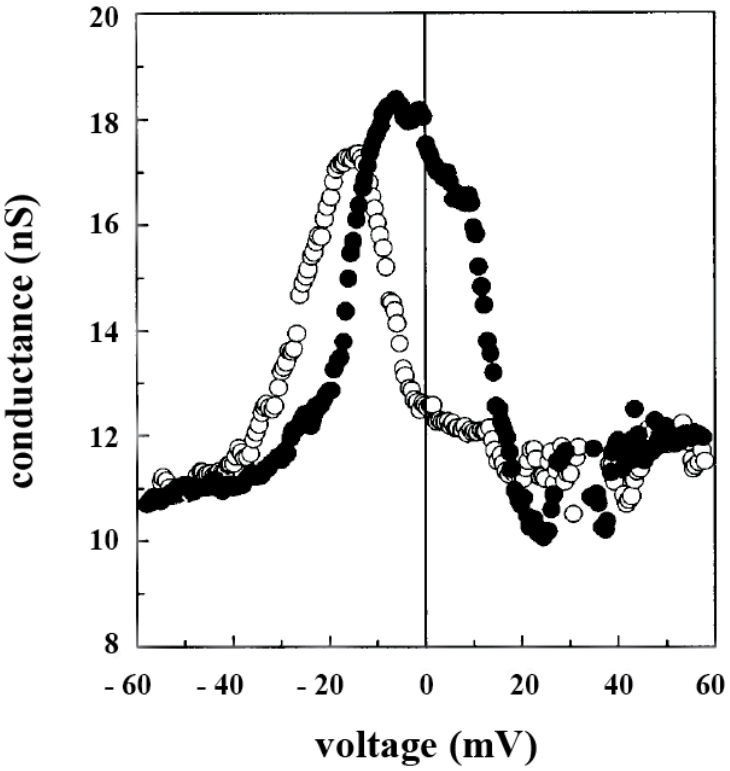

Fig.3 : **Bell-shaped voltage dependance of VDAC conductance.** In presence of an ATP gradient maximal channel conductance is observed between -15mV and -10mV. Higher potential values induce partial closure of the channels. ●Voltage change from negative to positive values. ○Voltage change from positive to negative values (Rostovsteva et *al*., 1997).

Electrophysical studies in planar phospholipid bilayers showed that reconstituted VDAC possesses bell-shaped voltage dependence **(Fig.3)**; with a pore displaying a canonical anion selective fully open state with a conductance of 4nS (1M KCl) when low voltages (+/- 10mV) are applied (Benz, 1994). It is assumed that this conformation permits passage of metabolites like ATP, ADP, inorganic phosphate and ions (Ca^{2+}, K^{+}, Na^{+} and preferentially Cl^{-}) across the mitochondrial outer membrane (Rostovtseva and Colombini, 1997). However, if higher voltages (+/- 25-50mV) are applied, VDAC shifts to a half open cation selective state only permeable to ions. A cationic fully open state of VDAC was also reported (Pavlov et al., 2005) but if this conformation is involved in transport of larger metabolites like ATP remains to be demonstrated. The ability of VDAC to switch between these open and closed states may be an important physiological regulation mechanism of metabolite flux *in vivo*.

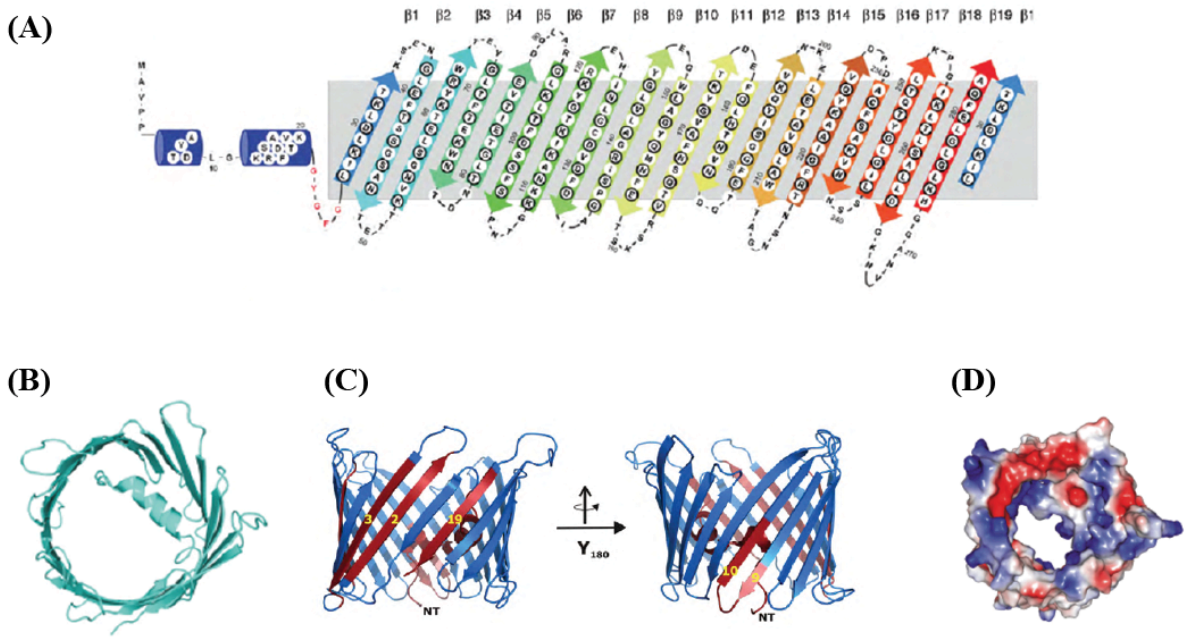

Fig.4 : Structure of VDAC. (A) Secondary topology of VDAC with 19 ß-strands (ß19 and ß1 closing the ß-barrel in a parallel arrangement) (Hiller et *al*., 2010). **(B)** Top view of human VDAC1. 3-D structure was solved by NMR and X-ray diffraction. The N-terminal helix protrudes into the lumen of the channel (Bayrhuber et *al*., 2008). **(C)** Side views of mouse VDAC1 with a 3-D structure solved by X-ray diffraction. Proposed voltage sensors are indicated in red (Ujwal et *al*., 2008). **(D)** Vacuum electrostatics illustrating charge distribution on human VDAC1 shown in (B). Negative charges are depicted in red and postive charges are depicted in blue (Summers and Court, 2010).

From a structural point of view VDAC forms a slightly elliptical 2,7-3,8nm x 2,4-3,1nm pore through the outer membrane with a height of 4,5nm and a constriction to 1,5-2,7nm x 1-1,7nm in the middle. It is assumed that this conformation represents the fully open state with an anion selective character, responsible for metabolite and ion transport. When the pore is partially closed it shifts to a cation selective state with a diameter of 1,9nm. The precise architecture of VDAC has been revealed by X-ray crystallography, nuclear magnetic resonance (NMR) and a combination of both techniques (Ujwal et al., 2008; Bayrhuber et al., 2008; Hiller et al., 2008). The obtained structures show that VDAC is organized in a unique monomeric ß-barrel composed of 19 antiparallel ß-strands with two parallel strands closing the ß-barrel **(Fig.4A)**. The N-terminal part of VDAC forms an α-helix located in the lumen of the channel, whereas the C-terminal part is embedded in the membrane **(Fig.4A+B)** (De Pinto et al., 1991). A key concept of voltage gating is the presence of voltage sensor domains in the channel. Biochemical approaches and site directed mutagenesis showed that positively charged amino acid residues at N-terminal positions are implicated in gating (Thomas et al., 1993). Based on these observations and structural data, several mechanisms of gating regulation by the N-terminal part (N-ter) of VDAC may be anticipated: (1) movement of N-ter in and out of the lumen creating a closed or opened conformation respectively, (2) movement of N-ter around a hinge inside the lumen causing open and closed states and (3) transition of N-ter from an α–helical structure aligning with the barrel wall to a less-structured element that interacts with the opposing barrel wall (Guo et al., 1995; Ujwal et al., 2008; De Pinto et al., 1990; Bayrhuber et al., 2008).

2.1.1.4 Native Assembly of VDAC in the mitochondrial outer Membrane

In addition to the structural data obtained by crystallography, previous studies analysed the native assembly of VDAC proteins in the mitochondrial outer membrane using atomic force microscopy (AFM) (Mannella et al., 1983; Hoogenboom et al., 2007; Gonçalves et al., 2007). Both studies confirmed the elliptical shape of a single VDAC and gave a first visual acknowledgment that VDAC is able to form a variety of oligomers **(Fig.5)**. However, none of the oligomers showed a pore diameter larger than that of a single VDAC, whereas it cannot be excluded that interaction of VDAC oligomers with other proteins, *e.g.* pro-apoptotic proteins, could lead to formation of megachannels with a larger diameter.

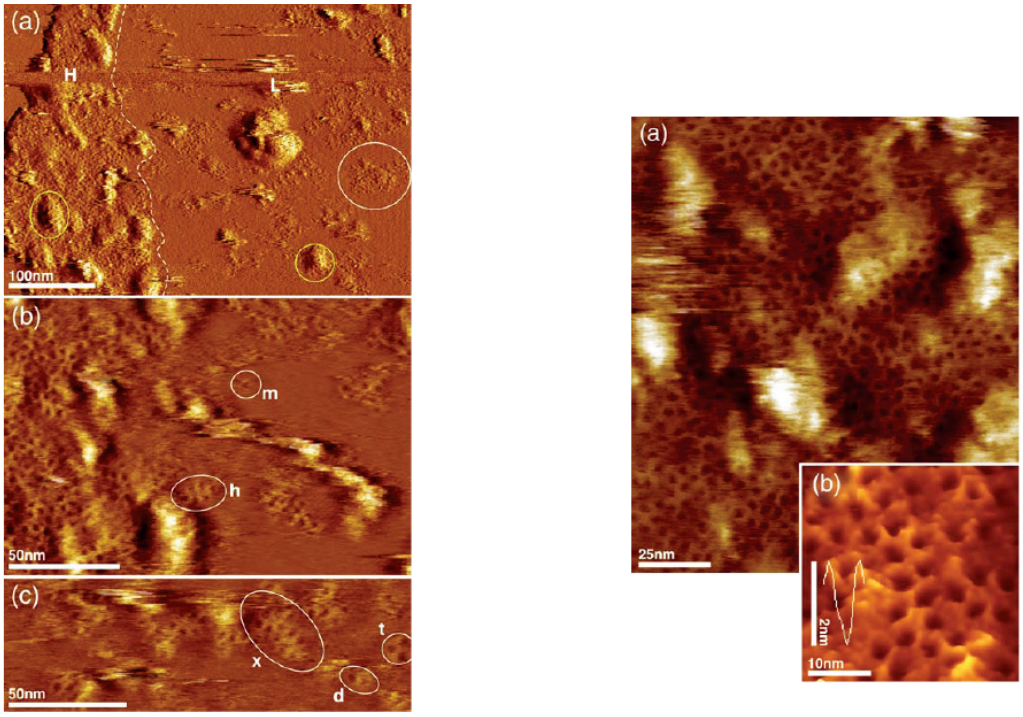

Fig.5 : Native assembly of VDAC in the mitochondrial outer membrane. **left panel** : **(a)** AFM image of a membrane patch containing low-density (L) and high density (D) protein domains. White and yellow outlines show protein corrugation and protusions respectively, distinguishable from the smooth lipid areas. **(b)** and **(c)** High-resolution topographs of low-density domains showing monomeric (m), dimeric (d), trimeric (t), hexameric (h), and arrays of oligomeric (x) VDACs. **right panel** : **(a)** High-resolution topograph of an array densely packed with VDAC. **(b)** Magnification of (a) showing eye-shaped VDAC (pore dimensions : 3.8nm x 2.7nm; height : 2nm) (Gonçalves et *al*., 2007).

2.2 Mitochondrial Protein Import

Mitochondria retained an entire genetic expression system in their matrix but only ~1% of the mitochondrial proteins are encoded by the mitochondrial genome. These proteins are typically integral inner membrane proteins of respiratory chain complexes that are synthesized on matrix ribosomes and inserted by the oxidase assembly (OXA) machinery (Preuss et al., 2005). The remaining 99% of mitochondrial proteins are encoded by the nuclear genome, synthesized on cytosolic ribosomes and imported into the different mitochondrial compartments by specialized machineries (Schmidt et al., 2010; Chacinska et al., 2009).

2.2.1 Mitochondrial Targeting Signals

Imported precursor proteins (preproteins) contain specific targeting signals guiding them to their functional destination in the mitochondrial subcompartments **(Fig.6)**. Generally,

two main groups of targeting signals can be distinguished (i) presequences, located at the N-terminal part of the preproteins, usually cleaved following import and (ii) internal targeting signals that remain part of the imported protein.

Import of most matrix directed preproteins is directed by an N-terminal presequence that forms an amphipathic α helix **(Fig6.A)** with a non consensus sequence of 15-50 amino acid residues possessing a hydrophobic and a positively charged surface recognized by the receptor proteins Tom20 and Tom22 respectively (Saitoh et al., 2007; Yamano et al., 2007). These α helixes also contain a cleavage site permitting processing of the imported protein by the mitochondrial processing peptidase (MPP) (Taylor et al., 2001). Some preproteins contain an additional uncleaved hydrophobic anchor causing arrest of translocation and insertion into the inner membrane, or even a cleaved hydrophobic sequence (bipartite presequence) removed by the inner membrane peptidase complex (IMP) with subsequent release into the intermembrane space (Glick et al., 1992) **(Fig6.A)**.

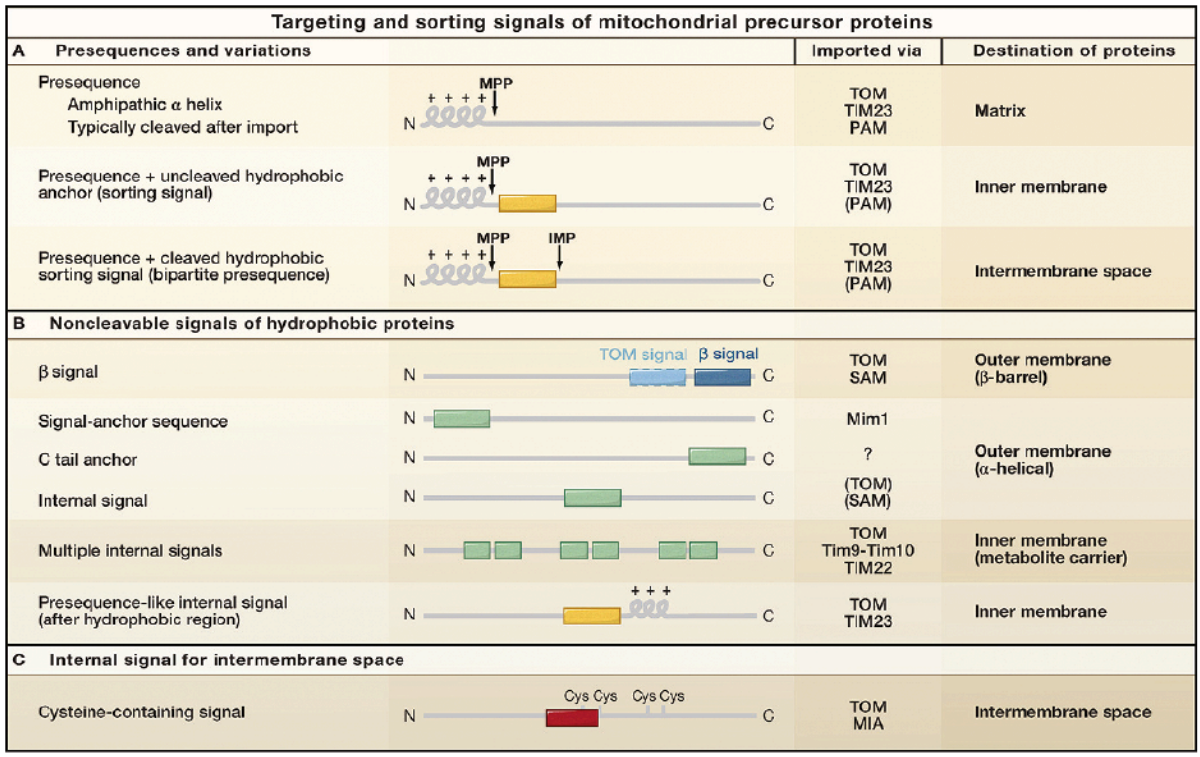

Fig.6 : Table summarizing targeting and sorting signals of mitochondrial precursor proteins. **(A)** Cleaved presequences and presequence variations directing precursor proteins to the matrix, the inner membrane and the intermembrane space. **(B)** Noncleaved targeting signals of precursor proteins inserted in the mitochondrial outer and inner membranes. **(C)** Internal mitochondrial intermembrane space targeting signal (MISS) targeting precursor proteins to the intermembrane space *via* the MIA machinery. **TOM** : Translocase of the Outer Membrane, **TIM23** : Presequence Translocase of the Inner Membrane, **TIM22** : Carrier Translocase of the Inner Membrane, **PAM** : Presequence Translocase-associated Motor, **Mim1** : Mitochondrial Import 1 protein, **SAM** : Sorting and Assembly machinery, **Tim9-Tim10** : small chaperones of the intermembrane space, **MIA** : Mitochondrial Intermembrane Space Assembly machinery, **MPP** : Mitochondrial Processing Peptidase, **IMP** : Inner Membrane Peptidase Complex (Chacinska et *al*., 2009).

All mitochondrial outer membrane proteins, the majority of integral inner membrane proteins and a few matrix directed proteins are devoid of a cleaved presequence, but contain internal targeting signals at various positions remaining in the mature imported molecule. Outer membrane proteins having a ß-barrel topology, *e.g.* Tom40 or VDAC1, contain an internal TOM signal necessary for the initial recognition at the mitochondrial surface and a ß signal in the last ß strand at their C-terminal region that is specifically recognized by the Sorting and Assembly Machinery (SAM) **(Fig6.B)** promoting insertion of proteins into the mitochondrial outer membrane (Kutik et al., 2008). Most of outer membrane proteins are, however, inserted by α helical transmembrane domains located in the middle or at the N-terminal and C-terminal parts of the imported protein (Beilharz et al., 2003; Otera et al., 2007; Stojanovski et al., 2007) **(Fig6.B)**. Inner membrane proteins belonging to the family of carrier proteins, *e.g.* ADP/ATP and phosphate carriers, are anchored by six transmembrane segments and contain their targeting information along the length of the protein **(Fig6.B)** each having about 10 amino acid residues. Some inner membrane proteins also contain an internal positively charged "presequence-like" signal often preceded by a hydrophobic sequence (Neupert and Herrmann, 2007; Chacinska et al., 2009) **(Fig6.B)**. Proteins directed to the intermembrane space have the mitochondrial intermembrane space signal (MISS) including a cysteine residue and a hydrophobic residue necessary for the binding and recognition by their receptor protein (Milenkovic et al., 2007, 2009; Sideris and Tokatlidis, 2007) **(Fig6.C)**.

2.2.2 Mitochondrial Protein Import Pathways

Currently, five protein import pathways have been described **(Fig.7)** that carry out the translocation of different classes of preproteins into the mitochondrial subcompartments (Neupert and Herrmann, 2007; Chacinska et al., 2009; Schmidt et al., 2010).

2.2.2.1 The Presequence Import Pathway

All imported preproteins pass the first mitochondrial membrane through the translocase of the outer membrane (TOM) complex. This complex is composed of the central channel-forming protein Tom40, the receptor proteins Tom20, Tom22 and Tom70, as well as of three small Tom proteins (Mokranjac and Neupert, 2009). Tom40 is an integral membrane protein with a 19-stranded ß-barrel topology (Zeth, 2010). The three small Tom proteins are involved in the assembly and stability of the TOM complex. Tom6 and Tom7 play

antagonistic roles; Tom6 is supposed to stabilize the TOM complex, whereas Tom7 has a more destabilizing effect by delaying early and late assembly steps of the TOM complex (Becker et al., 2011b). Tom5 exerts a complementary function to Tom6 and is also implicated in transfer of preproteins to the Tom40 channel (Becker et al., 2010; Dietmeier et al., 1997).

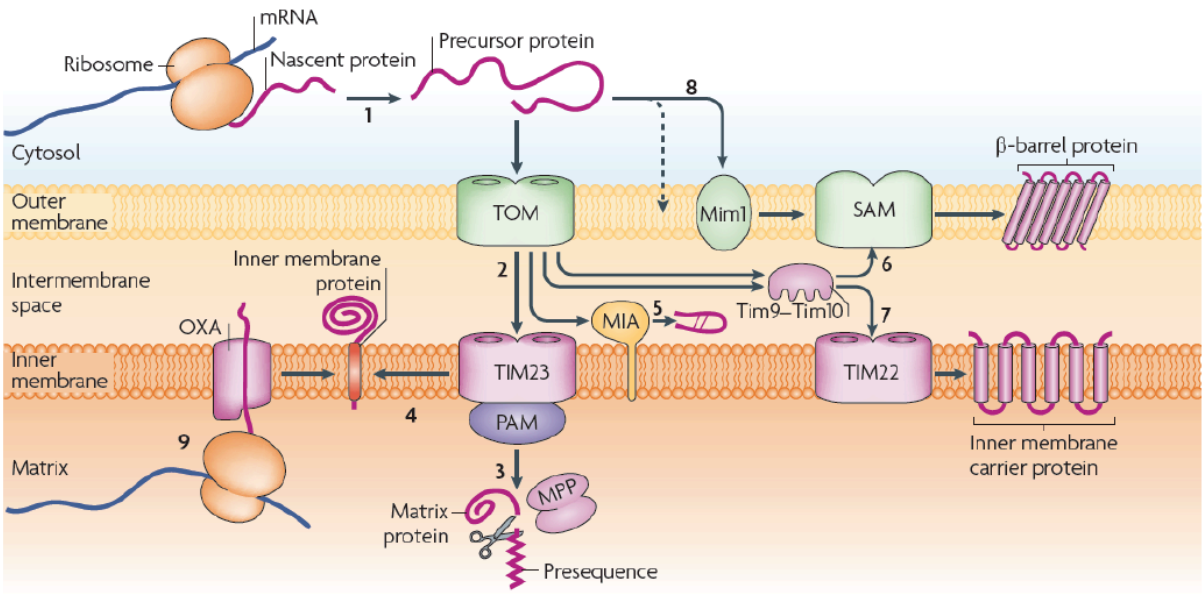

Fig.7 : Import pathways of mitochondrial proteins. Mitochondrial precursor proteins are synthesized on cytosolic ribosomes and imported through the translocase of the mitochondrial outer membrane (TOM) complex **(1)**. Arrived in the intermembrane space, the precursor proteins are guided to their destination *via* different sorting machineries **(2)**. Presequence carrying proteins imported into the matrix are translocated through the presequence translocase of the inner membrane (TIM23) complex with the help of the presequence translocase-associated motor (PAM). Presequences are cleaved off by the mitochondrial processing peptidase (MPP) **(3)**. Some proteins are laterally released from the TIM23 complex into the inner membrane **(4)**. The mitochondrial intermembrane space assembly (MIA) machinery is involved in import and oxydative folding of many intermembrane space proteins **(5)**. The Tim9-Tim10 chaperone complex transfers hydrophobic proteins either to the sorting and assembly machinery (SAM) complex, in the case of ß-barrel proteins of the outer membrane **(6)**, or to the TIM22 complex in the case of inner membrane carrier proteins **(7)**. α-helical precursor proteins are inserted into the outer membrane by the mitochondrial import 1 protein (Mim1) **(8)**. Proteins that are synthesized in the matrix on mitochondrial ribosomes are exported to the inner membrane by the oxidase assembly (OXA) machinery **(9)** (Schmidt et *al*., 2010).

The matrix-targeted import of preproteins happens *via* a sequential recognition of the presequence by various components of the import machinery **(Fig.7 step 2 and 3; Fig.8)**. The initial recognition of presequences on the mitochondrial surface occurs by the receptors Tom20 and Tom22. Tom20, the main receptor of matrix directed preproteins, is anchored by an N-terminal transmembrane domain exposing a hydrophilic domain to the cytosol that possesses a binding groove for the hydrophobic surface of the presequence located at the N-

terminal part of matrix targeted preproteins (Abe et al., 2000). The central receptor Tom22 spans the outer membrane in a N_{out}-C_{in} orientation exposing a highly negatively charged N-terminal domain to the cytosol, recognizing the positively charged surface of the presequence, and a short C-terminal domain to the intermembrane space. Tom22 connects Tom20 to the central translocation channel and it plays an important role in the overall integrity of the TOM complex (van Wilpe et al., 1999; Mayer et al., 1995). After translocation through the Tom40 channel, preproteins interact with the C-terminal part of Tom22 in the intermembrane space.

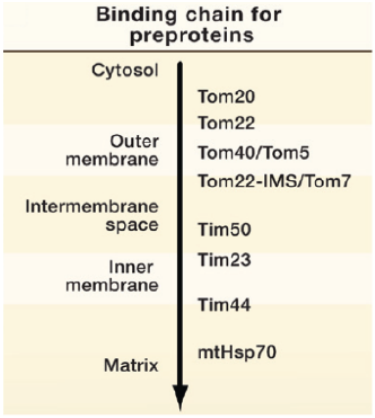

Fig.8 : Illustration of the sequential binding chain of presequence imported precursor proteins (Chacinska et *al*., 2009)

The passage across the mitochondrial inner membrane is ensured by the translocase of the inner membrane (TIM23) complex that is composed by the channel-forming Tim23 protein, Tim17, Tim50, Tim21 and Mgr2 (Mokranjac and Neupert, 2009; Gebert et al., 2012). Tim23, Tim50 and Tim21 expose domains to the intermembrane space that are involved in transient interactions between the TIM23 and the TOM complex. Tim50, tightly bound to the intermembrane space domain of Tim23, is the first component interacting with the preproteins and thus transfers the information of its entry to the import channel. Tim50 also plays an important role in absence of preproteins by closing the Tim23 channel, thereby avoiding leakiness of the inner membrane and dissipation of the electrochemical membrane potential ΔΨ (Meinecke et al., 2006). Tim21 competes with Tom22 for presequences and promotes release from the TOM complex and transfer to the Tim23 channel (Chacinska et al., 2005). Furthermore, Tim21 also favours interaction of the respiratory chain with the TIM23 complex to stimulate the ΔΨ dependant inner membrane insertion of preproteins containing a hydrophobic stop signal after the N-terminal presequence **(Fig.6A; Fig.7 step 4)**, a process requiring the activity of Tim17 (van der Laan et al., 2007; Chacinska et al., 2005). Δψ also activates the Tim23 channel and has an electrophoretic effect on the positively charged presequences to pull preproteins into the matrix compartment (Shariff et al., 2004; van der Laan et al., 2006; Krayl et al., 2007). Mgr2, a recently discovered subunit of the TIM23 complex, is necessary for an efficient TOM-TIM coupling and the recruitment of the respiratory chain complexes to the TIM23 complex (Gebert et al., 2012).

The translocation of presequence containing preproteins into the matrix requires the connection of the TIM23 complex, devoid of Tim21, to the presequence translocase-

associated motor (PAM). PAM is composed of Tim44 and its central component, the mitochondrial chaperone Hsp70 (mtHsp70) that binds emerging unfolded preproteins and drives their translocation into the matrix by an ATP-powered manner. mtHsp70 is stimulated by the nucleotide exchange factor Mge1, whereas Tim44 serves as a docking site to connect mtHsp70 to the TIM23 complex. Furthermore three membrane-bound co-chaperones coordinate the function of the mtHsp70; Pam18 stimulates the ATPase activity of mtHsp70 and Pam16 forms a complex with Pam18 to act as a negative regulator. Pam17 is involved in the TIM23-PAM interaction (Frazier et al., 2004; Kozany et al., 2004; Mokranjac et al., 2006; D'Silva et al., 2008). Two models were proposed to explain this translocation process: (i) the trapping or Brownian model where mtHsp70 binds the first segment of emerging preproteins to avoid backsliding. When a further segment of the same preprotein reaches the matrix, it is bound by mtHsp70 and favours its movement to the matrix lumen, (ii) the pulling model, where a conformational change of Tim44 leads to an active driving of the preproteins to the matrix (Chauwin et al., 1998).

2.2.2.2 The Carrier Import Pathway

Preproteins destined for the inner membrane are imported *via* the carrier pathway **(Fig.7 step 7)**. They are translated on cytosolic ribosomes and subsequently bound by cytosolic chaperones of the Hsp70 and Hsp90 families to prevent their aggregation and to guide them to the outer membrane receptor Tom70. This receptor is anchored by an N-terminal transmembrane segment into the outer membrane exposing hydrophilic domains to the cytosol and possessing binding sites for the Hsp70/Hsp90 chaperones that release the preprotein in an ATP dependent manner (Li et al., 2009; Young et al., 2003; Zara et al., 2009). The cytosolic domain of Tom70 is responsible for recognition of the targeting signals located on preproteins and contains 11 tetratricopeptide repeat motifs showing a preference for hydrophobic precursors (Chan et al., 2006; Wu and Sha, 2006). Hydrophobic preproteins owning internal targeting signals pass the outer membrane through the TOM complex in a loop structure to reach the intermembrane space, where two hexameric chaperone complexes, Tim9-Tim10 and Tim8-Tim13, bind the preproteins and guide them through the aqueous environment to the inner membrane (Webb et al., 2006; Wiedemann et al., 2001; Curran et al., 2002; Davis et al., 2007). Here they are inserted with the help of the TIM22 complex composed of two channel forming Tim22 proteins, the Tim54 protein and the Tim18 protein that is involved in the assembly of the TIM22 complex. The precursor protein is bound to the

TIM22 complex by a modified form of the intermembrane space chaperone, the Tim9-Tim10-Tim12 complex that is probably recognized by the exposed domain of Tim54. Activation of the Tim22 channels depends on the internal targeting signals and ΔΨ. Preproteins are likely inserted into the channel by a loop structure and laterally released into the lipid phase of the inner membrane (Rehling et al., 2003; Wagner et al., 2008).

2.2.2.3 The Mitochondrial intermembrane Space Import and Assembly (MIA) Pathway

Preproteins addressed to the intermembrane space are imported by the MIA pathway **(Fig.7 step 5)** that harbours two components of major importance; Mia40 and Erv1. Mia 40, an essential protein of the intermembrane space conserved in eukaryotes, serves as a receptor for incoming preproteins at the inner side of the outer membrane and holds oxidoreductase and chaperone activities. Homologues possess a highly conserved domain that is composed of

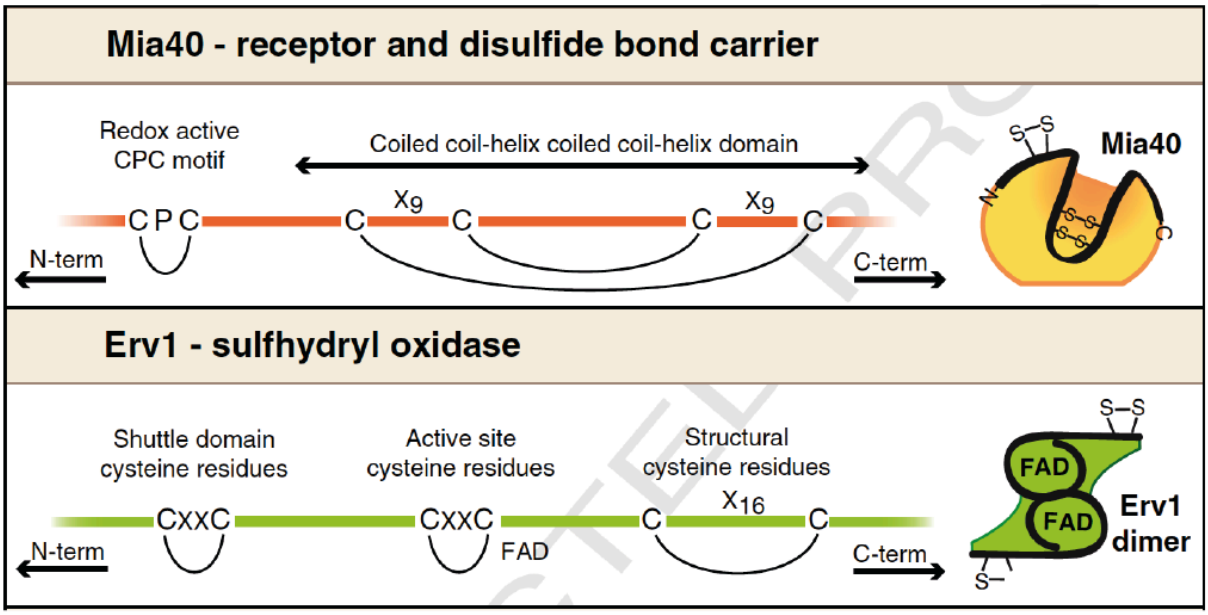

Fig.9 : Essential components of the MIA pathway. Mia40 has a conserved core domain with a redox active CPC motif interacting with Mia40 substrates and Erv1. The two CX_9C motifs confer a stable structure to Mia40. Erv1 contains two CXXC domains implicated in its activity, a first domain constituting the shuttle domain necessary for Erv1 function and a second domain forming the active site located near to the flavine adenine dinucleotide (FAD) binding site necessary for Erv1 dimerisation (Stojanovski et *al*., 2012).

three cysteine containing motifs; the redox active CPC motif and a twin CX_9C (X is an amino acid) motif implicated in the structural stability of Mia 40 that is important for its functional activity (Banci et al., 2009; Terziyska et al., 2009; Kawano et al., 2009). Erv1 belongs to the family of conserved sulfhydryl oxidases that share a flavin binding domain (FAD domain)

responsible for homodimerization of Erv1 (Fass, 2008). This essential protein also contains a catalytic domain and a shuttle domain with CXXC motifs necessary in Erv1 function and two cysteine residues stabilizing the structure of the protein **(Fig.9)** (Hofhaus et al., 2003).

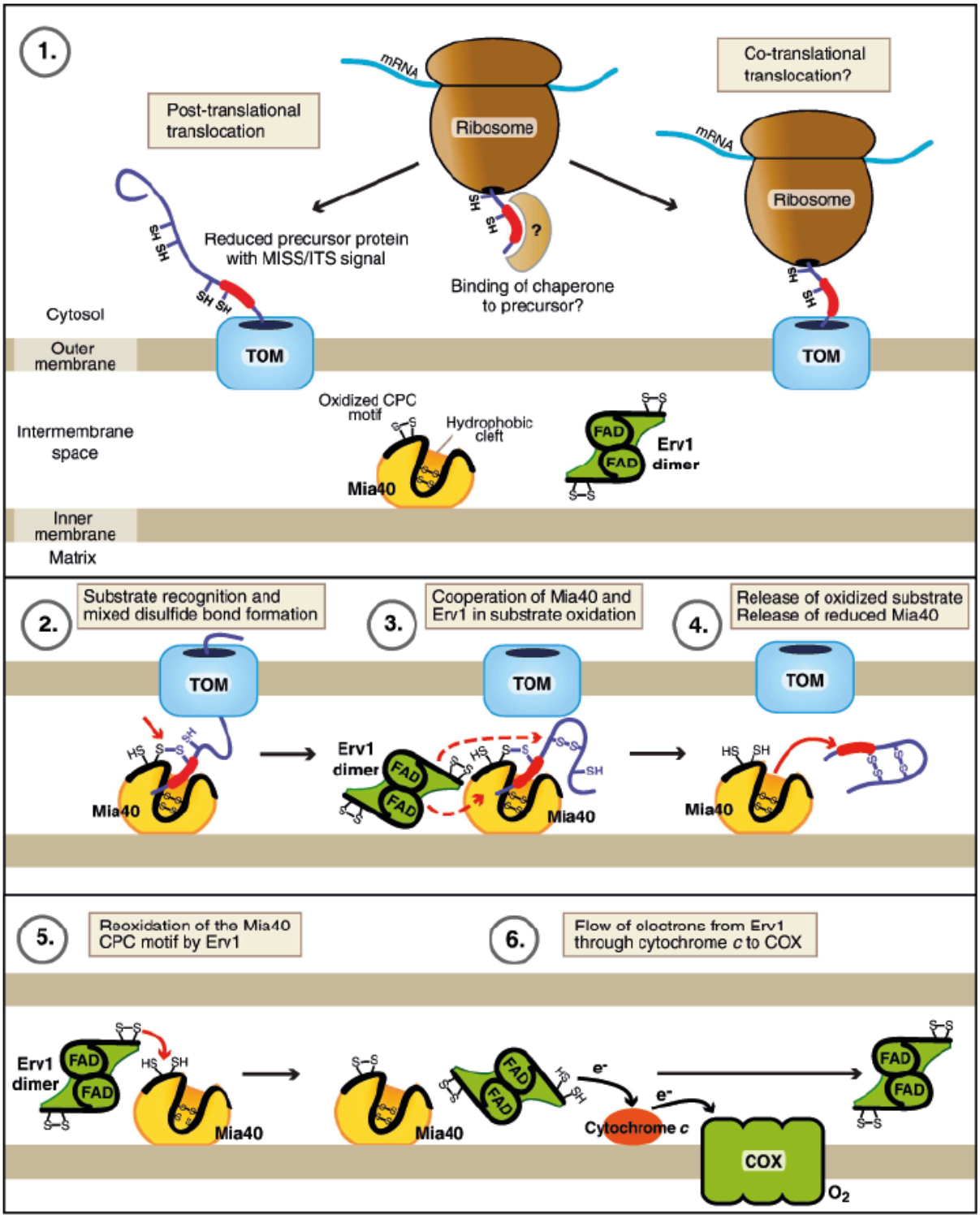

Fig.10 : Different steps of the oxydative biogenesis of intermembrane space proteins (MIA pathway) (Stojanovski et *al*., 2012).

Preproteins synthesized on cytosolic ribosomes are targeted to the TOM complex by a still unresolved mechanism and translocated in an unfolded and reduced state into the intermembrane space (Lutz et al., 2003) **(Fig.10 step 1)** where they are recognized in a receptor like manner by oxidized Mia40, due to the MISS targeting signal, with subsequent intermolecular disulphide bond formation between a cysteine of the preprotein and a first cysteine of the CPC redox active domain of Mia40 **(Fig.10 step 2)**. In the next step Erv1 and Mia40 cooperate to promote full oxidation of the preprotein that leaves Mia40 in a completely reduced state **(Fig.10 steps 3 and 4)**. Mia40 will be recharged by Erv1 to restore preprotein binding activity **(Fig.10 step 5)**. For this reason Erv1 accepts electrons from Mia40 in a reaction causing formation of another disulphide intermediate implicating the second cysteine of the CPC domain of Mia40. Erv1 is recycled by transferring gained electrons to the respiratory chain *via* cytochrome *c* **(Fig.10 step 6)**, thus increasing the reoxidation rate of Mia40 and potentially avoiding generation of reactive oxygen species (Stojanovski et al., 2012; Herrmann and Riemer, 2012).

2.2.2.4 The ß-barrel Import Pathway

Mitochondrial outer membrane proteins are exclusively imported from the cytosol and form two major families; proteins owning a ß-barrel topology and proteins inserted by terminal α-helical transmembrane domains.

Precursors of ß-barrel proteins are translocated through the outer membrane by the TOM complex and are inserted by a specialized protein complex, the sorting and assembly machinery (SAM) complex **(Fig.7 step 6)**. SAM is formed by the channel-forming core component Sam50 and two further subunits, Sam 37 and Sam35 (Wiedemann et al., 2003). Sam50 is a homologue of BamA, a member of the bacterial Omp85 protein family catalysing ß-barrel protein insertion into plasma membranes of Gram-negative bacteria, displaying its conserved character within human mitochondria (Paschen et al., 2003). After translocation, ß-barrel precursor proteins are bound by the intermembrane space chaperone complexes Tim9-Tim10 and Tim8-Tim13 that guide them to the SAM complex (Wiedemann et al., 2004). Sam35 recognizes the sorting signal located in the last C-terminal ß-strand of the preprotein that is released into the lipid phase with the help of Sam37 (Kutik et al., 2008; Chan and Lithgow, 2008), but the exact mechanisms of precursor insertion into Sam50 and its release are still unknown. Typical ß-barrel proteins, like VDAC and Tom40, are inserted with the help of this SAM complex, but maturation of the TOM complex follows a more sophisticated

route. Tom40 binds to the SAM complex and offers a platform for TOM complex assembly. A fraction of SAM, containing the Mdm10 (mitochondrial distribution and morphology 10) protein as an additional subunit, favours association of the central receptor Tom22 with Tom40 and its insertion into the membrane (Yamano et al., 2010; Meisinger et al., 2004; Stojanovski et al., 2007).

2.2.2.5 The outer Membrane Insertion of α-helical Proteins

Almost all outer membrane proteins are inserted *via* N-terminal, middle or C-terminal α-helical transmembrane domains, where the hydrophobic segments usually function as targeting signals **(Fig.6B)**. The integral outer membrane proteins Mim1 and Mim2 (mitochondrial import 1 and 2) play a crucial role in the biogenesis of these proteins **(Fig.7 step 8)** (Dimmer et al., 2012) and in this way intervene indirectly in the early assembly steps and the maturation of the TOM complex (Becker et al., 2010). The receptors Tom20 and Tom70 are examples for N-terminally anchored proteins, whereas the small Tom proteins, Tom5, Tom6 and Tom7 are anchored *via* their C-terminal domains (Popov-Celeketić et al., 2008; Thornton et al., 2010). Proteins possessing multiple transmembrane segments are imported with the help of the Tom70 receptor in a Mim1 depending manner (Becker et al., 2011a).

2.2.3 Regulation of the Mitochondrial Protein Import

The TOM complex is the main entry gate for all mitochondrial precursor proteins. Recently, the description of the mitochondrial phosphoproteome revealed that the TOM complex is highly phosphorylated at the outer membrane, raising the interest of how the preprotein import can be regulated. In fact two cytosolic protein kinases, the casein kinase 2 and the protein kinase A, were identified to be able to phosphorylate several proteins constituting the TOM complex, thereby regulating its function (Schmidt et al., 2011; Rao et al., 2011, 2012).

The casein kinase 2 (CK2), a highly conserved serine/threonine-selective tetrameric protein kinase composed of two α- and two β-subunits, is known for its contribution in many cellular processes like gene expression, signalling, protein synthesis, cell proliferation and apoptosis (Gao and Wang, 2006). This protein kinase is also implicated in the phosphorylation of the cytosolic domains of Tom proteins. Phosphorylation of serines at

positions 44 and 46 of the Tom22 precursor protein plays a dual role; it promotes targeting of Tom22 to mitochondria and association of Tom20 to the TOM complex. Tom20 itself is also phosphorylated at a serine on position 172, but mutation of this specific residue did not have an effect on its own targeting, neither on preprotein import following the presequence or the carrier pathways. Mim1, responsible for import of α-helical outer membrane proteins, also carries two essential serine residues on positions 12 and 16 that can be phosphorylated. Mutation of these sites leads to an impairment of Tom70 and Tom20 assembly into the TOM complex. The overall inactivation of CK2 shows drastic effects on whole mitochondrial protein import, illustrating the functional importance of this kinase in regulation and maturation of the TOM complex (Schmidt et al., 2011).

The protein kinase A (PKA), a cAMP dependent holoenzyme consisting of two regulatory and two catalytic subunits, is involved in numerous essential cellular processes like regulation of metabolic pathways, cellular growth, cell differentiation and many others (Vandamme et al., 2012). In the context of preprotein import, PKA phosphorylates a serine on position 174 of the receptor Tom70 under fermentive growth conditions. This specific phosphorylation impairs the capacity of the receptor to bind the Hsp70 moiety of the Hsp70/preprotein complex and hence hinders import of inner membrane targeted carrier proteins, necessary for metabolite transport into the mitochondrial matrix and subsequent stimulation of the respiration. This negative regulation process illustrates the capacity of the cell to adapt to metabolic conditions (Schmidt et al., 2011). A second substrate of PKA is the precursor of the Tom40 protein, whose phosphorylation at a serine on position 54 has an inhibitory effect on the import of the preprotein, thus impairing the biogenesis of the TOM complex (Rao et al., 2012).

These stimulatory and inhibitory effects of CK2 and PKA respectively illustrate in an elegant manner the multiple regulation of function and biogenesis of the TOM complex and preprotein import.

2.3 Nucleic Acid Import

The biogenesis of mitochondria requires import of a large number of proteins, but in addition to protein import, selective delivery of nucleic acids represents another process indispensable for a proper functioning of mitochondria. Naturally imported nucleic acids described up to date are small and non-coding, constituting mostly transfer RNAs (tRNAs) that guarantee translation of mitochondrial DNA encoded proteins. Artificial uptake of DNA into mitochondria has also been reported. Whereas mechanisms of protein import are well studied, processes involved in addressing nucleic acids into mitochondria are still raising fundamental questions.

2.3.1 Mitochondrial DNA Import

Mitochondrial DNA import has, in a first time, been described in plants. Isolated potato (*Solanum tuberosum*) mitochondria were able to import a linear 2,3kb plasmid derived from *Zea mays* that could be transcribed *in organello*, as demonstrated by RT-PCR and Southern blots. The import process depended on the double-stranded character of the DNA molecule and on the presence of the electrochemical membrane potential $\Delta\Psi$. The translocation through the mitochondrial outer membrane implicated VDAC, as confirmed by a specific import inhibition using the VDAC blocker ruthenium red and a pre-treatment with antibodies directed against potato VDAC. However, the assumed implication of the Adenine Nucleotide Transporter (ANT) in the passage across the mitochondrial inner membrane remained unclear (Koulintchenko et al., 2003). A second study demonstrated that the mitochondrial DNA import is also possible using isolated *Saccharomyces cerevisiae* and human mitochondria, showing that this phenomenon is not strictly specific to plants (Ibrahim et al., 2011). In agreement with previously obtained results, it could be shown that efficiency of mitochondrial DNA uptake decreased with increasing sizes of DNA templates, with a good import efficiency up to ~6,5kb and a complete absence of import above 10kb. However, the possibility of natural mitochondrial import of a linear 11,6kb fragment in the *Brassica napus* and the *Brassica rapa* species showed that, conversely to previous studies, sequence elements have to be responsible for mitochondrial import of larger DNA templates. Indeed, investigation of sequence elements revealed inverted repeats, localized at the *termini* of the imported linear 11,6kb DNA fragment, as being the specific sequence elements promoting its mitochondrial uptake because absence of these sequence elements abolished its import.

Furthermore, it was shown that external hydrolysis of ATP significantly enhanced mitochondrial DNA import. This fact could be explained by a possible implication of outer membrane protein phosphorylation that was slightly increased upon incubation of mitochondria with ATP. Preparation of mitochondria in phosphatase inhibiting conditions also significantly increased mitochondrial DNA uptake, strengthening the previously mentioned hypothesis.

2.3.2 Discovery and Versatility of tRNA Import

A first report suggesting the possibility that tRNAs could be imported into mitochondria dates back to 1967. The analysis of a mitochondrial tRNA fraction isolated from *Tetrahymena pyriformis* revealed that a large part of these tRNAs hybridize to nuclear DNA rather than to the mitochondrial DNA (Suyama, 1967). This hypothesis of mitochondrial tRNA import, however, was regarded with great scepticism at that time. In 1977 the next evidence for the presence of a cytosolic tRNA inside mitochondria was provided. In the yeast *Saccharomyces cerevisiae* it was shown that, from a preparation of mitochondrial tRNAs, one single tRNA, the isoacceptor $tRNA^{Lys(CUU)}$, hybridized exclusively to the nuclear DNA (Martin et al., 1977). This $tRNA^{Lys\ (CUU)}$ was then confirmed as being imported into mitochondria (Martin et al., 1979). At the end of '80s and beginning of '90, the first evidence of mitochondrial tRNA import was provided for plants, *e.g.* the species *Phaseolus vulgaris*, and the trypanosomatids *Leishmania tarantolae* and *Trypanosoma brucei* (Maréchal-Drouard et al., 1988; Simpson et al., 1989; Hancock and Hajduk, 1990a). Finally, in 1992 the first direct proof was given for the process of mitochondrial tRNA import, where it was possible to detect a foreign tagged tRNA inside mitochondria of a transgenic potato plant (Small et al., 1992).

The discovery of tRNA import in many eukaryotic microorganisms, like protozoa, fungi and algae, as well as in plants and animals, displays the diversity of this mechanism **(Table 2)**. Because mitochondria derive from an ancient α-proteobacteria, the possession of a complete set of mitochondrial tRNAs reflects the ancestral situation. Given the striking difference in tRNA import, even between closely related species, it is likely that the mitochondrial import has a polyphyletic origin (Schneider and Marechal-Drouard, 2000). The availability of a large number of mitochondrial DNA sequences allowed predictions of the number of mitochondrial tRNA genes in the corresponding organisms (O'Brien et al., 2009). By comparing the codon usage of these mitochondrial DNA encoded tRNAs with the

Class	Species/taxon	Kingdom	Amino acids specified by mitochondrial encoded tRNA genes	Amino acids specified by imported tRNAs	Redundant tRNA import
I	*Homo sapiens*	Metazoa	20	0	$tRNA^{Gln}$
	Saccharomyces cerevisiae	Fungi	20	0	$tRNA^{Lys}$ $tRNA^{Gln}$
	Allomyces macrogymus	Fungi	20	0	n.d.
	Oscarella carmella	Porifera	20	0	n.d.
II	*Didelphis virginiana*	Metazoa	19 (1 $tRNA^{Lys}$ pseudogene)	1 ($tRNA^{Lys(CUU)}$)	n.d.
	Reclinomonas americana	Excavata	19	1 ($tRNA^{Thr}$)	n.d.
	Phytophthora infestans	Chromalveolata	19	1 ($tRNA^{Thr}$)	n.d.
	Chondrus crispus	Archeaplastida	19	1 ($tRNA^{Thr}$)	n.d.
III	*Hyaloraphidium curvatum*	Fungi	7	13	n.d.
	Tetrahymena thermophila	Chromalveolata	7	13	-
	Arabidopsis thaliana	Archeaplastida	14	6	-
	Chlamidomonas reinhardtii	Archeaplastida	3	17	-
	Dictyostelium discoideum	Amoebozoa	14	6	n.d.
IV	Cnidaria	Metazoa	1 or 2 ($tRNA^{Met}$ and/or $tRNA^{Trp}$)	19 or 18	n.d.
	Trypanosomatidae	Excavata	0	20	-
	Apicomplexa	Chromalveolata	0	20	-

Table 2 : Diversity of mitochondrial tRNA import in eukaryotes

According to the completeness of the mitochondrial set of tRNA genes, eukaryotes can be subdivided into four classes.

Organisms of class I and class II possess a complete or almost complete set of mitochondrial tRNA genes respectively.

Class III organisms lack a considerable part of their mitochondrial tRNA genes and organisms of class IV are devoid of all or nearly all their mitochondrial tRNA genes. (adopted from Schneider, 2011)

complete mitochondrial genetic code, it was possible to anticipate the tRNAs that have to be imported in order to guarantee the translation of mitochondrial proteins. Nevertheless, limitations of this bioinformatic approach are the impossibility to predict *in organello* RNA editing events and the variation in the codon recognition by Wobble base pairing. In some rare cases, organisms import tRNAs even if they possess a complete set sufficient to assure mitochondrial translation, as the yeast *Saccharomyces cerevisiae* for example, that would be ignored by such a bioinformatic analysis. But the fact that such organisms are still capable of importing tRNAs would mean that this process is a universal feature of mitochondria conserved in eukaryotes. Indeed, this alternative hypothesis is strengthened by the demonstration that organisms owning a complete mitochondrial tRNA set are still able to import tRNAs, like mammalian mitochondria for example, importing cytosolic $tRNA^{Gln}$ and even yeast tRNAs by a cryptic mechanism (Kolesnikova et al., 2000, 2002; Rubio et al., 2008).

2.3.3 General and structural Characteristics of tRNAs

tRNAs represent a key family of molecules fulfilling an essential adaptor function during the translation of the genetic information by delivering amino acids to the nascent polypeptide chains that are synthesized on the ribosomes. Thereby, tRNAs act as bridging molecules between the four-letter genetic code and the twenty-letter code of amino acids in proteins. tRNA genes are transcribed by the RNA polymerase III in the nucleus upon recognition of two internal promoter sequences (called box A and box B) with release of pre-tRNAs undergoing eventual splicing and maturation processes inside the nucleus to achieve their functional structure. Finally, tRNAs are exported into the cytoplasm by the Ran-GTP binding ß-importin family proteins Los1/Exportin-t (Rubio and Hopper, 2011). Generally, tRNA molecules are relatively short lengthened with sizes around ~75 nucleotides, presenting the canonical secondary cloverleaf structure with a subdivision into two groups, class I and class II tRNAs **(Fig.11A)**. The interaction of tRNAs with their cognate aminoacyl-tRNA-synthethases (aaRS) requires the adaptation of the 3D L-shaped structure **(Fig.11B)**. Conserved and semiconserved tRNA residues undergoing tertiary interactions enable the folding and maintenance of this structure. Mitochondrial tRNAs, however, often represent unusual but remarkable structural features, as the mammalian $tRNA^{Ser(GCU)}$ for example that is lacking the complete D-arm. Despite their odd structural features, mitochondrial tRNAs are

still capable of adapting their required 3D L-shape structure to fulfil their functions (Giegé et al., 2012).

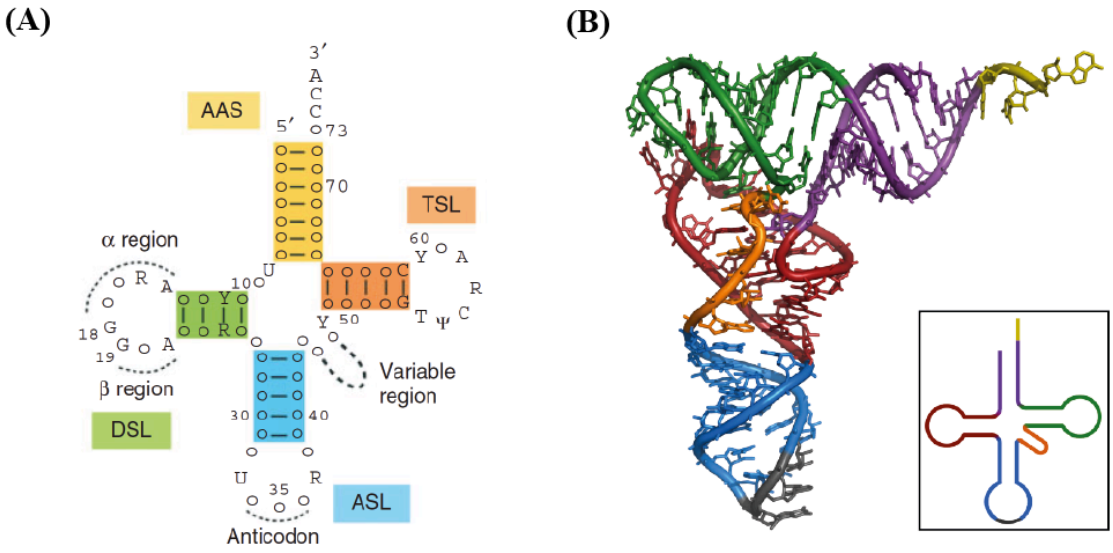

Fig.11 : tRNA structure. **(A)** Classical secondary cloverleaf structure of tRNA. From 5'→3' : AAS (Amino acid accepting stem) with 7 base pairs terminated at the 3'-end by $N_{73}CCA_{OH}$ (N_{73} being the discriminator base) and at the 5'-end by pN1 (with an additional N-1 in $tRNA^{His}$ isoacceptors); 2-nt connector (U_8, N_9) between AAS and DSL; DSL (D-stem loop) with a 4 base pair stem closed by a 7-11 nt D-loop (containing a variable content of dihydrouridines); ASL (Anticodon stem loop) with a 5 base pair stem and a 7 nt loop (containing U_{33}, R_{37} and the anticodon triplet N_{34}, N_{35}, N_{36}); variable region with 4 to 24 nt (4 or 5 nt in class I tRNAs and up to 24 nt arranged in a stem-loop in class II tRNAs); TSL (T-stem loop) with a 5 base pair stem and a 7 nt loop. nt = nucleotide, N = any nt (Giegé et *al*,. 2012). **(B)** Tertiary 3D L-shape structure of a *Saccharomyces cerevisiae* $tRNA^{Phe}$ (Shi and Moore, 2000). A network of tertiary interactions holds together the L-shape with a participation of 12 out of 23 conserved and semiconserved residues (Giegé et *al*,. 2012).

2.3.4 Mechanisms of mitochondrial RNA Import

All studied RNA import systems so far display significant discrepancies but share a common need being energy provided by ATP hydrolysis (Tarassov et al., 2007). The import mechanisms can be dissected into two distinct processes **(Fig.12)**; (i) the targeting of RNAs to the mitochondrial surface and (ii) their translocation across the double mitochondrial membrane. The first step requires a deviation from the cytoplasmic RNA pool, a procedure implicating cytosolic protein factors and specific import signals located on the imported RNAs, reflecting the specific nature of the RNA import process. Protein complexes carrying out the passage across the outer and inner mitochondrial membranes have only been poorly characterized yet. In the following sections I will outline the available information concerning this essential import pathway.

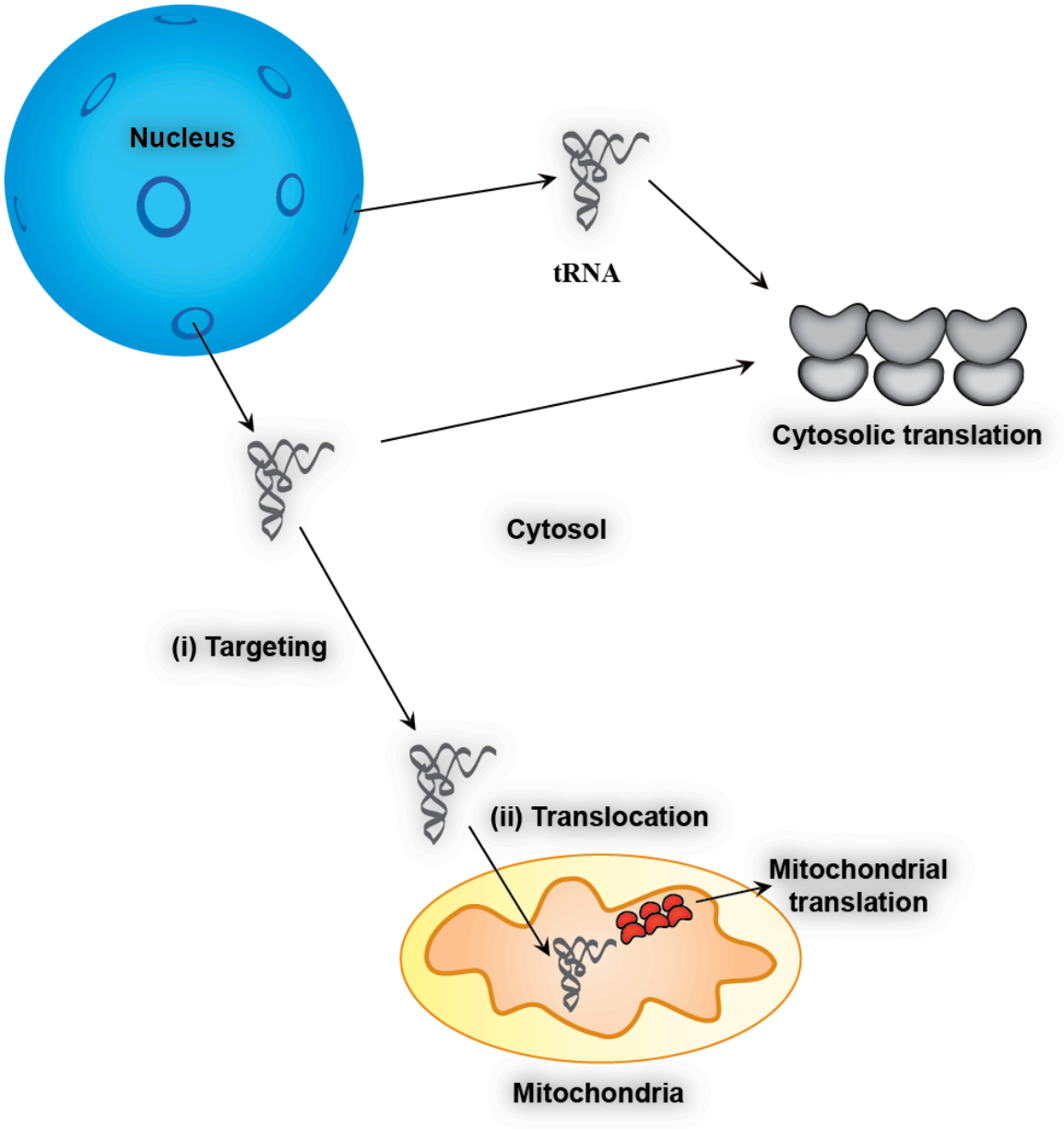

Fig.12 : Different steps of mitochondrial RNA import (here depicted for tRNA import). After transcription tRNAs are exported from the nucleus to the cytosol where they are involved in the process of cytosolic translation. (i) A small part is deviated from this process, targeted to the mitochondrial surface and (ii) translocated into mitochondria where imported tRNAs are used in mitochondrial translation.

2.3.4.1 RNA Import into mammalian Mitochondria

The mammalian mitochondrial genome encodes the two ribosomal RNAs, 12S rRNA and 16S rRNA, as well a complete set of 22 tRNAs sufficient for the translation of its genetic information (Florentz et al., 2003). For this reason mammalian mitochondria, mostly, do not import cytosolic tRNAs with the exception of a few marsupial animals, where import of a $tRNA^{Lys}$ was reported (Dörner et al., 2001). In addition, it was shown *in vivo* that the two isoacceptors $tRNA^{Glu(CUG)}$ and $tRNA^{Gln(UUG)}$ are located inside of mammalian mitochondria. *In vitro* import into isolated mitochondria also showed that the same two $tRNA^{Glu}$ are specifically imported in an ATP dependant manner but in absence of the electrochemical membrane potential $\Delta\Psi$ and cytosolic protein factors (Rubio et al., 2008).

Import of RNA components of ribonucleoprotein complexes into mammalian mitochondria was also suggested. A first candidate was the RNA part of the MRP RNase, a ribozyme possessing a dual localization to the nucleolus and the mitochondria. The central nucleotides 118-175 of MRP RNA promote its mitochondrial partitioning, where it is potentially involved in the initiation of the mitochondrial DNA replication by generation of primers (Li et al., 1994). The second candidate was the RNA part of the RNase P (H1 RNA), whose catalytic activity is involved in the maturation of precursor tRNA transcripts by processing their 5' leader sequence (Guerrier-Takada et al., 1983). It was shown that H1 RNA, derived from the nuclear form of RNase P, is associated to highly purified nuclease treated mitochondria and that it can be imported *in vitro* into isolated mammalian mitochondria (Puranam and Attardi, 2001; Wang et al., 2010). Other studies have, however, shown that the catalytic activity of mammalian RNase P is essentially carried out by a protein enzyme, suggesting that the ribozyme moiety was lost during the molecular evolution of this ribonucleoprotein (Holzmann et al., 2008; Gutmann et al., 2012). Regarding these observations one can hypothesize the presence of two distinct RNase P in mammalian mitochondria.

The 5S ribosomal RNA (5S rRNA) is an integral part of the large ribosomal subunit of almost all living organisms, with apparently essential functions in the translation process by linking different functional centers of the ribosome (Kiparisov et al., 2005). In addition to these features, 5S rRNA was also discovered in mammalian mitochondria (Magalhaes et al., 1998; Yoshionari et al., 1994). The mammalian mitochondrial DNA lost the 5S rRNA gene during evolution, thus the important abundance inside mitochondria can just be explained by its import. The import pathway adopted by 5S rRNA has been majorly described, where some

time ago it has already been shown that it depended on several conditions: (i) it needed ATP hydrolysis and the electrochemical membrane potential ΔΨ; (ii) it depended on protease-sensitive receptor proteins of the outer membrane; (iii) import required an intact and functional pre-protein import machinery and (iv) direction into mitochondria relied on soluble cytosolic proteins factors (Entelis et al., 2001).

5S rRNA has a size of ~120 nucleotides and is organized into a complex structure arranged in three major domains **(Fig.13A)**. The α-domain comprises helix I, whereas the domains ß and γ are formed by alternating helix loop structures. Directed mutagenesis analysis permitted to dissect the essential import determinants located in several structural domains of 5S rRNA **(Fig.13B)**. The ß-domain did not seem to have a crucial role in directing import of 5S rRNA because the domain itself could not be imported into mitochondria and replacement of two conserved nucleotides (A49, A50) in helix III, needed for binding of ribosomal proteins of the L18/eL5 family (Huber and Wool, 1984), did not cause significant changes in the 5S rRNA import efficiency. Even ablation of the whole helix III {Δ(28-51)} had no major effect on import. Because the isolated α and γ domains could be imported into mitochondria they were more closely investigated for potential import determinants. In the γ−domain it was shown that the breaking of helix V (A103G, C104G, C105G) and a destabilization of loop E (A100C) had no significant impact on the mitochondrial import. Interestingly, introduced mutations conferring a more closed and stable structure to the loop E and helix IV (A74G, U73A, A74U, A77C, U96A, G97A, G99U, A101U, U102A) generated 5S rRNA molecules displaying higher import efficiencies than the natural form, which is plausible because base exchanges or deletions causing profound disturbance in this structural elements (G97C, G98U, A101U, ΔU73, Δ78-98) lead to a significant decrease of 5S rRNA import. In the α-domain the loop A is an important element to preserve the natural 3D structure but deletion of two nucleotides (DC10, DU12) disturbing this structure only had a weak influence on 5S rRNA import. The disruption of helix I, however, (U111C+U112C, G7U, G8A, C9U) caused an import decease of ~50%. The combination of mutations touching at the same time these crucial structures of domains α+γ {U111C, U112C + Δ(78-98; G7U, G8A, C9U + Δ(78-98)} dramatically decreased 5S rRNA import indicating clearly that the two regions helix IV and helix I are responsible for the import of 5S rRNA, although one of them is sufficient to promote a mitochondrial localization to 5S rRNA (Smirnov et al., 2008).

5S rRNA import was shown to depend on soluble cytosolic protein factors. Based on import studies using combined cellular extracts, the hypothesis rose that there had to be at

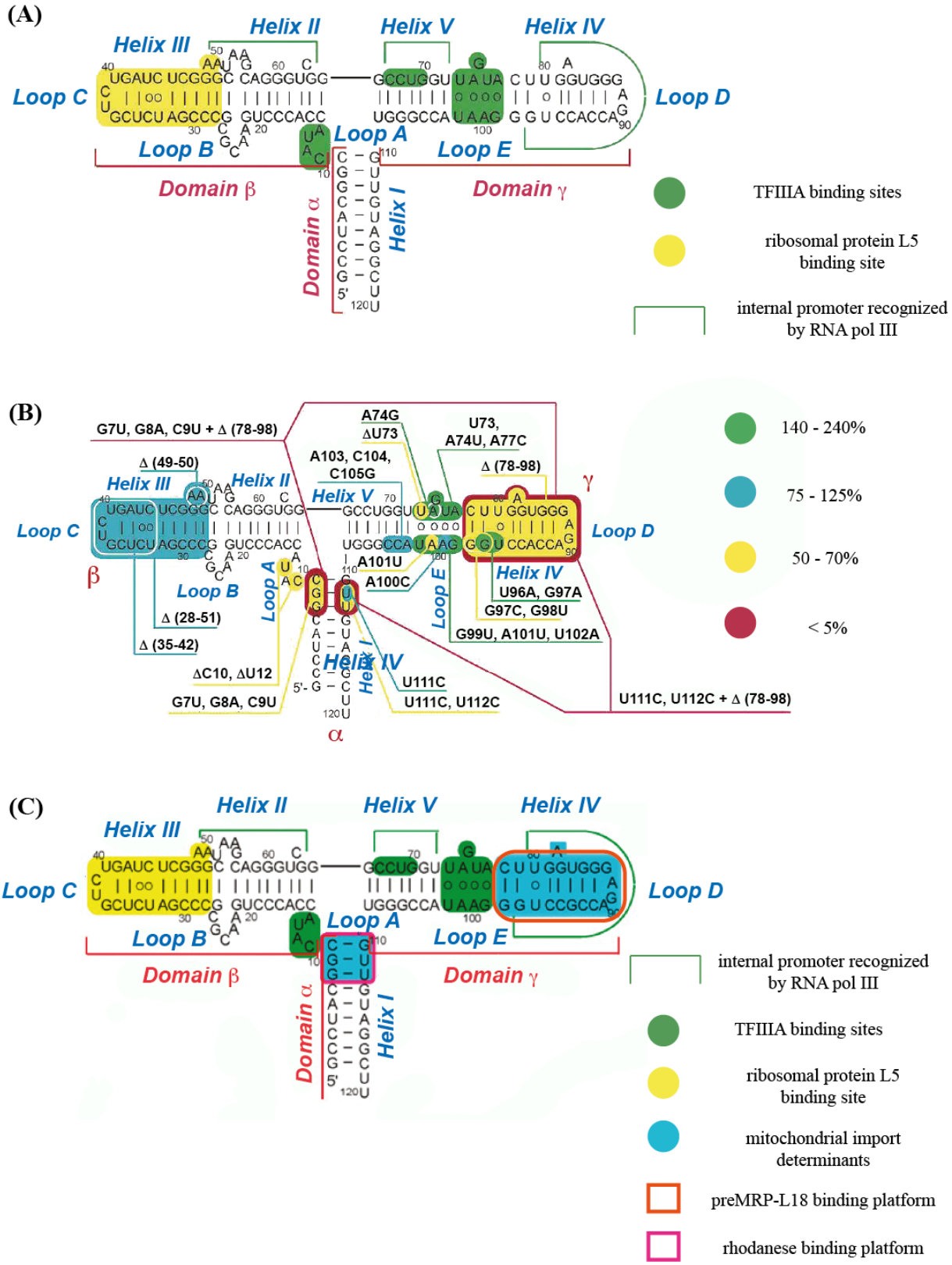

Fig.13 : 5S rRNA. (A) Secondary structure arrangement of human 5S rRNA. Binding sites for the transcription initiation factor III A (TFIII3A), for the ribosomal protein L5 and the promoter for RNA polymerase III are shown. **(B)** Mutation map of human 5S rRNA. Colors correspond to different import efficiencies *in vitro*. **(C)** Recapitulative map emphasizing binding platforms for the 5S rRNA import factors rhodanese and preMRP-L18, mitochondrial import determinants and structural elements mentionned in (A). (Smirnov et *al*., 2008, 2010, 2011).

least two different protein factors needed to import 5S rRNA into organelles. Indeed, screening for such proteins by North-Western analysis revealed the mitochondrial protein thiosulfate sulphurtransferase (rhodanese) that is involved in diverse processes such as cyanide detoxification, Fe/S cluster formation and in intracellular transport and regulatory pathways (Cipollone et al., 2007). *In vitro* import assays showed that recombinant rhodanese alone was not capable of directing 5S rRNA import but in combination with a cytosolic protein fraction, that itself had low import guiding capacities, import was restored as in presence of a complete cellular extract. The importance of rhodanese was emphasized by the fact that a pre-treatment of cytosolic protein extracts with rhodanese antibodies significantly decreased or completely abolished 5S rRNA import *in vitro*. *In vivo* knockdown of rhodanese by siRNA lead to an important drop of 5S rRNA import that was accompanied by an overall decrease of the mitochondrial translation activity. The interaction of the enzyme itself with the 5S rRNA was surprisingly more efficient when rhodanese was in a denatured state. This was in agreement with the finding that this enzyme bound in a co-translational manner to 5S rRNA that itself interacted with the nascent protein in a chaperone-like manner. Another interesting fact was that 5S rRNA had to be in a relaxed structure to bind efficiently to rhodanese. The structural elements of 5S rRNA binding to this enzyme are majorly located in the α-domain and to a lesser extent in the γ-domain **(Fig.13C)** as illustrated by affinity measurements with the help of gel-sift assays. These findings explained why these two domains are required for targeting 5S rRNA into mitochondria (Smirnov et al., 2010).

As mentioned before, 5S rRNA import depended, at least, on another cytosolic protein factor. With the help of North-Western analysis this second partner has been identified and turned out to be the precursor form of the mitochondrial ribosomal protein L18 (preMRP-L18), part of the large mitochondrial ribosomal subunit 16S. It was shown that this protein was able to interact with 5S rRNA *in vitro* and *in vivo*, and that this interaction was strictly dependent on the presence of helix IV and loop D, which are situated in the γ domain of 5S rRNA **(Fig.13C)** and already showed an essential character in directing its import. To validate that preMRP-L18 is an import factor, it was demonstrated that this protein, in combination with rhodanese, formed a minimal vehicle sufficient for *in vitro* import into isolated mitochondria. *In vivo*, a partial knockdown of preMRP-L18 by siRNA was in correlation with a decrease of 5S rRNA import and an overall inhibition of the mitochondrial translation, as observed already in the case of rhodanese knockdown. These results clearly illustrate that preMRP-L18 is needed to address 5S rRNA into mitochondria. Furthermore, preMRP-L18 turned out to be the necessary partner to confer to 5S rRNA its relaxed structure necessary for

the interaction with rhodanese. This sequence of chaperone events is very important in the mechanism of intracellular 5S rRNA traffic **(Fig.14)**. After export from the nucleus, 5S rRNA is bound by the ribosomal protein L5 and reimported into the nucleus to be integrated into the ribosome or it is captured by preMRP-L18, guiding 5S rRNA to the mitochondrial surface and conferring the structural rearrangement necessary for the interaction with rhodanese that is presumed to be the carrier of 5S rRNA during its mitochondrial import (Smirnov et al., 2011).

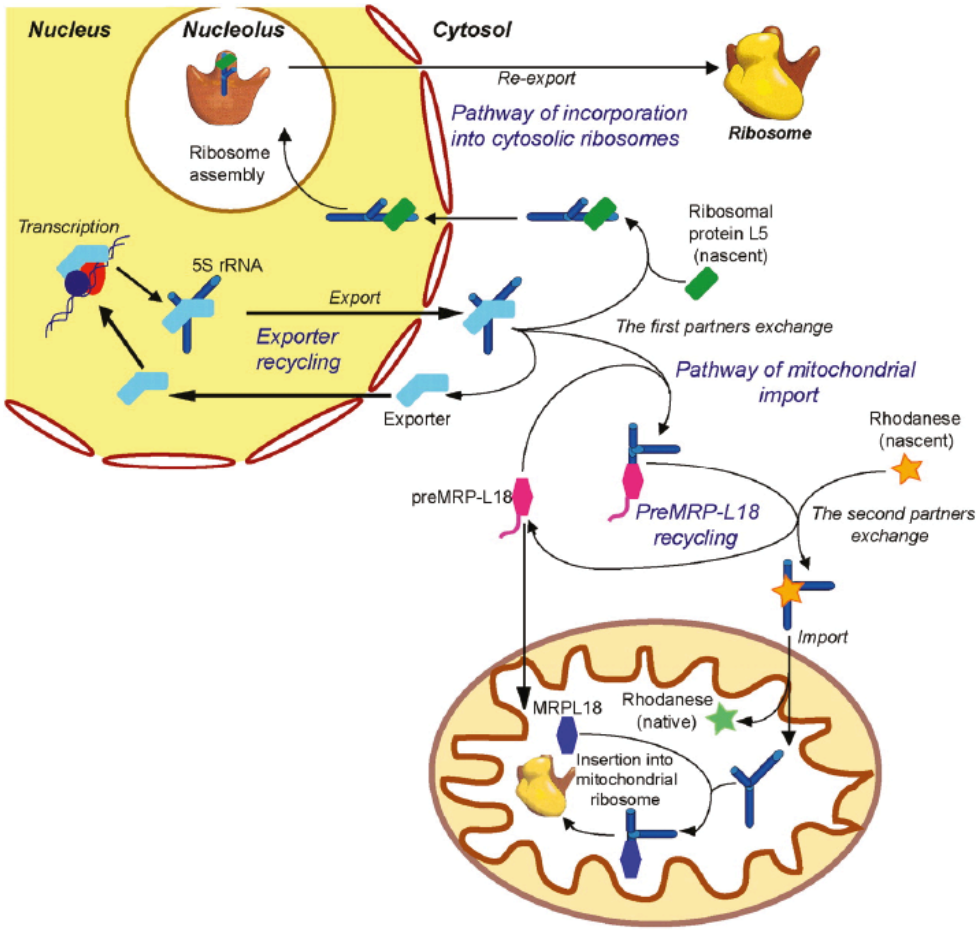

Fig.14 : Intracellular traffic of 5S rRNA. (Smirnov et *al*., 2011).

Concerning the translocation mechanism of 5S rRNA across the mitochondrial double membrane, some data is available describing the passage across the outer as well as the inner membranes. As already mentioned, 5S rRNA import was dependent on energy provided by ATP hydrolysis, on the electrochemical membrane potential $\Delta\Psi$ and on receptor proteins at the mitochondrial outer membrane. It has also been shown that the preprotein import machinery is involved in the mitochondrial transport of 5S rRNA: a chimeric non-unfoldable protein, composed of the mitochondrial targeted N-terminal part of rat ornithine

transcarbomylase (OTC) fused to the bovine pancreas trypsin inhibitor (BPTI), was able to block preprotein import as well as translocation of 5S rRNA into mammalian mitochondria (Entelis et al., 2001). Because this experimental approach permitted to block both Tom40 and Tim23 channels involved in preprotein import it was likely that the arrest of 5S rRNA import already occurred at the mitochondrial outer membrane, and it was not clear if 5S rRNA import continued through the Tim23 channel. Indeed, recent studies identified a new component potentially promoting RNA passage across the mitochondrial inner membrane, the polynucleotide phosphorylase (PNPASE), a 3'→ 5' exoribonuclease and polyA polymerase anchored in the mitochondrial inner membrane with an intermembrane space orientation (Chen et al., 2006). Ectopic expression of PNPASE in *Saccharomyces cerevisiae* demonstrated that, *in vitro* and *in vivo*, import of heterologous RNase P and MRP RNAs was increased compared to wild type cells and that expressed PNPASE even permitted import of 5S rRNA that is normally not present in yeast mitochondria. To put these results in a more physiologic context, *in vivo* import of 5S rRNA and the RNaseP and MRP RNAs was analysed in mammalian cells overexpressing PNPASE or being downregulated for PNPASE. Results confirmed that in both conditions import of different RNA species was augmented or decreased respectively (Wang et al., 2010).

2.3.4.2 Mitochondrial tRNA Import in Protozoa

Protozoa are a group of unicellular eukaryotic microorganisms building a very interesting model group to study tRNA import into mitochondria. In fact, during mitochondrial evolution protozoa lost a considerable part or even all their mitochondrial tRNA genes and by consequence corresponding tRNAs have to be imported from the cytosol (Schneider, 2011). Well studied members of this group are *Tetrahymena* (Rusconi and Cech, 1996a), apicomplexa (Esseiva et al., 2004) and trypanosomatids, where latter represent the most extreme case by importing all their cytosolic tRNAs required for mitochondrial translation (Hancock and Hajduk, 1990b).

These imported tRNAs have the interesting feature that they are functioning both in the cytosol and inside mitochondria, implying a distribution of functional aaRS in both compartments. Whereas eukaryotes, possessing a complete set of mitochondrial tRNAs, generally have two sets of compartment-specific aaRS, mitochondrial and cytosolic aaRS, (Duchêne et al., 2009), most part of imported tRNAs are aminoacylated by dually targeted aaRS in trypanosomes. So far, the dependence of the bacterial-like mitochondrial translation

system on its cytosolic counterparts required some unique evolutionary adaptations from the part of trypanosomes. *Trypanosoma brucei* for example, only has one single $tRNA^{Trp}$ that, inside mitochondria, needs to decipher the reassigned UGA codon (stop codon in cytosolic translation). This is achieved by a mitochondria-specific RNA editing event that converts the CCA anticodon of the imported $tRNA^{Trp}$ to a UCA anticodon (Alfonzo et al., 1999). The CCA anticodon, however, is a crucial identity element of the TrpRS and therefore the edited form of $tRNA^{Trp}$ cannot be charged inside mitochondria. For this reason trypanosomes evolved a mitochondria specific eukaryotic-type like TrpRS able to decode both, the cytoplasmic and the edited $tRNA^{Trp}$ anticodons (Charrière et al., 2006). In addition to this specific TrpRS, trypanosomal mitochondria also contain two other organelle specific aaRS, the AspRS and the LysRS, where latter one needs to be activated after import by cleavage of a C-terminal extension to be able to aminoacylate the $tRNA^{Lys}$ (Español et al., 2009).

Within the complete set of tRNAs in trypanosomes there are only two strictly cytoplasmic tRNAs, the initiator $tRNA^{Met}$ and the $tRNA^{Sec}$ (Tan et al., 2002b; Geslain et al., 2006). This can be explained by the facts that the mitochondrial DNA does not encode for selenoproteins and that the mitochondrial translation initiation is of a bacterial type using a different initiator $tRNA^{Met}$ carrying a formylated methionine. Latter situation therefore raises a fundamental problem because the imported cytosolic elongator $tRNA^{Met}$ cannot participate in translation initiation inside mitochondria. For this reason methionine bound to this tRNA becomes formylated by an unusual $tRNA^{Met}$-formyltransferase having a specificity for elongator tRNAs (Tan et al., 2002a).

The mitochondrial import of cytosolic tRNAs in protozoa requires the presence of specific targeting signals located within different structural elements interacting with cytosolic targeting factors. The species *Tetrahymena pyriformis* possesses three $tRNA^{Gln}$ isoacceptors, bearing UUA, CUA and UUG as anticodons. It was shown that only one of these tRNAs is imported, the $tRNA^{Glu(UUG)}$, where by directed mutagenesis it has been demonstrated that alteration of the anticodon sequence abolishes import and that the substitution of a single nucleotide in the anticodon (UU**A** → UU**G**) confers a mitochondrial localization to normally non-imported $tRNA^{Glu}$, thus illustrating that the anticodon functions as a mitochondrial import determinant in this tRNA (Rusconi and Cech, 1996a, 1996b). In the species *Leishmania tarentolae* systematic deletion studies, reconstruction and sequence analyses have shown that conserved motifs in the D-arm and the T-arm of imported tRNAs are necessary and sufficient to promote their mitochondrial import and that rather a structural arrangement is important in this context than the consensus sequence itself (Mahapatra et al.,

1998; Suyama et al., 1998; Bhattacharyya et al., 2002). Furthermore, it was also proposed that the cytosol specific post-transcriptional thiolations of the wobble position in the $tRNA^{Glu(UUC)}$ and $tRNA^{Glu(UUG)}$ act as specific import anti-determinants arresting these tRNA populations in the cytosol (Kaneko et al., 2003). In *Trypanosoma brucei* a *cis*-acting RNA motif {YGG(C/A)RRC} in the precursor of $tRNA^{Leu}$ was reported to be important for mitochondrial import but most import determinants were characterized on mature imported tRNAs (Sherrer et al., 2003; Tan et al., 2002b). The specificity of tRNA import in this organism relies on import determinants located in the T-arm of all imported tRNAs, the base pair 51-63. The non-imported initiator $tRNA^{Met}$ has the import anti-determinant base pair U51-A63 contributing to its strict cytosolic localization, whereas all other imported tRNAs carry a different base pair at this position. Interestingly, the U51-A63 base pair is also the main anti-determinant preventing binding of the translation elongation factor eEF1 to the initiator $tRNA^{Met}$. Introduction of this anti-determinant motif in imported tRNAs abolished their import, whereas *vice versa* replacement of the U51-A63 anti-determinant by another base pair in the normally non-imported tRNA confers mitochondrial import to latter one. The fact that the interaction of tRNAs with the elongation factor eEF1 is essential for their mitochondrial import defined eEF1 as the only identified cytosolic targeting factor in protozoa up to now (Bouzaidi-Tiali et al., 2007).

The translocation of tRNAs across the two mitochondrial membranes in protozoa was only studied in trypanosomes and a complete image of this process is not available yet. There is a consensus that tRNA import requires energy provided by ATP hydrolysis and eventually the electrochemical membrane potential $\Delta\Psi$ (Yermovsky-Kammerer and Hajduk, 1999; Rubio et al., 2000; Bouzaidi-Tiali et al., 2007). Concerning the translocation step itself there are some models that have been proposed. A first, and most debated one, has been described in the species *Leishmania tropica*. A protein, similar or identical to the tubulin antisense-binding protein (TAB), has been identified at the mitochondrial outer membrane but no receptor function of TAB neither a translocation activity across the outer membrane in the tRNA import process could be clarified (Mahapatra and Adhya, 1996; Adhya et al., 1997). The same research group proposed another protein complex of the mitochondrial inner membrane implicated in the translocation of tRNAs into the matrix, the 600 kDa multi-subunit RNA-import complex (RIC) (Chatterjee et al., 2006; Goswami et al., 2006; Adhya, 2008). This RIC complex contains three mitochondrial encoded and eight nuclear encoded subunits from which six were proposed to be important and sufficient to form a tRNA importing complex (Mukherjee et al., 2007). The two inner membrane receptor proteins RIC1

and RIC8A bind two potential types of RNAs, type I and type II RNAs respectively, characterized by distinct import motifs. These interactions show an allosteric behaviour potentially permitting regulation of tRNA import (Bhattacharyya et al., 2002, 2003). However, all of the work provided by this group is regarded with great scepticism because RIC could only be identified in *Leishmania tropica*. Moreover, some of the provided results also gave rise to an editorial concern (Schekman, 2010). In the species *Trypanosoma brucei* the single VDAC protein was shown not to be implicated in the translocation of tRNAs across the mitochondrial outer membrane (Pusnik et al., 2009). But a more recent *in vivo* study provided evidence that in *T.brucei* there is a connection between tRNA import and preprotein import mechanisms, sharing some common protein partners (Tschopp et al., 2011). From the preprotein import machinery only a few members have been identified yet; Sam50, the core subunit of the SAM complex, Tim17, a member of the Tim17/Tim22/Tim23 protein family and the highly conserved mitochondrial heat shock protein Hsp70 (Sharma et al., 2010; Singha et al., 2008). Whereas knockdown of Sam50 did not have any effect on tRNA import, the ablation of Tim17 and mtHsp70 impaired import of tRNAs into mitochondria. The recently identified archaic translocase of the outer mitochondrial membrane (ATOM) was shown to be the general entry gate for mitochondrial preproteins but its function in tRNA import has not been investigated yet (Pusnik et al., 2011).

2.3.4.3 Mitochondrial tRNA Import in Plants

Mitochondrial function and biogenesis in plants requires import of tRNAs from the cytoplasm into mitochondria. Although all studied plant systems so far were shown to import tRNAs, both the number and the identity of these tRNAs differ significantly, even between closely related species, illustrating the specificity of this import mechanism in different plant species (Kumar et al., 1996).

Usually, a tRNA encoded by the mitochondrial DNA and its cytosolic counterpart do not coexist inside plant mitochondria (Salinas et al., 2008). The specificity determining tRNA import into plant mitochondria was expected to occur by their ability to interact with their cognate aaRS. A first example is the $tRNA^{Ala(UGC)}$ from *Arabidopsis thaliana*, where the mutation of the AlaRS identity element U70C in the aminoacceptor stem abolished its aminoacylation and *in vivo* import into mitochondria of tobacco plants transformed with the $tRNA^{Ala}$ gene carrying the U70C mutation (Dietrich et al., 1996). But the heterologous co-expression of AlaRS and $tRNA^{Ala}$ in the yeast *Saccharomyces cerevisiae* was not sufficient to

direct the plant $tRNA^{Ala}$ inside yeast mitochondria, indicating that plants contain, at least, one additional cytosolic protein factor that directs import of $tRNA^{Ala}$ into their mitochondria (Mireau et al., 2000). The existence of other import determinants then aminoacylation identity elements was strengthened by another *in vivo* study using the $tRNA^{Val}$ from *Arabidopsis thaliana*. Expressed mutant $tRNA^{Val}$ forms with an altered aminoacylation identity (anticodon switch from AAC → CAU) were not aminoacylated *in vitro* and their *in vivo* import into mitochondria of transformed tobacco plants was suppressed. But the replacement of the D- and T-domains of $tRNA^{Val}$ with the corresponding domains of the non-imported elongator $tRNA^{Met}$ also lead to an absence of import, whereas the *in vitro* aminoacylation of these mutants was comparable to the native $tRNA^{Val}$ form (Delage et al., 2003b; Laforest et al., 2005). Another example that aminoacylation is not the only factor influencing tRNA import in plants was illustrated by *in vivo* import of $tRNA^{Gly}$ into mitochondria of transgenic tobacco plants. Three cytosolic $tRNA^{Gly}$ isoacceptors were identified in plant (Brubacher-Kauffmann et al., 1999), where in tobacco only the $tRNA^{Gly(UCC)}$ is imported and the $tRNA^{Gly(GCC)}$ is not. Sequence exchanges were performed between these two molecules and it was shown that the change of the anticodon (UCC → GCC) and the replacement of the D-domain from $tRNA^{Gly(GCC)}$ into the $tRNA^{Gly(UCC)}$ backbone had no or only poor effects on aminoacylation but abolished mitochondrial import of these mutant tRNAs (Salinas et al., 2005). Regarding the results obtained from these independent studies it became clear that it is not only the potential to be aminoacylated that confers mitochondrial import to tRNAs in plants. Furthermore, aminoacylation is known to be a prerequisite for nuclear export of tRNAs, so the absence of mitochondrial import in transgenic plants could be explained by a nuclear retention of non-aminoacylated tRNAs (Lund and Dahlberg, 1998). Thus, the challenge remains to identify the cytosolic protein factors targeting the imported tRNAs to the mitochondrial surface. The reason why certain tRNAs are preferentially imported into mitochondria was proposed in a study using the green algae *Chlamidomonas reinhardtii*. The amounts as well as the identity of an imported tRNA were shown to be correlated with the codon frequency and codon usage inside mitochondria (Vinogradova et al., 2009). This import regulation needs of course a feedback control from mitochondria to the cytosol, a signalling pathway that has not been investigated yet.

The translocation of tRNAs across the mitochondrial membranes has been studied in the potato *Solanum tuberosum*. *In vitro* import assays using a synthetic $tRNA^{Ala}$ transcript showed that the translocation process did not need any added cytosolic protein factors but that it was dependent on a functional respiratory chain, on energy provided by ATP hydrolysis and

on the electrochemical membrane potential ΔΨ. In addition, the import of $tRNA^{Ala}$ required receptor proteins located on the mitochondrial outer membrane that could bind the imported $tRNA^{Ala}$ in a quantity dependent manner. The use of the non-imported $tRNA^{Phe}$ and elongator $tRNA^{Met}$ as competitor molecules revealed, nevertheless, that the interaction of the imported $tRNA^{Ala}$ with receptor proteins was not specific. Such specificity might be induced *in vivo* by a proper protein-targeting factor delivering the tRNA-protein complex to its receptor. Import into the mitochondrial matrix was, however, much less compromised by the competitor RNAs leading to the suggestion that the mitochondrial membranes might act as specific barriers to exclude non-imported tRNAs (Delage et al., 2003a). Potential membrane proteins directly implicated in the translocation of tRNAs across the mitochondrial membranes were detected in a later study by using the North-Western approach. Results of this screening showed that the imported $tRNA^{Ala}$ was able to interact, *in vitro*, with the Voltage Dependent Anion Channel (VDAC) protein, as confirmed by affinity binding to membrane blotted VDAC and gel shift assays. In order to further investigate the involvement of VDAC in the passage of $tRNA^{Ala}$ across the outer mitochondrial membrane, *in vitro* import was performed in presence of VDAC antibodies and the drug ruthenium red, able to induce VDAC closure (Gincel et al., 2001). Indeed, both compounds blocked efficiently the import of $tRNA^{Ala}$ into mitochondria. To test the putative receptor function of the outer membrane proteins Tom20 and Tom40, *in vitro* import was assessed after mitochondria were pre-incubated with antibodies against these two proteins. Binding at the mitochondrial surface as well as import were efficiently blocked by the Tom20 and Tom40 antibodies. To investigate through which channel $tRNA^{Ala}$ is translocated competition experiments were performed using increasing amounts of a matrix-targeted protein together with the imported tRNA. In this way, it could be shown that tRNAs and preprotein cross the outer mitochondrial membrane using different import pathways because the tRNA import was not blocked by increasing amounts of added preproteins and *vice versa*. So there is strong evidence that $tRNA^{Ala}$ is imported into potato mitochondria *via* a VDAC dependent import pathway implicating proteins of the TOM complex as potential receptors (Salinas et al., 2006). But the passage of imported tRNAs across the mitochondrial inner membrane still remains to be solved.

2.3.4.4 Mitochondrial tRNA Import in Fungi

Analyses of mitochondrial genomes have shown that almost all species from the kingdom of fungi possess a complete set of tRNAs sufficient to guarantee the mitochondrial translation process. Two exceptions are the species *Spizellomyces punctatus* and *Harpochytrium sp*. that are partially devoid of mitochondrial tRNA genes and therefore require import of eight tRNAs from the cytosol (Schneider and Marechal-Drouard, 2000). In addition, it was also hypothesized that the yeast *Saccharomyces cerevisiae* imports two nuclear encoded $tRNA^{Gln}$, $tRNA^{Gln(CUG)}$ and $tRNA^{Gln(UUG)}$, together with the corresponding GlnRS to promote direct formation of the Gln-$tRNA^{Gln}$ in the organelle (Rinehart et al., 2005). These results were refuted by another study demonstrating that, indeed, no cytosolic $tRNA^{Gln}$ are imported into mitochondria of the yeast *Saccharomyces cerevisiae* and that Gln-$tRNA^{Gln}$ is formed inside mitochondria by the classical transamidation pathway involving the mitochondrial encoded $tRNA^{Gln}$, the cytosolic GluRS and the mitochondrial amidotransferase GatFAB (Frechin et al., 2009).

Another interesting finding has revealed the unexpected import of a small fraction of one single $tRNA^{Lys}$ isoacceptor into mitochondria of the yeast *Saccharomyces cerevisiae* (Martin et al., 1979). Yeast possesses three $tRNA^{Lys}$ isoacceptors; two cytosolic ones, the $tRNA^{Lys(UUU)}$ (tRK2) and the $tRNA^{Lys(CUU)}$ (tRK1), the latter being partially addressed to mitochondria. The third isoacceptor is the mitochondrial encoded $tRNA^{Lys(UUU)}$ (tRK3) **(Fig.15)**. Since the yeast mitochondrial genome encodes a full set of tRNAs, the reason as well as the function of the imported tRK1 were not clear. Evidence has, however, been provided implying the import of tRK1 from the cytosol in answer to an adaptation mechanism of the mitochondrial translation. Yeast cells where tRK1 import was blocked showed a strong growth defect at elevated temperatures (37°C). With the help of primer extension assays and special gel systems, it could be proved that the mitochondrial tRK3 became partially hypomodified at its anticodon wobble position U34, usually bearing the post-transcriptional modified 5-carboxymethylaminomethyl-2-thiouridine **(Fig.15)**. This modification normally confers to tRK3 the ability to read both mitochondrial AAA and AAG lysine codons (Martin et al., 1990), so the hypothesis was formulated that at elevated temperatures the rare AAG codon cannot be read anymore. This was in fact proved in a mitochondrial pulse-chase translation assay, where a specific decrease of the proteins Cox2 and Var1 has been observed, two proteins known to contain AAG codons in their ORFs (Foury et al., 1998). In experimental conditions permitting tRK1 import, the AAG codon could be read and the

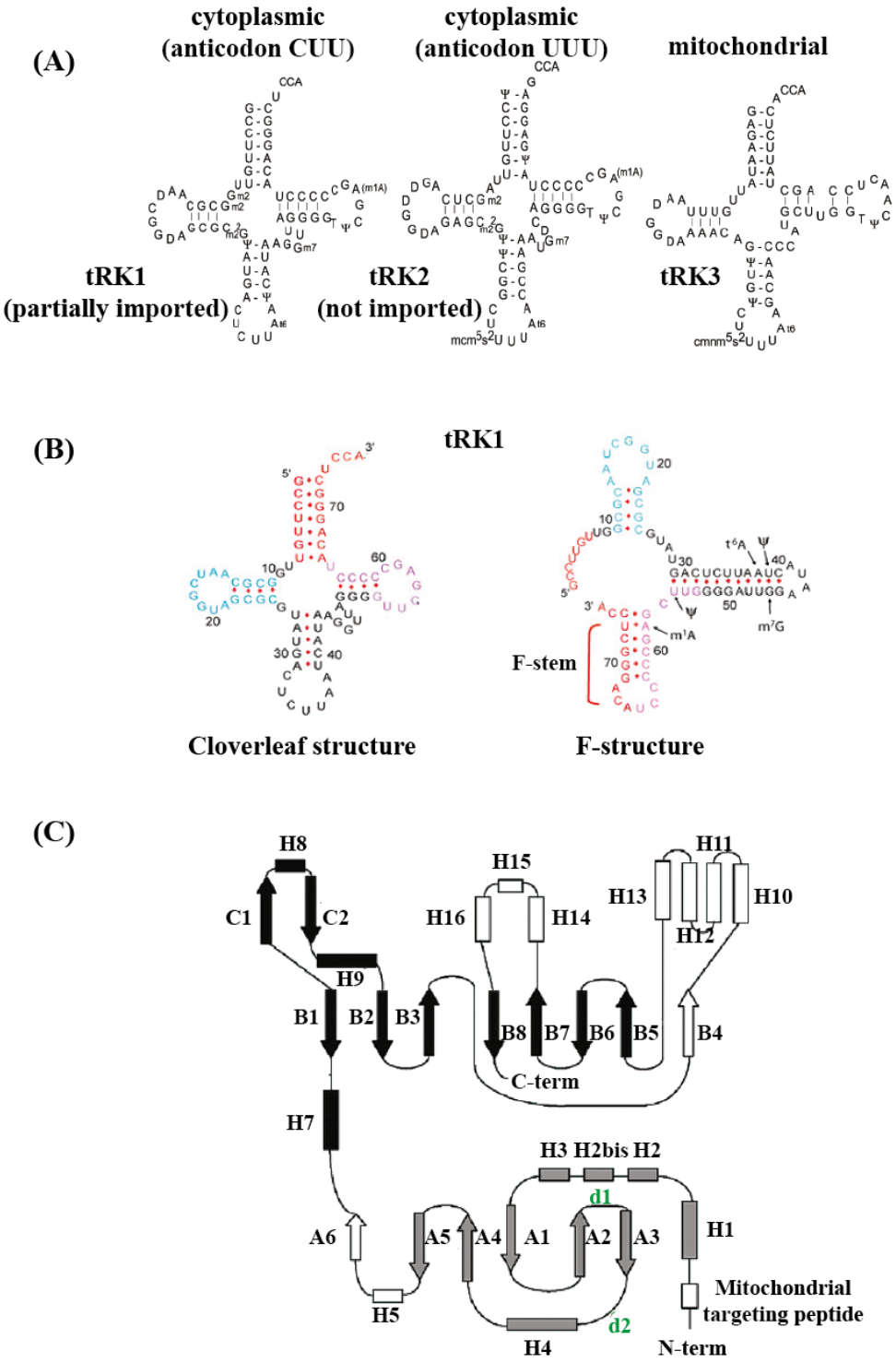

Fig.15 : Structures of tRK1 and preMSK. (A) Cloverleaf structures of cytoplasmic and mitochondrial *Saccharomyces cerevisiae* $tRNA^{Lys}$ (Kamenski et *al*,. 2007). **(B)** tRK1 cloverleaf structure and alternative F-structure upon interaction with enolase-2 (Kolesnikova et *al*,. 2010). **(C)** *In silico* spatial organization of *Saccharomyces cerevisiae* precursor form of mitochondrial lysyl-tRNA-synthetase (preMSK). Structural elements are annoteted according to the *E.coli* enzyme (Onesti et *al*,. 1995,2000). Active site elements of the C-terminal domain are in black, the N-terminal anticodon binding domain with oligonucleotide binding (OB) fold is in gray, the hinge region and "insertion sequences" are in white. H : helixes, B : ß element. (Kamenski et *al*,. 2007)

translation pattern as well as the quantitative abundance of Cox2 and Var1 has been restored **(Fig.16)**. These experiments illustrated for a first time the reason why a tRNA needs to be imported into mitochondria of an organism encoding a full set of tRNAs and demonstrated that this imported tRNA is requested to participate in the mitochondrial translation during stress conditions (Kamenski et al., 2007).

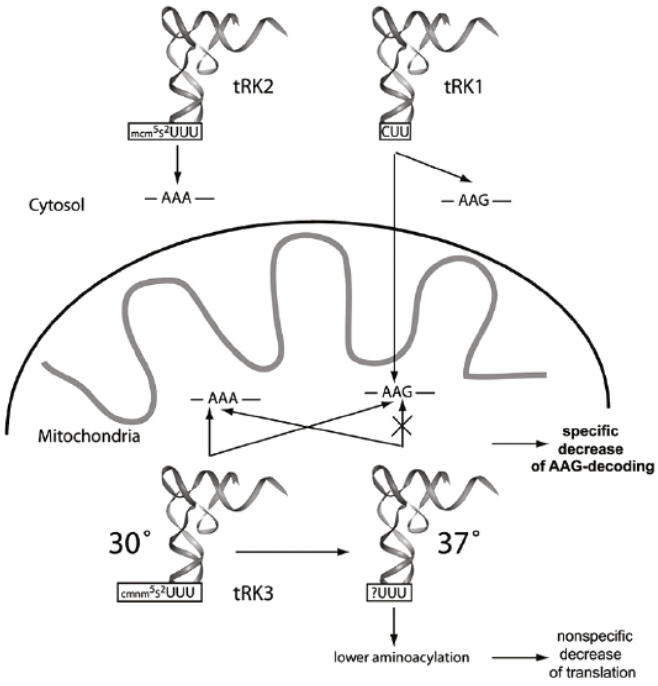

Fig.16 : Implication of tRK1 in mitochondrial translation. tRK1, decoding AAG, and tRK2, decoding AAA lysine codons, are required for cytosolic translation. Mitochondrial encoded tRK3 can decode both AAA and AAG codons at 30°C. At 37°C, the cmnm5s2U34 Wobble base becomes hypomodified, which renders AAG decoding more inefficient but without affecting AAA decoding. In this temperature stress conditions the imported tRK1 can complement for this defect (Kamenski et *al*., 2007).

The targeting mechanism guiding tRK1 from the cytoplasm to the mitochondrial surface is well characterized and consists in series of sequential interactions with essential proteinaceous import factors **(Fig.17)**. An overall prerequisite for mitochondrial tRK1 import is its aminoacylation by the cognate cytosolic LysRS (Tarassov et al., 1995a). Normally tRK1 is implicated in the cytosolic translation and its mitochondrial targeting requires a deviation from the cytoplasmic tRNA pool. The addressing factor accomplishing this job is the protein enolase-2 that usually catalyses the penultimate step of the glycolysis pathway. Deletion of the two yeast enolase isoforms, enolase-1 and enolase-2, lead to an almost complete arrest of tRK1 import *in vivo*, whereas expression of enolase-2 in the double deletion strain was able to complement this effect. Enolase-1 was, however, also able to partially restore tRK1 import. Introduction of a mutation in the catalytic site of enolase demonstrated that the catalytic activity of enolase was dispensable for its targeting activity. Another argument favouring the proposed role for this protein is its ability to bind tRK1 *in vitro* and to induce a

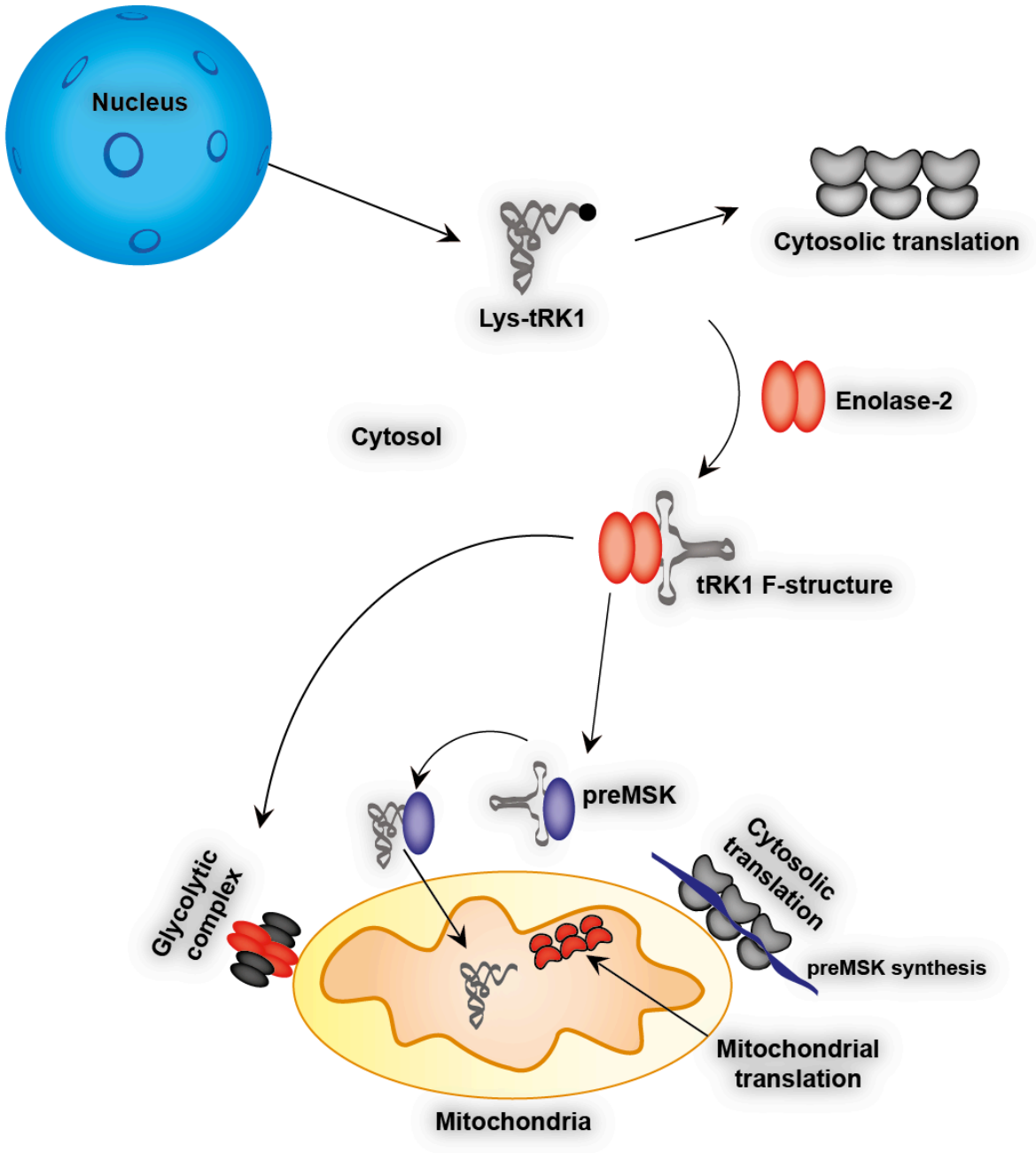

Fig.17 : Targeting of tRK1 to the mitochondrial surface in the yeast *Saccharomyces cerevisiae*. tRK1 is exported from the nucleus into the cytosol where it gets aminoacylated (Lys-tRK1) and used in the cytosolic translation process. A small part of tRK1 is deviated from the cytosolic tRNA pool by the glycolytic enzyme enolase-2 that has two functions : (i) it addresses tRK1 to the mitochondrial surface, where enolase-2 itself is integrated into the glycolytic complex and (ii) it acts as a chaperone folding tRK1 into an F-like structure that facilitates interaction with the second import factor, the precursor form of the mitochondrial lysyl-tRNA-synthetase (preMSK), synthesized on the periphery of mitochondria. Interaction with preMSK confers to tRK1 an L-shape like structure suitable for the use in the mitochondrial translation process (Entelis et *al*,. 2006; Kolesnikova et *al*,. 2010).

conformational change in tRK1 that enhances the interaction with the last import factor, the precursor form of the mitochondrial lysyl-tRNA-synthetase (preMSK) that has been shown to be indispensable for tRK1 import *in vitro* and *in vivo* (Entelis et al., 2006; Tarassov et al., 1995a).

The correct recognition between the imported tRK1 and the import directing protein factors requires import determinants on both partner molecules. The mitochondrial lysyl-tRNA-synthetase (MSK) is a class IIb aaRS composed of the catalytic C-terminal domain and the anticodon binding N-terminal domain that are linked by a flexible hinge region **(Fig.15)**. In order to study the essential domains of this protein involved in tRK1 import, a set of mutagenized preMSK versions bearing strategic deletions was created and tested for the ability to bind tRK1 and to promote its mitochondrial import. This kind of study permitted to discriminate that the N-terminal domain of preMSK alone is necessary and sufficient to direct import of tRK1 (Kamenski et al., 2007). More precisely, the region limited by the two α-helixes H5 and H7, comprising the end of the N-terminal part and the beginning of the hinge region, was shown to be the crucial domain involved in tRK1 import (Kamenski et al., 2010). Directed mutagenesis has also been the tool to identify the import determinant nucleotides in tRK1 by analysing the binding properties of the mutated transcripts to preMSK and by characterizing mitochondrial import of these transcripts. The anticodon region was shown to contain import determinants specifying its import selectivity because replacement of the anticodon arm of tRK1 by the one of tRK2 abolished completely mitochondrial import *in vivo* and *in vitro*. The most important position within this region seemed to be the wobble base C34 because introduction of this nucleotide into tRK2 conferred import to this normally strictly cytosolic tRNA. The import efficiency, however, was not very important, indicating that the nucleotide C34 is not only essential by itself but also in its context. This observation was strengthened by the fact that tRK1, bearing U34, was still efficiently imported into mitochondria (Entelis et al., 1998). The anticodon nucleotide U35 has been identified as main identity element for the cytosolic LysRS and mutation of this site strongly impaired the aminoacylation of tRK1 known to be a prerequisite for addressing tRK1 into mitochondria. Despite this fact, import of tRK1 was not or only slightly compromised by the single mutation of this nucleotide. Another interesting fact was that certain mutant transcripts could even be imported in a deacylated or misacylated state (Kolesnikova et al., 2002). In addition to the anticodon region, the aminoacceptor stem was also characterized as a region containing essential import determinants. The nucleotides C67, A68 and G69 of tRK1 were shown to be crucial because the replacement with their tRK2 counterparts lowered binding of preMSK and

blocked import of tRK1 (Entelis et al., 1998). The first base pair G1-C72 was also identified as an essential element of import selectivity *in vitro* and *in vivo*, which was illustrated by a mitochondrial import of a tRK2 mutant version containing this base pair. The mutation of the discriminator base U73 of tRK1 only resulted in a decreased import efficiency, but introduction of U73 lead to an import increase of tRK2 based transcripts, designating this nucleotide U73 as specific import determinant (Kazakova et al., 1999). Resuming the studies performed in order to identify tRK1 nucleotides as import determinants, it was clearly demonstrated that the residues C34, U73 and the first base pair C1-C72 act as elements specifying tRK1 import into mitochondria, whereas the nucleotides C67, A68, and G69, rather display a crucial character by acting as a preMSK binding platform.

What is the reason that makes these identified nucleotides so indispensable for the import of tRK1 into mitochondria? When enolase-2 has been discovered as a first protein factor in the sequential interaction cascade responsible for guiding tRK1 to the mitochondrial surface, a chaperone activity has been assumed for this protein in order to facilitate the further interaction of tRK1 with preMSK. Recently, it has been shown with the help of the in-gel FRET approach that, upon interaction of tRK1 with enolase-2, tRK1 adopted an alternative so-called F-structure, where the T-stem and the 3'-end of tRK1 are brought together to form the F-stem **(Fig.15)** (Kolesnikova et al., 2010). So it is very likely that the stabilisation of this alternative F-structure at the 3'-end is a crucial factor defining the specificity of tRK1 import into mitochondria by facilitating the interaction of tRK1 with preMSK. The above-mentioned import determinants are involved in the stabilisation of this alternative F-structure. This hypothesis is encouraged by *in silico* analysis of predicted secondary structures, demonstrating that the strictly cytosolic tRK2 is not able to form a stable F-stem in contrast to a mutant possessing nucleotides at positions 72 and 73 of tRK2 stabilizing the F-structure, thus increasing the import of these mutant versions. This may also explain why the first base pair G1-C72 of tRK1 is an import determinant because this canonical base pairing favours stability of the formed F-stem. The discriminator base at position 73 of tRNAs were shown to influence the stability of the first base pair of the aminoacceptor stem, thus the implication of the discriminator base U73 of tRK1 in keeping F-stem stability may be justified by such fact (Lee et al., 1993). In the F-structure, the anticodon nucleotides are involved in the formation of a long hairpin structure potentially determining the overall structure stability **(Fig.15)**. This explains the important character of the nucleotide C34 because it stabilises the hairpin structure; introduction of U34 leads to formation of three consecutive non-canonical G-U base pairs destabilizing the long hairpin. These findings provided a first evidence for a

participation of a secondary RNA structure rearrangement in the mechanism of mitochondrial import selectivity, since in other studies this process was rather attributed to changes in the classical tertiary or 3D structure of imported tRNAs (Goswami et al., 2003; Salinas et al., 2005).

After targeting to the mitochondrial surface, tRK1 needs to be translocated across the mitochondrial outer and inner membranes. Only little information about this final step in the import process is available up to now. One study has demonstrated that the import process is dependent on ATP provided energy and on the electrochemical membrane potential $\Delta\Psi$. In addition, it has been shown that import of tRK1 is sensitive to protease treatment, thus illustrating the dependence on outer mitochondrial receptor proteins. Hence, mitochondrial import of tRK1 has been investigated in yeast strains carrying deletions for the outer membrane receptor proteins Tom20 and Tom70 implicated in the import of matrix-targeted and inner-membrane inserted preproteins respectively. The protein Tim44, part of the presequence translocation-associated motor PAM, was also analysed for its implication in tRK1 import. Indeed, results obtained *in vitro* and *in vivo* have shown that import of tRK1 was abolished when the proteins Tom20 and Tim44 were absent, whereas the deletion of Tom70 did not have any effect (Tarassov et al., 1995b). These results raised the hypothesis that the imported tRK1 and its targeting factor preMSK might be translocated as a complex through the mitochondrial membranes. This idea, however, is still dealing with the fundamental dogma telling that a partial unfolding of preproteins occurs during their passage into the matrix. In this way it remains unclear how and if tRK1 can be imported in complex with preMSK.

OBJECTIVES

OBJECTIVES OF THE THESIS WORK

The main objective of my thesis work was the identification and characterization of mitochondrial outer and inner membrane proteins that are involved in the translocation of tRK1 into mitochondria of the yeast *Saccharomyces cerevisiae*. In this work, the deciphering of the translocation mechanism was mainly focused on the passage of tRK1 across the mitochondrial outer membrane. To achieve this objective, the following tasks have been set:

- Exploitation of broad-spectrum screening approaches in order to identify mitochondrial membrane proteins interacting with the imported tRK1. To this aim we took advantage of the North-Western approach and crosslinking combined with immunoprecipitation (CLIP).

- To characterize the implication of the identified candidate proteins in the translocation mechanism, import of tRK1 was studied *in vitro* and *in vivo* using the corresponding mutant yeast strains.

- The translocation of tRK1 across the mitochondrial outer membrane was assessed by studying the involvement of the two main channel-forming proteins, the Voltage-Dependent Anion Channel (VDAC1 or Por1) and the Tom40 protein of the preprotein import machinery.

- The assembly and stability of the TOM complex and of VDAC1 oligomers was analyzed in context with tRK1 translocation through the mitochondrial outer membrane.

- The requirements for soluble cytosolic targeting factors were defined for different import pathways of tRK1 across the outer membrane.

RESULTS AND DISCUSSION

II) RESULTS AND DISCUSSION

1. tRNA TRANSLOCATION ACROSS THE MITOCHONDRIAL OUTER MEMBRANE

After addressing of tRK1 to the mitochondrial surface, the first barrier to cross is the mitochondrial outer membrane. To identify potential candidate proteins interacting with the imported tRK1 we decided to apply first systematic screening approaches.

1.1 Identification of mitochondrial outer Membrane Proteins interacting with tRK1

In the yeast *Saccharomyces cerevisiae* it was shown that protease digestion of receptor proteins located at the mitochondrial outer membrane abolished import of tRK1. Indeed, the Tom20 protein of the TOM complex, fulfilling the function as receptor for matrix targeted preproteins, was shown to be essential for internalization of tRK1 (Tarassov et al., 1995). These observations lead to the assumption that proteins playing the role of receptors and/or translocators of tRK1 should have RNA-binding properties. To identify potential proteins interacting with tRK1, North-Western analysis was carried out on mitochondrial lysates of a wild type strain and a strain carrying a deletion for the *VDAC1* or *POR1* gene (*por1*Δ strain) in presence of the radiolabelled aminoacylated tRK1 **(Fig. 18A)**. The reason to compare the presence of potential tRK1 binding proteins in these two strains was based on the fact that the VDAC1 protein was involved in tRNA import in plants (Salinas et al., 2006). Band patterns obtained after North-Western are represented on **(Fig.18B)**. Zones containing proteins having potential tRK1-binding capacities were subjected to mass spectrometry analysis and identified proteins were sorted according to their mitochondrial localization in the outer membrane (OM), the inner membrane (IM), the intermembrane space (IMS) and the matrix compartment (M). The studies were mainly focused on OM proteins responsible for the first steps in the translocation pathway of tRK1 into mitochondria. Potential protein candidates identified in the wild type strain were VDAC1 and Tom5, whereas in the *por1*Δ strain components of the TOM complex of the preprotein import machinery have been found, namely Tom40, Tom20 and Tom22 **(Table 3, TableS1)**.

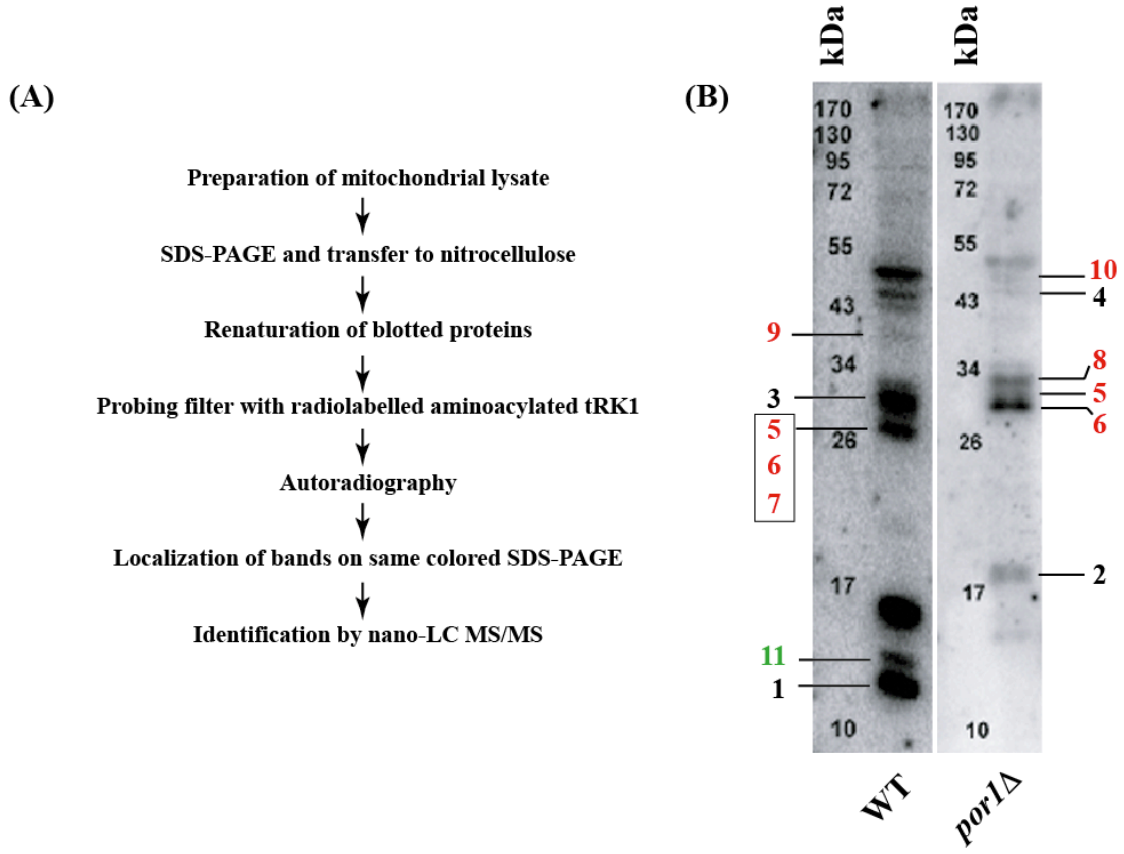

Fig.18 : Identification of tRK1 interacting proteins by North-Western analysis. (A) Technical procedure of the North-Western approach. **(B)** Autoradiogram of North-Western blot performed on mitochondrial lysates derived from wild type (WT) and *por1*Δ strains. **Bold black numbers** : Indicate bands in which mitochondrial outer membrane proteins were identified. **Bold red numbers** : Indicate bands in which mitochondrial inner membrane proteins were identified. **Bold green number** : Indicates band in which mitochondrial matrix proteins were identified. Boxed numbers : Multiple proteins identified in a single band.

An alternative permitting the characterization of mitochondrial membrane proteins interacting physically with tRK1 was offered by the crosslinking and immunoprecipitation (CLIP) approach that has been performed on isolated mitochondria of a wild type strain. To this aim, *in vitro* import was performed using a tRK1 transcript (BrU-tRK1) synthesized in presence of the modified photoactivable base 5-bromouridine. Upon UV irradiation BrU-tRK1 can covalently bind to proteins that interact with tRK1 during import into mitochondria yielding stable BrU-tRK1/protein complexes. In absence of ATP, tRK1 cannot be imported into mitochondria (Tarassov et al., 2007) and probably accumulates at the mitochondrial outer membrane where it interacts with its receptor and/or translocator proteins. Therefore, in order to favor binding of tRK1 to the mitochondrial surface and to lower dissociation of formed complexes between tRK1 and outer membrane proteins, the import and crosslinking

Identified mitochondrial proteins	Position of band on NW autoradiogram	Wild type	*por1*Δ
TOM 5 (component of the translocase of outer membrane complex)	**1**	+	-
TOM 20 and TOM 22 (components of the translocaseof outer membrane complex)	**2**	-	+
VDAC1 (Voltage-Dependent Anion Channel)	**3**	+	-
TOM 40 (component of the translocase of outer membrane complex)	**4**	-	+
MIR 1 (Phosphate carrier)	**5**	+	+
PET 9 (ADP/ATP carrier)	**6**	+	+
AIM 37 (subunit of MINOS complex)	**7**	+	-
PHB 1 (Prohibitin 1)	**8**	-	+
PHB 2 (Prohibitin 2)	**9**	+	-
TIM 50 (component of the translocase of inner membrane 23 complex)	**10**	-	+
HSP 10 (mitochondrial co-chaperone)	**11**	+	-

Table 3 : Mitochondrial proteins identified by North-Western screening. Bold numbers indicate corresponding signal position on the Nort-Western (NW) autoradiogram. **Black numbers** : mitochondrial outer membrane proteins. **Red numbers** : mitochondrial inner membrane proteins. **Green number** : mitochondrial matrix protein. (+) and (-) indicate if the protein was identified in the corresponding yeast strain or not, respectively.

Mitochondrial localization	Identified proteins	Function and/or name of identified proteins
Outer membrane	**VDAC 1**	(Voltage dependent anion channel 1)
	TOM 40	(Channel-forming protein of the TOM complex)
	TOM 71	(Receptor protein of the TOM complex)
Inner membrane	**PHB 1**	(Prohibitin 1)
	PHB 2	(Prohibitin 2)
	PET 9	(ADP/ATP carrier)
	MIR 1	(Phosphate carrier)
	YMC 1	(Carrier protein involved in oleate metabolism and glutamate biosynthesis)
	MOS 1	(Subunit of MINOS complex)
	AIM 5	(Subunit of MINOS complex)
	FMP 10	(Uncharacterized mitochondrial membrane protein)
	YNR040W	(Uncharacterized mitochondrial membrane protein)
	YDL027C	(Uncharacterized mitochondrial membrane protein)
	YER077C	(Uncharacterized mitochondrial membrane protein)
Matrix	**HSP 60**	(Mitochondrial protein chaperone)
	Mitochondrial ribosomal proteins of the small and large subunit (cf. Table S2)	

Table 4 : Mitochondrial proteins identified by crosslinking and immunoprecipitation (CLIP) analysis. Identified proteins were grouped according to their mitochondrial localisation. Uncharacterized mitochodrial membrane proteins are represented by their systematic gene names.

procedures were performed in absence of an external ATP source. BrU-tRK1/protein complexes were immunoprecipitated by an antibody directed against 5-bromouridine and eluted proteins were identified by mass spectrometry analysis. By this method it was possible to identify the two most abundant proteins of the mitochondrial outer membrane, VDAC1 and Tom40, and a receptor protein of the TOM complex, Tom71 (**Table 4, Table S2**).

RNA import into mitochondria of *Saccharomyces cerevisiae*, but also into mitochondria of mammalian cells, anticipated the necessity for components and the integrity of the preprotein import machinery (Tarassov et al., 1995; Entelis et al., 2001). With the help of our systematic screening approaches we were able to confirm the interaction of tRK1 with proteins of the preprotein import machinery during its binding and translocation steps through the mitochondrial outer membrane. The results, however, also imply a new candidate protein, VDAC1, which has not been proposed yet as an element of the tRK1 import machinery of *S.cerevisiae* mitochondria. Due to the known channel properties of VDAC1, it was interesting to hypothesize that this protein could also be implicated in the translocation of tRK1 across the mitochondrial outer membrane. Regarding the fact that in the *por1*Δ strain only components of the preprotein import machinery have been identified, it might be attractive to propose the co-existence of two alternative import pathways across the mitochondrial outer membrane. In order to test this hypothesis, identified candidate proteins were investigated in further details.

1.2 Import of tRK1 is mediated by the VDAC and the TOM Channel

1.2.1 Functional and physical Integrity of isolated Mitochondria from Saccharomyces cerevisiae Strains

In order to guarantee the functional integrity of mitochondria isolated from different *S.cerevisiae* strains that were used in our *in vitro* studies, their respiration rates were analyzed by oxygraphy **(Table 5, Annex A)**. Mitochondria from the corresponding wild type, *por1*Δ, *por2*Δ, *tom5*Δ, *tom6*Δ, *tom7*Δ and *tom20*Δ_{112} yeast strains were able to respire in a cyanide sensitive way on added substrates (succinate, ethanol, NADH) and were coupled as illustrated by the respiratory control. Mitochondria from the *por1*Δ strain, however, showed a decreased respiratory rate compared to mitochondria from the other strains. 4,4'-diisothiocyano-2,2'-stilbenedisulfonic acid (DIDS), an anion selective channel blocker capable of inhibiting VDAC (Thinnes et al., 1994), reduced the respiration of wild type and *tom5*Δ mitochondria to

Yeast strain	Succinate (state 4)	Ethanol	NADH	FCCP (state 3u, succinate based)	Respiratory control (V3u/V4)	DIDS
BY n=32	34±9	123±12	49±1	85±37	2,5±0,9	16±2
*tom5*Δ n=3	21±2	128±9	44±12	75±37	3,6±1,6	n.d.
*tom6*Δ n=1	140	n.d.	n.d.	270	1,9	n.d.
*tom7*Δ n=1	80	n.d.	n.d.	160	2	n.d.
tom20Δ_{112} n=4	24±7,5	n.d.	n.d.	27±7,5	1,2±0,12	n.d.
*por1*Δ n=3	10±3	117±14	23±7	22±8	2,2±1,1	16±4
*por2*Δ n=3	29±8	121±22	41±11	83±17	2,9±0,5	8

Table 5. Respiration rates of *Saccharomyces cerevisiae* mitochondria from wild type (BY) and deletion strains. Respiration rates are indicated in [nmol $O_2 \cdot min^{-1} \cdot mg^{-1}$ mitochondrial protein] with corresponding standard deviations. V3u and V4 represent respiration rates of mitochondria at the uncoupled state (state 3u) and the state 4 respectively. Concentrations of substates and other chemical compounds used were as follows : [succinate] = 10mM, [ethanol] = 1mM, [NADH] = 1mM, [FCCP] = 0,5-1·10^{-8} M, [DIDS] = 0,5mM. n.d. : not determined.

a similar rate as the one observed in *por1*Δ mitochondria, with an even more prominent effect in the *por2*Δ mitochondria. In addition to their functional integrity, isolated mitochondria were also checked for their physical integrity. The intactness of mitochondrial inner and outer membranes was assessed using the citrate synthase assay reflecting the accessibility of externally added substrates to the matrix-localized enzyme citrate synthase (Matlib et al., 1979). All our mitochondrial preparations had an overall integrity >95%. The intactness of the mitochondrial outer membrane was checked by accessibility of externally added cytochrome *c* to the respiratory chain during respiration measurements by oxygraphy. Isolated mitochondria from used strains had an outer membrane integrity in the range of 85-95%. These functional and stability tests showed that mitochondria isolated from different yeast strains fulfilled the criteria to be used in further experiments.

As VDAC1 is the main translocator for metabolites across the mitochondrial outer membrane (Benz, 1994), the decrease of the respiration rate in the *por1*Δ strain and in presence of the channel blocker DIDS can be explained by a limited access of substrates to the respiratory chain. The supply of metabolites in absence of VDAC1 can be assured by the channel activity of the Tom40 protein of the preprotein import machinery (Kmita and Budzińska, 2000; Antos et al., 2001) that becomes upregulated in absence of the VDAC1 protein to permit adaptation of the outer membrane permeability (Kmita et al., 2004).

1.2.2 tRK1 Translocation into reconstituted Vesicles proceeds via VDAC and the Tom40 Channel

Previous studies have shown that import of tRK1 into mitochondria of *S.cerevisiae* requires the presence of a functional preprotein import machinery (Tarassov et al., 1995). Nevertheless, the exact implication mechanism of proteins shown to play a role in tRK1 import has not been described, neither the proteins ensuring the role of translocators through the mitochondrial outer membrane. With the help of our screening approaches we could identify the channel-forming proteins VDAC1 and Tom40 as potential candidates implicated in tRK1 import into mitochondria of *S.cerevisiae*. In order to assess the role of these two proteins in the translocation mechanism across the mitochondrial outer membrane, we decided to investigate their participation in a simplified model that was developed with isolated mitochondrial outer membrane vesicles (OMVs) derived from wild type (WT), *por1*Δ and *por2*Δ mitochondria.

In order to evaluate the purity of the prepared OMVs, different fractions were analyzed during the isolation procedure for the presence of specific marker enzymes: M, initial mitochondrial preparation used for OMV isolation; IM/M, pellet obtained after hypotonic shock representing the inner mitochondrial membrane and the matrix compartment; OMV, prepared outer membrane vesicles. Citrate synthase (CS) and adenylate kinase (ADK) are marker enzymes of the mitochondrial matrix and the intermembrane space respectively and succinate dehydrogenase (SDH) is a specific marker of the mitochondrial inner membrane. Activities of these enzymes were measured according to (Sottocasa et al., 1967; Ernster and Luylenstierna, 1970; Matlib et al., 1979) and were normalized to the protein content of the corresponding fraction. CS and SDH were equally distributed in the IM/M fraction, whereas ADK was almost absent, indicating that the hypotonic treatment of mitochondria disrupted the mitochondrial outer membrane. Prepared OMV fractions of

mitochondria from different yeast strains were practically devoid of any contamination by other mitochondrial subcompartments as illustrated by the low SDH and ADK activities in these OMV fractions **(Table 6)**.

	Citrate synthase			Succinate dehydrogenase			Adenylate kinase		
	WT	*por1*Δ	*por2*Δ	WT	*por1*Δ	*por2*Δ	WT	*por1*Δ	*por2*Δ
M	91±4	104±12	93±14	107±17	79±11	87±7	227±34	258±41	196±22
IM/M	122±9	131±8	129±11	123±7	114±9	109±8	11,5±3	7,3±2,5	4,8±2,3
OMV	nd	nd	nd	0,7±0,4	1,2±0,3	1,3±0,2	3,2±0,2	2,1±1,1	1,4±0,3

Table 6 : Activity of marker enzymes in different mitochondrial fractions [nmol • min^{-1} • mg^{-1} mitochondrial protein]. M : isolated mitochondria; IM/M : inner membrane and matrix fraction; OMV : outer membrane vesicles.

In addition, VDAC1 was present in prepared OMVs at about the same level as in mitochondria initially used for the OMV preparation **(Fig.19)**.

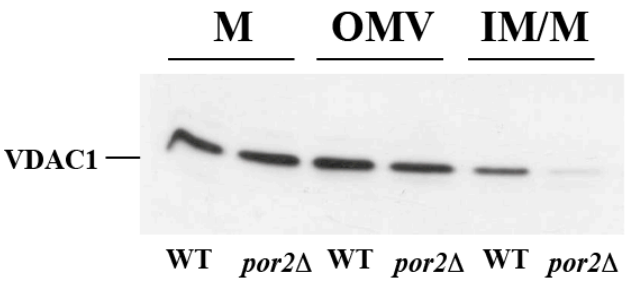

Fig.19 : Immunoblot illustrating VDAC1 distribution in fractions after isolation of mitochondrial outer membrane vesicles from wild type (WT) and *por2*Δ strains.
M – mitochondria, OMV - outer membrane vesicles, IM/M – inner mitochondrial membrane and matrix fraction. Isolated fractions, equalized to the initial volume of fractionation, were subjected to 10% SDS-PAGE and immunodecoration was done with antibodies directed against VDAC1.

For *in vitro* import studies it was crucial that OMVs exposed the mitochondrial outer membrane proteins in the right orientation in order to guarantee proper interactions of tRK1 with its receptor and translocator proteins. Indeed, prepared OMVs had an outside-out orientation as illustrated by trypsin accessibility to the cytosolic part of the Tom70 protein of the TOM complex **(Fig.20)**. The stability of OMVs was checked by a coupled enzymatic reaction explained in detail in **(Fig.21)**. Measurements confirmed that OMVs were stable in time at applied experimental conditions **(Fig.22A)**. In addition, time-dependent tRK1 *in vitro*

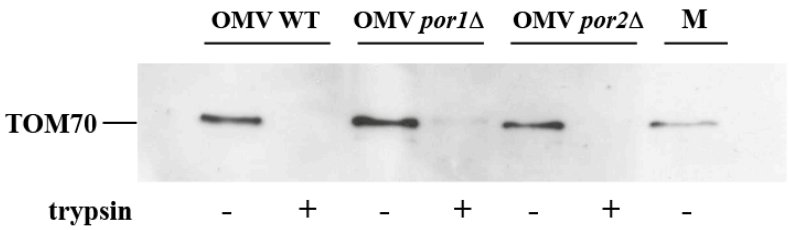

Fig.20 : Outside-out orientation of outer membrane vesicles (OMVs). Obtained vesicles were treated with trypsin (+) or not (-) and analyzed by immunodecoration with antibodies directed against the cytosolic part of the outer membrane protein TOM70. OMV WT: Outer membrane vesicles derived from a wild type strain, OMV *por1*Δ: Outer membrane vesicles derived from a *por1*Δ strain, OMV *por2*Δ: Outer membrane vesicles derived from a *por2*Δ strain, M : mitochondrial lystate.

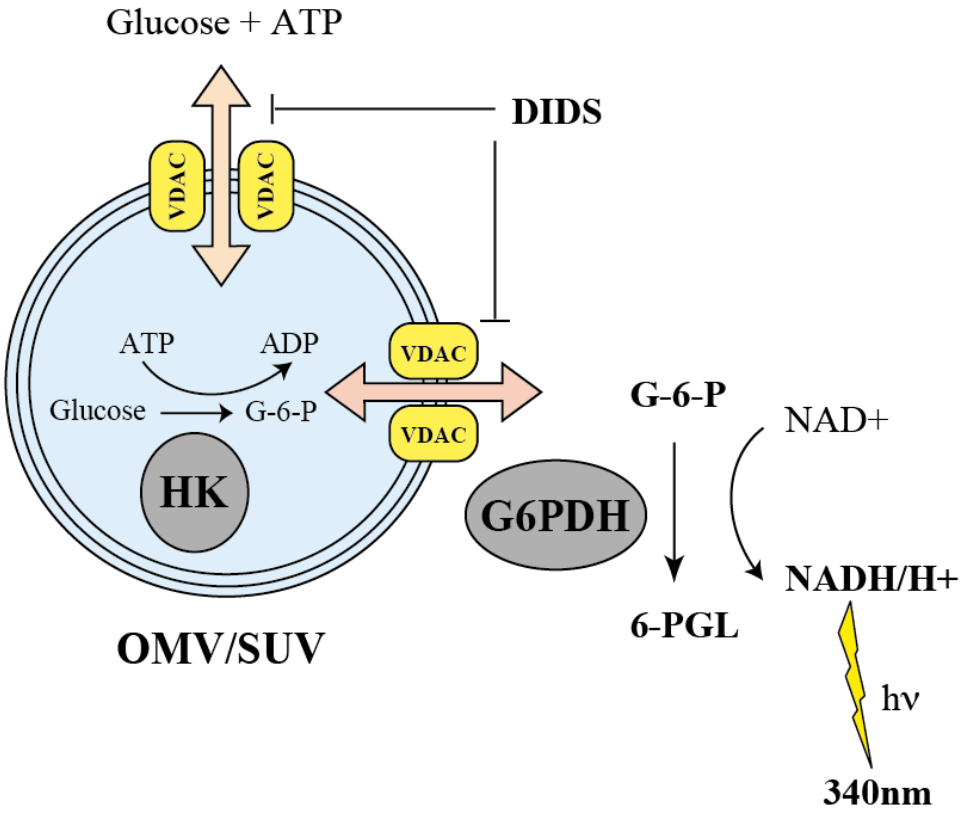

Fig.21 : Scheme illustrating the stability test of prepared outer membrane vesicles (OMVs) or small unilamellar vesicles (SUVs). OMVs or SUVs were loaded with yeast hexokinase (HK) by sonication and incubated at 30°C in presence of D-glucose and ATP that entered the vesicles *via* the VDAC channels. Inside vesicles, HK catalyzed transformation of glucose to glucose-6-phosphate (G-6-P) that diffused outside the OMVs/SUVs through the VDAC channels. Extravesicular G-6-P was oxidized to 6-phosphogluconolactone (6-PGL) by glucose-6-phosphate dehydrogenase (G6PDH) accompanied by an equimolar reduction of NAD+ to NADH that was monitored spectrophotometrically at 340nm. DIDS (50-500µM) was used to block VDAC channels in order to investigate the leakiness of the prepared OMVs/SUVs, assuming that DIDS completely blocked VDAC channels. Total amount of loaded HK was checked by solving OMVs/SUVs by digitonin and by measuring HK activity.

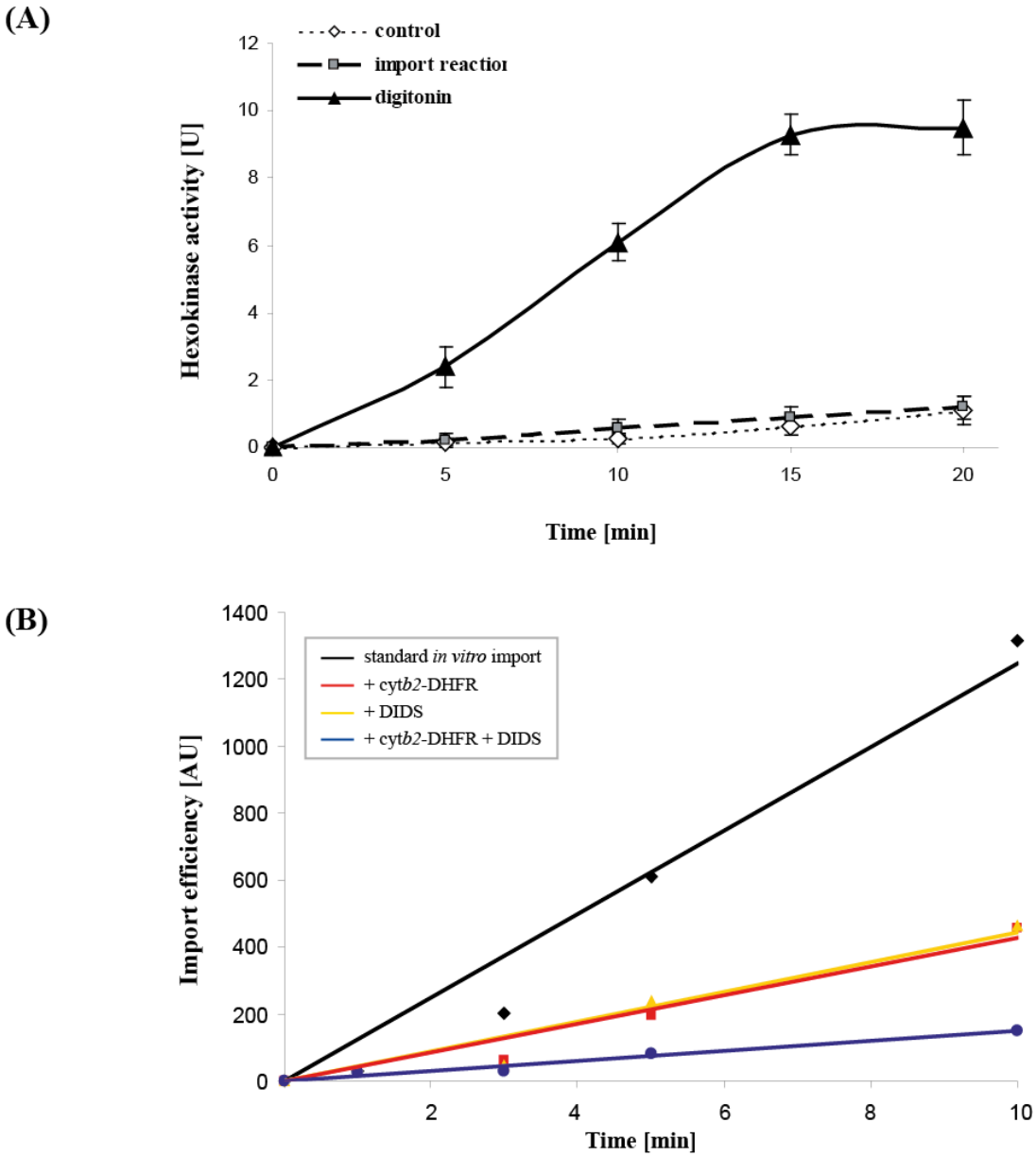

Fig.22 : Characterisation of outer membrane vesicles. (A) Outer membrane vesicles are stable in time at experimental conditions of *in vitro* tRK1 import. Amount of loaded hexkinase (HK) was checked by solving OMVs by digitonin and by measuring total HK activity in supernatant at indicated times after sedimentation of OMVs at 100000g. Leakiness of OMVs was investigated by measuring HK activity in supernatants of untreated OMVs (control) and in supernatants of OMVs in tRK1 *in vitro* import conditions in presence of tRK1 and import directing proteins enolase-2 and preMSK (import reaction). This graph is representative for OMVs derived from wild type mitochondria. HK activity [U] = µmol • min^{-1}. **(B) Linear character of time dependant *in vitro* tRK1 import into OMVs.** tRK1 import kinetics was monitored by autoradiography and tRK1 import was quantified as explained in material and methods. Used colors: black for standard tRK1 *in vitro* import reaction; red for tRK1 *in vitro* import reaction into OMVs pre-treated with cyt*b2*-DHFR; yellow for tRK1 *in vitro* import reaction into OMVs pre-treated with 1mM DIDS and blue for tRK1 *in vitro* import reaction into OMVs pre-treated with cyt*b2*-DHFR and DIDS. [AU] = Arbitrary unit.

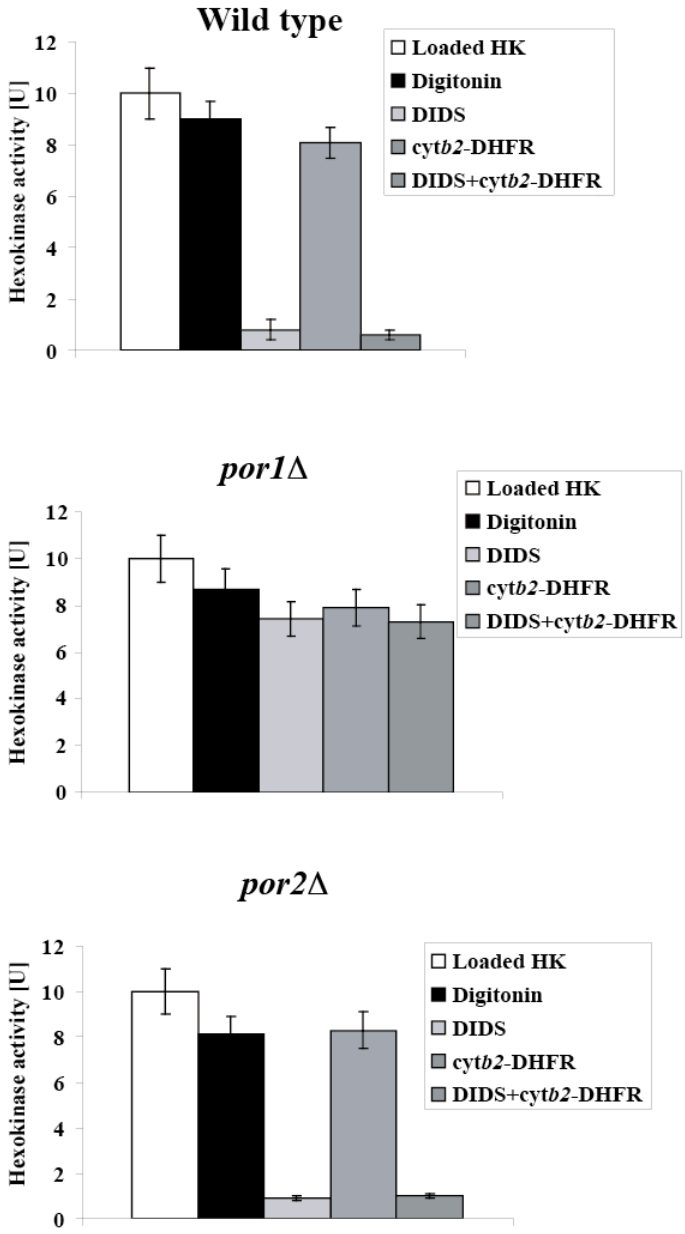

Fig.23 : Substrate access to hexokinase (HK) through channels of OMVs derived from outer mitochondrial membranes of wild type, *por1*Δ *and por2*Δ strains in presence of DIDS and/or cyt*b2*-DHFR. Loaded HK : Activity of total HK that was used to be loaded into OMVs. Digitonin : Activity of HK that was loaded into OMVs lysed by digitonin. DIDS : Activity of loaded HK in presence of 50-500µM DIDS. cyt*b2*-DHFR : Activity of loaded HK in presence of cyt*b2*-DHFR. DIDS + cyt*b2*-DHFR : Activity of loaded HK in presence of DIDS and cyt*b2*-DHFR. Hexokinase (HK), ([U] : µmol • min^{-1}).

import into OMVs displayed a linear character and confirmed that the import reaction was still in a linear phase after 5 minutes, the time frame that has been used in the following tRK1 *in vitro* import reactions into OMVs **(Fig.22B)**. In order to assess the functionality of channels in prepared OMVs, substrate access to loaded hexokinase (HK) was checked as described in **(Fig.21)** in presence of the VDAC1 channel blocker DIDS and/or the Tom40 channel blocking protein cyt*b2*-DHFR **(Fig.23)**. This protein consists in a fusion between the N-terminal 167 residues of the *S.cerevisiae* cytochrome *b2*, devoid of the residues 47-65 forming the intermembrane space sorting signal, and the entire mouse dihydrofolate reductase (DHFR). Cyt*b2*-DHFR can be imported into isolated mitochondria due to the matrix-targeting signal localized at the N-terminal part of the fused cytochrome *b2* moiety. In presence of the drug methotrexate, a structural analog of the DHFR substrate folate, the DHFR part of the fusion protein acquires a stable non-unfoldable 3D structure that hinders the complete import of cyt*b2*-DHFR into mitochondria thereby spanning the two mitochondrial membranes (Dekker et al., 1997). In OMVs deriving from wild type (WT) and *por2*Δ yeast strains application of DIDS was sufficient to prevent entry of HK substrates into OMVs, demonstrating that VDAC1 was present and functional in gating substrates into OMVs. Blocking of the Tom40 channel in *por1*Δ derived OMVs did not significantly decrease the access of substrates to HK, meaning that substrates could enter OMVs *via* another channel or that cyt*b2*-DHFR did not block the Tom40 channel in an efficient manner **(Fig.23)**. This could have been a consequence of the fact that OMVs lacked mitochondrial inner membranes, which are required for formation of mitochondrial contact sites between the TOM and TIM complexes and for a proper functioning of the pre-protein import machinery (Reichert and Neupert, 2002). Nevertheless, this set of control experiments confirmed that our model to study *in vitro* import of tRK1 into OMVs was valid.

In vitro tRK1 import into OMVs (100µg protein/assay) derived from WT, *por1*Δ and *por2*Δ mitochondria was analyzed in presence of the Tom40 channel-blocking protein cyt*b2*-DHFR (1µg/import reaction) or/and the VDAC inhibitor DIDS (0,25mM). The corresponding autoradiogram of *in vitro* import reactions into different OMVs is represented on **(Fig.24A)**. Pre-incubation of different OMVs with cyt*b2*-DHFR or DIDS decreased import of tRK1 by ~50% and ~60% respectively, compared to control import conditions into OMVs derived from WT mitochondria, where no cyt*b2*-DHFR or DIDS was applied **(Fig.24B+C)**. If both channel-blocking agents were applied together, translocation was inhibited by ~80-90% **(Fig.24D)**.

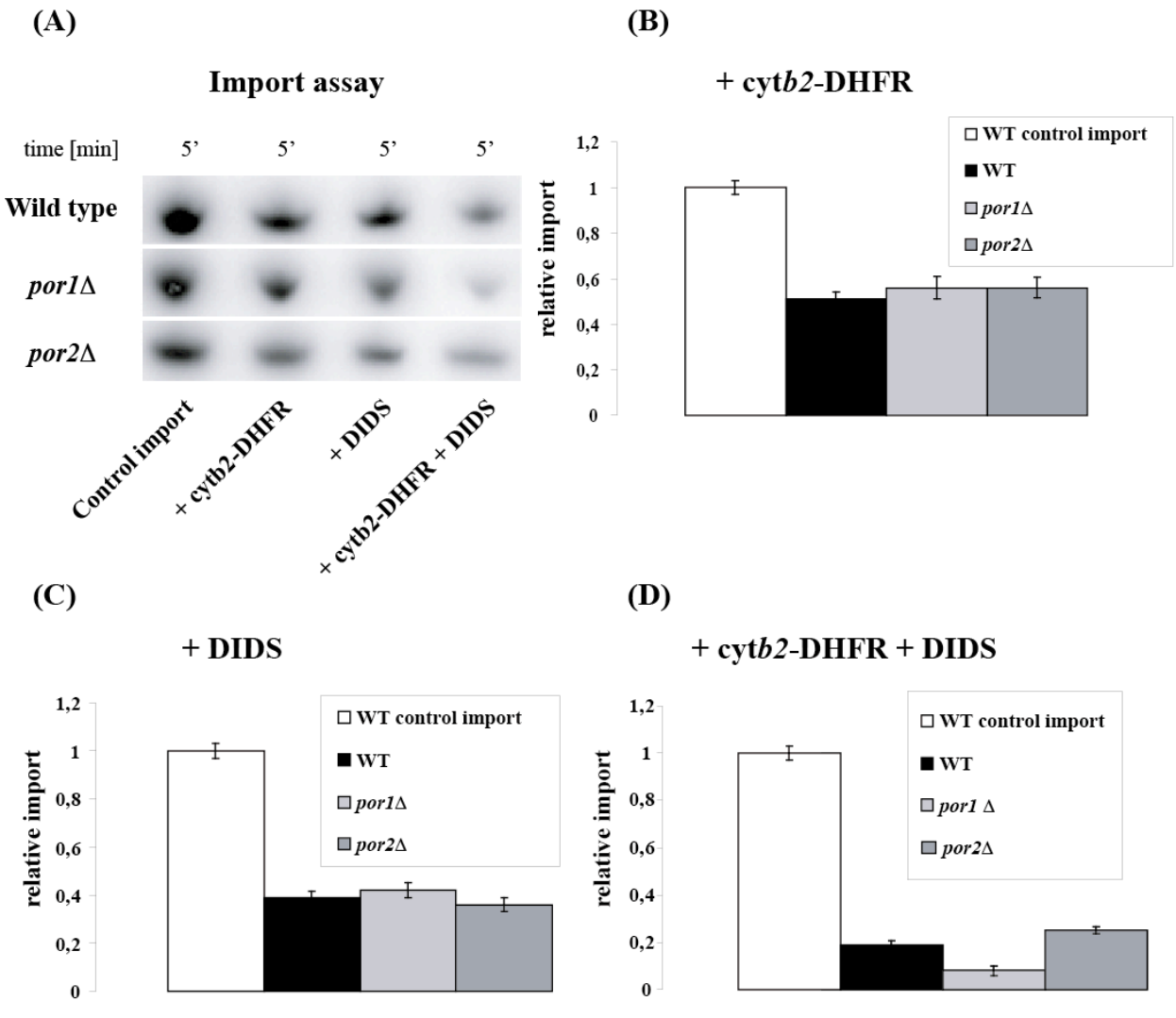

Fig.24 : *In vitro* import of tRK1 into OMVs derived form wild type (WT), *por1*Δ and *por2* Δ mitochondria. **(A)** Autoradiogram of tRK1 *in vitro* imports into OMVs (100µg protein/assay) derived from different yeast strains. **(B)** Plot illustrating *in vitro* import of tRK1 into OMVs in presence of cyt*b2*-DHFR (1µg/assay). **(C)** Plot illustrating *in vitro* import of tRK1 into OMVs in presence of 0,25mM DIDS. **(D)** Plot illustrating *in vitro* import of tRK1 into OMVs in presence of 0,25mM DIDS + cyt*b2*-DHFR (1µg/assay). **(B)-(D)** : Import into OMVs derived from WT mitochondria was set to 1).

To investigate the implication of the VDAC proteins in closer detail, small unilamellar vesicles (SUVs) reconstituted with purified VDAC1 **(Fig.25A)** and VDAC2 **(Fig.25B)** proteins were used. Stability tests and functional characterization were carried out in the same way as for previously described OMVs and prepared SUVs were shown to be suitable to study import of tRK1. The corresponding autoradiogram of *in vitro* import reactions into different SUVs is represented in **(Fig.26A)**. Indeed, it could be demonstrated that SUVs+VDAC1 were able to internalize tRK1 in a DIDS-sensitive way. The presence of 0,25mM DIDS caused an import decrease of ~95%. Interestingly, SUVs+VDAC2 were also able to import tRK1, still the import efficiency was ~50% of the one obtained with

SUVs+VDAC1. This import process was also shown to be sensitive to DIDS (0,25mM) that almost completely inhibited the internalization of tRK1 **(Fig.26B)**.

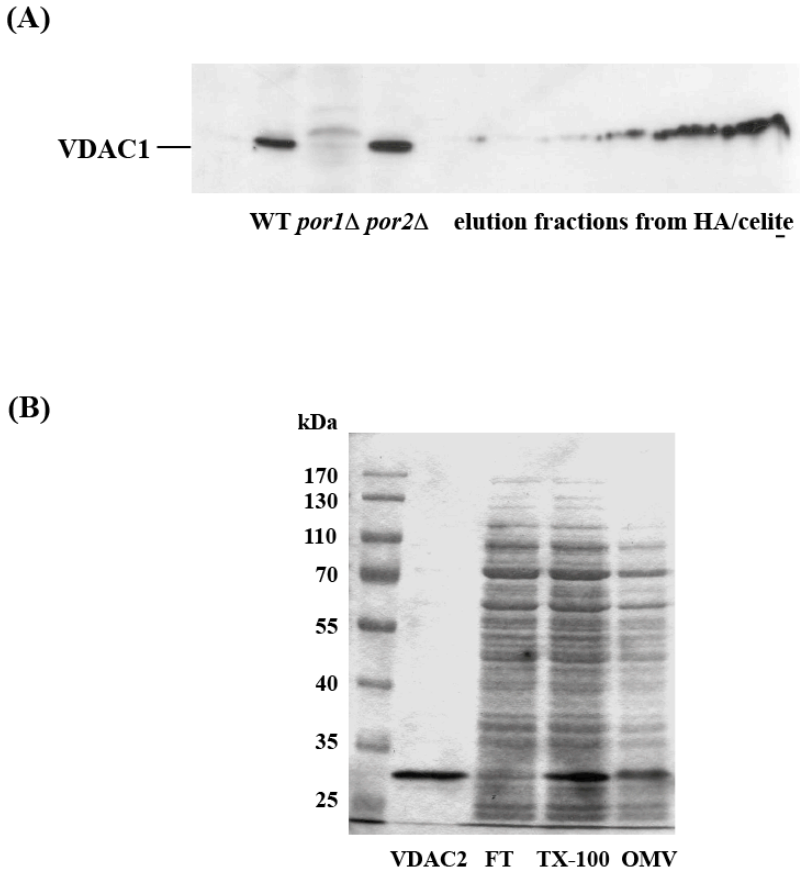

Fig.25 : Purification of VDAC1 and VDAC2 from *S.cerevisiae*. (A) Purification of VDAC1. Mitochondrial lysates from indicated strains and several consecutive elution fractions from hydroxyapatite/celite535 column were analyzed by Western blot using antibodies directed against VDAC1 from *S.cerevisiae*. **(B) Purifications of VDAC2.** Silver stained 10% SDS-PAGE of the various fractions obtained during VDAC2 purification. TX-100 : supernatant from sedimented extract obtained after 2% Triton X-100 treatment of *por1*Δ mitochondria; FT : flow-through from hydroxyapatite/celite535 column; OMV : Outer membrane vesicles obtained from *por1*Δ mitochondria; VDAC2 : 100ng of VDAC2 eluted from hydroxyapatite/celite535 column.

Considering the results of the tRK1 import studies into different OMVs and SUVs, it is probable that Tom40 and VDAC channels are both implicated in the translocation mechanism through the mitochondrial outer membrane. The hypothesis was supported by an almost complete arrest of import if these two channels were blocked simultaneously. At least in this experimental system a major role may be attributed to the channels formed by the VDAC proteins because application of DIDS showed a stronger inhibitory effect on tRK1 uptake into OMVs than cyt*b2*-DHFR. In addition, DIDS virtually blocked the internalization

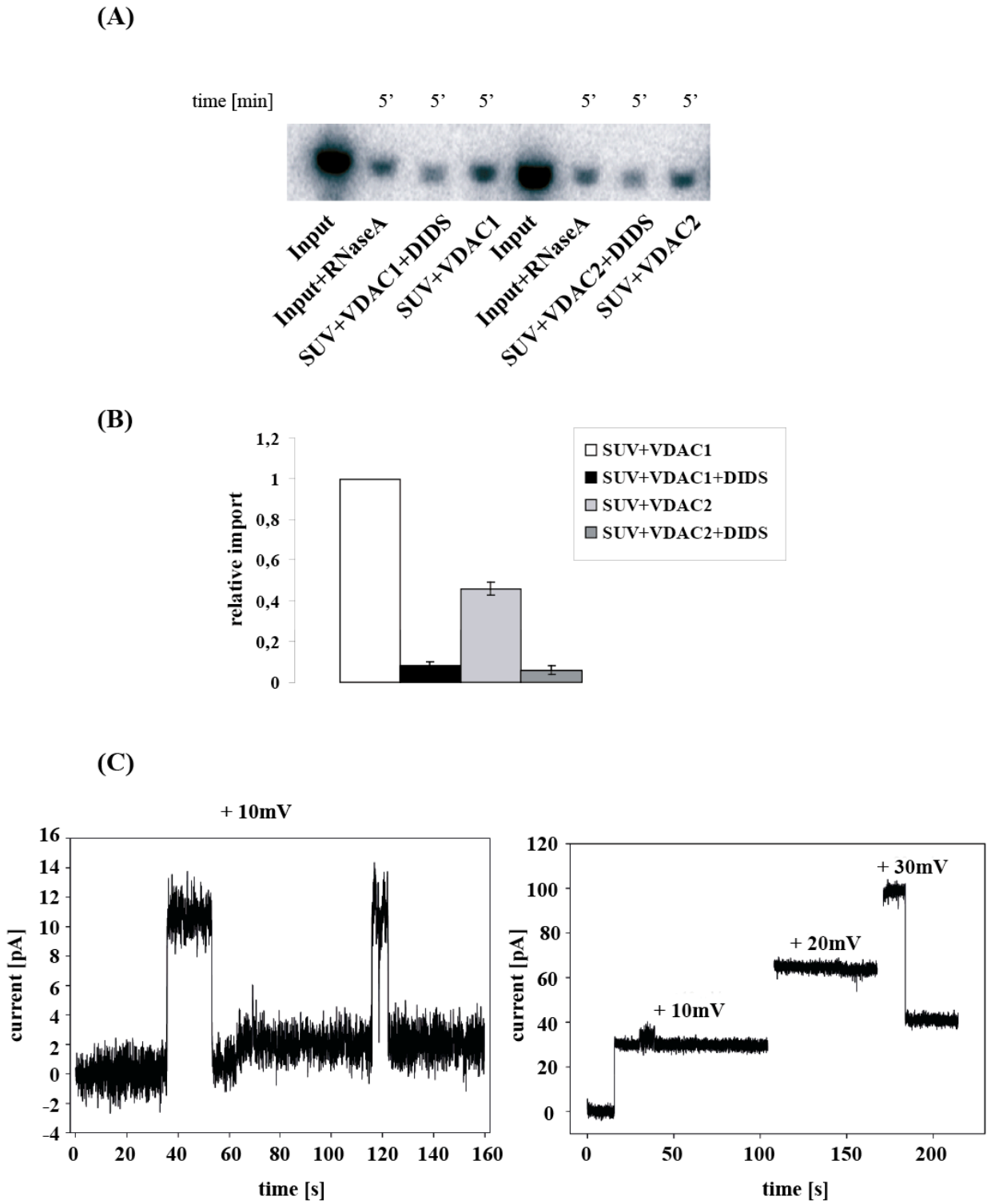

Fig.26 : *In vitro* of tRK1 into small unilamellar vesicles (SUVs) reconstituted with VDAC1 or VDAC2. **(A)** Autoradiogram illustrating *in vitro* tRK1 import into SUVs reconstitued with VDAC1 or VDAC2 in presence or absence of DIDS (0,25mM). Imports were performed in 100µl SUV solution containing 0,1µg of reconstituted protein. **(B)** Plot illustrating *in vitro* import of tRK1 into SUVs (import into SUV+VDAC1 was set to 1). **(C)** Voltage dependent conductivity of VDAC2 channels in presence of 1M KCl. left panel : channel recording performed with an applied potential of +10mV. right panel : channel recording performed at applied voltages of +10mV, +20mV and +30mV.

of tRK1 into SUVs reconstituted with VDAC proteins. Pre-incubation of *por1*Δ OMVs in presence of cyt*b2*-DHFR, however, did not permit a complete inhibition of the import process. This could have been a consequence of the fact that OMVs lack mitochondrial inner membranes, required for a proper functioning of the pre-protein import machinery as stressed above (Reichert and Neupert, 2002). Such a situation may have caused an inefficient import of cyt*b2*-DHFR and thereby could have partially hindered blocking of the Tom40 channel. Another possibility might be a possible channel formation by the VDAC2 protein, which could permit the translocation process of tRK1 as it was shown by import into SUVs reconstituted with purified VDAC2 **(Fig.26A+B)**. These results were rather unexpected because until now the dogma persisted that in *S.cerevisiae* the second VDAC isoform, VDAC2, was devoid of any channel activity. However, the fact that in a *por1*Δ mutant overexpression of VDAC2 was able to complement the temperature sensitive growth defect (Blachly-Dyson et al., 1997) may support our hypothesis that VDAC2 could be able to generate channels if VDAC1 is absent.

To test our hypothesis, we analyzed the channel-forming capacity of purified VDAC2 reconstituted in a diphytanoylphosphatidylcholine membrane in presence of 1M KCl and 10mM Tris-HCl pH 7,4 according to (Rostovtseva and Bezrukov, 1998; Rostovtseva et al., 2006). First, the amount of added VDAC2 was titrated until the amount necessary for generation of a minimal current level could be determined, assuming that this situation represented the recording of the channel-forming capacity of a single reconstituted VDAC2 protein. At the applied voltage of +10mV a channel opening could be recorded generating a current of ~11pA, corresponding to a conductance of 1,1nS. After 120s flickering down to ~2pA could be seen **(Fig.26C left panel)**. In a second independent experiment the channel formation was analyzed at different applied voltages with a larger amount of VDAC2, reflecting this time the recording of the channel-forming capacity of multiple VDAC2 proteins. In this way, it could be demonstrated that the application of +10mV generated a current of ~35pA and that doubling of applied voltage from +10mV to +20mV also produced a proportionally raised current from ~30pA to ~70pA respectively. At +30mV the current was shortly raised to ~105 pA but then suddenly dropped down to ~40pA **(Fig.26C right panel)**.

The biophysical properties of reconstituted VDAC2 proteins reminded the ones that were reported for reconstituted VDAC1 proteins, which display a channel activity at low applied voltages from 10-20mV, corresponding to the anion selective fully open state. In the case of VDAC2, the single channel conductivity of 1,1nS was, however, ~4-fold lower than usually observed for VDAC1, where single channel conductivity is about 4nS in 1M KCl. At

voltages >30mV, conductivity of multiple VDAC2 channels dropped down indicating that a population of these channels adopted a closed substate, a situation that is also characteristic for VDAC1 proteins (Blachly-Dyson and Forte, 2001). Thus, our obtained results showed that reconstituted VDAC2 was, indeed, capable of forming channels in artificial membranes, which could also promote translocation of tRK1 into SUVs containing the VDAC2 protein.

1.2.3 tRK1 Translocation into Mitochondria proceeds through the VDAC1 and the Tom40 Channel

In vitro import studies of tRK1 into OMVs and SUVs demonstrated that the VDAC and Tom40 channels are potentially involved in the translocation mechanism across the mitochondrial outer membrane. Still, these models represent an artificial situation in which the functional state of the studied channels may not be properly regulated because important contacts between outer and inner membrane proteins have been disrupted. In order to analyze the implication of the proposed channels in a more physiologic context, tRK1 import into mitochondria has been investigated.

The involvement of VDAC proteins in translocation of tRK1 was checked by *in vitro* import studies into mitochondria of wild type (WT), *por1*Δ and *por2*Δ strains. Indeed, *por1*Δ mitochondria had an import efficiency that was decreased by ~80% compared to the import into WT mitochondria, whereas *por2*Δ mitochondria obtained from a deletion mutant of the second VDAC isoform, VDAC2, had an import efficiency that was comparable to WT mitochondria **(Fig.27A)**. To complement these results obtained *in vitro*, Northern blot hybridizations were performed to investigate *in vivo* import of tRK1 into mitochondria of above described strains. Import was reduced by ~70% in the *por1*Δ strain compared to the situation in WT, while the *por2*Δ mutant showed no significant import decrease, which is in agreement with our results obtained *in vitro* **(Fig.27B)**.

In order to obtain a more conclusive picture about the involvement of the channels formed by the VDAC and the Tom40 proteins, their participation in tRK1 translocation through the mitochondrial outer membrane has been investigated. The role of VDAC proteins was assessed with the help of the channel blocker DIDS. *TOM40* is an essential gene, which makes that the corresponding deletion mutant cannot be used for *in vitro* import studies. Therefore, the importance of the Tom40 channel was analyzed with the help of the chimeric protein cyt*b2*-DHFR described in the previous section. Indeed, pre-incubation of isolated mitochondria with the protein cyt*b2*-DHFR (1µg/50µg of mitochondrial protein) in presence

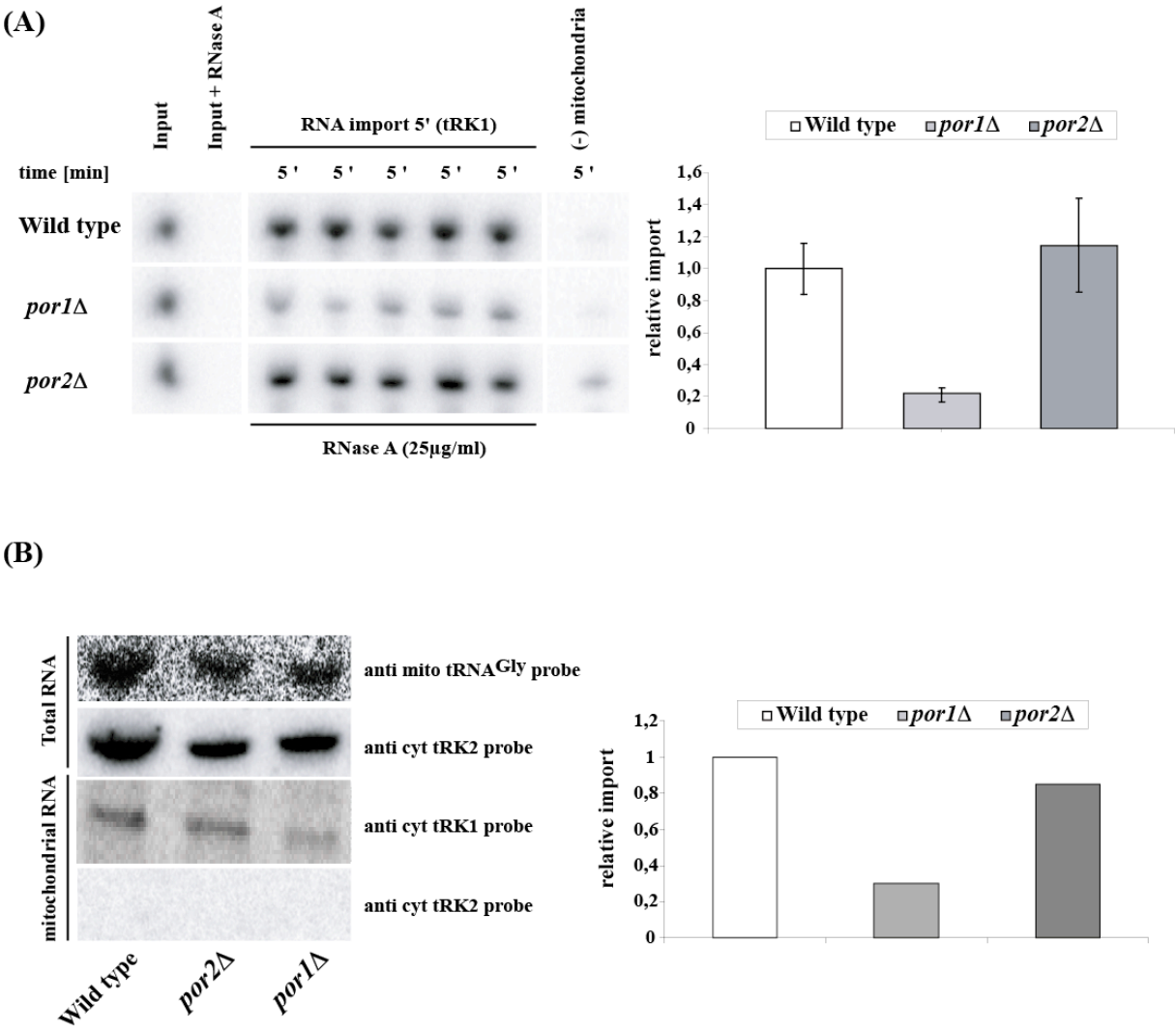

Fig.27 : *In vitro* and *in vivo* import of tRK1 into mitochondria of *Saccharomyces cerevisiae*. (A) *In vitro* import of tRK1 into isolated mitochondria of wild type, *por1*Δ and *por2*Δ cells. **(left)** Autoradiogram of tRK1 *in vitro* imports (performed in 5 repeats). **(right)** Plot illustrating relative imports of tRK1 (import in wild type strain was set to 1 and error bars were calculated as explained in materiel and methods). **(B)** Northern blot illustrating *in vivo* import of tRK1 into mitochondria of wild type, *por1*Δ and *por2*Δ strains. anti mito $tRNA^{Gly}$: probe directed against mitochondrial $tRNA^{Gly}$; anti cyt tRK2 : probe directed against cytoplasmic $tRNA^{Lys(UUU)}$ (tRK2); anti cyt tRK1 : probe directed against partially imported cytoplasmic $tRNA^{Lys(CUU)}$ (tRK1).

of methotrexate (2µM) decreased the import of the matrix directed precursor form of mitochondrial lysyl-tRNA-synthetase (preMSK), used here as the control of blocking efficiency, by 10-fold in WT mitochondria and by 4- to 5-fold in *por1*Δ and *por2*Δ mitochondria respectively **(Fig.28A right panel)**. These results confirmed the validity of our model and gave us the possibility to study the implication of the Tom40 channel in tRK1 import into isolated mitochondria.

In vitro import of tRK1 into isolated mitochondria of WT, *por1*Δ and *por2*Δ yeast strains in presence or absence of the channel blocking compounds DIDS and/or cyt*b2*-DHFR has been analyzed **(Fig.28A left panel)**. Upon addition of DIDS (0,25mM) import of tRK1 was reduced by ~80% in WT and *por1*Δ mitochondria and it was almost completely abolished in *por2*Δ mitochondria compared to the control import condition in WT mitochondria. Pre-incubation of mitochondria with the protein cyt*b2*-DHFR only showed an inhibitory effect in *por1*Δ mitochondria where tRK1 import was decreased by ~50% compared to the control import into WT mitochondria. The application of both channel-blocking compounds together, however, completely blocked the translocation of tRK1 through the mitochondrial outer membrane **(Fig.28B+C)**.

The obtained results clearly demonstrate that tRK1 translocation across the mitochondrial outer membrane mainly occurs through the channel formed by the VDAC1 protein because import into *por1*Δ mitochondria or blocking of the VDAC1 channel by DIDS of WT and *por2*Δ mitochondria reduced import by ~70-90%, whereas blocking of the Tom40 channel had no influence on tRK1 import into WT and *por2*Δ mitochondria, where VDAC1 was present. In absence of the VDAC1 protein, however, or in conditions where it is blocked by DIDS, the Tom40 channel is able to support the import of tRK1, which is illustrated by the fact that import was completely abolished if the two channel-forming proteins were blocked. The remaining import of tRK1 in case of cyt*b2*-DHFR pretreatment of *por1*Δ mitochondria may be explained by the less effective blocking of the Tom40 channel, where after five minutes preMSK could still be partially imported **(Fig.28A right panel)**. In these conditions, the accessible Tom40 channels may permit translocation of tRK1 into *por1*Δ mitochondria. Purified VDAC2 was shown to form channels in unilamellar membranes and its reconstitution into SUVs permitted internalization of tRK1 in a DIDS sensitive way **(Fig.26)**. *In vitro* and *in vivo* import of tRK1 into *por2*Δ mitochondria, however, was comparable to the one observed into WT mitochondria and partial blocking of the Tom40 channel in the *por2*Δ mitochondria *in vitro* did not have any detectable effect on tRK1 import. These results gave further proofs that tRK1 translocation into mitochondria proceeded primarily *via* the VDAC1 channel. There

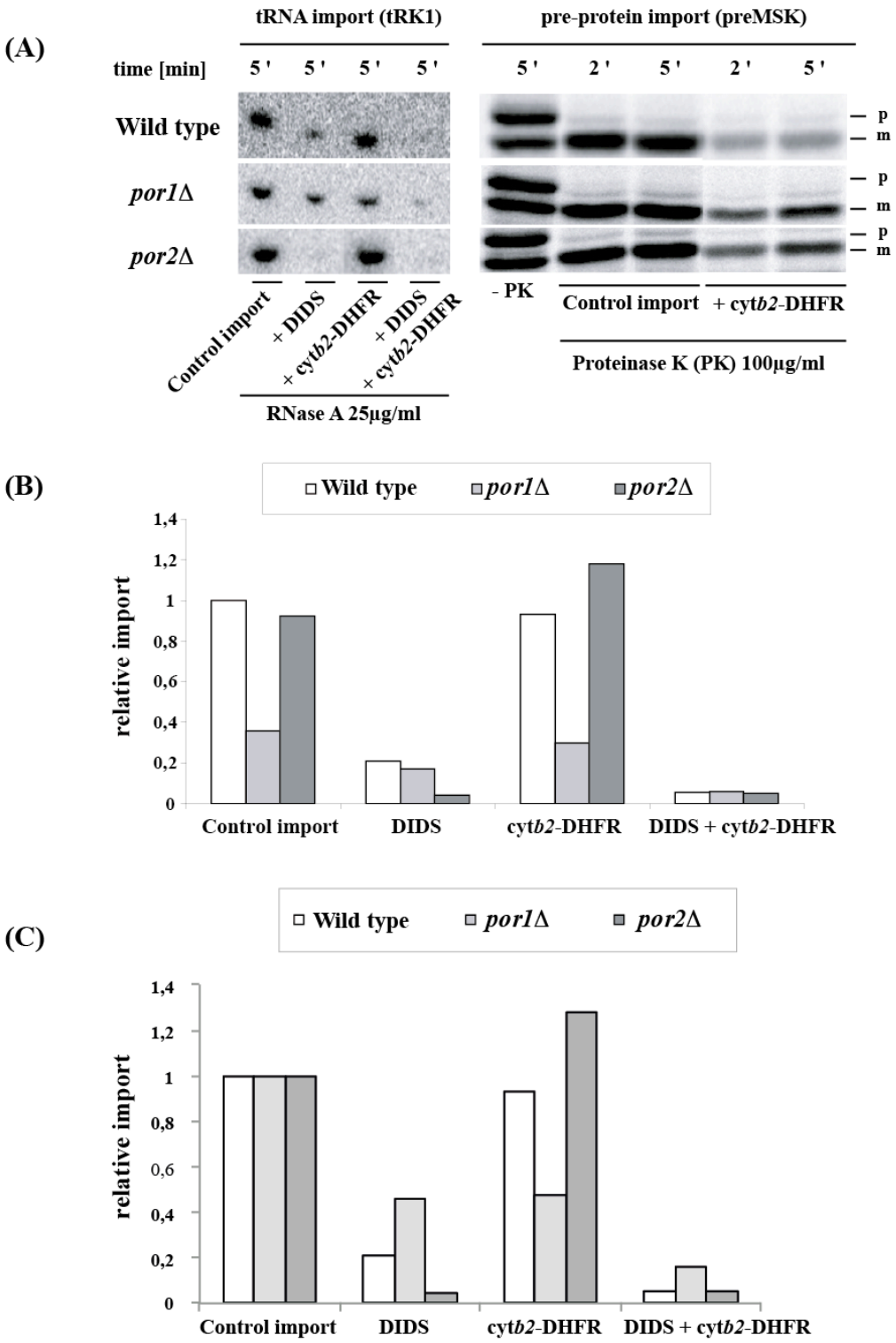

Fig.28 : ***In vitro*** **import of tRK1 into isolated mitochondria of wild type, *por1*Δ and *por2*Δ cells without or in presence of DIDS and/or cyt*b2*-DHFR. (A) left panel** : Autoradiogram of tRK1 imports in presence of DIDS (0,25mM) and/or cyt*b2*-DHFR (1µg/50µg mitochondrial protein); **right panel** : Autoradiogram of imports of precursor form of mitochondrial lysyl-tRNA-synthetase (preMSK); p : precursor form of preMSK; m : mature processed form of preMSK; PK : Proteinase K. cyt*b2*-DHFR was used in presence of 2µM methotrexate. **(B)** Plot illustrating relative imports of tRK1 in different strains and different conditions (control import in wild type strain was set to 1). **(C)** Plot illustrating relative imports of tRK1 in different strains and different conditions (control imports of the different strains were set to 1).

could be several reasons why the VDAC2 proteins seems dispensable: (i) the opening state of eventually formed VDAC2 channels may be negatively regulated if VDAC1 is expressed, (ii) if the VDAC1 gene is deleted, the low endogenous expression level of VDAC2 (Blachly-Dyson et al., 1997) may be insufficient to promote tRK1 import, even if VDAC2 would be able to form channels in the mitochondrial outer membranes and (iii) the Tom40 channel offers an alternative pathway permitting the passage of tRK1 through the mitochondrial outer membrane. The latter reason is strengthened by the fact that in absence of VDAC1 Tom40 becomes upregulated and that these channels
can be used as an alternative entry gate for metabolites (Kmita and Budzińska, 2000; Kmita et al., 2004). Another argument linking the VDAC1 and the Tom40 import pathways is their potential common evolutionary precursor. Both proteins display significant similarities with the bacterial Omp85 protein family and have the same 19-stranded ß-barrel structure that form channels implicated in transport of metabolites or precursor proteins (Zeth, 2010). Despite their divergent functions, the capacity of RNA translocation through the mitochondrial outer membrane may be a conserved feature of these two channels with a preference for VDAC1 that has acquired an anion selective character.

1.2.4 tRK1 Import induces Formation of VDAC1 Oligomers

VDAC1 and Tom40 form channels in the mitochondrial outer membrane that participate in the translocation of tRK1. With the help of electron microscopy and conductance measurements it has been shown that Tom40 is able to form pores possessing a diameter of 2-5nm (Ahting et al., 1999, 2001). Theoretically, the size of this pore could be sufficient to permit passage of correctly folded tRK1 molecules that can adopt structural conformations with sizes of about 25Å-45Å (Kolesnikova et al., 2010). In its anion selective fully open state, VDAC1 was reported to form eye-shaped 3,5nm x 3,1nm pores with a lumen constriction possessing a diameter of ~1,5nm (Summers and Court, 2010). The size of this channel renders the translocation of folded tRK1 molecules less probable. On the other hand, VDAC1 has the ability to form oligomeric structures in the mitochondrial outer membrane that are presumed to generate megachannels participating in the apoptosis triggering mechanism by facilitating the release of cytochrome *c* from the intermembrane space to the cytosol (Mannella et al., 1983; Hoogenboom et al., 2007; Gonçalves et al., 2007; Keinan et al., 2010).

These last facts encouraged us to investigate if VDAC1 is able to form oligomeric structures upon import of tRK1 into mitochondria. To this aim, *in vitro* import reactions were carried out in presence of tRK1 and potentially formed VDAC1 oligomers were stabilized by the chemical protein-protein crosslinker 3-Maleimidobenzoic acid *N*-hydroxysuccinimide ester (MBS) **(Fig.29)**. Indeed, in presence of tRK1, specific formation of a prominent crosslinking product migrating at ~65kDa could be visualized by Western blot using an antibody against VDAC1. If mitochondria were treated by DIDS (0,5mM), formation of this product was decreased and yielded a product with higher mobility. When ATP was omitted from the import reaction, formation of the ~65kDa crosslinking product was enhanced and further oligomers migrating between ~115-120kDa became visible. In absence of the import directing protein factors enolase-2 and preMSK, VDAC1 oligomerization was absent.

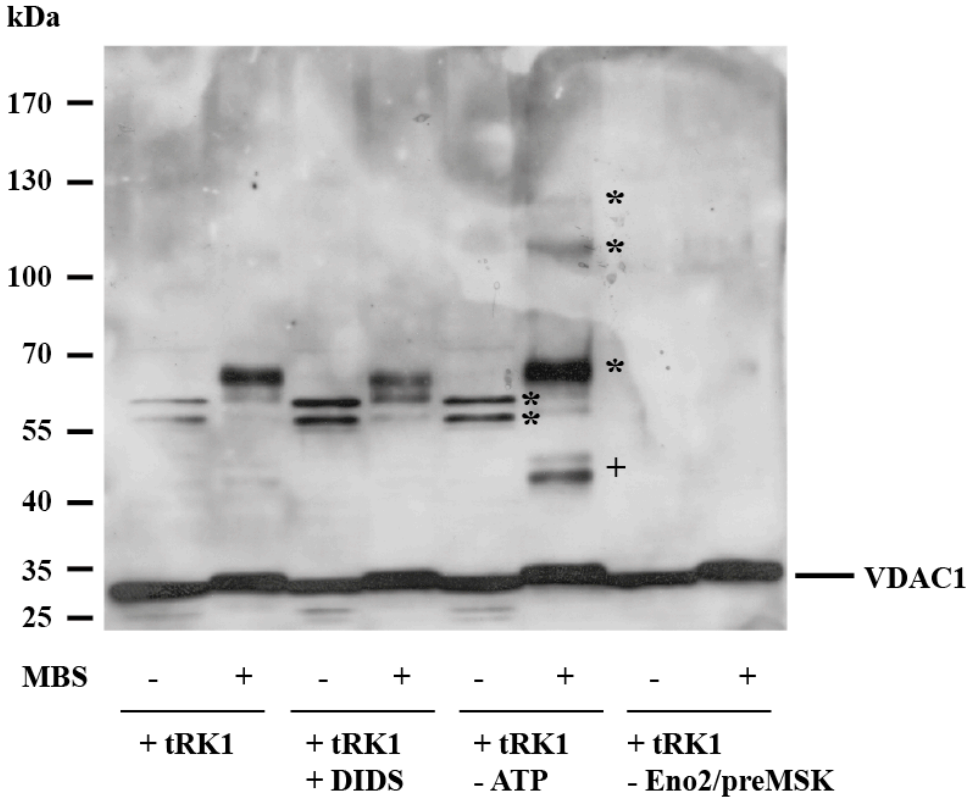

Fig.29 : Formation of VDAC1 oligomers at the mitochondrial outer membrane upon tRK1 import. (+ tRK1) : Standard import reaction, (+ tRK1+DIDS) : Import in presence of 0,5mM DIDS, (+tRK1-ATP) : Import in absence of ATP, (+tRK1-Eno2/preMSK) : Import in absence of import directing proteins enolase-2 and preMSK. (*) Possible VDAC1 oligomers. (+) Heterooligomers between VDAC1 and unknown proteins. Monomeric VDAC1 migration level is indicated (32kDa).VDAC1 was monitored by Western blot. MBS : 3-Maleimidobenzoic acid N-hydroxysuccinimide ester was used at a final concentration of 1mM.

These results suggest that VDAC1 formed oligomeric structures upon import of tRK1 into mitochondria. The crosslinking products migrating at ~65kDa and ~115-120kDa probably represent the dimeric and tetrameric forms of VDAC1 respectively. DIDS, known for its capacity to block the VDAC1 channel, also seems to change the conformation of VDAC1 oligomers. A part of the ~65kDa complex adopted a more compact structure with higher mobility. This compact structure could represent a conformation unsuitable for tRK1 translocation and could give an additional explanation for the ability of DIDS to inhibit tRK1 import into mitochondria. In absence of ATP, tRK1 cannot be imported (Tarassov et al., 2007) and probably accumulates at the mitochondrial outer membrane. This situation favored the formation of VDAC1 oligomers and strengthens the hypothesis that interaction of tRK1 with VDAC1 at the mitochondrial surface lead to VDAC1 oligomerization that could be involved in the tRK1 translocation mechanism. Import directing proteins enolase-2 and preMSK are known for their chaperone activities that could also confer to tRK1 the structural conformation needed for the interaction with its receptor proteins at the mitochondrial outer membrane. In absence of these two protein factors, tRK1 binding to receptor proteins should therefore not take place. Indeed, if enolase-2 and preMSK were omitted, VDAC1 oligomerization was completely absent, indicating that the binding of tRK1 to the mitochondrial outer membrane receptor proteins could be necessary to induce the formation of VDAC1 oligomers. Furthermore, it is also possible that VDAC1 formed crosslinking products with other unknown proteins of the mitochondrial outer membrane yielding a potential heterooligomer that could be visualized at ~40kDa. One can hypothesize that these proteins in complex with VDAC1 could possess regulatory functions either on the channeling capacities or on the generation of VDAC1 oligomers.

1.3 Energy Requirements for tRK1 Import into Mitochondria of *Saccharomyces cerevisiae*

In all studied RNA import systems translocation of RNA molecules inside mitochondria was dependent on energy delivered by ATP hydrolysis (Entelis et al., 2001; Salinas et al., 2008). The role of the electrochemical membrane potential $\Delta\Psi$, which is indispensable for import of preproteins into mitochondria (Schleyer et al., 1982; Eilers et al., 1987), has not been thoroughly investigated for its implication in the RNA import mechanism, while available data are somewhat contradictory.

For this reason, we studied *in vitro* import of tRK1 into mitochondria of a wild type *S.cerevisiae* strain in presence or absence of ATP and/or the electrochemical membrane potential ΔΨ **(Fig.30)**.

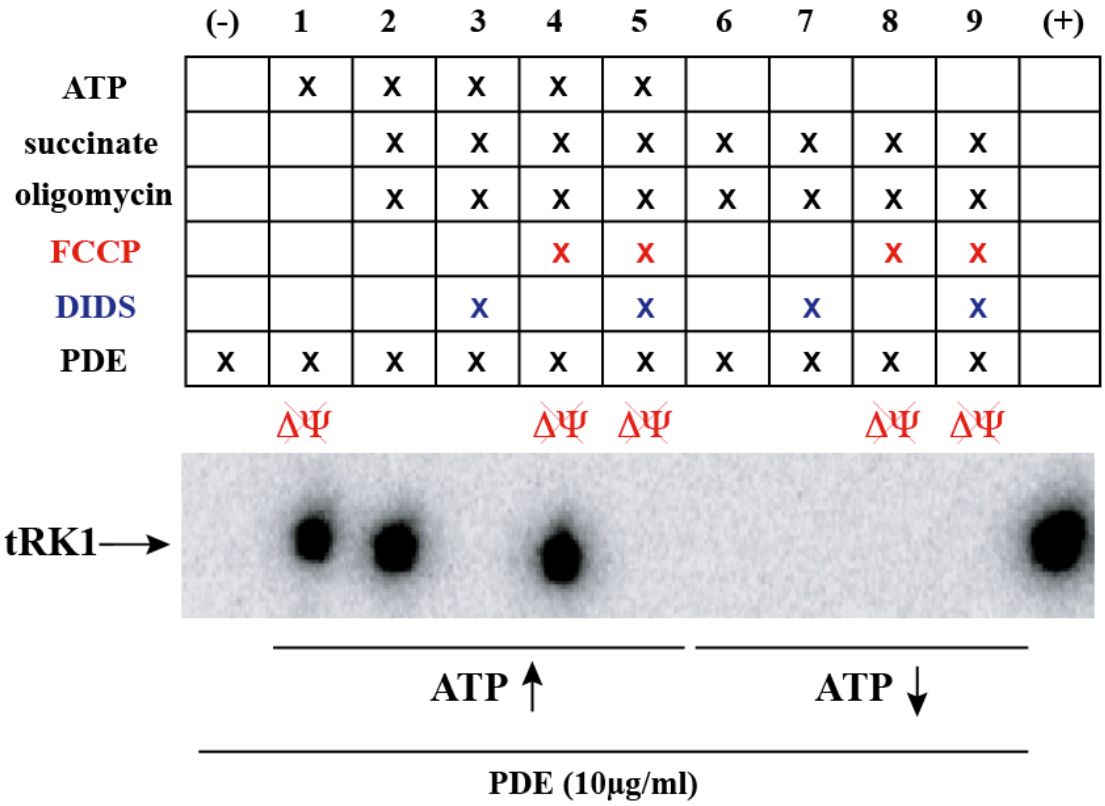

Fig.30 : Impact of ATP and the electrochemical membrane potential ΔΨ on tRK1 import. *In vitro* import of tRK1 into mitochondria of wild type cells was performed in presence (lanes 1-4) or absence (lanes 5-9) of ATP and/or the electrochemical membrane potential ΔΨ. ATP was used at a final concentration of 5mM. FCCP (Carbonyl cyanide-p-trifluoromethoxyphenylhydrazone) (10nM) marked in red; DIDS (4,4'-Diisothiocyano-2,2'-stilbenedisulfonic acid) (0,5mM) marked in blue; PDE (Phosphodiesterase) (10µg/ml). Oligomycin (50µM). lanes 1-9 : *In vitro* tRK1 import reactions performed during 5 minutes; (-) : PDE activity control; (+) : Input.

Manipulation of ΔΨ was achieved by treating mitochondria with different chemical compounds; (i) import assays were performed in presence of the protonophore trifluorocarbonylcyanide phenylhydrazone (FCCP) (10nM) that causes leakiness of protons through the mitochondrial inner membrane and thereby dissipated the proton-motive force generated by the respiratory chain, (ii) manipulation of the respiratory chain activity, achieved by omission of energizing substrates, *e.g.* succinate or NADH, or by oligomycin (50µM) inhibition of the F_1F_0-ATPase, offered another set of possibilities to influence ΔΨ. The

VDAC1 channel blocker DIDS (0,5mM) was used in order to assess the importance of this channel in presence and absence of ATP and/or ΔΨ. While import was performed in absence of ATP, tRK1 could not be translocated inside mitochondria, whereas addition of ATP restored import of tRK1 even if ΔΨ was depleted or inhibited. DIDS was able to block tRK1 import in any condition **(Fig.30)**.

In this way, it could be confirmed that passage of tRK1 through the mitochondrial outer membrane was dependent on VDAC1 and on the presence of ATP, whereas ΔΨ was not required in the conditions used in our study. ATP could have a role at different steps of the tRK1 import mechanism; (i) at the cytosolic side it could promote transfer of tRK1 from the targeting factors to the receptor proteins and (ii) inside mitochondria ATP may be crucial to favor active translocation of the negatively charged tRK1 molecule against the countercurrent of the electrochemical gradient into the matrix compartment. The fact that the polyanionic tRK1 molecule needs to be transported into the negatively charged matrix compartment could explain why depletion of ΔΨ had no influence on tRK1 import. The results obtained during this work were, however, in contradiction with previous studies that demonstrated the necessity of the electrochemical membrane potential ΔΨ for *in vitro* tRK1 import into WT mitochondria (Tarassov et al., 1995). These discrepancies could be explained by different experimental conditions. Indeed, in the previous work a complete cytosolic soluble protein fraction was used to direct import of tRK1 into WT mitochondria. In these conditions, additional protein factors, in addition to enolase-2 and preMSK, could alter the structural conformation of tRK1 and trigger a preferential use of the Tom40 dependent import pathway. In that case, it was assumed that tRK1 and preMSK could be translocated as a complex through the mitochondrial membranes *via* the preprotein import machinery, which would explain the necessity for the electrochemical membrane potential ΔΨ. In this work, the used tRK1 *in vitro* import system, working with the necessary but sufficient import directing proteins enolase-2 and preMSK alone, lead to a preferential use of the VDAC1 dependent import pathway. In these conditions, it may be possible that preMSK was just needed as a chaperone to confer a suitable conformation to tRK1 necessary for its interaction with receptor proteins and/or for its translocation through VDAC1 channels. This fact could explain why tRK1 translocation *via* the VDAC1 dependent import pathway was not dependent on the electrochemical membrane potential ΔΨ in experimental conditions used in our study.

1.4 Impact of the TOM Complex Stability on tRK1 Import into Mitochondria

The TOM complex harbors three small proteins, Tom5, Tom6 and Tom7 that are differentially implicated in the biogenesis and the stability of this complex as well as in the mitochondrial import of preproteins (Alconada et al., 1995; Dietmeier et al., 1997). Tom5 and Tom6 exert complementary functions by promoting the early assembly steps and the stability of the TOM complex at a platform built by the SAM machinery (Becker et al., 2010). The Tom7 protein in contrast, possesses antagonistic functions to Tom5 and Tom6 by delaying the assembly of Tom40 to the SAM complex and by hindering the early assembly step of the TOM complex. Tom7 also binds to the Mdm10 protein and disturbs assembly of Tom22 during the late stage of TOM complex maturation (Becker et al., 2011). As previously shown Tom40 participates in the translocation of tRK1 across the mitochondrial membrane and for this reason we were interested to which degree the TOM complex stability could be implicated in the tRK1 import mechanism.

In order to evaluate the impact of the TOM complex stability on tRK1 translocation, *in vitro* tRK1 import assays were performed into mitochondria of wild type (WT), *tom5*Δ, *tom6*Δ and *tom7*Δ *S.cerevisiae* strains **(Fig.31)**. tRK1 internalization was not compromised in the *tom6*Δ and the *tom7*Δ strains but surprisingly import was ~3-fold higher in the *tom5*Δ strain compared to import into WT mitochondria. In every case, tRK1 import was sensitive to the VDAC1 channel blocker DIDS but inhibition at 12.5μM was ~10-fold more prominent on import into mitochondria of *tom5*Δ and *tom6*Δ strains compared to the situation in WT and *tom7*Δ strains.

The stability of the TOM complex did not seem to play a crucial role during import of tRK1. The increased DIDS sensitivity of tRK1 import in the *tom5*Δ and the *tom6*Δ mutant strains, where stability and maturation of the TOM complex are compromised, could point to a preferential use of the VDAC1 dependent import pathway in these conditions. Alternatively, it could be hypothesized that the presence of Tom5 in WT cells could influence the channeling activity of the VDAC1 protein or its oligomerization, attributing a potential regulatory function to this protein on the tRK1 import mechanism.

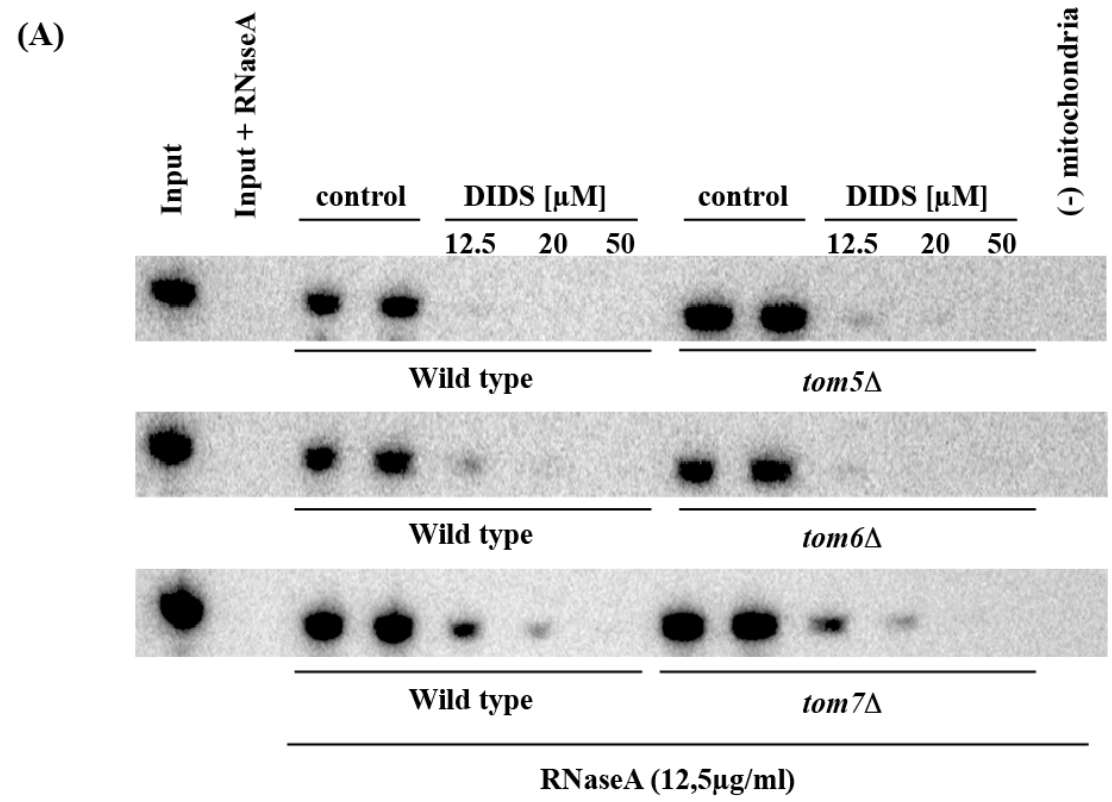

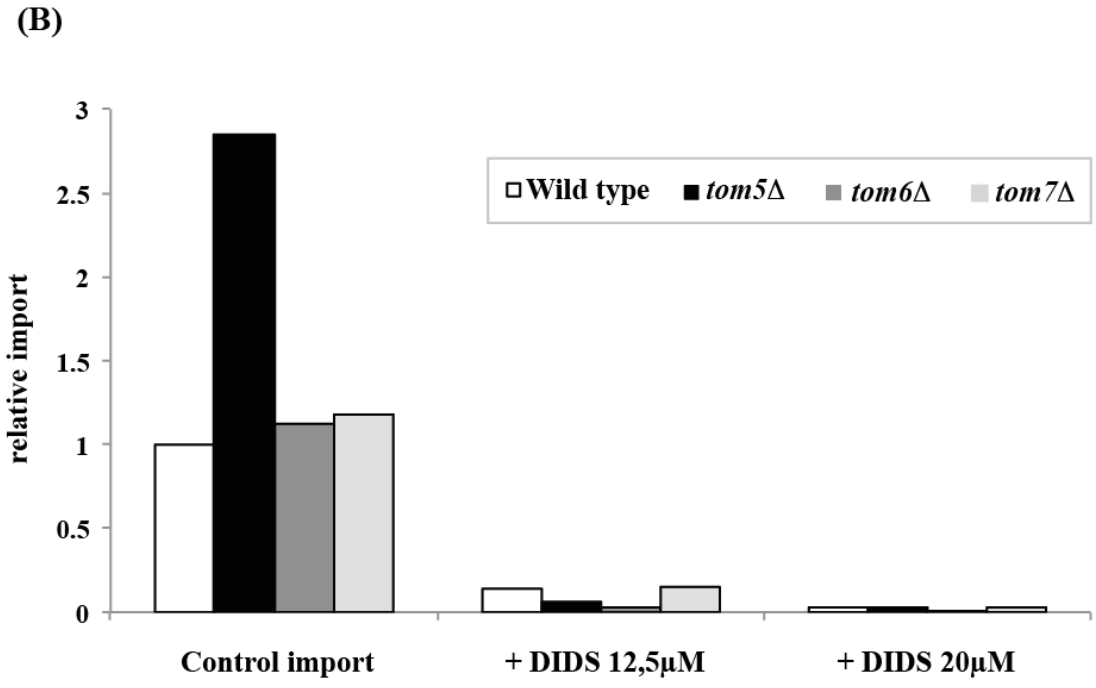

Fig.31 : Impact of the TOM complex stability on *in vitro* tRK1 import into isolated mitochondria. **(A)** Autoradiogram illustrating tRK1 import into isolated mitochondria of wild type (WT), *tom5*Δ, *tom6*Δ and *tom7*Δ *S.cerevisiae* strains in absence or presence of DIDS. Import reactions were performed for 5 minutes. **(B)** Plot illustrating relative tRK1 import into mitochondria of different *S.cerevisiae* strains (control import into WT mitochondria was set to 1 for each independent experiment).

1.5 The VDAC1 and Tom40 dependent Import Pathways show different Requirements for Import directing Protein Factors

tRNA import systems in protists, plants, mammals and fungi were shown to differ significantly in the need and the nature of import directing cytosolic protein factors (Rubio and Hopper, 2011). Early studies of tRK1 import into mitochondria of *S.cerevisiae* demonstrated a strict requirement of an intact preprotein import machinery together with a crude fraction of soluble cytosolic proteins to direct import of tRK1 (Tarassov et al., 1995). *In vitro* import of tRNAs into plant mitochondria, however, was shown to rely on the VDAC1 protein without any need for added cytosolic protein factors (Delage et al., 2003; Salinas et al., 2006). The results obtained in this work demonstrated that tRK1 translocation into mitochondria of *S.cerevisiae* can also use a VDAC1 dependent import pathway that can be complemented by translocation through the Tom40 channel.

For this reason we decided to assess the importance of the import directing proteins, enolase-2 and preMSK, in conditions where tRK1 should principally use the VDAC1 dependent import pathway. To this aim, we used a mutant *S.cerevisiae* strain encoding a Tom20 protein bearing a C-terminal deletion (*tom20*Δ_{112}) (Moczko et al., 1994). The C-terminal domain of Tom20 possesses a binding groove for the mitochondrial targeting sequences of preproteins and disruption of this part should theoretically lead to an ablation of preprotein import. Indeed, it could be shown that preMSK was not imported into mitochondria of the *tom20*Δ_{112} yeast strain **(Fig.32A)**, assuming that in these conditions tRK1 could only enter *tom20*Δ_{112} mitochondria *via* the VDAC1 dependent import pathway. *In vitro* import of tRK1 into WT and *tom20*Δ_{112} mitochondria was analyzed in control import conditions (+Eno-2/preMSK), in absence of import directing proteins factors (-Eno-2/preMSK) and in presence of DIDS **(Fig.32B+C)**. *tom20*Δ_{112} mitochondria displayed a ~4.5-fold higher import efficiency than WT mitochondria. In addition, *tom20*Δ_{112} mitochondria were even able to internalize tRK1 in absence of Eno-2/preMSK with an efficiency ~2-fold higher than WT mitochondria in control import conditions. The VDAC1 blocker DIDS was able to inhibit significantly tRK1 import in both studied strains.

The fact that deletion of the C-terminal part of the *TOM20* gene caused such an increase of tRK1 import reminded of the situation observed in the *tom5*Δ mutant, where tRK1 internalization was also significantly enhanced. These observations were, however, rather unexpected because it had been described that the VDAC1 biogenesis pathway and especially

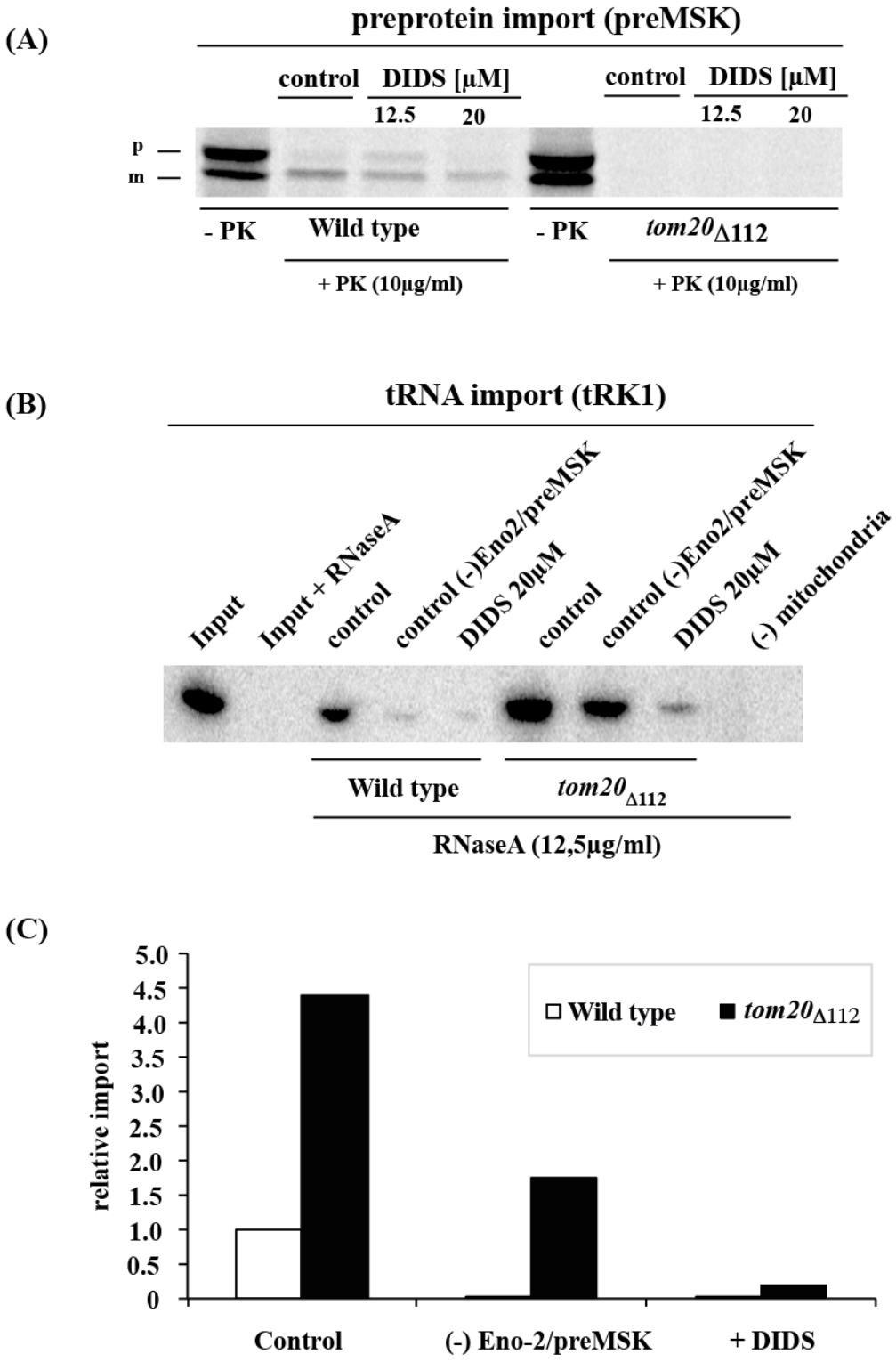

Fig.32 : The VDAC1 and Tom40 import pathways have different requirements for import directing protein factors. (A) Autoradiogram illustrating *in vitro* import of preMSK into isolated mitochondria of wild type (WT) and tom20$_{\Delta 112}$ *S.cerevisiae* strains in absence or presence of DIDS (20µM). p : precursor form of MSK (preMSK); m : mature processed form of MSK. Import reactions were carried out for 5min. **(B)** Autoradiogram illustrating *in vitro* import of tRK1 into isolated mitochondria of wild type (WT) and tom20$_{\Delta 112}$ *S.cerevisiae* strains in absence or presence of DIDS (20µM) and import directing protein factors enolase-2 and preMSK. Import reactions were carried out for 5min. **(C)** Plot showing *in vitro* import of tRK1 into mitochondria of above described strains and conditions (control import into WT mitochondria was set to 1).

the assembly of VDAC1 into oligomeric high molecular weight complexes was dependent on Tom5 and Tom20 proteins. Nevertheless, VDAC1 import and assembly was not completely absent and *tom5*Δ and *tom20*Δ mutant cells were still capable of assembling VDAC1 into oligomeric complexes, yet with efficiencies of 50% and 30% respectively compared to wild type cells (Krimmer et al., 2001). Thus, it might be possible that the Tom20 protein together with Tom5 could, in addition to their tasks in the preprotein import, exert regulatory functions on the tRK1 import pathway by changing the gating properties of VDAC1 in WT cells. The discrepancies between the previous study, where *tom20*Δ_{112} cells did not import tRK1, and this work could be explained by different experimental conditions. In the previous work a complete cytosolic soluble protein fraction was used to direct import of tRK1 into *tom20*Δ_{112} mitochondria. In these conditions, additional protein factors could alter the structural conformation of tRK1 and trigger a preferential use of the Tom40 dependent import pathway. In our above-described experiments, we used a more artificial and "minimal" *in vitro* import system with Eno-2 and preMSK as import directing protein factors, which could confer to tRK1 a conformation suitable for a favored translocation implying the VDAC1 dependent import pathway. This explanation is in agreement with the fact that tRK1 import into WT and *tom20*Δ_{112} mitochondria was sensitive to DIDS. Because preMSK is not imported into *tom20*Δ_{112} mitochondria **(Fig.32A)** it can also be concluded that tRK1 and preMSK are not imported as a complex in case of the VDAC1 dependent import pathway, a fact that has often been presumed in literature in context of tRK1 import through the preprotein import machinery (Tarassov et al., 1995; Salinas et al., 2008; Schneider, 2011). Another striking observation was the internalization of tRK1 into *tom20*Δ_{112} mitochondria in absence of the import directing protein factors Eno-2/preMSK. These results mean that, at least *in vitro*, tRK1 can be imported into isolated mitochondria *via* the VDAC1 dependent import pathway without any cytosolic protein factors, which is also the case for *in vitro* tRNA import into plant mitochondria (Delage et al., 2003). Moreover, the fact that preMSK is dispensable for tRK1 import *in vitro* is in agreement with recently published data demonstrating *in vivo* import of tRK1 into mitochondria of a *msk1*Δ *S.cerevisiae* strain (Sepuri et al., 2012).

Publication 1

(submitted)

RNA translocation across the mitochondrial membrane is mediated by alternative channels

Tom Schirtz, Geng Wang, Eriko Shimada, Mikhail Vysokikh, Nina Entelis, Michael A. Teitell, Ivan Tarassov, Carla M. Koehler

RNA translocation across the outer mitochondrial membrane is mediated by alternative channels

Tom Schirtz,[1,7] Geng Wang,[2,7] Eriko Shimada,[3], Mikhail Vyssokikh,[1,4] Nina Entelis,[1] Michael A. Teitell,[3,5,6] Ivan Tarassov,[1,*] Carla M. Koehler[2,5,*]

[1]"Génétique Moléculaire, Génomique, Microbiologie" (GMGM), UMR 7156, Université de Strasbourg - CNRS, Strasbourg 67084, France.

[2]Department of Chemistry and Biochemistry, University of California at Los Angeles, CA 90095, USA.

[3]Department of Pathology and Laboratory Medicine, University of California at Los Angeles, CA 90095, USA.

[4]Belozersky Institute of Physico-Chemical Biology, M. V. Lomonossov Moscow State University, Moscow 119991, Russia.

[5]Molecular Biology Institute, University of California at Los Angeles, CA 90095, USA.

[6]Jonsson Comprehensive Cancer Center, Broad Stem Cell Research Center, California NanoSystems Institute, University of California at Los Angeles, CA 90095, USA.

[7]These authors contributed equally to this work

[*]Correspondence: i.tarassov@unistra.fr (I.T.), koehler@chem.ucla.edu (C.M.K),

Running Title: TOM and VDAC channels import RNA into mitochondria

Keywords: mitochondria / RNA import /porin / TOM / outer membrane / translocation channel

SUMMARY

Mitochondria are an essential and semi-autonomous organelle of eukaryotic cells that interact continuously with nuclear and cytosolic compartments with functions ranging from oxidative phosphorylation to apoptosis. Numerous micro- and macromolecules are imported into mitochondria, including small non-coding RNAs, although the mechanisms of RNA translocation across the double mitochondrial membranes are not resolved and may vary between species. Here, we report the first mechanistic step of RNA translocation across the mitochondrial outer membrane by analysing two main pore-forming machineries, the translocase of the outer membrane (TOM)-related proteins and the Voltage Dependent Anion Channel (VDAC or porin). In these studies, complementary experimental models are used including isolated VDAC reconstituted in artificial lipid vesicles, purified mitochondrial outer membranes, isolated yeast and human mitochondria, and finally intact yeast and human cells, along with naturally imported or with artificially targeted RNAs. We demonstrate that both TOM and VDAC machineries are used to internalize RNAs independently or in concert, and potentially with different substrate specificities. Thus, transport of RNA across the outer membrane displays a remarkable flexibility.

INTRODUCTION

Mitochondria are intracellular organelles within eukaryotic cells that are responsible for a large number of essential and non-essential processes, including respiration, ATP-generation, synthesis of amino acids, oxidation of fatty acids, regulation of reactive oxygen species, apoptosis, and others (Scheffler 2001b; Scheffler 2001a). Mitochondria are also implicated in the aging process and in many grave, mostly incurable diseases (Larsson and Clayton 1995; Wallace 1999; Wallace and Lott 2004). A unique feature of this organelle is protection by a double membrane and the presence of a second cellular genome, the mitochondrial genome

(mtDNA), in the inner matrix compartment. mtDNA, although different in organization and size among species, codes for only a minor part of the macromolecules present in the organelle. The vast majority of mitochondrial proteins are encoded within the nucleus and targeted, or imported, into mitochondria by mechanisms studied in great detail (Pfanner et al. 1992; Neupert and Herrmann 2007; Chacinska et al. 2009). Much less is known about RNA import, although this pathway is universal. Imported RNAs have been identified in the mitochondria of protozoans, plants, fungi, and animals. In contrast to mitochondrial protein import, RNA import mechanisms and the nature of the imported RNAs seems to differ from one system to another, suggesting that RNA import pathways may have developed independently several times during evolution (Salinas et al. 2008). The only common feature for all RNA import events described so far is the necessity of energy in the form of ATP hydrolysis and maintenance of the mitochondrial inner membrane (IM) electrochemical potential. Additional properties of RNA import mechanisms show an apparent diversity. Some RNA substrates require specific import factors. For example, enolase and cytosolic precursors of aminoacyl-tRNA synthetases are required for $tRNA^{Lys}$ import in yeast (Tarassov et al. 1995b; Entelis et al. 2006) and rhodanese and the precursor of mitochondrial ribosomal protein MRP-L18 are required for 5S rRNA import in human cells (Smirnov et al. 2010; Smirnov et al. 2011a). Nevertheless, at the current state of knowledge, one cannot rule out common molecular mechanisms involving different protein factors (Salinas et al. 2008; Rubio and Hopper 2011; Smirnov et al. 2011a).

Arguably, the most intriguing step of mitochondrial RNA import is the translocation of negatively charged RNAs across the double mitochondrial membrane, which is counter-current to the electrochemical gradient. In plants, which import a subset of mitochondrial tRNAs, porin (or Voltage-Dependent Anion Channel, VDAC) was implicated in RNA translocation at the outer membrane, and the TOM proteins constituting the GIP (General

Insertion Pore) could also be involved (Salinas et al. 2006; Sieber et al. 2011). In yeast, the TIM/TOM machinery needed to be intact and functional for $tRNA^{Lys}$ import (Tarassov et al. 1995a), although there is no direct evidence that RNAs transit through the pre-protein channel. Similar *in vitro* requirements were found for natural 5S rRNA and artificial tRNA import in human mitochondria (Entelis et al. 2001a). Finally, endogenous PNPASE localized in the intermembrane space (IMS) was recently shown to regulate the import of the RNA component of RNase P (*H1* RNA), *MRP* RNA, and *5S* rRNA into mammalian mitochondria and, through ectopic expression, to regulate RNA import into yeast mitochondria (Wang et al. 2010). All of these studies combined suggest either differences in RNA import mechanisms in different systems or they reveal similar mechanisms with different component requirements. To address this central mechanistic issue, we compared yeast and human systems for mitochondrial RNA import and, by exploiting a large range of techniques and model systems *in vitro* and *in vivo*, demonstrate that small RNAs imported into mitochondria either naturally or in engineered systems can cross the outer membrane (OM) by using one or both TOM and VDAC channels. Our results establish the flexibility of the mitochondrial RNA import pathway and indicate a closer evolutionary relationship between these mechanisms among species than previously anticipated.

RESULTS

VDAC and Tom Proteins are Candidate RNA Translocators

It was previously shown that yeast and mammalian mitochondrial outer membrane (OM)-associated proteins sensitive to protease treatment are essential for RNA internalization (Tarassov et al. 1995a; Entelis et al. 2001a). To examine whether PNPASE affects this requirement, yeast mitochondria with or without ectopic PNPASE expression (Wang et al. 2010) were isolated and treated with trypsin in an isotonic buffer. Trypsin degraded the OM

protein Tom70p but not the mitochondrial intermembrane space (IMS) protein Mia40p, indicating that mitochondrial integrity was not compromised (Figure 1A). Radiolabeled human *H1* RNA was imported into protease treated or untreated mitochondria. PNPASE expression in untreated mitochondria resulted in a ~4-fold increase in *H1* import, following nuclease treatment to remove nonimported RNA, as anticipated (Figure 1B) (Chen et al. 2006; Wang et al. 2010). In contrast, trypsin treatment of intact mitochondria decreased *H1* RNA import by 95% in PNPASE-expressing mitochondria and 75% in vector-only mitochondria, (Figure 1B). These results strongly suggest that one or more mitochondrial OM proteins are required for PNPASE-augmented RNA import into isolated yeast mitochondria.

We postulated that proteins involved in RNA translocation have RNA-binding properties. To screen for yeast mitochondrial membrane proteins that interact with a naturally imported RNA, North-Western assays were performed on mitochondrial protein extracts from wild type (WT) and *Δpor1* strains in the presence of radiolabeled aminoacylated $tRNA^{Lys(CUU)}$ (tRK1). Por1p was initially chosen because of the VDAC requirement in plants (Salinas et al. 2006; Sieber et al. 2011). Autoradiograms showed distinct banding patterns between the two yeast strains. This was followed by a systematic nano-LC MS/MS mass spectrometry analysis of all potential zones containing RNA-interactants (Figure 1C, Table S1). Identified mitochondrial proteins were sorted according to their localization within the OM, IMS, inner membrane (IM), and matrix and further assessed for the presence of potential nucleotide-binding motifs in each sequence. We subsequently focused on mitochondrial OM proteins as the first step in the RNA import pathway. Our analysis revealed that the main OM proteins potentially interacting with tRK1 in the WT strain were Por1p and small receptor protein Tom5p, whereas in mitochondria from the *Δpor1* strain, only Tom40p, Tom22p, and Tom20p components of the TOM complex were detected (Table 1 and S2). We therefore examined two channels, Tom40p and Por1p in greater detail.

tRNA Import into Reconstituted OM Vesicles is *via* the VDAC or TOM Channels

A simplified model system for assessing RNA import independent of transcript processing was developed with mitochondrial OM vesicles (OMV) derived from different yeast strains, as described in the Experimental Procedures. During the isolation and purification of OMV, aliquots from the following fractions were separated for analyses of purity: M, the initial swollen mitochondrial suspension in 10 mM Tris HCl; IM/M, the IM pellet including mitochondrial matrix after 12,000 x *g* sedimentation; and OMV, the OM fraction. The activity of marker enzymes in these 3 fractions was measured, normalized to protein content, and their distribution is listed in Table S3. In the OMV fraction citrate synthase (CS) activity was not detectable, whereas CS activity was present at similar levels in M and IM/M fractions for all yeast strains examined. Succinate dehydrogenase (SDH) activity was also distributed between the M, IM/M, and OMV fractions, with only 0.5% to 1.5% of the total SDH activity present in the OMV fraction, consistent with previously reported results (Mihara et al. 1982). Indeed, Western blots show that Por1p is present at about the same level in fractions M and OMV for both WT and Δ*por2* yeast strain used as control (Figure S1).

Functionality of the OMV porin and TOM channels was confirmed with different tests (see detailed description in Supplementary Material & Methods and in Figures S2-S5A). Time-dependent tRK1 import into OMV showed linear transport kinetics (Figure S5B) for the time interval tested. After validation of the OMV model, *in vitro* import of tRK1 into isolated OMV was studied (Figure 2A). The addition of the competing import substrate, cyt b_2-DHFR plus methotrexate to block transport, into WT and *Δpor1* OMV inhibited tRK1 import by 50%, and the addition of the porin inhibitor DIDS into WT and *Δpor1* OMV reduced tRK1 import by 60%. Combining the two inhibitors increased inhibition to 90% and 80% in *Δpor1* and WT OMV, respectively. Taken together, these OMV import assays strongly suggest that Por1p and the Tom40 channel both mediate tRK1 transport.

To further study the role of different channels in tRK1 import, purified Por1p (Figure S6) was reconstituted into small unilamellar vesicles (SUV). The intactness and stability of SUV during the tRK1 import assay was tested as described for OMV (data not shown) and tRK1 import was compared with both OMV and WT mitochondria (Figure 2B). DIDS efficiently inhibited tRK1 uptake whereas cytb_2-DHFR addition was ineffective because Tom40 was absent in the reconstituted SUV. In contrast to the 4-fold inhibition in OMV and WT mitochondria, DIDS reduced tRK1 import by 15-fold.

tRNA Import into Yeast Mitochondria is Through the Porin or TOM Channels

To evaluate open versus closed candidate import channels, mitochondria were obtained from WT and *Δpor1* yeast strains. To test functional integrity of the isolated mitochondria, respiration was quantified by measurements of cyanide-resistant oxygen consumption for different respiratory substrates (Table 2). Our data suggest that Por1p is essential for metabolite transport into mitochondria, which is in agreement with OMV and SUV studies on hexokinase substrate availability. However, even without the main metabolite channel Por1p, substrate oxidation in mitochondria from the *Δpor1* strain is still very efficient, confirming studies that showed metabolite import can be partially recovered through alternative OM β-barrel protein channels (see Discussion). Indeed, the intactness of the OM for mitochondria from both strains was found comparable and calculated values of the membrane integrity were >85%, which corresponds to essentially intact mitochondria preparations. Taken together, comparable data for respiratory capacity, coupling, and intactness of the OM for mitochondria from WT and *Δpor1* strains confirm that the two strains are suitable for further studies of tRK1 import.

We next examined the involvement of Por1p in mitochondrial tRNA import with isolated WT and *Δpor1* mitochondria (Figure 3A).Consistent with the OMV data in the *Δpor1*

mutant, the import of tRK1 is reduced to ~20% of the WT level. To extend these *in vitro* assays *in vivo*, the import of tRK1 into mitochondria of the corresponding strains was measured by Northern analysis (Figure 3B). Indeed, tRK1 import was markedly reduced in the mutant strains, especially in the *Δpor1* strain, in agreement with the *in vitro* results. Together with prior data implicating the TOM complex in tRK1 import (Tarassov et al. 1995a; Entelis et al. 2001a), our analysis herein favors the participation of both channels in the RNA import pathway.

Replicating OMV and SUV studies in isolated yeast mitochondria, the importance of Por1p was analyzed by the addition of the specific porin inhibitor DIDS, whereas the role of Tom40p was assessed by blocking with the precursors cytochrome (cyt) b_2-DHFR. We first established the amount of cyt b_2-DHFR that was needed to inhibit protein import into the matrix by blocking the import of pre-MSK protein (Figure 4A, right panel). Pre-MSK import was impaired by ~10-fold and ~5-fold into WT and *Δpor1* mitochondria, respectively (Figure 4A, left panel). tRK1 import into isolated WT and *Δpor1* mitochondria with or without DIDS and/or cyt b_2-DHFR, respectively, was decreased by 60% in *Δpor1* mitochondria, while DIDS treatment inhibited import by 80% in WT mitochondria and an additional 20% in *Δpor1* mitochondria (Figure 4A, right panel). Finally, cyt b_2-DHFR addition blocked import in combination with DIDS treatment in all strains (Figures 4B and 4C). These results show that Por1p is the major channel for tRK1 translocation, while in the absence of Por1p, the Tom40p channel supports RNA import.

Whereas Por1p-mediated tRK1 import through the OM is likely independent from the electrochemical membrane potential ($\Delta\Psi$) of the IM, its dependence on ATP in the mitochondrial matrix is less clear. In all systems examined to date, mitochondrial tRNA import was dependent on energy provided by ATP hydrolysis (reviewed in Entelis et al. 2001b; Salinas et al. 2008). Interestingly, the $\Delta\Psi$, which is indispensable for pre-protein

import (Schleyer et al. 1982; Eilers et al. 1987), has not been thoroughly evaluated for its role in RNA import and the published data appears inconclusive. Therefore, the import of tRK1 into isolated yeast mitochondria was examined with or without added ATP and/or in presence and absence of the ΔΨ. The ΔΨ was depleted by performing import reactions in the absence of a substrate, such as succinate, or by addition of the protonophore FCCP. These assays were also performed with or without DIDS to evaluate this RNA import channel. The data show that ATP exclusion blocked tRK1 import, even with a high ΔΨ (Figure 4D). Conversely, ATP addition enabled tRK1 import in the absence of ΔΨ, possibly through unblocked Por1p or, Tom40 in the case of *Δpor1* mitochondria.

PNPASE-augmented RNA Import into Yeast Mitochondria is *via* the VDAC Channel

The import of human *H1* RNA can be augmented in yeast mitochondria, both *in vitro* and *in vivo*, by ectopic expression of the human *PNPT1* gene, encoding PNPASE, in yeast (Wang et al. 2010). To identify OM proteins required for this non-physiologic import, the *in vitro* import assay was performed on mitochondria isolated from specific yeast deletion strains. Guidance for strain usage was provided by prior published results (Salinas et al. 2006; Salinas et al. 2008) and those described above. The data show that the import of *H1* RNA is markedly impaired in *Δpor1* PNPASE-expressing yeast mitochondria (Figures 5A and 5C), whereas import is essentially unaffected in *Δtom70* PNPASE-expressing yeast mitochondria compared to WT controls (Figures 5B and 5D). The non-involvement of the Tom70p receptor is consistent with results obtained for tRK1 import previously (Tarassov et al. 1995a), and, more importantly, is in good agreement with the importance of porin for RNA translocation. These data strongly suggest that the porin channel is used for PNPASE-augmented RNA import into yeast mitochondria, in the same way that the porin channel is used to import tRK1 without ectopic PNPASE expression.

H1 RNA Import in Human Mitochondria Proceeds Through VDAC

To determine whether the channels for RNA import into yeast mitochondria are similar in mammalian mitochondria, the case of *H1* RNA import was investigated. Mitochondrial RNAs (mtRNAs) are transcribed as long polycistronic transcripts, which then undergo processing to generate individual mRNAs, tRNAs and rRNAs (Bonawitz et al. 2006). One of the RNA processing steps requires the RNase P enzyme, which contains *H1* RNA as one of its essential components (Thomas et al. 2000; Kikovska et al. 2007; Wang et al. 2010; Mercer et al. 2011). *VDAC* involvement was assessed in HeLa cells using a shRNA approach. Of the three VDAC proteins (VDAC1, 2, 3) in human cells, VDAC1 is the most abundant isoform in almost all cell types (Yamamoto et al. 2006; De Pinto et al. 2010). A reproducible ~60% reduction in VDAC1 steady-state protein expression was achieved using shRNA (Figure 6A). Mitochondria from WT and VDAC-knockdown HeLa cells were isolated for import assays using radiolabeled *H1* RNA. A ~2-fold reduction in the amount of imported *H1* RNA was detected in the VDAC1-knockdown mitochondria compared to a WT control (Figure 6B). This result, however, could be from a general effect of VDAC1 knockdown on mitochondrial function. To exclude this possibility, an independent antibody-blocking approach against VDAC1 was used in the import assay with WT mitochondria. Mitochondria were pre-incubated with VDAC1 antibody, TOMM40 antibody or control buffer only. The import assay was then performed using antibody-treated or untreated mitochondria. WT mitochondria exposed to VDAC1 antibody showed a ~2 fold reduction in imported *H1* RNA compared to control mitochondria (Figure 6C), suggesting that human VDAC mediates RNA import into mammalian mitochondria. Antibody against TOMM40 inhibited, although not completely, the import of a protein precursor Su9-DHFR into mitochondria, showing that channel blocking was partially effective. At this level of channel inhibition, we did not detect a marked effect on *H1* RNA import into mitochondria (Figure 6C). This result could suggest

the preferential use of the VDAC-channel for RNA translocation and/or substrate specificity of the two channels for distinct types of RNA. To confirm that VDAC directly mediates *H1* RNA import, a co-immunoprecipitation assay was performed using antibodies against either VDAC or TOMM40. Radiolabeled *H1*, or a control non-imported mitochondrial-encoded $tRNA^{Lys}$ precursor, was incubated with isolated HeLa mitochondria and the samples were UV-crosslinked. Following this, mitochondria were lysed and VDAC or TOMM40 were isolated by immunoprecipitation. When *H1* RNA was used as the import substrate and VDAC1 antibody was used for immunoprecipitation, the radiolabeled RNA copurified with VDAC1 (Figure 6D). To a lesser extent, the radiolabeled RNA also copurified with TOMM40, suggesting preferential use of a VDAC1-containing channel for *H1* RNA import. These results support a direct interaction of the imported RNA with the VDAC channel, and to a lesser extent the TOMM40 channel, which are in agreement with both *in vivo* and *in vitro* import assays.

Since the accumulated data in yeast and mammalian mitochondria indicate that VDAC1 is part of the OM RNA import channel, we predict that VDAC1 knockdown would reduce *H1* RNA in mitochondria and thereby cause incomplete processing of long mtRNA transcripts. Therefore, mitochondrial *H1* RNA was quantified in WT and VDAC1-knockdown mitochondria in intact cells using RT-PCR. A markedly greater amount of *H1* RNA was detected in WT compared to VDAC1-knockdown mitochondria (Figure 7A). mtRNA transcript processing was then examined by RT-PCR using primers that annealed to mRNAs in long transcripts that were separated by two or three tRNAs. For example, *COX1* and *COX2* are separated by $tRNA^{Ser}$ and $tRNA^{Asp}$, whereas *ND4* and *ND5* are separated by $tRNA^{His}$, $tRNA^{Ser}$ and $tRNA^{Leu}$ in long mtRNA transcripts (Figure 7B). Increased amounts of partially or completely unprocessed mtRNA precursor transcripts were detected in VDAC-knockdown compared to WT mitochondria (Figure 7B). This increase in partially or completely

unprocessed mtRNA long transcripts with VDAC1 knockdown further supports the involvement of VDAC in the import of small nucleus-encoded RNAs, in this case *H1* RNA, into mammalian mitochondria.

Prior studies showed that PNPASE knockdown in mammalian cells impaired nucleus-encoded small RNA import, which reduced oxidative phosphorylation and disrupted the mitochondrial network structure (Chen et al. 2006; Wang et al. 2010). These mitochondrial features were also examined in VDAC1-knockdown HeLa cells. Similar to PNPASE-deficient cells, a ~1.5 to 2-fold decrease in the steady-state amount of mitochondrion-encoded COX2 protein was detected in the VDAC1-knockdown cells, whereas no strong difference in the amount of TOMM40 or PNPASE, mitochondrial proteins encoded in the nucleus, was detected (Figure S7A). This decreased steady-state COX2 abundance with reduced VDAC1 could result from impaired translation of mitochondrion-encoded proteins. An in vivo mitochondrial translation assay showed that all mitochondrial-encoded proteins, including COX2, in VDAC1-knockdown cells were present at ~50% of the WT control level (Figure S7B). In addition, MitoTracker green staining showed fragmentation of the mitochondrial network in the VDAC1-knockdown cells, similar to the fragmentation detected previously when RNA import was impaired by PNPASE knockdown (Figure S7C). Finally, VDAC1-knockdown cells were examined for oxygen consumption and showed ~70% of the respiration rate of WT control cells (Figure S7D). Combined, these results indicate that the VDAC1-containing OM channel directly mediates RNA import into mitochondria and that VDAC1 reduction leads to defects in mitochondrial function and structure that are similar to those seen by PNPASE reduction.

DISCUSSION

Multiple Pathways or a Conserved RNA Import Pathway with Distinct Substrate Requirements?

RNA import into mitochondria has been described in a wide variety of species including protists (*Toxoplasma*, *Tetrahymena*, *Chlamydomonas*, trypanosomatids, and yeast), higher plants (liverwort, tobacco, potato, bean, *Arabidopsis*, wheat, and maize) and animals (Entelis et al. 2001b), making this process at least quasi-universal amongst eukaryotes. It is generally thought that mitochondrial RNA import mechanisms developed independently in different taxa, and therefore it would be difficult to arrive at a universal mechanism for this process (Schneider and Marechal-Drouard 2000). Common features include an ATP requirement and the involvement of membrane-bound proteinase-sensitive receptors. ATP may be crucial at different steps of translocation starting from release of tRNA-precursor protein complex from cytosolic partners like enolase upon binding to the receptors on the mitochondrial surface. Upon translocation, ATP might be essential for two aspects – providing energy needed to deliver the polyanionic RNA molecule to the negatively-charged mitochondrial matrix and for functioning mitochondrial chaperones facilitating the uptake of precursor proteins to mitochondria. Indeed, the ATP/ADP ratio in mitochondria modulates the state of the IM adenine nucleotide translocator that can form a tight inter-membrane complex with porin at contact sites where it regulates the gating properties of VDAC (Antos et al. 2001). Recent critical examination of the data accumulated from various species has resulted in significant progress in understanding the driving forces and universal features of this process (Salinas et al. 2008; Duchene et al. 2009; Rubio and Hopper 2011). However, tRNA import, although representing the most common type of RNA delivery into mitochondria, appears somewhat special and thus not sufficient to establish a general RNA import mechanism. Recent results

for 5S rRNA, *H1* RNA, and *MRP* RNA mitochondrial import reported from various vertebrate species (Yoshionari et al. 1994; Magalhaes et al. 1998; Puranam and Attardi 2001; Wang et al. 2010) provide an opportunity to fill in key knowledge gaps and take a fresh look at the process of RNA import with an enhanced level of understanding (Smirnov et al. 2008; Smirnov et al. 2010; Smirnov et al. 2011a). Data from these studies suggest that imported RNAs have to escape cytosolic channeling and be transferred to the mitochondrial surface. To accommodate these two prerequisites, both cytosolic and mitochondrial proteins are likely involved. Furthermore, in several cases the RNA itself undergoes conformational changes upon interaction with these proteins to enable its trafficking and import (Smirnov et al. 2008; Kolesnikova et al. 2010b; Smirnov et al. 2011a). In situations where the targeting step of various RNA molecules appears to share much more common features than formerly suggested, we propose here that the translocation step, in which the transport of RNA across the double mitochondrial membrane occurs, shows an even higher level of mechanistic conservation between species. This idea is supported by protein content of mitochondrial membranes, which is relatively conserved amongst species, and by the observation that additional micro- and macromolecular transport events, including metabolite transport, protein import, and ionic channeling appear mechanistically conserved in all eukaryotes.

To date, three main translocation machineries have been implicated in mitochondrial RNA import: 1) the TOM/TIM protein import apparatus (yeast, plants); 2) the VDAC/porin metabolite transport system (plants); and 3) a suggested RNA-specific complex, termed RIC, composed of several unrelated proteins in trypanosomatids (for review, see Salinas et al. 2008; Rubio and Hopper 2011); recently, identification of this complex was subject to a critical discussion (Schekman 2010). We considered the controversial data for involvement by the RIC trypanosmal system (Schekman 2010) and decided to focus our efforts on the first two systems. This focus was further justified by the recent suggestion that both systems may

be evolutionarily, or at least structurally, related, putting VDAC/porins and Tom40 proteins in the same group of membrane inserted β-barrel transporters (Zeth 2010). Also, it was shown that Tom40 can compensate for the lack of porin in metabolite transport across the OM (Anthos et al, 2001). In the present study, we showed that both systems could transport small non-coding RNAs across the outer mitochondrial membrane, but with different substrate preferences and specificities.

The use of VDAC1-containing channels for mitochondrial RNA import in both yeast and mammalian cells indicates that specific features, if not most of the pathway, are conserved, providing a solid starting point for complete characterizations of the entire RNA import pathway. With the OM channels identified, a key next step would be to decipher how RNAs cross the mitochondrial IM. It would also be of high interest to determine the substrate selectivity and preferences of different OM channels and potentially different pathways. Whether there is one single pathway with different tributaries or multiple individual pathways provides fertile ground for continuing investigations.

How do RNAs Cross the Mitochondrial OM and what happens thereafter?

Both VDAC and Tom40 proteins form outer mitochondrial transmembrane channels. Folded RNAs seem possible to transport through the TOM channel, whose diameter was estimated as ~2.5 nm (Ahting et al. 1999; Ahting et al. 2001). In striking contrast, the possible involvement of the porin channel in folded RNA import appears sterically enigmatic, since this channel has been established as a transporter for lower molecular weight metabolites. Therefore, RNAs imported through the VDAC channel are most likely unfolded or thoroughly restructured. Since VDAC is an anion channel, it may facilitate the unfolding of negatively charged RNA substrates. This would be interesting and add a layer of complexity and selectivity to the preference of specific RNAs through specific channels. Alternatively, we opine that more

intricate rearrangements take place that may involve formation of new oligomeric complexes of porins capable of facilitating RNA translocation. The first possibility relies on the known properties of porins to change their conductivity state upon interacting with IM proteins, such as the adenine nucleotide translocator (Dihanich et al. 1987; Benz et al. 1990; Benz and Brdiczka 1992). However, our procedure for OMV generation excludes IM proteins, making this possibility less likely. In this context, Tom40 proteins maintain functionally active VDAC complexes through interactions with the small adaptor Tom proteins, Tom5, Tom6, and Tom7 (Becker et al. 2010). One can hypothesize that one of these proteins may influence OM permeability. Such a hypothesis would be in agreement with reports in which Tom5 was required for porin-related functions, especially for directing oligomer formation (Mannella 1982; Krimmer et al. 2001; Hoogenboom et al. 2007).

Assuming that small RNA transport is sterically possible through both channels by adapting the RNA structure (Entelis et al. 2006; Kolesnikova et al. 2010a; Smirnov et al. 2010; Smirnov et al. 2011b), the following question arises - what is the driving force for delivering polyanion molecules into a negatively charged compartment? We recently performed experiments by crosslinking 5-bromouridine labelled tRK1 with proteins during translocation, an approach commonly designed as CLIP (Cross-linking and Immuno precipitaton). Preliminary anaylses (not shown here) obtained identified, in addition to Tom41 and VDAC1, other candidate proteins including mtHsp60, Hsc82, Pam18, Tom71, Phb1 and Phb2. We therefore tentatively hypothesize that vectorised RNA transfer may be based on irreversible ATP hydrolysis by motor proteins and chaperones in the matrix. For the Tom40-directed pathway, we suggest the involvement of a compartmentalised system of protein import. Once Tom71 binds the carrier preprotein-RNA complex, it passes through the OM in a folded state. The RNA moiety is hidden from interactions directly with channels comprised of Tom40 and Tim23 and bound to Pam18 during this first irreversible ATP-driven motor

protein translocation. Next, the RNA is complexed with mitochondrial HSP60 and HSC82 chaperones, with the carrier preprotein undergoing a second ATP-dependent unfolding step. At this stage, the RNA probably is freed and subsequently binds to additional interactants. For the VDAC1-mediated pathway, we suggest a limited free diffusion mechanism where two channels cooperate and facilitate delivery of free RNA or RNA in a complex with protein. Once the RNA is recognized by an interior sensor of VDAC as a polyanion, labelled RNA is bound by VDAC1, possibly by a loose attachment to the nucleotide binding mojety of VDAC1. With dissociation and diffusion into the IMS, the RNA might then bind the 250nm channel of the IM composed of prohibitins 1 and 2. In fact, it has been established that this complex can fulfil the task of a chaperone and direct substrate translocation by energy-dependant conformational changes (Osman et al. 2009). The last step upon arrival in the matrix through the PHB1/2 channel could be ATP hydrolysis-dependent unfolding and maintenance involving matrix chaperones, with subsequent binding of the RNA to its functional interactants, each different for each imported RNA species. Such a sequence of events, schematically represented in Fig. S8, is for the moment still purely hypothetical and awaits further experimentation for validation, but is in reasonable agreement with currently available data and provides directly testable hypotheses for evaluation.

MATERIALS AND METHODS

Strains, Plasmids, Antibodies and Growth Conditions

WT *Saccharomyces cerevisiae* strains W303 (*MAT*a RNAs) and BY4742 (*MATα*) were used for the isolation of mitochondria. Deletion mutant strain *Δpor1* based on the genetic background of BY4742 were purchased from Euroscarf (http://web.uni-frankfurt.de/fb15/mikro/euroscarf/). For mitochondria isolation purposes, yeast cells were grown on corresponding YPGlyGluc media (yeast extract 1%, peptone 2%, glycerol 4% and

glucose 0.5%) to reach an OD_{600nm} = 3.5 - 4. *E.coli* BMH 71-18 strain was transformed with pUHE73-1 plasmid, containing the cyt b_2-DHFR gene, and grown overnight in LB (yeast extract 0,5%, peptone 1%, NaCl 0,5%) in presence of 100µg/ml ampicillin. Prior to IPTG induction, cells were diluted and grown to OD_{600nm} = 0.8. Other yeast strains were previously described (Dihanich et al. 1987; Koehler et al. 1998). Both strains were grown and maintained in synthetic complete media minus the amino acid for marker selection. HeLa and HEK293 cells cultured in DMEM supplemented with 10% fetal bovine serum. Stable VDAC1 knockdown cell lines were established by transfection of HEK293 cells with VDAC1 shRNA construct, VSVg and Hit60 packaging vectors using BioT reagent (Bioland Scientific LLC). The harvested viruses were used to infect HeLa cells and cells were selected with 3 µg/mL puromycin. All the PNPASE, Su9-DHFR and H1 RNA plasmids were previously described (Chen et al. 2006; Rainey et al. 2006; Wang et al. 2010). The shRNA vectors for VDAC1 silencing were purchase from Sigma. The following dilutions were used for each antibody: PNPASE (Chen et al., 2006; Rainey et al., 2006), Porin (Abcam), VDAC1 (Abcam), TOMM40, COX2 (Santa Cruz Biotech.), and HRP-conjugated mouse and rabbit secondary antibody (Thermo Fisher Scientific).

Mitochondrial RNA Purification

Mitochondria were isolated based on a published procedure by *Daum et al. 1982* with slight modifications and its functional integrity was approved (for details see Supplemental methods). Mitochondria were treated with 25 µg/mL S7 micrococcal nuclease at 27°C for 30 min in nuclease buffer (0.6 M Sorbitol, 20 mM $MgCl_2$, 5 mM $CaCl_2$, 20 mM Tris-pH 8.0). The reaction was stopped by addition of 20 mM EGTA. The mitochondria were then solubilized in SDS buffer (100 mM NaCl, 1 % SDS, 20 mM Tris-Cl pH 7.4) at 65°C for 5 min. RNA was extracted using TRIzol (Invitrogen) reagent, treated with DNase I (Roche) for

1hr at 37°C in the manufacturer supplied buffer and DNase I was heat inactivated at 65°C for 10 min.

Purification of Recombinant Proteins

The recombinant enolase-2 was purified according to the procedures described in Entelis et al. (2006). The recombinant fusion protein cytb_2-DHFR, consisting of the first 167 amino acids of the *S. cerevisiae* cytochrome b_2 and mouse dihydrofolate reductase, was overexpressed from pUHE73-1 plasmid in *E.coli* BMH 71-18 strain by induction for 1h at 37°C in presence of 1 mM IPTG. Inclusion bodies containing cyt b_2-DHFR were purified according to Koll et al. (1992). A crude fraction of cyt b_2-DHFR, obtained from inclusion bodies was further purified by passage through a pre-packed PD10 desalting column (GE Healthcare) to exchange the buffer to 20 mM MES-KOH pH 6, and by subsequent cation exchange chromatography on Mono-S column (Pharmacia Biotech) with the AKTÄ FPLC system (Amersham Pharmacia Biotech). A single protein peak corresponding to cyt b_2-DHFR was detected at OD_{280nm} and eluted between 300-350 mM on a linear (from 0 to 500 mM) KCl gradient. Peak fractions of 0.5 ml size were collected and combined after verification of purity on SDS-PAGE, aliquoted and stored at –80˚C. The recombinant precursor of *S. cerevisiae* mitochondrial lysyl-tRNA synthetase, preMSK, was purified in its native form from the *E.coli BL21* strain transformed with the expression vector pET3 (Invitrogen).

Crosslinking and Immunoprecipitation Assay

Immediately after import, the imported RNA and mitochondrial proteins were UV crosslinked (1.8 J in Stratalinker). The mitochondria were then solubilized in lysis buffer (150 mM NaCl, 10% glycerol, 1% Triton X-100, 2 mM EDTA, 20 mM Tris-Cl pH 8.0) containing protease inhibitor (Roche). Insoluble materials were removed by centrifugation at 20,000 *g* for 30 min

at 4°C. The lysates were pre-cleared with protein A-Sepharose beads (Pharmacia) by incubating for 1 hour at 4°C, and immunoprecipitated using 5 μg of antibody conjugated to protein A-Sepharose beads for 2 hours at 4°C. The beads were then washed 6 times with lysis buffer. The immunoprecipitate was boiled in SDS loading buffer, separated on SDS-PAGE and analyzed by autoradiography.

Synthesis of $tRNA^{Lys(CUU)}$ (tRK1), Radioactive Labelling and Aminoacylation

The plasmid used for *in vitro* transcription of the $tRNA^{Lys(CUU)}$ (tRK1) gene was constructed by cloning the corresponding PCR product of the tRNA gene in a pUC119 vector under the control of a T7 promoter. The gene was cloned in order to have a *Bst NI* restriction site at its 5' end yielding a 3'CCA-OH terminus after digestion. T7 transcription was carried out using the T7 RiboMAX™ Large Scale RNA production system (Promega) and the corresponding T7 transcript (tRK1) was gel purified on a denaturating 10% 8M Urea PAGE. tRK1 was 5' labelled with γ^{32}P-ATP using T4 polynucleotide kinase (10U 1h 37°C) and gel purified on a denaturating 10% 8M Urea PAGE. Prior to aminoacylation, tRK1 was refolded by heating at 90°C for 1' in presence of 10mM $MgCl_2$ and cooling down at room temperature for 15'. Subsequent aminoacylation was carried out in aminoacylation buffer (100mM Tris-HCl pH7.5, 30mM KCl, 10mM $MgCl_2$, 2mM ATP, 1mM DTT, 0.05mM Lys) for 10' at 37°C in presence of 1nM recombinant lysyl-tRNA-synthetase (KRS). Aminoacylated tRK1 was phenol extracted, ethanol precipitated and dissolved in 10mM sodium acetate pH5.

Isolation and Reconstitution of Por1p for *in vitro* Studies

The pellets containing the membrane fraction from yeast mitochondria (WT and *Δpor1* strains) that were subjected to hypotonic shock were solubilized with Triton X-100 to purify Por1p (see above). One-step hydroxyapatite/celite column chromatography was applied to

purify Por1p (DePinto et *al*. 1987). The yield of Por1p was about 5 mg/L yeast culture and the protein concentration was determined using the calculated extinction coefficient at 280 nm of 24050 $(mol/L)^{-1}cm^{-1}$ (Bay and Court, 2009). Protein purity was monitored by SDS-PAGE and was estimated to be at least 95%, based on silver staining of gels or by Western blot with monoclonal antibodies against yeast VDAC1. Isolated Por1p was reconstituted into SUV in the presence of ergosterol using modifications of the procedure described by Mannella et *al.* 1991. Its functional state in SUV was investigated by access test for enzymes included in vesicles interior (see Supplemental methods).

ol extraction, precipitated with ethanol, and analysed as described above for mitochondria.

Subfractionation of Mitochondria and Preparation of OMV

WT and deletion mutant strains were grown and mitochondria were isolated as described above. Outer mitochondrial membrane isolation and preparation of outside-out sealed vesicles was performed essentially as described by Schatz and co-workers (Schatz, EMBO J, 1983). OM purity was estimated by the absence of succinate dehydrogenase activity (IM marker) (Sottocasa et al. 1967), myokinase (IMS marker), citrate synthase (matrix marker) and porin (OM marker). Detection of porin was performed after separation of proteins on SDS-PAGE followed by Western blot using rabbit polyclonal antibodies developed against *S. cerevisiae* porin. Intactness of OM vesicles was checked as described above (preparation of SUV with hexokinase activity accessibility based test). Assays of tRK1 import into OMV were carried out as described above for isolated mitochondria and SUV.

North-Western Hybridization

Sucrose gradient purified mitochondria were used to prepare a total lysate separated on a 12% SDS-PAGE (50 µg mitochondrial protein) in duplicates. One gel was stained by Coomassie

blue and the other identical gel was transferred on nitrocellulose membrane (Invitrogen). This membrane was incubated in renaturation buffer (0.1% v/v Nonidet NP-40, 0.1 M Tris-HCl, pH 7.5) at 4°C for 6h and then washed (3 x 10' at 4°C) in hybridization buffer (10 mM Tris-HCl pH7.5, 5 mM $MgCl_2$, 1% bovine serum albumin). Hybridization was carried out in presence of 5' labeled aminoacylated tRK1 transcript (100 cps, 15h, 4°C). The membrane was washed again in hybridization buffer (3 x 10' at 4°C) and exposed to a PhophorImager plate (Fuji). Autoradiographies were developed using TyphoonTrio scanner and images were treated in ImageQuant™TL program.

Other detailed methods are described in the Supplementary material.

REFERENCES

Ahting, U., Thieffry, M., Engelhardt, H., Hegerl, R., Neupert, W., and Nussberger, S. 2001. Tom40, the pore-forming component of the protein-conducting TOM channel in the outer membrane of mitochondria. *J Cell Biol* **153**(6): 1151-1160.

Ahting, U., Thun, C., Hegerl, R., Typke, D., Nargang, F.E., Neupert, W., and Nussberger, S. 1999. The TOM core complex: the general protein import pore of the outer membrane of mitochondria. *J Cell Biol* **147**(5): 959-968.

Antos, N., Stobienia, O., Budzinska, M., and Kmita, H. 2001. Under conditions of insufficient permeability of VDAC1, external NADH may use the TOM complex channel to cross the outer membrane of Saccharomyces cerevisiae mitochondria. *J Bioenerg Biomembr* **33**(2): 119-126.

Becker, T., Guiard, B., Thornton, N., Zufall, N., Stroud, D.A., Wiedemann, N., and Pfanner, N. 2010. Assembly of the mitochondrial protein import channel: role of Tom5 in two-stage interaction of Tom40 with the SAM complex. *Mol Biol Cell* **21**(18): 3106-3113.

Benz, R. and Brdiczka, D. 1992. The cation-selective substate of the mitochondrial outer membrane pore: single-channel conductance and influence on intermembrane and peripheral kinases. *J Bioenerg Biomembr* **24**(1): 33-39.

Benz, R., Kottke, M., and Brdiczka, D. 1990. The cationically selective state of the mitochondrial outer membrane pore: a study with intact mitochondria and reconstituted mitochondrial porin. *Biochim Biophys Acta* **1022**(3): 311-318.

Bonawitz, N.D., Clayton, D.A., and Shadel, G.S. 2006. Initiation and beyond: multiple functions of the human mitochondrial transcription machinery. *Mol Cell* **24**(6): 813-825.

Chacinska, A., Koehler, C.M., Milenkovic, D., Lithgow, T., and Pfanner, N. 2009. Importing mitochondrial proteins: machineries and mechanisms. *Cell* **138**(4): 628-644.

Chen, H.W., Rainey, R.N., Balatoni, C.E., Dawson, D.W., Troke, J.J., Wasiak, S., Hong, J.S., McBride, H.M., Koehler, C.M., Teitell, M.A. et al. 2006. Mammalian polynucleotide phosphorylase is an intermembrane space RNase that maintains mitochondrial homeostasis. *Mol Cell Biol* **26**(22): 8475-8487.

De Pinto, V., Guarino, F., Guarnera, A., Messina, A., Reina, S., Tomasello, F.M., Palermo, V., and Mazzoni, C. 2010. Characterization of human VDAC isoforms: a peculiar function for VDAC3? *Biochimica et biophysica acta* **1797**(6-7): 1268-1275.

Dihanich, M., Suda, K., and Schatz, G. 1987. A yeast mutant lacking mitochondrial porin is respiratory-deficient, but can recover respiration with simultaneous accumulation of an 86-kd extramitochondrial protein. *Embo J* **6**(3): 723-728.

Duchene, A.M., Pujol, C., and Marechal-Drouard, L. 2009. Import of tRNAs and aminoacyl-tRNA synthetases into mitochondria. *Curr Genet* **55**(1): 1-18.

Eilers, M., Oppliger, W., and Schatz, G. 1987. Both ATP and an energized inner membrane are required to import a purified precursor protein into mitochondria. *Embo J* **6**(4): 1073-1077.

Entelis, N., Brandina, I., Kamenski, P., Krasheninnikov, I.A., Martin, R.P., and Tarassov, I. 2006. A glycolytic enzyme, enolase, is recruited as a cofactor of tRNA targeting toward mitochondria in Saccharomyces cerevisiae. *Genes Dev* **20**: 1609-1620.

Entelis, N.S., Kolesnikova, O.A., Dogan, S., Martin, R.P., and Tarassov, I.A. 2001a. 5 S rRNA and tRNA import into human mitochondria. Comparison of in vitro requirements. *J Biol Chem* **276**(49): 45642-45653.

Entelis, N.S., Kolesnikova, O.A., Martin, R.P., and Tarassov, I.A. 2001b. RNA delivery into mitochondria. *Adv Drug Deliv Rev* **49**(1-2): 199-215.

Hoogenboom, B.W., Suda, K., Engel, A., and Fotiadis, D. 2007. The supramolecular assemblies of voltage-dependent anion channels in the native membrane. *J Mol Biol* **370**(2): 246-255.

Kikovska, E., Svard, S.G., and Kirsebom, L.A. 2007. Eukaryotic RNase P RNA mediates cleavage in the absence of protein. *Proc Natl Acad Sci U S A* **104**(7): 2062-2067.

Koehler, C.M., Jarosch, E., Tokatlidis, K., Schmid, K., Schweyen, R.J., and Schatz, G. 1998. Import of mitochondrial carriers mediated by essential proteins of the intermembrane space. *Science* **279**(5349): 369-373.

Kolesnikova, O., Kazakova, H., Comte, C., Steinberg, S., Kamenski, P., Martin, R.P., Tarassov, I., and Entelis, N. 2010a. Selection of RNA aptamers imported into yeast and human mitochondria. *RNA* **16**(5): 926-941.

Krimmer, T., Rapaport, D., Ryan, M.T., Meisinger, C., Kassenbrock, C.K., Blachly-Dyson, E., Forte, M., Douglas, M.G., Neupert, W., Nargang, F.E. et al. 2001. Biogenesis of porin of the outer mitochondrial membrane involves an import pathway via receptors and the general import pore of the TOM complex. *J Cell Biol* **152**(2): 289-300.

Larsson, N.G. and Clayton, D.A. 1995. Molecular genetic aspects of human mitochondrial disorders. *Annu Rev Genet* **29**: 151-178.

Magalhaes, P.J., Andreu, A.L., and Schon, E.A. 1998. Evidence for the presence of 5S rRNA in mammalian mitochondria. *Mol Biol Cell* **9**(9): 2375-2382.

Mannella, C.A. 1982. Structure of the outer mitochondrial membrane: ordered arrays of porelike subunits in outer-membrane fractions from Neurospora crassa mitochondria. *J Cell Biol* **94**(3): 680-687.

Mercer, T.R., Neph, S., Dinger, M.E., Crawford, J., Smith, M.A., Shearwood, A.M., Haugen, E., Bracken, C.P., Rackham, O., Stamatoyannopoulos, J.A. et al. 2011. The human mitochondrial transcriptome. *Cell* **146**(4): 645-658.

Mihara, K., Blobel, G., and Sato, R. 1982. In vitro synthesis and integration into mitochondria of porin, a major protein of the outer mitochondrial membrane of Saccharomyces cerevisiae. *Proc Natl Acad Sci U S A* **79**(23): 7102-7106.

Neupert, W. and Herrmann, J.M. 2007. Translocation of proteins into mitochondria. *Annu Rev Biochem* **76**: 723-749.

Osman, C., Merkwirth, C., and Langer, T. 2009. Prohibitins and the functional compartmentalization of mitochondrial membranes. *J Cell Sci* **122**(Pt 21): 3823-3830.

Pfanner, N., Rassow, J., van der Klei, I.J., and Neupert, W. 1992. A dynamic model of the mitochondrial protein import machinery. *Cell* **68**(6): 999-1002.

Puranam, R.S. and Attardi, G. 2001. The RNase P associated with HeLa cell mitochondria contains an essential RNA component identical in sequence to that of the nuclear RNase P. *Mol Cell Biol* **21**(2): 548-561.

Rainey, R.N., Glavin, J.D., Chen, H.W., French, S.W., Teitell, M.A., and Koehler, C.M. 2006. A new function in translocation for the mitochondrial i-AAA protease Yme1: import of polynucleotide phosphorylase into the intermembrane space. *Mol Cell Biol* **26**(22): 8488-8497.

Rubio, M.A. and Hopper, A.K. 2011. Transfer RNA travels from the cytoplasm to organelles. *Wiley Interdiscip Rev RNA* **2**(6): 802-817.

Salinas, T., Duchene, A.M., Delage, L., Nilsson, S., Glaser, E., Zaepfel, M., and Marechal-Drouard, L. 2006. The voltage-dependent anion channel, a major component of the tRNA import machinery in plant mitochondria. *Proc Natl Acad Sci U S A* **103**(48): 18362-18367.

Salinas, T., Duchene, A.M., and Marechal-Drouard, L. 2008. Recent advances in tRNA mitochondrial import. *Trends Biochem Sci* **33**(7): 320-329.

Scheffler, I.E. 2001a. A century of mitochondrial research: achievements and perspectives. *Mitochondrion* **1**(1): 3-31.

-. 2001b. Mitochondria make a come back. *Adv Drug Deliv Rev* **49**(1-2): 3-26.

Schekman, R. 2010. Editorial expression of concern for Goswami S. et al, "A bifunctional tRNA import receptor from Leishmania mitochondria". *Proc Natl Acad Sci U S A* **107**(20): 9476.

Schleyer, M., Schmidt, B., and Neupert, W. 1982. Requirement of a membrane potential for the posttranslational transfer of proteins into mitochondria. *Eur J Biochem* **125**(1): 109-116.

Schneider, A. and Marechal-Drouard, L. 2000. Mitochondrial tRNA import: are there distinct mechanisms? *Trends Cell Biol* **10**(12): 509-513.

Sieber, F., Placido, A., El Farouk-Ameqrane, S., Duchene, A.M., and Marechal-Drouard, L. 2011. A protein shuttle system to target RNA into mitochondria. *Nucleic Acids Res* **39**(14): e96.

Smirnov, A., Comte, C., Mager-Heckel, A.M., Addis, V., Krasheninnikov, I.A., Martin, R.P., Entelis, N., and Tarassov, I. 2010. Mitochondrial enzyme rhodanese is essential for 5 S ribosomal RNA import into human mitochondria. *J Biol Chem* **285**(40): 30792-30803.

Smirnov, A., Entelis, N., Martin, R.P., and Tarassov, I. 2011a. Biological significance of 5S rRNA import into human mitochondria: role of ribosomal protein MRP-L18. *Genes Dev* **25**(12): 1289-1305.

Smirnov, A., Tarassov, I., Mager-Heckel, A.M., Letzelter, M., Martin, R.P., Krasheninnikov, I.A., and Entelis, N. 2008. Two distinct structural elements of 5S rRNA are needed for its import into human mitochondria. *Rna* **14**(4): 749-759.

Sottocasa, G.L., Kuylenstierna, B., Ernster, L., and Bergstrand, A. 1967. An electron-transport system associated with the outer membrane of liver mitochondria. A biochemical and morphological study. *J Cell Biol* **32**(2): 415-438.

Tarassov, I., Entelis, N., and Martin, R.P. 1995a. An intact protein translocating machinery is required for mitochondrial import of a yeast cytoplasmic tRNA. *J Mol Biol* **245**(4): 315-323.

-. 1995b. Mitochondrial import of a cytoplasmic lysine-tRNA in yeast is mediated by cooperation of cytoplasmic and mitochondrial lysyl-tRNA synthetases. *Embo J* **14**(14): 3461-3471.

Thomas, B.C., Chamberlain, J., Engelke, D.R., and Gegenheimer, P. 2000. Evidence for an RNA-based catalytic mechanism in eukaryotic nuclear ribonuclease P. *Rna* **6**(4): 554-562.

Wallace, D.C. 1999. Mitochondrial diseases in man and mouse. *Science* **283**(5407): 1482-1488.

Wallace, D.C. and Lott, M.T. 2004. "MITOMAP: A Human Mitochondrial Genome Database". *http://wwwmitomaporg*.

Wang, G., Chen, H.W., Oktay, Y., Zhang, J., Allen, E.L., Smith, G.M., Fan, K.C., Hong, J.S., French, S.W., McCaffery, J.M. et al. 2010. PNPASE Regulates RNA Import into Mitochondria. *Cell* **142**(3): 456-467.

Yamamoto, T., Yamada, A., Watanabe, M., Yoshimura, Y., Yamazaki, N., Yoshimura, Y., Yamauchi, T., Kataoka, M., Nagata, T., Terada, H. et al. 2006. VDAC1, having a shorter N-terminus than VDAC2 but showing the same migration in an SDS-polyacrylamide gel, is the predominant form expressed in mitochondria of various tissues. *Journal of proteome research* **5**(12): 3336-3344.

Yoshionari, S., Koike, T., Yokogawa, T., Nishikawa, K., Ueda, T., Miura, K., and Watanabe, K. 1994. Existence of nuclear-encoded 5S-rRNA in bovine mitochondria. *FEBS Lett* **338**(2): 137-142.

Zeth, K. 2010. Structure and evolution of mitochondrial outer membrane proteins of beta-barrel topology. *Biochim Biophys Acta* **1797**(6-7): 1292-1299.

SUPPLEMENTAL INFORMATION

Supplemental Information includes eight figures, three tables, Supplemental Methods and Supplemental References and can be found with this article online.

ACKNOWLEDGMENTS

We thank P. Hammann and L. Kuhn (IBMC - CNRS, Strasbourg, France) and L. Sabatier (ECPM, Strasbourg, France) for mass-spectrometry analysis and A.-M. Heckel-Mager (UMR 7156 CNRS - Université de Strasbourg, France) for extensive technical assistance. This work was supported by the CNRS, Université de Strasbourg, Moscow State University, AFM (Association Française contre les Myopathies), ANR (Agence Nationale de la Recherche), FRM (Fondation pour la Recherche Médicale), the French National Program "Investissement d'Avenir" (Labex MitoCross), the NIH (GM061721, GM073981, CA90571, and CA156674), the American Heart Association (0640076N), the California Institute of Regenerative Medicine (RS1-00313 and RB1-01397), and the Broad Stem Cell Research Center at UCLA.

FIGURE LEGENDS

Figure 1. Mitochondrial OM Proteins Potentially Involved in RNA Import.

(A) Immunoblots of untreated or trypsin-treated isolated yeast mitochondria with (PNP) or without (Vec) ectopic PNPASE expression. Tom70p marks the OM and Mia40p marks the IMS. (B) Radiolabeled human *H1* RNA was imported into mitochondria treated as in 'A'. Exogenous nuclease addition removed unimported RNA. The input is 1%, the arrow denotes full-length *H1* RNA, and the asterisk denotes a product that may be degraded or processed. (C) North-Western analysis of mitochondrial proteins from WT and *Δpor1* interacting with tRK1. Left panel- technical procedure of North-Western analysis. Right panel - autoradiograph of North-Western blot, bold numbers show the band in which mitochondrial outer membrane proteins were identified (see also Table 1 and Table S1).

Figure 2. In vitro Import Analysis of tRK1.

(A) tRK1 was imported into OMV derived from WT and *Δpor1* OMV for 5 min in the presence of cyt b_2-DHFR, DIDS, or both. Import was quantitated from the autoradiogram and the inhibition is presented in bar graphs. (B) tRK1 was imported into SUV reconstituted with purified Por1p in the presence cyt b_2-DHFR, DIDS, or both. Quantitation from the autoradiogram is presented as in 'A'. RNase A is included as a positive control to degrade tRK1 (see also Figures S1-S6 and Tables S2 and S3) .

Figure 3. tRK1 Import in Yeast Mitochondria.

(A) In vitro import of tRK1 into isolated mitochondria of WT and *Δpor1* cells. Left - autoradiographies of in vitro tRK1 imports (performed in 5 repeats). Right - plot illustrating relative imports of tRK1 (import in WT strain was set to 1 and error bars were calculated as

explained in material and methods). (B) Northern blot illustrating in vivo import of tRK1 into mitochondria from WT and *Δpor1* cells. Anti mito $tRNA^{Gly}$: probe directed against mitochondrial tRNAGly; anti cyt tRK2: probe directed against cytoplasmic $tRNA^{Lys}$(UUU) (tRK2); anti cyt tRK1: probe directed against partially imported cytoplasmic $tRNA^{Lys}$(CUU) (tRK1).

Figure 4. In vitro Import of tRK1 into Isolated Mitochondria of WT and *Δpor1* Strains Without or With DIDS and/or cyt b_2-DHFR Protein.

(A) Autoradiographies of tRK1 imports and imports of precursor form of mitochondrial lysyl-tRNA-synthetase (preMSK); p: precursor form of preMSK; m: mature processed form of preMSK; PK: Proteinase K. (B) Plot illustrating relative imports of tRK1 in different strains and different conditions (control import in WT strain was set to 1). (C) Plots illustrating relative imports of tRK1 in different conditions to control imports within each studied strain (control imports of the different strains were set to 1). (D) In vitro import of tRK1 into mitochondria of WT cells in presence or absence of ATP and/or ΔΨ.

Figure 5. PNPASE-mediated RNA Import into Yeast Mitochondria Dependence on Porin.

(A) Immunoblots of WT control and Δpor1 yeast mitochondria with (PNP) or without (Vec) PNPASE expression. OM protein Tom70 was the loading control. (B) Import of radiolabeled H1 RNA into WT control or *Δpor1* isolated yeast mitochondria with (PNP) or without (Vec) PNPASE expression. (C) Immunoblots of WT control and *Δtom70* yeast mitochondria with (PNP) or without (Vec) PNPASE expression. OM protein Por1 was the loading control. (D) Import of radiolabeled H1 RNA into WT control or *Δtom70* isolated yeast mitochondria with (PNP) or without (Vec) PNPASE expression.

Figure 6. *H1* RNA Translocates into Mammalian Mitochondria Through the VDAC (Porin) Channel.

(A) Immunoblots of WT control or VDAC1 knockdown (KD) HeLa cell mitochondria. OM protein TOM40 is the loading control. (B) Radiolabeled *H1* RNA was imported into isolated WT or KD HeLa cell mitochondria and quantified by autoradiography. Import reactions were repeated with 1X and 2X amounts of *H1* RNA. (C) WT mitochondria isolated from HeLa cells were treated with antibodies against VDAC1 and TOMM40 or with buffer only. This was followed by *H1* RNA (top panel) or protein import with Su9-DHFR (p: precursor; m: mature) as a substrate (bottom panel). (D) Crosslinking of radiolabeled *H1* RNA and immunoprecipitation of VDAC1. $tRNA^{Lys}$ was used as negative control for non-imported RNA and TOMM40 antibody was used as a negative control for the immunoprecipitation assay.

Figure 7. VDAC1 Knockdown Reduces *H1* RNA Import and the Processing of Mitochondrial-encoded RNA Transcripts in vivo.

(A) RNA was isolated from whole cell lysate (Total) or mitochondria (Mito) of WT control or VDAC1 knockdown (KD) HeLa cells. RT-PCR was performed using specific primers to amplify *H1* RNA or *COX1* mtRNA as a control. (B) Accumulation of unprocessed mitochondrial transcripts in the VDAC1 knockdown cells. RNA was isolated from WT mitochondria, and RT-PCR was performed with the primers shown in the upper scheme. S: $tRNA^{Ser}$, D: $tRNA^{Asp}$, H: $tRNA^{His}$, L: $tRNA^{Lys}$. (see also Figure S7).

Table 1. Outer membrane proteins identified by Nano-LC MS/MS for bands localised according tRK1-positive signal position on North-Western hybridization.

Identified mitochondrial outer membrane proteins	Position of band on NW autograph (Fig. S1)	Wild type	ΔPOR1
TOM5 (component of the translocase of outer membrane complex)	**1**	+	-
TOM20 and **TOM22** (component of the translocase of outer membrane complex)	**2**	-	+
POR1 (Porin 1 or Voltage Dependant Anion Channel)	**3**	+	-
TOM40 (component of the translocase of outer membrane complex)	**4**	-	+

Table 2. Respiration of yeast mitochondria from wild type and deletion strains. Rate of respiration in nmole O_2/min*mg of mitochondrial protein. V3u and V4 are respiration rates at uncoupled state (state3u) and state 4, respectively.

Yeast strain	Succinate (state4)	Ethanol	NADH	FCCP, (state3u, succinate based)	Respiratory control, V3u/V4	DIDS, 0.5mM
BY, n=32	34±9	123±12	49±1	85±37	2,5±0,9	16±2
W303, n=9	54±18	134±19	54±8	124±31	2,5±0,8	30±4
ΔPor1, n=3	10±3	117±14	23±7	22±8	2,2±1,1	16±4

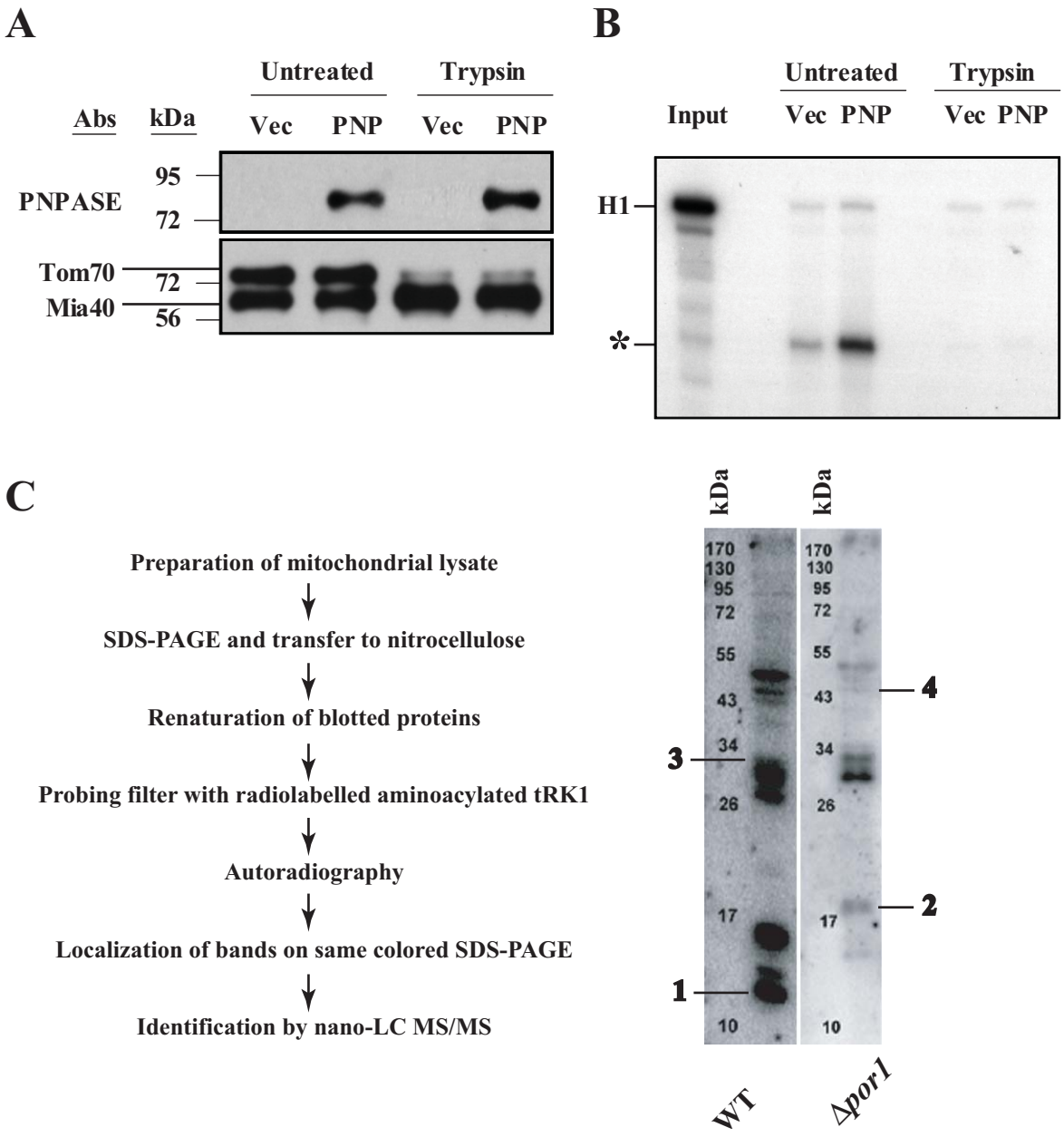
A
Untreated
Trypsin
Abs
kDa
Vec
PNP
Vec
PNP
PNPASE
95
72
Tom70
72
Mia40
56
B
Input
Untreated
Trypsin
Vec PNP
Vec PNP
H1
*
C
Preparation of mitochondrial lysate
SDS-PAGE and transfer to nitrocellulose
Renaturation of blotted proteins
Probing filter with radiolabelled aminoacylated tRK1
Autoradiography
Localization of bands on same colored SDS-PAGE
Identification by nano-LC MS/MS
kDa
kDa
170
130
95
72
55
43
34
26
17
10
1
2
3
4
WT
Δpor1

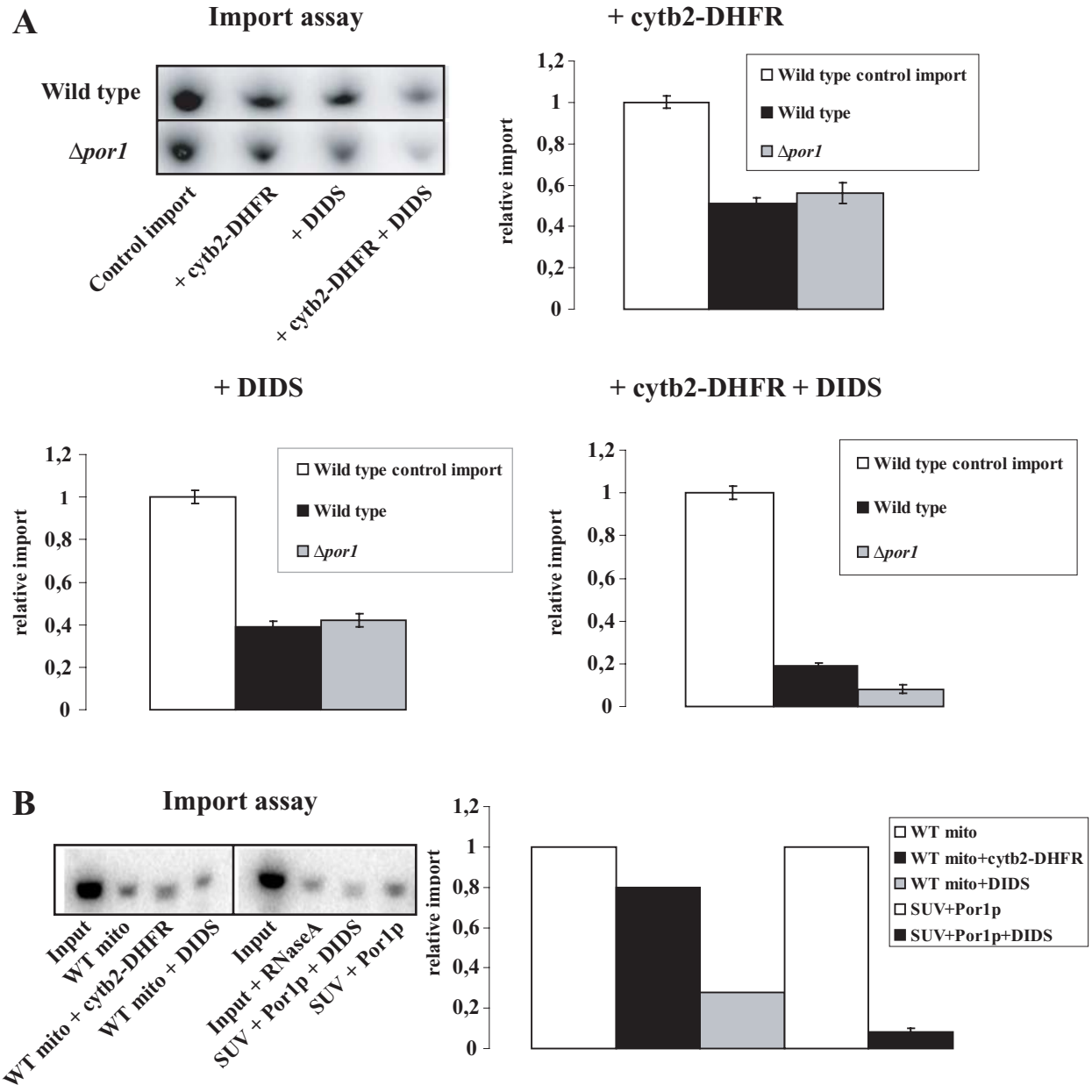
A
Import assay
Wild type
Δpor1
Control import
+ cytb2-DHFR
+ DIDS
+ cytb2-DHFR + DIDS
+ cytb2-DHFR
relative import
1,2
1
0,8
0,6
0,4
0,2
0
Wild type control import
Wild type
Δpor1
+ DIDS
+ cytb2-DHFR + DIDS
B
Import assay
Input
WT mito
WT mito + cytb2-DHFR
WT mito + DIDS
Input
Input + RNaseA
SUV + Por1p + DIDS
SUV + Por1p
WT mito
WT mito+cytb2-DHFR
WT mito+DIDS
SUV+Por1p
SUV+Por1p+DIDS

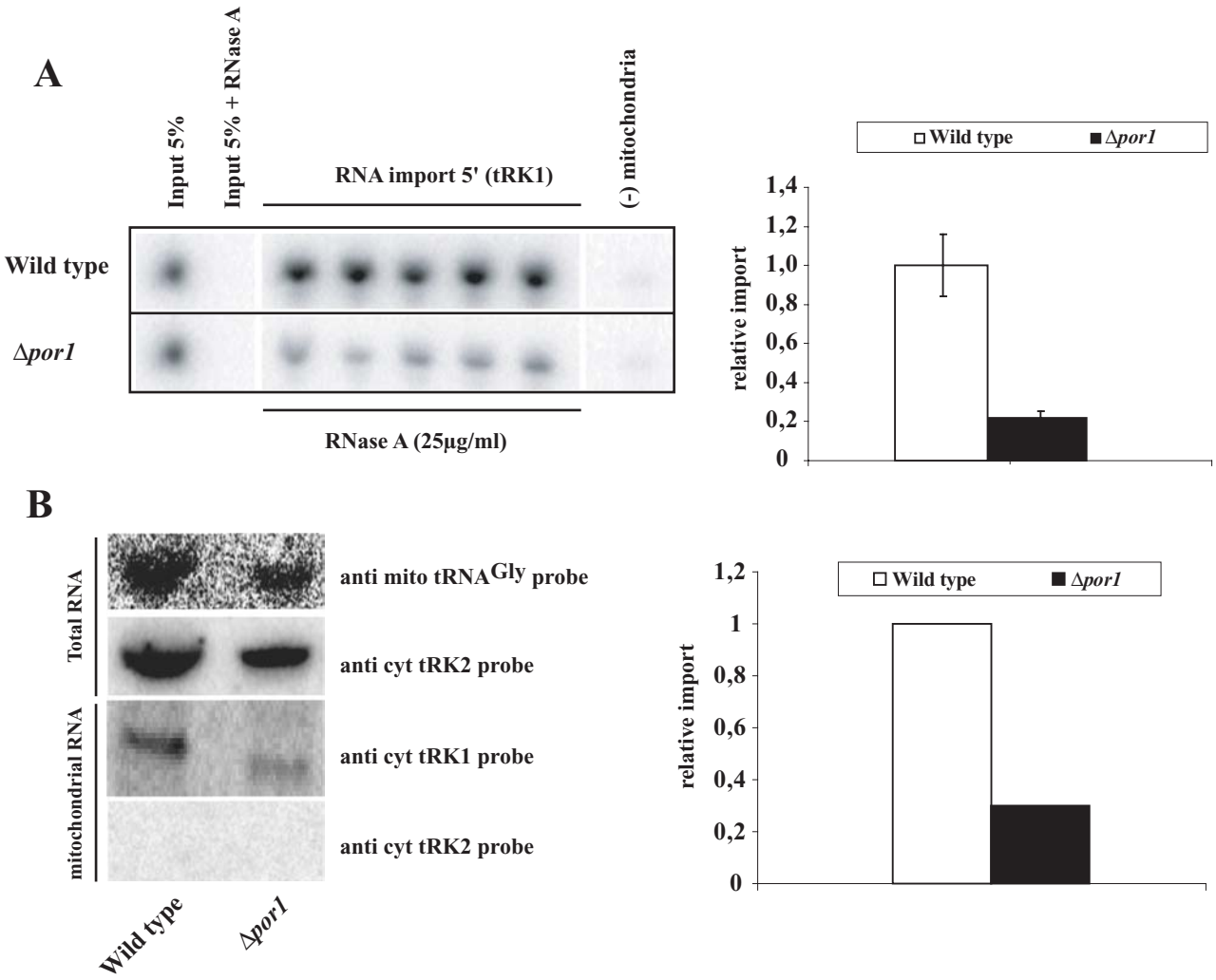
A
Input 5%
Input 5% + RNase A
RNA import 5' (tRK1)
(-) mitochondria
Wild type
Δpor1
RNase A (25µg/ml)
Wild type
Δpor1
relative import
1,4
1,2
1,0
0,8
0,6
0,4
0,2
0
B
Total RNA
mitochondrial RNA
anti mito tRNAGly probe
anti cyt tRK2 probe
anti cyt tRK1 probe
anti cyt tRK2 probe
Wild type
Δpor1
Wild type
Δpor1
relative import
1,2
1
0,8
0,6
0,4
0,2
0

A

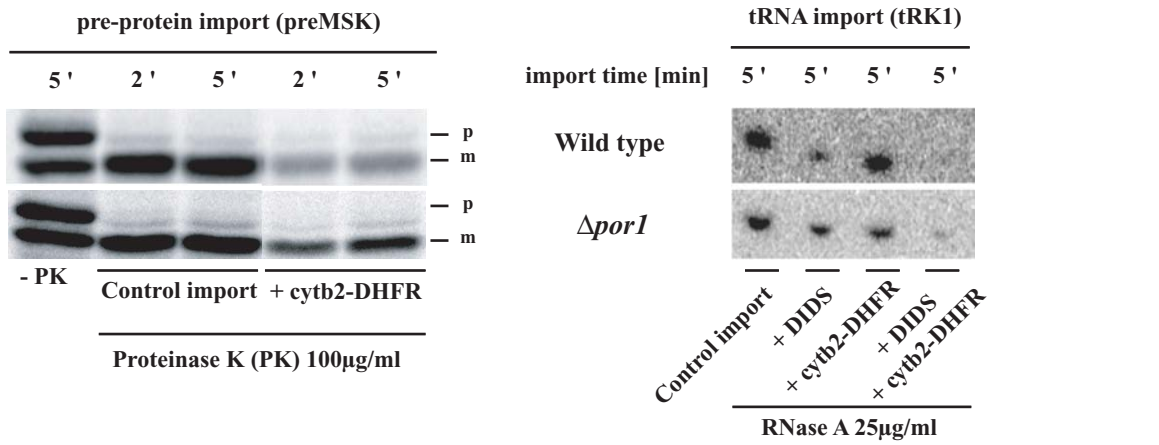

B

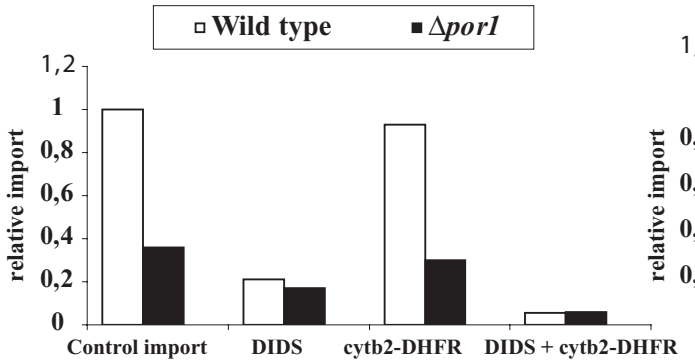

C

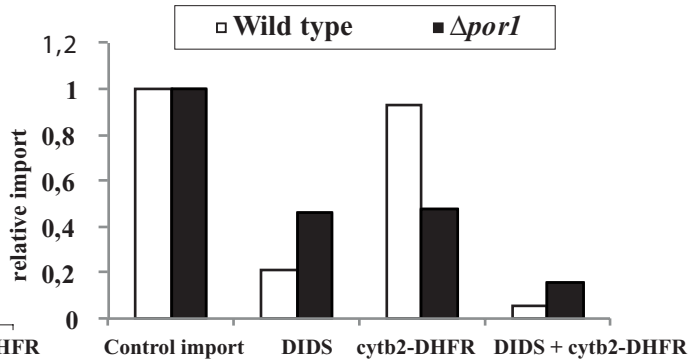

D

Mitochondria, 0,1mg	-	+	+	+	+	+	+	+	+	+	-	-
5 mM ATP	-	+	+	+	+	+	-	-	-	-	-	-
5 mM succinate	-	-	+	+	+	+	+	+	+	+	-	-
1 µg oligomycin	-	-	+	+	+	+	+	+	+	+	-	-
1 µM FCCP	-	-	-	-	+	+	-	-	+	+	-	+
0.5 mM DIDS	-	-	-	+	-	+	-	+	-	+	-	-
Nuclease 1U	+	+	+	+	+	+	+	+	+	+	-	-
ΔΨ		-	+	+	-	-	+	+	-	-		
tRK1												

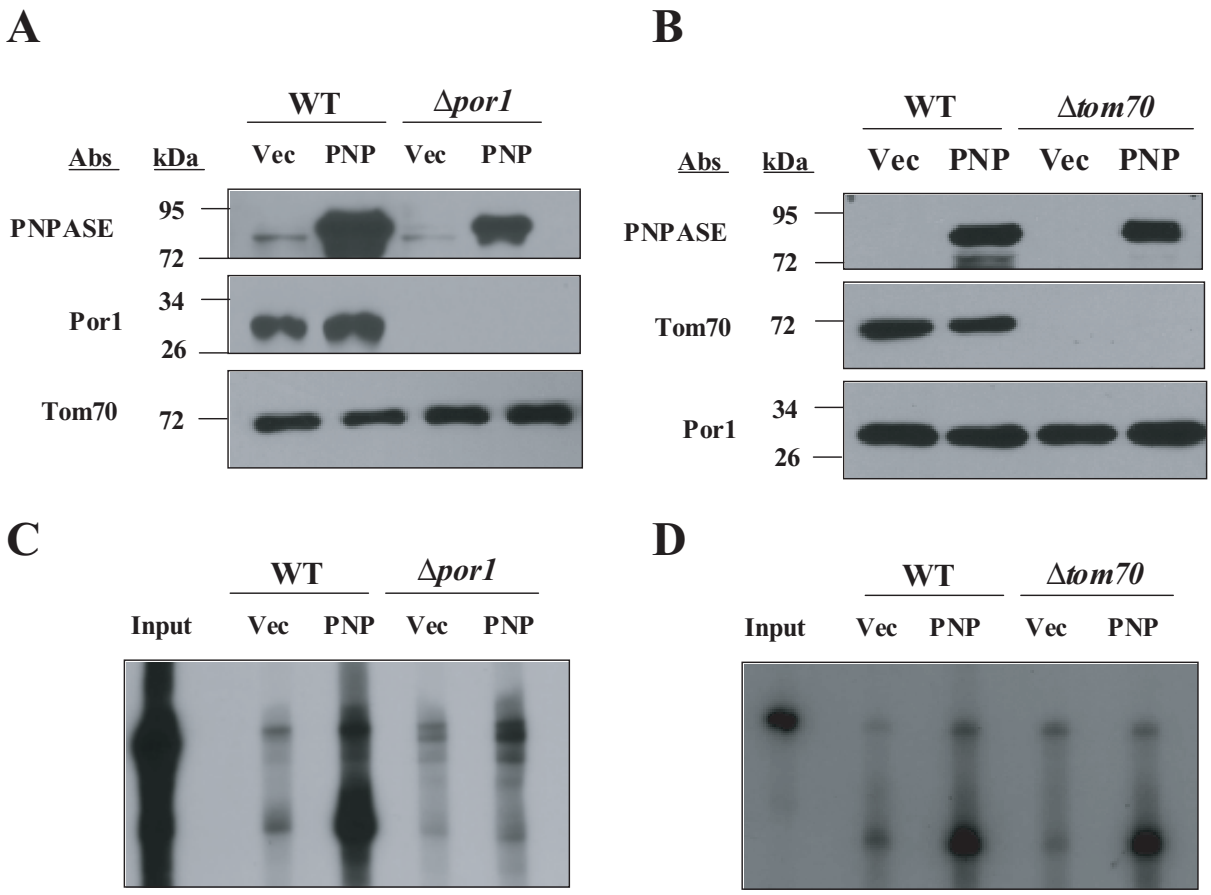
A
WT
Δpor1
Abs
kDa
Vec
PNP
Vec
PNP
PNPASE
95
72
Por1
34
26
Tom70
72
B
WT
Δtom70
Abs
kDa
Vec
PNP
Vec
PNP
PNPASE
95
72
Tom70
72
Por1
34
26
C
WT
Δpor1
Input
Vec
PNP
Vec
PNP
D
WT
Δtom70
Input
Vec
PNP
Vec
PNP

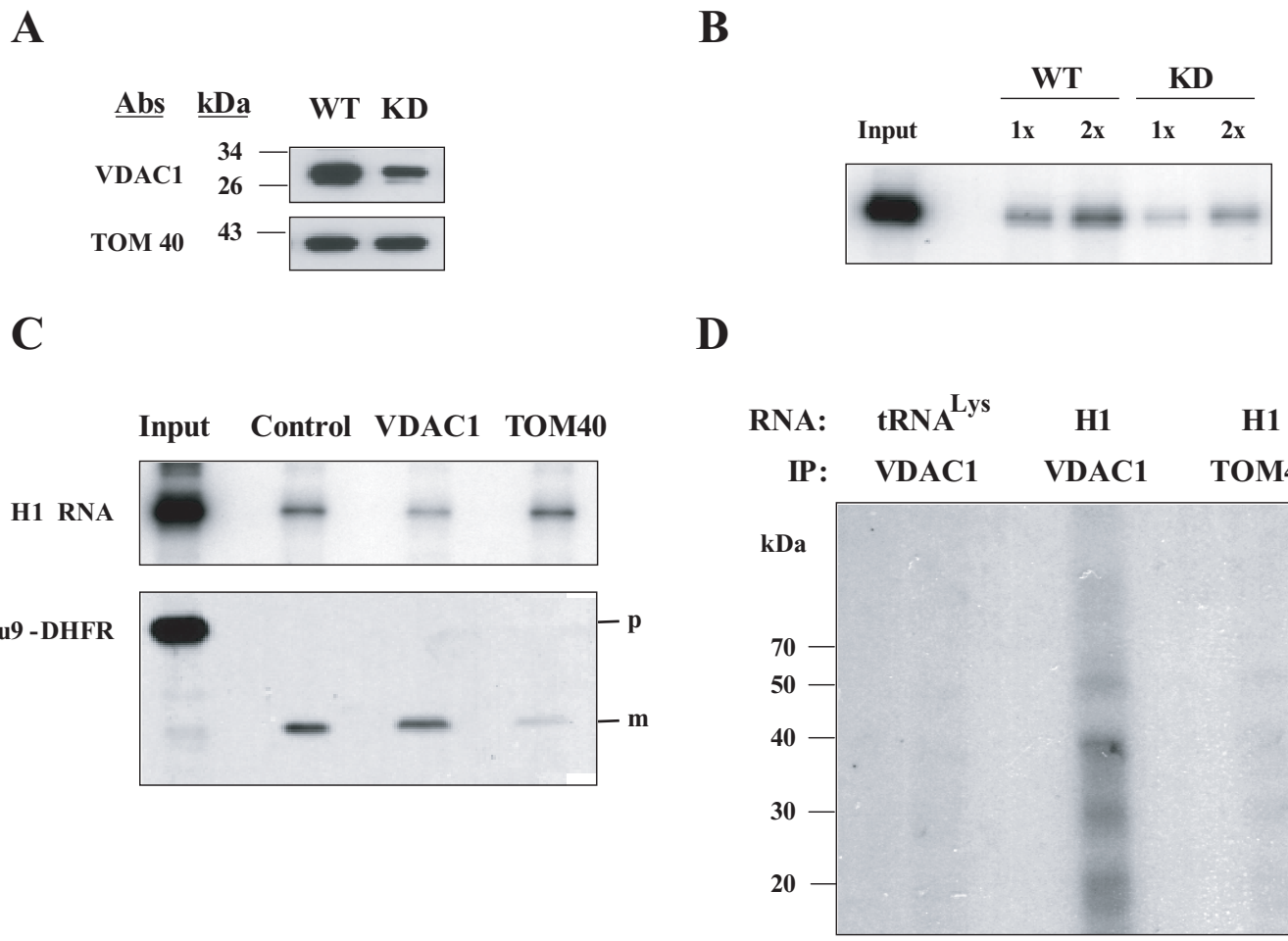
A
Abs
kDa
WT
KD
VDAC1
34
26
TOM 40
43
B
WT
KD
Input
1x
2x
1x
2x
C
Input
Control
VDAC1
TOM40
H1 RNA
Su9 -DHFR
p
m
D
RNA:
tRNA^Lys
H1
H1
IP:
VDAC1
VDAC1
TOM40
kDa
70
50
40
30
20

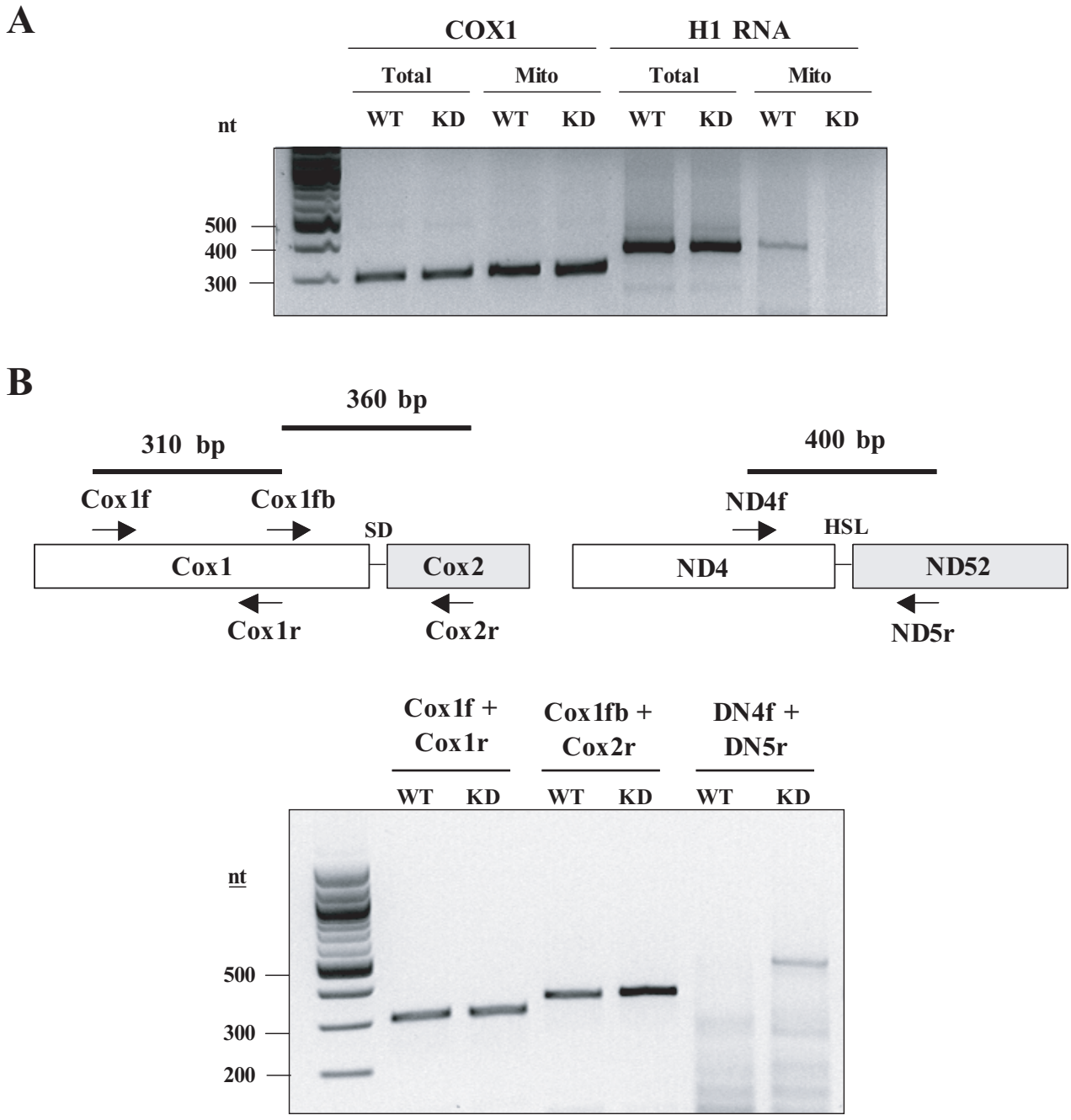
A
COX1
H1 RNA
Total
Mito
Total
Mito
WT KD WT KD WT KD WT KD
nt
500
400
300
B
360 bp
310 bp
400 bp
Cox1f
Cox1fb
SD
ND4f
HSL
Cox1
Cox2
ND4
ND52
Cox1r
Cox2r
ND5r
Cox1f + Cox1r
Cox1fb + Cox2r
DN4f + DN5r
WT KD WT KD WT KD
nt
500
300
200

Genes & Development

Supplemental Material

RNA translocation across the outer mitochondrial membrane is mediated by alternative channels

Tom Schirtz, Geng Wang, Eriko Shimada, Mikhail Vyssokikh, Nina Entelis, Michael A. Teitell, Ivan Tarassov, Carla M. Koehler

Content:

Supplemental Methods

Isolation and characterisation of mitochondria

Overnight grown yeast cells were harvested (2000 x *g* 15' at 20°C), then washed twice with sterile water. Spheroplasting was achieved by incubating cells (1 g wet weight/10 ml) at 37°C for 20'-30' with slight shaking in spheroplasting buffer (1.35 M sorbitol, 1 mM EDTA, 1 mM EGTA, 0.2 M Na-phosphate pH 7.4) containing 15 mg Zymolyase 20T/g wet cells. Spheroplasting was checked by measuring an OD_{600nm} drop (10-15x) in water. Spheroplasts were then harvested by centrifugation at 1000 x *g* for 10' at 4°C and washed once in spheroplast washing buffer (0.75 M sorbitol, 0.4 M mannitol, 0.1% bovine serum albumin, 10 mM HEPES-NaOH, pH 7). Total cell lysate was obtained by lysing spheroplasts (0.2 g/ml) in breakage buffer BB (0.6 M sorbitol, 0.5 mM EDTA, 0.1% bovine serum albumin, 10 mM HEPES-NaOH, pH 7), containing a protease inhibitor cocktail (Roche), with 10-15 strokes in a Dounce homogenizer (Wheaton) using the "loose" pestle. Cellular debris was removed by differential centrifugation (3000 x *g* 10' at 4°C) and a crude mitochondrial preparation was obtained by centrifugation of the clarified lysate (10000 x *g* 20' at 4°C). If needed, the crude mitochondrial preparation was further purified by centrifugation (10000 x *g* 45' at 4°C) through a discontinuous sucrose gradient (60%-32%-23%-15% in BB), where pure mitochondria were recovered from the 60%-32% interphase and washed again in breakage buffer (10000 x *g* 20' at 4°C). Complete mitochondrial integrity was checked with the citrate synthase assay (Matlib et al., 1979) and the integrity of the OM was assessed by accessibility of externally added cytochrome *c* to the respiratory chain during respiration measurements. Prepared mitochondria usually had a complete integrity of >90%. Integrity of the OM was calculated according to the equation I = (1-$\mathcal{V}$ iso./ $\mathcal{V}$hypo.) x 100, where I is intactness in %, $\mathcal{V}$ iso. and $\mathcal{V}$ hypo. are the KCN-sensitive rates

of oxygen consumption of isotonic or hypotonically incubated mitochondria, respectively. This value was normally in between 80%-90%. Respiratory control was calculated according to the Chance method as ratio of respiration rates at metabolic states 3 and state 4 was in a range from 2 to 4 (Chance and Williams, 1955).

Reconstitution of Porin into Vesicles

Mixture of egg yolk L-a-phosphatidyl choline, L-a-phosphatidyl ethanolamine, L-a-phosphatidyl inositol, L-a-phosphatidyl serine, egg lecithin L-a-phosphatidic acid and cardiolipin (all reagents obtained from Sigma) with ratio 46:33:10:1:4:6 *m*/*m*/*m* was dissolved in chloroform and evaporated at room temperature under a stream of argon for 1 hour. Dried lipids/sterol mixture (between 10 and 11 mg) was resuspended in 400 µl ice-cold 10 mM Tris HCl buffer (pH 7.0), containing 1 mM EDTA (TE). The resulting cloudy suspension was diluted and sonicated on ice (Fisher Scientific Sonifier Model 300) to yield the stock suspension of SUVs (20 mg/ml). Stock SUV suspensions lacking ergosterol were prepared by the same method. Porin was preincubated with ergosterol (Sigma) - 50µl of protein solution (20 µg/ml) diluted in TE was mixed with 50 µl 1% ergosterol resuspended in TE and the mixture was gently shaked in ice for 10 min. Thereafter, 100 µl of this mixture was added to 0.6 ml of 1% Triton X-100 and 50 µl of SUV stock solution. Resulting 0.75 ml were mixed with 150 µl of SUV stock solution and subjected to 3 freeze-thaw cycles (liquid N_2, room temperature). Obtained vesicles with reconstituted porin were called VDAC-SUV, versus control SUV, where porin was absent. Liposomes lacking porin were prepared by the same method with adequate amount of 2% Triton X-100 solution in TE instead of porin solution.

Determination of Functional State of Porin Reconstituted in SUV

To test the functional state of reconstituted porin in VDAC-SUV, its ability to form channels for metabolites was studied by developed original method. For this test hexokinase (2.7.1.1., ATP:D-hexose 6-phosphotransferase) from *S. cerevisiae* (Sigma) was used, assuming that this glycolytic enzyme with a molecular weight of 54 kDa cannot pass the porin channel (cut-off is in 2- 6 kD). The enzyme (approximately 10 U) was included by sonication (3 *x* 10s) (45% of maximal power of Fisher Scientific Sonifier Model 300) in VDAC-SUV containing 10 μg of porin. Loaded vesicles were washed from non-included enzyme by sedimentation at 100 ,000 x *g* at 4˚C for 1 h (Beckman TL100 bench top ultracentrifuge). Absence of non-included enzyme and the amount of specific activity loaded in vesicles were checked spectrophotometrically with bacterial glucose 6-phosphate dehydrogenase as coupling enzyme added in excess and NAD+ as a second substrate. Glucose (2 mM) and ATP (5 mM) were added to 100 μl of VDAC-SUV as substrates of hexokinase reaction and formation of NADH, measured at 340 nm in 1 cm quartz cuvettes on Beckman Coulter DU730 spectrophotometer, was used for calculation of hexokinase activity. Specific blocker of porin channel DIDS was used in a concentration from 50 to 500 μM to prevent transport of ATP and glucose into hexokinase-loaded vesicles through the reconstituted porin. In control, experiments with vesicles without porin or without ergosterol were used and formation of NADH was compared to that using the VDAC-SUV. Full activity of loaded hexokinase was calculated for digitonin (50 μg) treated SUV after its complete solubilisation.

Import of tRK1 and preMSK into Mitochondria

In vitro import assays (100 µl) were carried out in import mixture (10 mM HEPES-NaOH pH7, 0.6 M sorbitol, 10 mM succinate, 2 mM NADH, 1 mM $MgCl_2$, 30 mM KCl, 5 mM ATP) for indicated times at 30°C containing 50-100 µg of crude mitochondria (mitochondrial protein), 3 pmol of 5' labelled aminoacylated tRK1 transcript, 21 pmol recombinant yeast enolase-2 (Eno-2) and 4,4pmol recombinant mitochondrial pre-lysyl-tRNA-synthetase (preMSK). Non imported tRK1 was degraded by adding 1V of 2x RNaseA solution (25 µg/ml RNaseA, 0.6 M sorbitol, 8 mM $MgCl_2$, 10 mM HEPES-NaOH pH 7) for 10' at 0°C. The reaction was stopped with 5 volumes of breakage buffer containing 5 mM EDTA. Mitochondria were pelleted by centrifugation (13000 x *g* 5' at 4°C), the pellet transferred in a fresh tube and washed again. The mitochondrial pellet was then lysed in 100 µl lysis buffer (0.1 M sodium acetate pH 5, 1% SDS, 0.1% DEPC) at 100°C for 1' and the mitochondrial RNAs were extracted with hot phenol (55°C) and ethanol precipitated in the presence of 10 µg *E.coli* carrier RNAs. Isolated mitochondrial RNAs were separated by electrophoresis on a denaturating 10% 8M Urea PAGE, the gel was fixed (10% EtOH/10% acetic acid), dried and exposed to a PhosphorImager plate (Fuji). Autoradiographies were revealed using a TyphoonTrio scanner. The treatment of images and subsequent calculations of import efficiencies were done with the help of the ImageQuant™TL program. For representation of relative imports on the plots, error bars were calculated according to the standard deviation for parallel experiments.

DIDS (4,4'-Diisothiocyano-2,2'-stilbenedisulfonic acid) (Thinnes et al., 1994) was used at 0.25 mM. To block the TOM40 channel of the pre-protein import machinery, the recombinant cyt b_2-DHFR (26 pmol) was imported in presence of 2 µM methotrexate. Blocking was tested by inhibition of *in vitro* import of preMSK. To determine the requirement of the TOM40 channel on

tRK1 import, cyt b_2-DHFR treated mitochondria were used for *in vitro* tRK1 import. *In vitro* import assays of preMSK (100 µl) were carried out in import mixture (10 mM HEPES-NaOH pH 7, 0.6 M sorbitol, 10 mM succinate, 2 mM NADH, 1 mM $MgCl_2$, 30 mM KCl, 5 mM ATP) for indicated times at 25°C. Non imported preMSK was degraded by proteinase K treatment (100 µg/ml) for 2' at 25°C. The reaction was stopped with 9 volumes of ice cold BB containing 1 mM PMSF. Mitochondria were pelleted and washed once again with BB+PMSF before uptake in Laemmli buffer. Proteins were separated on a 12% SDS-gel, which was fixed, dried and exposed to a PhosphorImager plate.

***In Vitro* Transcription and Import of H1 RNA**

Import substrate RNA were transcribed from PCR templates by incubating 800 ng PCR template with SP6 RNA Polymerase (New England Biolabs) at 40°C for 15 minutes in SP6 transcription buffer (40 mM Tris-Cl pH 7.5, 6 mM $MgCl_2$, 2 mM spermidine, 0.1 mg/mL BSA) with 0.5 mM rNTP without GTP, 5 mM methyl G-Cap (New England Biolabs) , 10 mM DTT and ^{32}P rCTP (~1 mCi/ml) (MP Biomedical). The rGTP was then added to the reaction to a final concentration of 0.5 mM and allowed to incubate for 90 minutes at 40°C. Import substrates for mammalian experiments were transcribed using Ambion Sp6 MEGAscript® Kit according to manufacturer's protocol. All yeast strains were grown at stationary phase for 2 days in selection medium. Yeast and mammalian mitochondrial isolation procedure were previously described (Chen et al., 2006; Rainey et al., 2006) . The import assay for yeast mitochondria was performed in 200 µl volume by incubating 100 µg of isolated mitochondria at room temperature for 5 min in import buffer (0.6 M sorbitol, 2 mM KH_2PO_4, 50 mM KCl, 50 mM Hepes-KOH pH 7.1, 10 mM $MgCl_2$, 2.5 mM EDTA, and 1 mg/mL BSA 5 mM ATP, 2 mM DTT, 5 mM NADH) and subsequently

adding 5 pmol of radiolabeled RNA and incubating for an additional 5 min at room temperature for import. Then, mitochondria were pelleted at 11,000 x *g*, rinsed with wash buffer (0.6 M sorbitol and 20 mM Tris-Cl pH 8.0), and treated with 25 µg/mL S7 micrococcal nuclease at 27°C for 30 minutes. Total RNA was isolated as described above, analyzed by electrophoresis on an 8M urea-5% Acrylamide gel, and visualized by autoradiography. Mammalian import assays were performed using buffer containing 0.225 M mannitol plus 0.075 M sucrose instead of 0.6 M sorbitol, and 20 mM succinate instead of 5 mM NADH was used.

Import of tRK1 into VDAC-SUV

Assays of tRK1 import into VDAC-SUV (100 µl of vesicles/assay) were carried out as described above for isolated mitochondria. For such purposes vesicles were dialysed overnight at 4˚C against import mixture (10 mM HEPES-NaOH, pH 6.8, 0.44 M sorbitol, 10mM succinate, 3 mM NADH, 2.5 mM $MgCl_2$). After completion of tRK1 import, vesicles were treated with RNaseA (25 µg/ml) for 10' on ice and sedimented at 100,000 x *g* for 1 h at 4˚C (Beckman TL100 bench top ultracentrifuge). tRK1 was isolated from the pellet of VDAC- SUV by hot phenol.

Oxygen Consumption Measurement in Mammalian Cells

Cells were seeded at 50,000 cells/well in a XF24 Extracellular Flux Analyzer cell culture plate (Seahorse Bioscience) and incubated in the 37°C incubator with 5% CO_2 for 24 hr. The oxygen consumption rate was measured using the XF24 Extracellular Flux Analyzer (Zhang et al., 2012).

Synthesis of ^{35}S-Met labelled preMSK

^{35}S-Met labelled preMSK was synthesized in rabbit reticulocyte lysate (TnT® T7 Quick for PCR DNA, Promega). The template consisted in a PCR product of the preMSK gene under T7 promoter.

In vivo Mitochondrial Translation

In vivo mitochondrial translation assays were performed as previously described (Hao and Moraes, 1996). Semi-confluent cells (0.5×10^6) were incubated in DMEM with 10% dialyzed FCS lacking methionine and cysteine and supplemented with 0.2 mg/ml emetine for 5 min at 37 ºC. 200 µCi/ml of PRO-MIX^{TM} L-[^{35}S] methionine and cysteine (MP Biomedical.) was added followed by 30 min incubation at 37 ºC. Cells were washed with PBS, lysed, and analyzed by 14% SDS-PAGE and autoradiography.

RT-PCR Analysis

Isolated mitochondrial RNA were subject to RT-PCR using the AccessQuick™ RT-PCR kit (Promega) and a specific reverse primer. The AMV reverse transcriptase were denatured at 95°C for 5 min and PCR amplification were performed in the same tube after addition of the specific forward primer.

Northern Blot Analysis

Total RNAs were extracted from spheroplasts by addition of 1 volume of lysis buffer (0.1 M sodium acetate pH 5, 1% SDS) and 1 volume of hot phenol (55°C) with subsequent vortexing, centrifugation (16,000 x *g* 10' at 4°C) and precipitation from aqueous phase. For isolation of

mitochondrial RNAs, mitochondria (1 mg/ml) were treated with RNase A (100 μg/ml) for 15' on ice and the reaction was stopped by addition of 5 volumes of BB buffer (0.6 M sorbitol, 10 mM HEPES-NaOH, pH 7) containing 5 mM EDTA. Mitochondrial RNAs were extracted as described for total RNAs. Total and mitochondrial RNAs were separated by electrohopresis on a 8M urea-10% acrylamide gel and transferred onto a Hybond-N membrane (Amersham) in transfer buffer (17 mM NaH_2PO_4/8 mM Na_2HPO_4 pH 6.5). Subsequent hybridizations were carried out with radiolabeled probes directed against tRK1, mitochondrial and total tRNAs followed by exposing to a PhosphorImager plate.

CLIP (Cross-link with Immunoprecipitation).

5-bromodeoxyuridine labelled tRK1 (by T7 transcription) was imported to yest BY strain derived mitochondria at standard *in vitro* import conditions, followed by 312nm irradiation. After import, mitochondria were lysed by osmotic shock in presence of 0.5% Triton X-100 and the lysate was incubated 1h with biotin - conjugated anti-5-bromodeoxyuridine antibodies (Sigme-Aldrich) at 4˚C and gentle shaking. The mixture was then incubated overnight with streptavidine sepharose, washed by the lysis buffer and crosslinked complexes of labelled tRK1 and mitochondrial proteins were eluted by low pH buffer. Eluted fractions were seprated on a 4-20% gradient SDS PAAG, the bands visualised by Coomassie staining, excised and analysed by MALDI and LC/MS after trypsin digestion.

Mass Spectrometry Analysis

For identification of proteins interacting with tRK1, the corresponding bands on the stained gel were localized relative to the signals obtained by the North-Western hybridization and cut for mass spectrometry analysis (Nano LC/MS/MS).

Supplemental References

Chance, B., and Williams, G.R. (1955). Respiratory enzymes in oxidative phosphorylation. III. The steady state. J. Biol. Chem. *217*, 409-427.

Chen, H.W., Rainey, R.N., Balatoni, C.E., Dawson, D.W., Troke, J.J., Wasiak, S., Hong, J.S., McBride, H.M., Koehler, C.M., Teitell, M.A.*, et al.* (2006). Mammalian polynucleotide phosphorylase is an intermembrane space RNase that maintains mitochondrial homeostasis. Mol. Cell. Biol. *26*, 8475-8487.

Hao, H., and Moraes, C.T. (1996). Functional and molecular mitochondrial abnormalities associated with a C --> T transition at position 3256 of the human mitochondrial genome. The effects of a pathogenic mitochondrial tRNA point mutation in organelle translation and RNA processing. J. Biol. Chem. *271*, 2347-2352.

Matlib, M.A., Shannon, W.A., Jr., and Srere, P.A. (1979). Measurement of matrix enzyme activity in situ in isolated mitochondria made permeable with toluene. Methods Enzymol. *56*, 544-550.

Rainey, R.N., Glavin, J.D., Chen, H.W., French, S.W., Teitell, M.A., and Koehler, C.M. (2006). A new function in translocation for the mitochondrial i-AAA protease Yme1: import of polynucleotide phosphorylase into the intermembrane space. Mol. Cell. Biol. *26*, 8488-8497.

Thinnes, F.P., Florke, H., Winkelbach, H., Stadtmuller, U., Heiden, M., Karabinos, A., Hesse, D., Kratzin, H.D., Fleer, E., and Hilschmann, N. (1994). Channel active mammalian porin, purified from crude membrane fractions of human B lymphocytes or bovine skeletal muscle, reversibly binds the stilbene-disulfonate group of the chloride channel blocker DIDS. Biol. Chem. Hoppe Seyler *375*, 315-322.

Zhang, J., Nuebel, E., Wisidagama, D.R., Setoguchi, K., Hong, J.S., Van Horn, C.M., Imam, S.S., Vergnes, L., Malone, C.S., Koehler, C.M.*, et al.* (2012). Measuring energy metabolism in cultured cells, including human pluripotent stem cells and differentiated cells. Nature Protoc. *7*, 1068-1085.

Table S1, related to Figure 1. Mass Spectrometry Analysis of Proteins that Bound to the Aminoacylated tRK1

Sample name	Mitochondrial fraction L = lysate; OM = outer membrane; IM = inner membrane	MS/MS sample name	Protein name	Protein accession numbers	Protein molecular weight (Da)
Por1 deletant	OM	E041529 (F068412)	Mitochondrial import receptor subunit TOM40; Mitochondrial import site protein ISP42; Translocase of outer membrane 40 kDa subunit	gi|124912,gi|15945907,gi|190408429,gi|207342175,gi|227419,gi|3838,gi|51013493,gi|6323859,gi|736300	17 713,9
	OM	E041531 (F068414)	TOM20	gi|1323117,gi|151943359,gi|190406898,gi|207345161,gi|406600,gi|45269441,gi|453432,gi|464308,gi|6321519	18 388,8
	OM	E041531 (F068414)	TOM22	gi|1302070,gi|1352638,gi|151944406,gi|190409118,gi|6223340,gi|6324198,gi|854506	24 391,3
	OM	E041532 (F068415)	CDP-diacylglycerol--serine O-phosphatidyltransferase; AltName: Phosphatidylserine synthase	gi|131441,gi|359736,gi|4248,gi|603618,gi|6320864	23 494,9
	OM, ER	E041533 (F068416)	CDP-diacylglycerol--serine O-phosphatidyltransferase; AltName: Phosphatidylserine synthase	gi|131441,gi|359736,gi|4248,gi|603618,gi|6320864	20 545,7
	OM, ER	E041537 (F068420)	CDP-diacylglycerol--serine O-phosphatidyltransferase; AltName:Phosphatidylserine synthase	gi|131441,gi|359736,gi|4248,gi|603618,gi|6320864	33 839,4
	OM, ER	E041540 (F068423)	CDP-diacylglycerol--serine O-phosphatidyltransferase; AltName: Phosphatidylserine synthase	gi|131441,gi|359736,gi|4248,gi|603618,gi|6320864	34 334,2
	OM	E041542 (F068425)	Mitochondrial NADH-cytochrome b5 reductase, involved in ergosterol biosynthesis	gi|147223225,gi|1490392,gi|151941658,gi|1582554,gi|187609654,gi|190409689,gi|207343618,gi|407497,gi|486258,gi|549725,gi|6322699	39 449,0
	OM	E041544 (F068427)	Mitochondrial import receptor subunit TOM40; Mitochondrial import site protein ISP42; Translocase of outer membrane 40 kDa subunit	gi|124912,gi|15945907,gi|190408429,gi|207342175,gi|227419,gi|3838,gi|51013493,gi|6323859,gi|736300	41 198,6
	OM	E041547 (F068430)	FAA1	gi|1420696,gi|151945398,gi|190407617,gi|207340896,gi|266448,gi|3692,gi|6324893,gi|940848	44 368,2
BY	OM	E041477 (F068379)	Tom 5 (translocase of the outer membrane)	gi|151942907,gi|190408058,gi|207340260,gi|2498696,gi|45270628,gi|6325391	5 966,7
	OM	E041486 (F068388)	POR1	gi|1301923,gi|151944477,gi|190409046,gi|6324273,gi|68846657,gi|994830	30 411,5
	OM	E041489 (F068391)	POR1	gi|1301923,gi|151944477,gi|190409046,gi|6324273,gi|68846657,gi|994830	30 411,5
	OM	E041493 (F068395)	POR1	gi|1301923,gi|151944477,gi|190409046,gi|6324273,gi|68846657,gi|994830	30 411,5
	OM	E041494 (F068396)	POR1	gi|1301923,gi|151944477,gi|190409046,gi|6324273,gi|68846657,gi|994830	30 411,5
	OM	E041495 (F068397)	unnamed protein product Primary component of eisosomes, which are large immobile cell cortex structures associated with endocytosis; null mutants show activation of Pkc1p/Ypk1p stress resistance pathways; detected in phosphorylated state in mitochondria	gi|1323125,gi|151943363,gi|1723685,gi|190406894,gi|207345156,gi|6321523	38 332,3
	OM	E041497 (F068399)	delta(24)-sterol C-methyltransferase	gi|151946153,gi|190408231,gi|207342464,gi|39103685,gi|396515,gi|462024,gi|619251,gi|6323635,gi|854482	43 413,6
	OM	E041499 (F068401)	delta(24)-sterol C-methyltransferase	gi|151946153,gi|190408231,gi|207342464,gi|39103685,gi|396515,gi|462024,gi|619251,gi|6323635,gi|854482	43 413,6
BY	IM	E041479 (F068381)	F1F0 ATP synthase subunit e [Saccharomyces cerevisiae YJM789]	gi|151942299,gi|190404736,gi|3913153,gi|45269331,gi|6320529	10 857,8
	IM	E041482 (F068384)	Chain H, Crystal Structure Of Yeast Mitochondrial F1-Atpase	gi|11938911,gi|11938920,gi|11938929	14 535,2
	IM	E041483 (F068385)	cytochrome C oxidase chain IV precursor [Saccharomyces cerevisiae]	gi|1143560,gi|117090,gi|1322805,gi|151943629,gi|190407127,gi|3582,gi|6321251	17 124,8
	IM	E041483 (F068385)	Chain F, Yeast Cytochrome Bc1 Complex With Stigmatellin	gi|14579632,gi|151942490,gi|1717954,gi|188036286,gi|188036297,gi|188036309,gi|188036320,gi|190404554,gi|20151124,gi|20151135,gi|6320738,gi|927796	14 547,7
	IM	E041486 (F068388)	Aim37 Putative protein of unknown function; non-tagged protein is detected in purified mitochondria; null mutant is viable and displays reduced respiratory growth and reduced frequency of mitochondrial genome loss	gi|1302012,gi|151944434,gi|1730757,gi|190409089,gi|207341725,gi|51012859,gi|6324229,gi|71064099,gi|929853	26 942,5
	IM	E041490 (F068392)	Atp4p F(1)F(0)-ATPase complex delta subunit	gi|1147615,gi|151942718,gi|190407875,gi|207340536,gi|51013403,gi|6325179	26 907,5
	IM	E041493 (F068395)	ADP/ATP carrier [Saccharomyces cerevisiae YJM789]	gi|151946364,gi|170958,gi|396555,gi|536035,gi|584738,gi|602894,gi|6319441	34 409,9
	IM	E041494 (F068396)	Lpi11p, protein of mito carrier family	gi|1244780,gi|190407824,gi|20138947,gi|207340610,gi|6325123	34 189,0
	IM	E041494 (F068396)	suppressor of cytochrome oxidase deficiency [Saccharomyces cerevisiae YJM789]	gi|151946417,gi|1587582,gi|207347782,gi|498753,gi|536232,gi|585972,gi|6319498	34 872,6
	IM	E041494 (F068396)	Cytochrome c1, heme protein, mitochondrial; Ubiquinol-cytochrome-c reductase complex cytochrome c1 subunit; Cytochrome c-1; Cytochrome b-c1 complex subunit 4;Complex III subunit 4; Complex III subunit IV	gi|117766,gi|1420211,gi|14277715,gi|145579629,gi|151945691,gi|188036283,gi|188036294,gi|188036306,gi|188036317,gi|190407400,gi|20151121,gi|20151132,gi	34 037,3
	IM	E041494 (F068396)	MIR1 [Saccharomyces cerevisiae]	gi|1015764,gi|1019698,gi|127277,gi|151945144,gi|171957,gi|190409551,gi|207343823,gi|227212,gi|296863,gi|45269717,gi|6322537	32 795,8
	IM	E041494 (F068396)	Succinate dehydrogenase [ubiquinone] iron-sulfur subunit, mitochondrial;Iron-sulfur subunit of complex II; Ip	gi|118619,gi|1360235,gi|151941130,gi|172549,gi|190406009,gi|207343274,gi|45270268,gi|6322987	30 214,3
	IM	E041494 (F068396)	ADP/ATP carrier [Saccharomyces cerevisiae YJM789]	gi|151946364,gi|170958,gi|396555,gi|536035,gi|584738,gi|602894,gi|6319441	34 409,9
	IM	E041497 (F068399)	Cytochrome bc1 complex subunit 2, mitochondrial; Ubiquinol-cytochrome-c reductase complex core protein 2; Core protein II; Complex III subunit 2;	gi|136696,gi|14277713,gi|14557627,gi|151942961,gi|188036281,gi|188036292,gi|188036304,gi|188036315,gi|20151119,gi|20151130,gi|24158772,gi|34811037,gi	40 461,7
	IM	E041501 (F068403)	Chain D, Crystal Structure Of Yeast Mitochondrial F1-Atpase	gi|11938907,gi|11938908,gi|11938909,gi|11938916,gi|11938917,gi|11938918,gi|119389925,gi|119389926,gi|119389927	51 109,1
Por1 deletant	IM	E041524 (F068407)	QCR8 [Saccharomyces cerevisiae] part of bc1	gi|1008356,gi|14277719,gi|14557633,gi|151944963,gi|188036287,gi|188036298,gi|188036310,gi|188036321,gi|190409345,gi|20151125,gi|20151136,gi|24158778	10 956,8
	IM	E041524 (F068407)	F1F0 ATP synthase subunit f	gi|151942350,gi|1763252,gi|190404687,gi|2493092,gi|6320585,gi|849198	11 294,6
	IM	E041524 (F068407)	Mitochondrial ATP synthase g subunit	gi|1314094,gi|151942809,gi|190407964,gi|2493096,gi|51013411,gi|6325277,gi|887598	12 903,9
	IM	E041526 (F068409)	Cytochrome c oxidase polypeptide 6, mitochondrial; Cytochrome c oxidase polypeptide VI	gi|117093,gi|151943997,gi|171295,gi|190405834,gi|45270446,gi|488164,gi|6321842	17 324,2
	IM	E041526 (F068409)	protein is detected in highly purified mitochondria and orthologous to human gene BRP44L;	gi|1322599,gi|1723875,gi|45270862,gi|6321358	14 978,3
	IM	E041526 (F068409)	Chain H, Crystal Structure Of Yeast Mitochondrial F1-Atpase	gi|11938911,gi|11938920,gi|11938929	14 535,2
	IM	E041529 (F068412)	ADP/ATP carrier [Saccharomyces cerevisiae YJM789]	gi|151946364,gi|170958,gi|396555,gi|536035,gi|584738,gi|602894,gi|6319441	20 231,2
	IM	E041530 (F068413)	Chain G, Crystal Structure Of Yeast Mitochondrial F1-Atpase	gi|11938910,gi|11938919,gi|11938928,gi|151946430,gi|190408794,gi|37359702,gi|45269621,gi|473609,gi|483826,gi|536260,gi|584817,gi|6319513	16 704,9
	IM	E041530 (F068413)	Chain D, Crystal Structure Of Yeast Mitochondrial F1-Atpase	gi|11938907,gi|11938908,gi|11938909,gi|11938916,gi|11938917,gi|11938918,gi|119389925,gi|119389926,gi|119389927	20 640,2
-	IM	E041531 (F068414)	Chain D, Crystal Structure Of Yeast Mitochondrial F1-Atpase	gi|11938907,gi|11938908,gi|11938909,gi|11938916,gi|11938917,gi|11938918,gi|119389925,gi|119389926,gi|119389927	16 772,9
	IM	E041532 (F068415)	Chain D, Crystal Structure Of Yeast Mitochondrial F1-Atpase	gi|11938907,gi|11938908,gi|11938909,gi|11938916,gi|11938917,gi|11938918,gi|119389925,gi|119389926,gi|119389927	23 133,0
	IM	E041533 (F068416)	Chain A, Crystal Structure Of Yeast Mitochondrial F1-Atpase	gi|11938904,gi|11938905,gi|11938906,gi|11938913,gi|11938914,gi|11938915,gi|11938922,gi|11938923,gi|11938924,gi|151946302,gi|1660995,gi|17111	23 347,4
	IM	E041534 (F068417)	Chain A, Crystal Structure Of Yeast Mitochondrial F1-Atpase	gi|11938904,gi|11938905,gi|11938906,gi|11938913,gi|11938914,gi|11938915,gi|11938922,gi|11938923,gi|11938924,gi|151946302,gi|1660995,gi|17111	34 037,3
	IM	E041534 (F068417)	ADP/ATP carrier [Saccharomyces cerevisiae YJM789]	gi|151946364,gi|170958,gi|396555,gi|536035,gi|584738,gi|602894,gi|6319441	27 591,7
	IM	E041534 (F068417)	Succinate dehydrogenase [ubiquinone] iron-sulfur subunit, mitochondrial; Iron-sulfur subunit of complex II	gi|118619,gi|1360235,gi|151941130,gi|172549,gi|190406009,gi|207343274,gi|45270268,gi|6322987	34 409,9
	IM	E041534 (F068417)	Cytochrome b-c1 complex subunit 2, mitochondrial; Ubiquinol-cytochrome-c reductase complex core protein 2; Core protein II; Complex III subunit 2	gi|136696,gi|14277713,gi|14557627,gi|151942961,gi|188036281,gi|188036292,gi|188036304,gi|188036315,gi|20151119,gi|20151130,gi|24158772,gi|34811037,gi	30 214,3
	IM	E041535 (F068418)	MIR1 [Saccharomyces cerevisiae]	gi|1015764,gi|1019698,gi|127277,gi|151945144,gi|171957,gi|190409551,gi|207343823,gi|227212,gi|296863,gi|45269717,gi|6322537	32 797,3
	IM	E041535 (F068418)	Cytochrome bc1 complex subunit 2, mitochondrial; Ubiquinol-cytochrome-c reductase complex core protein 2; Core protein II;Complex III subunit 2	gi|136696,gi|14277713,gi|14557627,gi|151942961,gi|188036281,gi|188036292,gi|188036304,gi|188036315,gi|20151119,gi|20151130,gi|24158772,gi|34811037,gi	32 795,8
	IM	E041535 (F068418)	ADP/ATP carrier [Saccharomyces cerevisiae YJM789]	gi|151946364,gi|170958,gi|396555,gi|536035,gi|584738,gi|602894,gi|6319441	31 330,0
	IM	E041536 (F068419)	Probable electron transfer flavoprotein subunit beta	gi|1169560,gi|1323371,gi|151943484,gi|190406783,gi|207344982,gi|45270646,gi|6321646,gi|790498	33 699,4
	IM	E041536 (F068419)	Chain C, Structure Of The Yeast Cytochrome Bc1 Complex	gi|14277714,gi|14557628,gi|152030930,gi|188036282,gi|188036293,gi|188036305,gi|188036316,gi|20151120,gi|20151131,gi|24158773,gi|30179770,gi|34811038	28 741,7
	IM	E041536 (F068419)	Cytochrome b-c1 complex subunit 2, mitochondrial;Ubiquinol-cytochrome-c reductase complex core protein 2; Core protein II; Complex III subunit 2	gi|136696,gi|14277713,gi|14557627,gi|151942961,gi|188036281,gi|188036292,gi|188036304,gi|188036315,gi|20151119,gi|20151130,gi|24158772,gi|34811037,gi	33 199,7
	IM	E041536 (F068419)	hypothetical protein SCRG_03207 (2-oxoacid dehydrogenases acyltransferase)	gi|190409060	32 795,8
	IM	E041538 (F068421)	protein is detected in highly purified mitochondria	gi|1279689,gi|1431001,gi|151941968,gi|190405042,gi|207346907,gi|56404748,gi|6320178	32 795,8
	IM	E041538 (F068421)	Cytochrome c oxidase subunit 2; Cytochrome c oxidase polypeptide II	gi|117050,gi|13512,gi|13613,gi|152030934,gi|157072434,gi|157072436,gi|157072438,gi|16944801,gi|2511678,gi|29293743,gi|3158146,gi|31581148,gi|31581150,	31 409,8
	IM	E041538 (F068421)	Chain G, Crystal Structure Of Yeast Mitochondrial F1-Atpase	gi|11938910,gi|11938919,gi|11938928,gi|151946430,gi|190408794,gi|37359702,gi|45269621,gi|473609,gi|483826,gi|536260,gi|584817,gi|6319513	32 795,8
	IM	E041538 (F068421)	Chain D, Crystal Structure Of Yeast Mitochondrial F1-Atpase	gi|11938907,gi|11938908,gi|11938909,gi|11938916,gi|11938917,gi|11938918,gi|119389925,gi|119389926,gi|119389927	34 334,2
	IM	E041540 (F068423)	Chain D, Crystal Structure Of Yeast Mitochondrial F1-Atpase	gi|11938907,gi|11938908,gi|11938909,gi|11938916,gi|11938917,gi|11938918,gi|119389925,gi|119389926,gi|119389927	33 199,7
	IM	E041540 (F068423)	PHB1 [Saccharomyces cerevisiae]	gi|1323219,gi|151943412,gi|1730544,gi|190406850,gi|207345078,gi|45270082,gi|6321571	33 839,4
	IM	E041540 (F068423)	PHB1 [Saccharomyces cerevisiae]	gi|1323219,gi|151943412,gi|1730544,gi|190406850,gi|207345078,gi|45270082,gi|6321571	33 839,4
	IM	E041541 (F068424)	Ypr128cp ATP/ADP carrier	gi|1066487,gi|151942903,gi|190408053,gi|207340274,gi|6325385,gi|74676404	39 708,6
	IM	E041542 (F068425)	ADP/ATP carrier [Saccharomyces cerevisiae YJM789]	gi|151946364,gi|170958,gi|396555,gi|536035,gi|584738,gi|602894,gi|6319441	34 409,9
	IM	E041542 (F068425)	Chain D, Crystal Structure Of Yeast Mitochondrial F1-Atpase	gi|11938907,gi|11938908,gi|11938909,gi|11938916,gi|11938917,gi|11938918,gi|119389925,gi|119389926,gi|119389927	35 728,6
	IM	E041544 (F068427)	pyruvate dehydrogenase alpha subunit (E1 alpha) [Saccharomyces cerevisiae YJM789]	gi|151944896,gi|172108,gi|190405734,gi|207345769,gi|298059,gi|37362644,gi|603419,gi|730222	42 021,3
	IM	E041544 (F068427)	Chain A, Crystal Structure Of Yeast Mitochondrial F1-Atpase	gi|11938904,gi|11938905,gi|11938906,gi|11938913,gi|11938914,gi|11938915,gi|11938922,gi|11938923,gi|11938924,gi|151946302,gi|1660995,gi|17111	44 629,2
	IM	E041545 (F068428)	Chain A, Crystal Structure Of Yeast Mitochondrial F1-Atpase	gi|11938904,gi|11938905,gi|11938906,gi|11938913,gi|11938914,gi|11938915,gi|11938922,gi|11938923,gi|11938924,gi|151946302,gi|1660995,gi|17111	44 976,6
	IM	E041546 (F068429)	Chain A, Crystal Structure Of Yeast Mitochondrial F1-Atpase	gi|11938904,gi|11938905,gi|11938906,gi|11938913,gi|11938914,gi|11938915,gi|11938922,gi|11938923,gi|11938924,gi|151946302,gi|1660995,gi|17111	44 135,9
	IM	E041546 (F068429)	Cytochrome bc1 complex subunit 1, mitochondrial; Ubiquinol-cytochrome-c reductase complex core protein 1; Core protein I; Complex III subunit 1	gi|136693,gi|171256,gi|463264,gi|51013545,gi|536065,gi|6319426	44 721,6
	IM	E041546 (F068429)	pyruvate dehydrogenase alpha subunit (E1 alpha) [Saccharomyces cerevisiae YJM789]	gi|151944896,gi|172108,gi|190405734,gi|207345769,gi|298059,gi|37362644,gi|603419,gi|730222	50 211,0
	IM	E041546 (F068429)	Beta subunit of succinyl-CoA ligase	gi|1323442,gi|151943518,gi|1711580,gi|6321683	46 326,4
	IM	E041547 (F068430)	Ypl063wp [Saccharomyces cerevisiae] TIM50P	gi|1079679,gi|151942732,gi|190407889,gi|207340520,gi|6325194,gi|74676305	46 884,1
	IM	E041548 (F068431)	Ypl063wp [Saccharomyces cerevisiae] TIM50P	gi|1079679,gi|151942732,gi|190407889,gi|207340520,gi|6325194,gi|74676305	52 594,1
BY	matrix	E041479 (F068381)	HSP10 [Saccharomyces cerevisiae]	gi|1420125,gi|151945648,gi|190407360,gi|453447,gi|51013895,gi|521088,gi|6324594,gi|729121,gi|829130	11 354,4
	matrix	E041479 (F068381)	MRP-S19 unnamed protein product [Saccharomyces cerevisiae]	gi|1302539,gi|151944566,gi|1730677,gi|190408964,gi|6324365	10 257,4
	matrix	E041482 (F068384)	MRP-L28 conserved protein [Saccharomyces cerevisiae YJM789]	gi|151941589,gi|190409866,gi|45270522,gi|486501,gi|549618,gi|6322902,gi|78100834	15 632,5
	matrix	E041482 (F068384)	MRP-L28 YmL28 [Saccharomyces cerevisiae YJM789]	gi|151942427,gi|172768,gi|190404614,gi|51013851,gi|6174960,gi|6320670,gi|927728	17 324,7
	matrix	E041482 (F068384)	Rim1 Single-stranded DNA-binding protein essential for mitochondrial genome maintenance; involved in mitochondrial DNA replication; Rim1p [Saccharomyces cerevisiae]	gi|10383791,gi|14588940,gi|151943849,gi|190406464,gi|254074,gi|417647	15 368,6
	matrix	E041483 (F068385)	unnamed protein product, colocalizes with mitochondrial ribosomes [Saccharomyces cerevisiae]	gi|1302213,gi|42742305,gi|6000057,gi|85681851	20 132,7
	matrix	E041485 (F068387)	Protein associated with the mitochondrial nucleoid with similarity to E. coli L7/L12 ribosomal protein	gi|1322579,gi|151943736,gi|1723848,gi|190407028,gi|207345332,gi|6321369	20 632,8
	matrix	E041486 (F068388)	Superoxide dismutase [Mn], mitochondrial	gi|134681,gi|151943950,gi|190405793,gi|207344789,gi|217035334,gi|4514,gi|45269533,gi|500704,gi|6321796	24 076,3
	matrix	E041497 (F068399)	Ketol-acid reductoisomerase, mitochondrial; Acetohydroxy-acid reductoisomerase; Alpha-keto-beta-hydroxylacil reductoisomerase	gi|124371,gi|151940879,gi|190405401,gi|207342795,gi|3827,gi|609403,gi|6323387,gi|957238	44 351,9
	matrix	E041484 (F068386)	ARS-binding factor; involved in mito DNA replication [Saccharomyces cerevisiae YJM789]	gi|151946230,gi|190408303,gi|207342356,gi|2815294,gi|398988,gi|45269826,gi|6323717,gi|763019	21 545,3
por1 deletant					
	matrix	E041524 (F068407)	Thioredoxin-3, mitochondrial	gi|140543,gi|151943894,gi|164519455,gi|164519456,gi|164519457,gi|164519458,gi|164519459,gi|164519460,gi|190406501,gi|1907220,gi|6319925	14 414,8
	matrix	E041526 (F068409)	Ypl059wp ROS detox	gi|1079683,gi|151942735,gi|190407892,gi|3025275,gi|45720877,gi|6325198	16 914,3
	matrix	E041526 (F068409)	YmL34 60S component	gi|151941749,gi|1582535,gi|190409673,gi|407512,gi|486297,gi|51013525,gi|548805,gi|6322678	14 886,8
	matrix	E041526 (F068409)	conserved protein [Saccharomyces cerevisiae YJM789]	gi|151941589,gi|190409866,gi|45270522,gi|486501,gi|549618,gi|6322902,gi|78100834	15 632,5
	matrix	E041526 (F068409)	YmL28 60S component	gi|151942427,gi|172768,gi|190404614,gi|51013851,gi|6174960,gi|6320670,gi|927728	17 324,7
	matrix	E041529 (F068412)	IBM1 [Saccharomyces cerevisiae]	gi|1208238,gi|151943108,gi|190406271,gi|45270492,gi|557817,gi|6322138,gi|731809	17 117,8
	matrix	E041530 (F068413)	Heat shock protein 60, mitochondrial;Stimulator factor I 66 kDa component; P66; CPN60	gi|123579,gi|151941093,gi|171720,gi|190405319,gi|207342889,gi|226279,gi|577181,gi|6323288	17 453,2
	matrix	E041531 (F068414)	unnamed protein product [Saccharomyces cerevisiae]	gi|1322579,gi|151943736,gi|1723848,gi|190407028,gi|207345332,gi|6321369	20 252,9
	matrix	E041532 (F068415)	conserved protein [Saccharomyces cerevisiae YJM789]	gi|151944142,gi|190405972,gi|45270102,gi|551327,gi|6321992,gi|731767	20 252,9
	matrix	E041534 (F068417)	YDR296W [Saccharomyces cerevisiae]	gi|45269361,gi|6320502,gi|6526399,gi|74583565,gi|849216	34 872,6
	matrix	E041534 (F068417)	YDR296W [Saccharomyces cerevisiae] mtDNA recombination	gi|45269361,gi|6320502,gi|6526399,gi|74583565,gi|849216	32 795,8
	matrix	E041534 (F068417)	IDH1 [Saccharomyces cerevisiae]	gi|1301886,gi|151944495,gi|167013430,gi|167013432,gi|167013434,gi|167013436,gi|167013438,gi|167013440,gi|167013442,gi|167013444,gi|167013446,gi|16701	31 794,8
	matrix	E041536 (F068419)	Isocitrate dehydrogenase [NADP], mitochondrial;IDH; Oxalosuccinate decarboxylase; NADP(+)-specific ICDH; IDP	gi|1241602,gi|1431074,gi|151941934,gi|171749,gi|190405075,gi|19350651,gi|193506512,gi|193506513,gi|193506514,gi|193506515,gi|193506516,gi|193506517,gi	34 409,9
	matrix	E041536 (F068419)	YmL5/7 [Saccharomyces cerevisiae YJM789]	gi|151942214,gi|1710597,gi|190404813,gi|207346552,gi|45269381,gi|6320443,gi|817823	34 409,9
	matrix	E041536 (F068419)	mitochondrial ribosomal protein [Saccharomyces cerevisiae YJM789]	gi|151942101,gi|190404923,gi|207346717,gi|45269259,gi|46810393,gi|6320321,gi|747890	33 082,2
	matrix	E041536 (F068419)	mitochondrial ribosomal protein [Saccharomyces cerevisiae YJM789]	gi|151945891,gi|190408413,gi|207342209,gi|2500474,gi|6323842,gi|854458	34 334,2
	matrix	E041536 (F068419)	54S ribosomal protein L24, mitochondrial; YmL14/YmL24	gi|1350795,gi|151945896,gi|190408418,gi|45269854,gi|6323847,gi|642285	34 037,3
	matrix	E041536 (F068419)	Ketol-acid reductoisomerase, mitochondrial; Acetohydroxy-acid reductoisomerase;Alpha-keto-beta-hydroxylacil reductoisomerase	gi|124371,gi|151940879,gi|190405401,gi|207342795,gi|3827,gi|609403,gi|6323387,gi|957238	34 447,5
	matrix	E041538 (F068421)	conserved protein [Saccharomyces cerevisiae YJM789]	gi|151944143,gi|190405973,gi|207344502,gi|458946,gi|6321993,gi|731768	29 157,5
	matrix	E041538 (F068421)	DNA binding protein [Saccharomyces cerevisiae YJM789]	gi|151945946,gi|190408467,gi|207342128,gi|2497200,gi|6323897,gi|736307	34 096,7
	matrix	E041538 (F068421)	Heat shock protein 60, mitochondrial;Stimulator factor I 66 kDa component; P66; CPN60	gi|123579,gi|151941093,gi|171720,gi|190405319,gi|207342889,gi|226279,gi|577181,gi|6323288	35 015,4
	matrix	E041541 (F068424)	malate dehydrogenase	gi|171892,gi|190409745,gi|486125,gi|547901,gi|6322765	36 350,8
	matrix	E041543 (F068426)	IDH1 [Saccharomyces cerevisiae]	gi|1301886,gi|151944495,gi|167013430,gi|167013432,gi|167013434,gi|167013436,gi|167013438,gi|167013440,gi|167013442,gi|167013444,gi|167013446,gi|16701	43 579,5
	matrix	E041543 (F068426)	SSC1 [Saccharomyces cerevisiae]	gi|1015701,gi|1197073,gi|123636,gi|151945113,gi|171463,gi|190409522,gi|207343868,gi|6322505,gi|717089	44 351,9
	matrix	E041546 (F068429)	Isocitrate dehydrogenase [NADP], mitochondrial; IDH; Oxalosuccinate decarboxylase; NADP(+)-specific ICDH; IDP	gi|124160,gi|1431074,gi|151941934,gi|171749,gi|190405075,gi|19350651,gi|193506512,gi|193506513,gi|193506514,gi|193506515,gi|193506516,gi|193506517,gi	45 854,4
	matrix	E041546 (F068429)	mitochondrial ribosomal small subunit component [Saccharomyces cerevisiae YJM789]	gi|151943936,gi|171982,gi|190405778,gi|207344804,gi|417730,gi|45270660,gi|500819,gi|6321782	51 109,1
	matrix	E041548 (F068431)	unknown [Saccharomyces cerevisiae]	gi|1122358,gi|1431482,gi|151942028,gi|190404991,gi|207346829,gi|2506374,gi|51830224,gi|6320241	50 014,6
	matrix	E041548 (F068431)	unnamed protein product [Saccharomyces cerevisiae]	gi|1420808,gi|151945449,gi|207340808,gi|2506349,gi|6324950	50 413,6

Table S2, related to Figure 1. Identified peptides of outer membrane proteins found in bands, corresponding to tRK1 positive signal on North Western assay

Strain	Protein name	Identification probability	Number of unique peptides	Percentage sequence coverage	Peptide sequence
Wild type	TOM 5 (5,97kD)	93.7%	1	30%	MFGLPQQEVSEEEKR
	POR1 (30,41kD)	100%	15	59,4%	AKQPVKDGPLSTNVEAK - DFYHATPAAFDVQTTTANGIK - DGPLSTNVEAK - GAFDLCLK - LEFANLTPGLK - LEFANLTPGLKNELITSLTPGVAK - LPNSNVNIEFATR - NELITSLTPGVAK - NINDLLNK - QLLRPGVTLGVGSSFDALK - SAVLNTTFTQPFFTAR - SPPVYSDISR - VSDSGIVTLAYK - YAMALSYFAK - YLPDASSQVK
ΔPOR1	TOM20 (20,3kD)	99.8%	2	16,4%	ALTVYPQPADLLGIYQR - EATFTTNVENGER
	TOM22 (16,8kD)	99.9%	3	24,3%	IVALK - QTISNFFGFTSSFVR - TFDLQSDANNILAQGEK
	TOM40 (42kD)	99.1%	2	10,3%	SAPTPLAEASQIPTIPALSPLTAK - TDGSAPGDAGVSYLTR

Table S3, related to Figure 1. Activity of marker enzymes in mitochondrial fractions, nmole/min* mg protein.

	Citrate synthase				Succinate dehydrogenase				Adenylate kinase			
	WT	ΔPOR1	ΔPOR2	ΔTOM5	WT	ΔPOR1	ΔPOR2	ΔTOM5	WT	ΔPOR1	ΔPOR2	ΔTOM5
M	91±4	104±12	93±14	94±11	107 ±17	92±8	79±11	87±7	227 ±34	258±41	196±22	214±19
IM/M	122±9	131±8	129±11	136±9	123 ±7	125±6	114±9	109±8	11.5 ±3.0	7.3±2.5	4.8±2.3	6.5±3.1
OMV	nd	nd	nd	nd	0.5± 0.2	0.7±0.4	1.2±0.3	1.3±0.2	3.2± 0.2	2.1±1.1	1.4±0.3	1.7±0.8

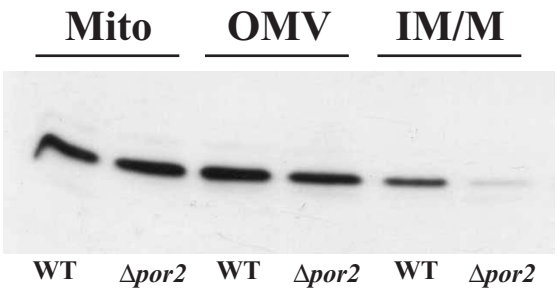

Fig. S1. Immunoblot illustrating VDAC1 distribution in fractions after isolation of mitochondrial outer membrane vesicles from wild type and Δ*por2* strains. Mito – mitochondria, OMV - outer membrane vesicles, IMM/M – inner mitochondrial membrane and matrix fraction. Isolated fractions, equalized to initial volume of fractionation were subjected to 10% SDS-PAGE and immunodecoration was done with antibodies directed against VDAC1.

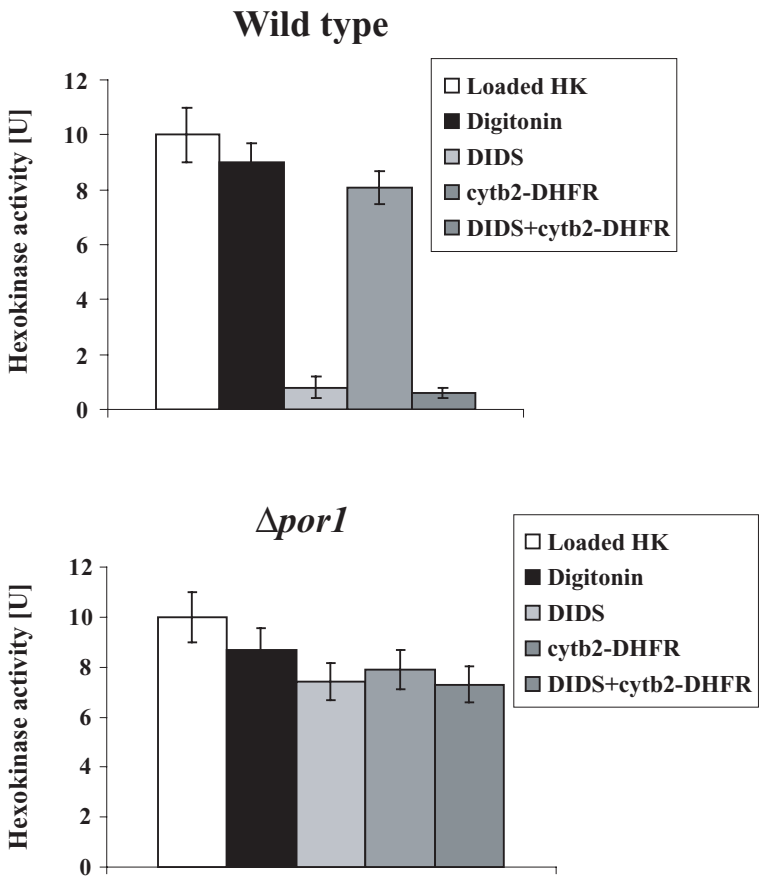

Fig. S2. : Substrate access to hexokinase through channels of OMVs reconstituted with outer mitochondrial membranes from wild type and Δ*por1* strains. Hexokinase (HK), ([U] : μmol/min)

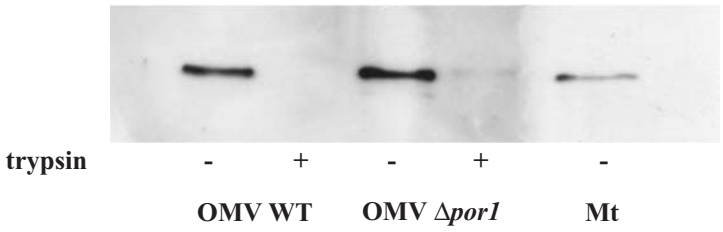

Fig. S3. Outside out orientation of OMV. Vesicles were treated with trypsin and its proteins were separated by SDS-PAGE and immunodecorated with antibodies directed against cytosolic part of outer membrane protein TOM70. OMV WT: outer membrane vesicles from wild type strain, OMV Δ*por1*: outer membrane vesicles from Δ*por1* strain, Mt: mitochondrial lysate

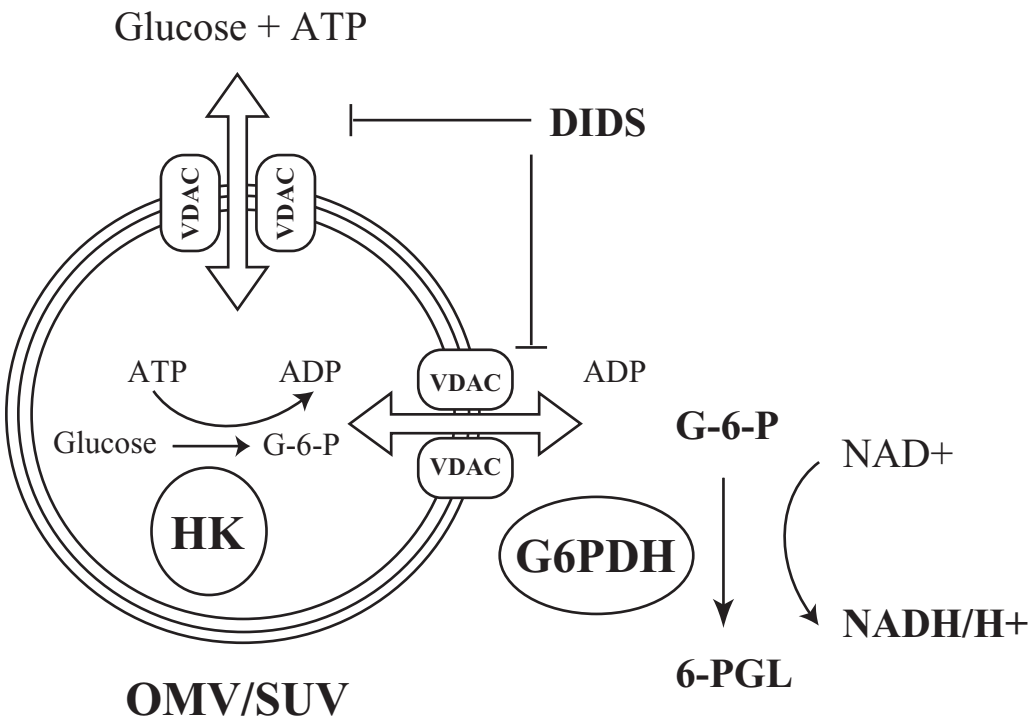

Fig. S4. Scheme illustrating the stability test of prepared outer membrane vesicles (OMVs) or small unilamellar vesicles (SUVs). OMVs or SUVs are loaded with yeast hexokinase (HK) by sonication and incubated at 30˚C in presence of D-glucose and ATP that enter the vesicles via the VDAC channels. Inside of the vesicles HK produces glucose-6-phosphate (G-6-P) that diffuses outside the VDAC channels. Extravesicular G-6-P is oxidized to 6-phosphogluconolactone (6-PGL) by glucose-6-phosphate dehydrogenase (G6PDH) accompanied by an equimolar reduction of NAD+ to NADH that is monitored spectrophotometrically at 340nm. DIDS is used to block VDAC channels in order to investigate the leakiness of the prepares OMVs/SUVs, assuming that DIDS completely blocks VDAC channels. Total amount of loaded HK was checked by solving OMVs/SUVs by digitonin.

A

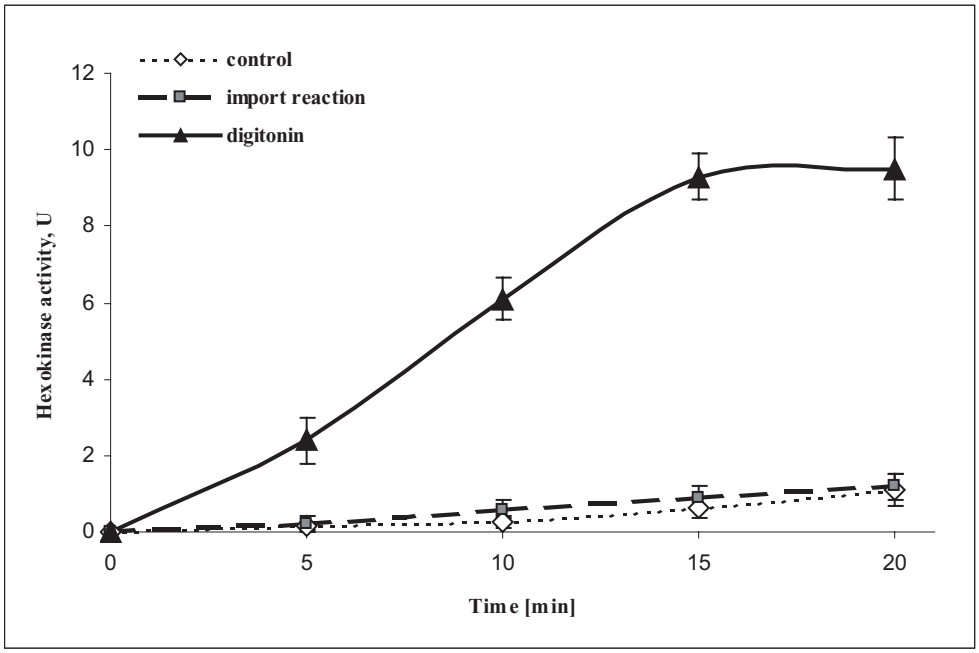

B

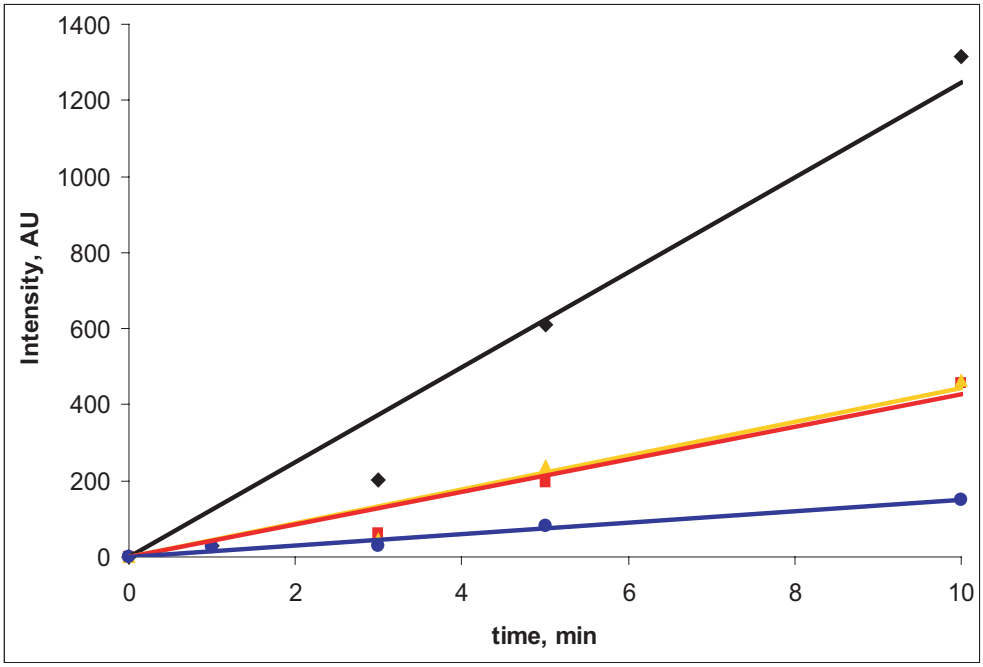

Fig. S5. Characterisation of outer membrane vesicles
A - Outer membrane vesicles are stable in time at experimental conditions of tRK1 *in vitro* import. Amount of loaded HK was checked by solving OMVs by digitonin and measuring total activity in supernatant at indicated times and conditions after sedimentation of OMVs at 100000g, 45 min. Leakiness of OMVs was investigated by measuring of HK activity in supernatans for untreated OMVs (control) and for OMVs at tRK1 *in vitro* import conditions in presence of tRK1 and import directing proteins. This graph is representative for OMVs derived from wild type mitochondria. B- **Linear character of time dependant tRK1 *in vitro* import into OMVs.** tRK1 import kinetics was monitored by autoradiography and tRK1 spots intensity was quantified as explained in material and methods. Used colors: black for standard tRK1 *in vitro* import reaction; red for tRK1 *in vitro* import reaction into OMVs pre-treated with cytb2-DHFR; yellow for tRK1 *in vitro* import reaction into OMVs pre-treated with 1mM DIDS and blue for tRK1 *in vitro* import reaction into OMVs pre-treated with cytb2-DHFR and DIDS.

WT Δ*por1* Δ*por2* elution fractions from HA/celite

Fig. S6. Purification of VDAC1 from *S.cerevisiae*. Mitochondrial lysates from indicated strains and several consequtive elution fractions from hydroxyapatite/celite535 column were analyzed by Western blot using antibodies directed against single peptide of VDAC1 from *S.cerevisiae*.

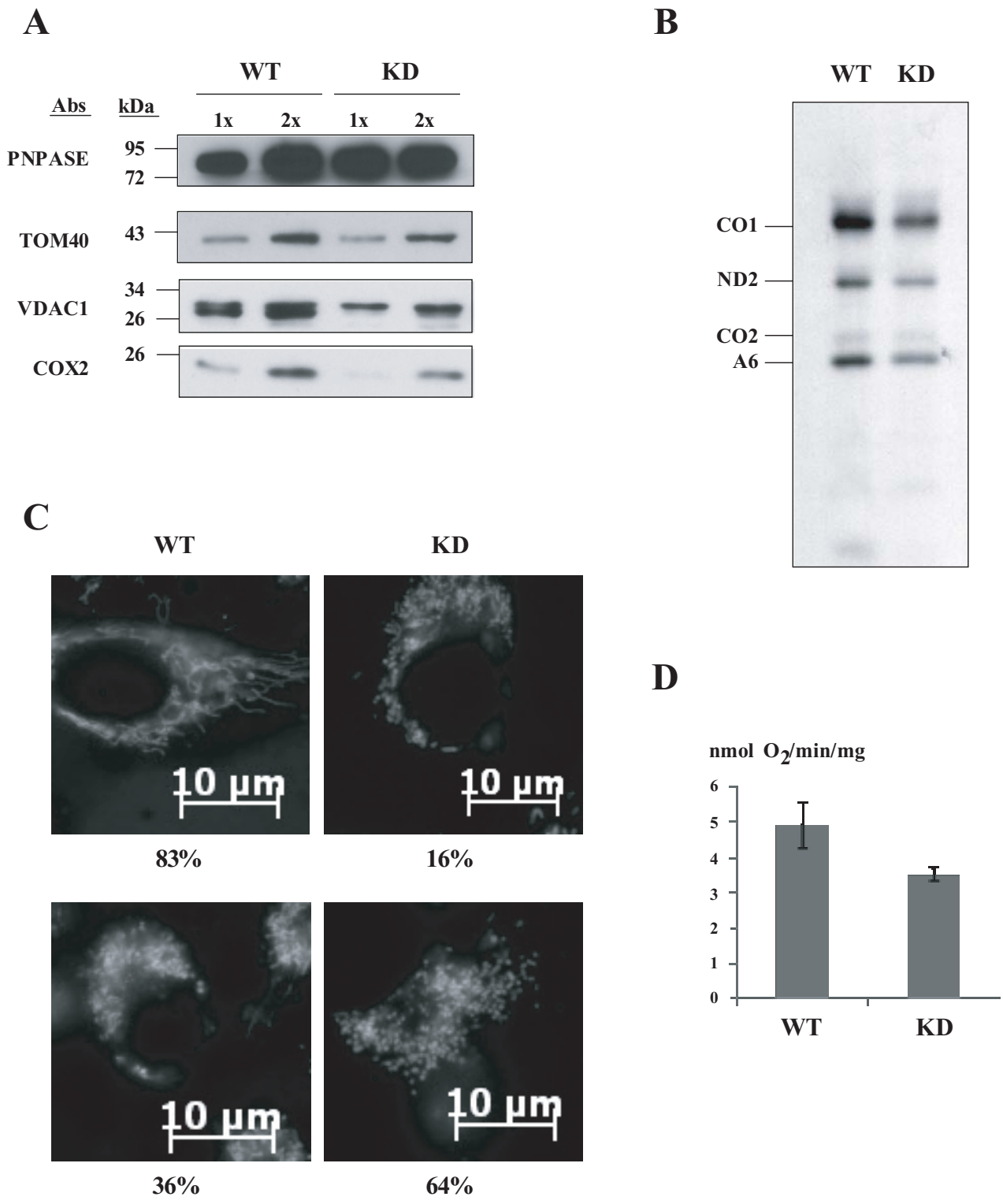

Fig. S7. VDAC1 knockdown impairs mitochondrial functions and structure. (A) Steady-state expression of nucleus and mitochondrion-encoded proteins in wild type (WT) control and VDAC1 knockdown (KD) mitochondria. For each mitochondria 20µg (1X) and 40µg (2X) protein was loaded per lane. **(B)** *In vivo* mitochondrial translation of wild type (WT) control or VDAC1 knockdown (KD) HeLa cells. **(C)** Mitochondrial structure in wild type (WT) control or VDAC1 knockdown (KD) cells shown by Mito-Tracker green staining. Representative images and summarized percentages from 8 fields with over 160 examined cells for each situation are shown. (D) Oxygen consumption of wild type (WT) control or VDAC1 knockdown (KD) cells measured by an XF24 Extracellular Flux Analyzer.

CONCLUSIONS AND PERSPECTIVES

III) CONCLUSIONS AND PERSPECTIVES

The results obtained during this work permitted to draw the following conclusions :

- With the help of North-Western and CLIP analysis it was possible to identify two sets of mitochondrial outer membrane proteins suggesting two possible tRNA import pathways.

- *In vitro* and *in vivo* import studies confirmed the existence of two import pathways across the mitochondrial outer membrane, a VDAC1 dependent import pathway and a Tom40 dependent import pathway.

- Import of tRK1 into isolated mitochondria was shown to induce VDAC1 oligomerization that could promote the translocation of tRK1 through the mitochondrial outer membrane.

- The VDAC1 dependent import pathway can have different requirements for import directing protein factors from that dependent on Tom40.

- Destabilisation of the TOM complex did not have significant consequences on tRK1 import.

- Tom5 and Tom20 proteins of the preprotein import machinery could possess regulatory functions on VDAC1 channelling properties.

The *in vitro* import studies of tRK1 into outer membrane vesicles (OMVs), small unilamellar vesicles (SUVs) and isolated mitochondria gave us the possibility to outline the translocation pathway of tRK1 through the mitochondrial outer membrane. While the channels formed by VDAC proteins could be investigated in detail by a combination of genetic and biochemical approaches, the implication of the Tom40 channel could only be partially characterized with the help of the channel-blocking protein cyt*b2*-DHFR. The essential character of the *TOM40* gene (Baker et al., 1990) would render a genetic analysis of

its implication in tRK1 import quite difficult. For this reason, it will be of substantial importance to study translocation of tRK1 into SUVs reconstituted with the purified or the recombinant Tom40 protein in absence and presence of the blocking protein cyt*b2*-DHFR. In addition, similar import studies could be performed into SUVs reconstituted with the purified TOM complex, giving the possibility to study the Tom40 channel in a more physiologic environment.

3D-structure determinations of VDAC1 demonstrated that this protein possesses a 25 residue-long N-terminal region that was shown to be important for channel gating and conductance of ions and metabolites through the channel (Bayrhuber et al., 2008; Ujwal et al., 2008). Within this N-terminal part of VDAC1 it is known that lysine residues act at strategic positions as potential voltage sensors defining the ion selective state of the channel (Choudhary et al., 2010). In that context, it would be attractive to study tRK1 import in *por1*Δ yeast strains expressing different mutant versions of VDAC1 with systematically truncated N-*termini* or bearing specific site mutations for residues implicated in voltage sensoring.

Deletion of the small Tom protein Tom5 and the receptor protein Tom20 lead to a significant increase of *in vitro* tRK1 import compared to import into wild type mitochondria. To complement these results, it will be essential to study *in vivo* import of tRK1 into mitochondria of *tom5*Δ and *tom20*Δ strains by Northern blot. In the same context, *in vivo* import of tRK1 into mitochondria of *tom6*Δ and *tom7*Δ yeast strains should also be assessed to obtain a more conclusive picture in terms of TOM complex stability impact on tRK1 import. In order to investigate the proposed regulatory functions of Tom5 and Tom20 on the channelling capacities of VDAC1, it will also be necessary to compare *in vitro* import of tRK1 into SUVs reconstituted with VDAC1 together with Tom5 and/or Tom20 to *in vitro* import of tRK1 into SUVs reconstituted with VDAC1 alone.

Recently two new mitochondrial outer membrane proteins, Om14p and Om45p, interacting with VDAC1 have been described (Lauffer et al., 2012). The interactome of the Om14p protein with mitochondrial inner membrane proteins resembles the protein set that we identified by North-Western and CLIP analysis **(Table3, Table4 and Table S2)**. It is possible that Om14p and Om45p facilitate formation of contact sites between VDAC1 and mitochondrial inner membrane proteins by playing the role of adaptor proteins. In that context it would be interesting to investigate the role of Om14p and Om45p in tRK1 import by studying latter in the corresponding mutant yeast strains.

This work was mainly focused on the characterisation of identified mitochondrial outer membrane proteins for their implication in tRK1 import into mitochondria. Crosslinking combined with immunoprecipitation (CLIP) has already been performed in conditions that favoured the identification of mitochondrial outer membrane proteins interacting with tRK1 and permitted us to detect VDAC1, Tom40 and Tom71. This preliminary experiment was, however, only done with a wild type strain where, according to our results, tRK1 import preferentially occurs *via* the VDAC1 dependent import pathway. In order to identify further mitochondrial outer membrane proteins implicated in the Tom40 dependent import pathway by CLIP analysis, similar experiments should be performed using the *por1*Δ strain.

The major purpose of future studies investigating tRK1 import should be focused on the identification of mitochondrial inner membrane proteins responsible for translocation of tRK1 into the matrix compartment. The screening for mitochondrial proteins interacting with tRK1 by North-Western and CLIP analysis has already lead to the identification of several mitochondrial inner membrane proteins **(Table3, Table4, TableS1 and Table S2)**. Potential candidates are Pet9 (ATP/ADP carrier), Mir1 (Phosphate Carrier), Phb1 and Phb2 (Prohibitin 1 and Prohibitin 2) and Tim50 (subunit of the TIM23 complex). The implication of ATP/ADP carriers was already studied in plant mitochondria by blocking this carrier protein with atractyloside that prevents the exchange of ATP and ADP at the level of the mitochondrial inner membrane. Blocking of ATP/ADP carriers was shown to have no effect on tRNA import into plant mitochondria (Salinas et al., 2006). From the other proposed candidates, prohibitin proteins seem to be the most interesting ones because it is known that Phb1 and Phb2 form large megadalton ring-like structures in the mitochondrial inner membrane defining a channel with a pore diameter of 20-25nm (Osman et al., 2009). For this reason, it will be of particular interest to study tRK1 import into mitochondria of yeast strains carrying deletions for Phb1 and/or Phb2. Proteins belonging to the recently described mitochondrial inner-membrane organizing system (MINOS complex) were also identified by our screening approaches, namely Mos1, Aim5 and Aim37. These proteins were probably co-immunoprecipitated with the tRK1/VDAC1 complex because it is known that VDAC1 interacts with subunits of the MINOS complex (Harner et al., 2011; Hoppins et al., 2011; van der Laan et al., 2012).

To verify and complement these preliminary results, identification of inner membrane proteins should be finalized by the CLIP approach. A crucial factor for a promising outcome by this method is a good efficiency of complex formation between tRK1 and its interacting proteins during the import process. To raise the probability of complex formation between

tRK1 and inner membrane proteins, the velocity of the import reaction should be decreased. A first possibility would be to reduce the temperature during import. In addition, inhibition of the mitochondrial respiratory chain activity could provide another mean to slow down the translocation across the inner membrane. Finally, the identified inner membrane candidate proteins will be investigated for their implication in the tRK1 import mechanism by studying *in vitro* and *in vivo* import into mitochondria of the corresponding deletion mutants.

Based on the results obtained in this work it is possible to draw a hypothetical model of the tRNA import mechanism into mitochondria of *Saccharomyces cerevisiae* **(Fig.33)**. If we assume that tRNA transport through VDAC1 and Tom40 channels will be sterically possible, the following question can be stressed: what could be the driving force to deliver a polyanionic tRNA molecule into the matrix compartment surrounded by a negatively charged mitochondrial inner membrane ? We hypothesize that such a vector transfer could be based on an irreversible tRNA binding step in the matrix. Our preliminary data obtained by CLIP analysis support our idea that, indeed, ATP-driven chaperone proteins could be implicated in this binding step **(Table3 and Table4)**. Concerning tRNA import *via* the Tom40 dependent import pathway we propose a compartmentalized system. The tRNA arrives in complex with its carrier protein(s) and the complex probably binds to the receptor protein Tom71 of the TOM complex. The tRNA/protein complex could then adopt a conformation in which the tRNA moiety would be hidden in the complex. Latter will be subsequently translocated through the mitochondrial outer and inner membranes by the preprotein import machinery. After passage into the matrix compartment, the tRNA/protein complex is bound *via* is protein moiety by the presequence translocase-associated motor (PAM), an interaction probably representing a first irreversible step. Then, the tRNA/protein complex is taken in charge by the mitochondrial heat-shock protein (mtHsp60), where the imported preprotein undergoes folding and the RNA possibly dissociates. Free tRNA could be subsequently bound by mitochondrial elongation factors that would guide it to mitoribosomes. This last step is also strengthened by the fact that in our CLIP analysis numerous mitoribosomal proteins have been identified **(Table S2)**. In the context of the VDAC1 dependent import pathway we can propose a limited diffusion mechanism implicating the cooperation of the channel-forming proteins VDAC1 and prohibitins (Phb1/Phb2 complex) that could facilitate the delivery of free tRNA to the matrix compartment. The tRNA probably arrives at the mitochondrial surface in complex with its targeting protein(s), where it binds to the receptor protein Tom71. The tRNA/protein complex could split at this step and, due to its anion selective character, VDAC1 interacts with the polyanionic tRNA and could promote partial unfolding to ease the

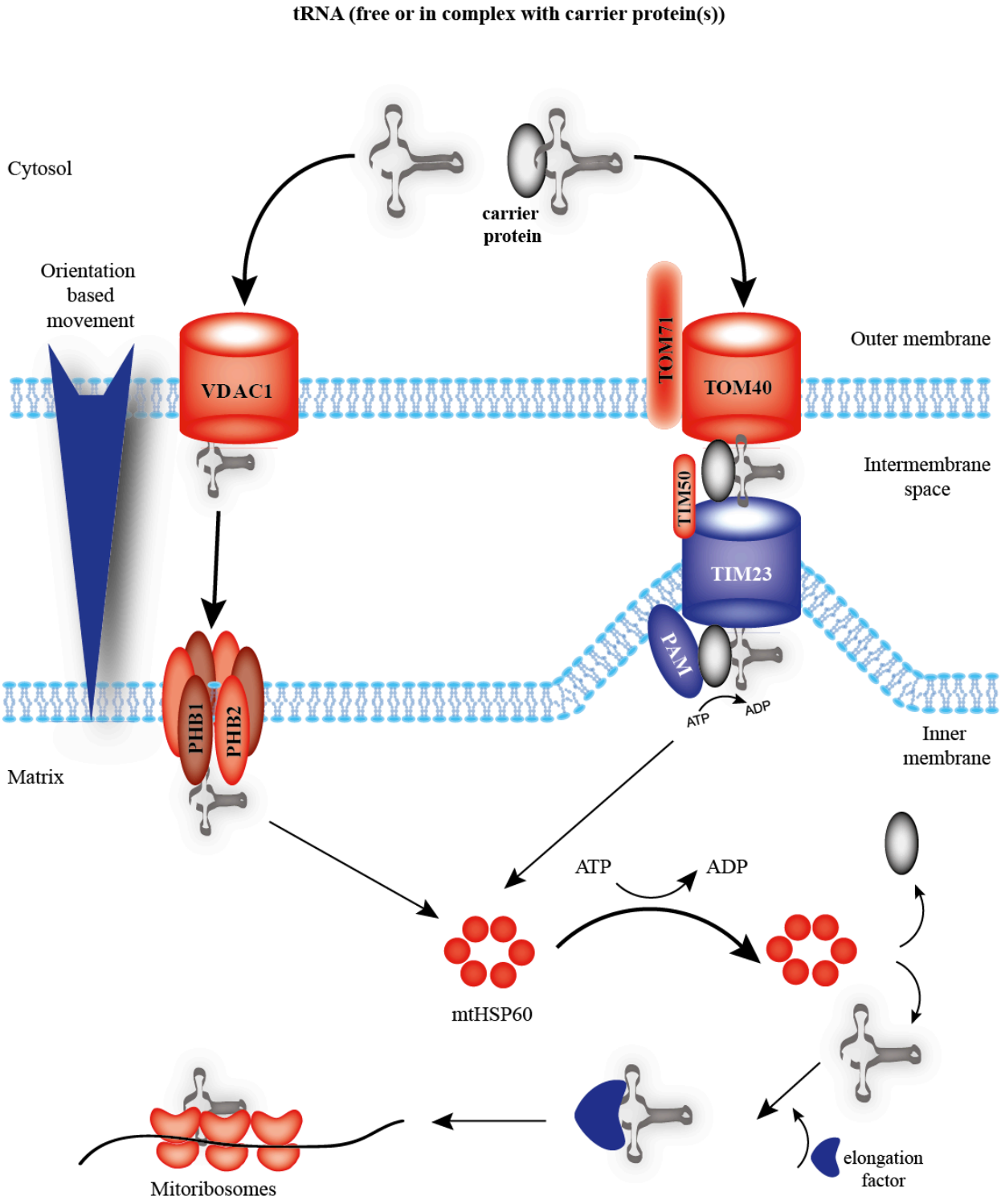

Fig.33 : Hypothetical model of RNA import into mitochondria of *Saccharomyces cerevisiae.* Proteins drawn in red were identified by CLIP followed by subsequent mass spectrometry analysis. VDAC1 : Voltage-Dependent Anion Channel 1; TOM : translocase of the mitochondrial outer membrane; TIM : translocase of the mitochondrial inner membrane; PAM : presequence translocase-associated motor; mtHSP60 : mitochondrial chaperone protein; PHB 1+2 : Prohibitins 1+2.

passage across the channel. Alternatively, our results permit the suggestion that VDAC1 arranges into oligomeric high molecular weight complexes with formation of megachannels that could promote the translocation of tRNAs through the mitochondrial outer membrane. Once delivered into the intermembrane space, tRNAs might bind to the prohibitin complex, which forms a 1,2MDa ring-like structure in the mitochondrial inner membrane with a channel size of 20-25nm (Osman et al., 2009) that has the appropriate size to deliver tRNAs into the matrix compartment. After this final translocation step, tRNAs could be bound by the nucleotide binding motifs of mtHsp60, which were also shown to be capable of interacting with single stranded DNA during mitochondrial DNA replication (Kaufman et al., 2000). After ATP dependent refolding, tRNAs will be released, bound by mitochondrial elongation factors and used in the mitochondrial translation system.

OTHER PROJECT

IV) Other project : Correction of the Consequences of mitochondrial 3243A>G Mutation in the *MT-TL1* Gene causing the MELAS Syndrome by tRNA Import into Mitochondria

In parallel to my main project that consisted in "Studying the translocation mechanism of tRK1 into mitochondria of *Saccharomyces cerevisiae*" I was also participating in a collaboration study entitled "Correction of the Consequences of mitochondrial 3243A>G Mutation in the *MT-TL1* Gene causing the MELAS Syndrome by tRNA Import into Mitochondria" aiming to rescue the MELAS mutation consequences by allotopic expression of recombinant tRNA versions based on the yeast *Saccharomyces cerevisiae* $tRNA^{Lys(CUU)}$ (tRK1) and $tRNA^{Lys(UUU)}$ (tRK2) in human cells.

It is known that human mitochondria are able to import yeast tRK1 and mutant versions based on tRK2 containing the import determinant base pair G1-C72 (Kazakova et al., 1999). Previous studies already demonstrated that such recombinant yeast tRNAs could be successfully imported into human mitochondria and that they were able to rescue defects of the A8344G mutation causing the MERFF syndrome (Kolesnikova et al., 2000, 2004). The same strategy was pursued in this project in order to rescue the MELAS mutation consequences. MELAS (Mitochondrial encephalomyopathy, lactic acidosis and stroke-like episodes) is a mitochondrial disease that particularly affects the nervous system and muscles. In most cases, MELAS is caused by point mutations in the mitochondrial $tRNA^{Leu(UUR)}$ (*MT-TL1* gene), where the base substitution 3243A>G was one of the mutations that have been associated with the MELAS syndrome (Goto et al., 1990). During this project I was responsible to construct the recombinant tRNA versions and to analyse their import capacity into human mitochondria after transient transfection of cybrid cell lines bearing the MELAS mutation. Recombinant tRK1 and tRK2 molecules were produced by site directed mutagenesis with the goal to introduce the mitochondrial import determinants in the case of tRK2 based recombinant molecules (G1-C72 base pair), the aminoacylation identity for the human mitochondrial leucyl-tRNA-synthetase (A73) and the anticodons UAA and CAA necessary for the decoding of leucine codons during mitochondrial protein synthesis. Finally, it was possible to produce two recombinant transcripts based on tRK1, $tRK1^{(UAA)}$ and $tRK1^{(CAA)}$, and one recombinant transcript based on tRK2, $tRK2^{(CAA)}$. After transient transfection of MELAS cybrid cell lines, it could be shown that all three recombinant tRNA versions could be imported with different efficiencies into mitochondria of MELAS cybrid cells lines. The same versions were also validated by stable expression of the corresponding

genes in MELAS cybrid cell lines and were found to partially correct mitochondrial defects caused by the mutation.

Publication 2

Correction of the Consequences of mitochondrial 3243A>G mutation in the *MT-TL1* gene causing the MELAS syndrome by tRNA import into mitochondria

Olga Z. Karicheva, Olga A. Kolesnikova, Tom Schirtz, Mikhail Y. Vysokikh, Anne-Marie Mager-Heckel, Anne Lombès, Abdeldjalil Boucheham, Igor A. Krasheninnikov, Robert P. Martin, Nina Entelis and Ivan Tarassov. Nucleic Acids Res. 2011 Oct;39(18):8173-86.

Published online 30 June 2011

Nucleic Acids Research, 2011, Vol. 39, No. 18 ***8173–8186***
doi:10.1093/nar/gkr546

Correction of the consequences of mitochondrial 3243A>G mutation in the *MT-TL1* gene causing the MELAS syndrome by tRNA import into mitochondria

Olga Z. Karicheva[1,2], Olga A. Kolesnikova[1,2], Tom Schirtz[1], Mikhail Y. Vysokikh[1,3], Anne-Marie Mager-Heckel[1], Anne Lombès[4], Abdeldjalil Boucheham[1], Igor A. Krasheninnikov[2], Robert P. Martin[1], Nina Entelis[1] and Ivan Tarassov[1,*]

[1]UMR 7156 University of Strasbourg (UdS) - CNRS, Molecular Genetics, Genomics & Microbiology, Strasbourg 67084, France, [2]Department of Molecular Biology, Biology Faculty, [3]Belozersky Institute of Physico-Chemical Biology, M. V. Lomonossov Moscow State University, Moscow, Russia 119991 and [4]Centre de Recherche de l'Institut du Cerveau et de la Moëlle (CRICM); INSERM UMRS 975, CNRS UMR 7225, UPMC, Paris, France 75651

Received March 22, 2011; Revised and Accepted June 14, 2011

ABSTRACT

Mutations in human mitochondrial DNA are often associated with incurable human neuromuscular diseases. Among these mutations, an important number have been identified in tRNA genes, including 29 in the gene *MT-TL1* coding for the $tRNA^{Leu(UUR)}$. The m.3243A>G mutation was described as the major cause of the MELAS syndrome (mitochondrial encephalomyopathy with lactic acidosis and stroke-like episodes). This mutation was reported to reduce $tRNA^{Leu(UUR)}$ aminoacylation and modification of its anti-codon wobble position, which results in a defective mitochondrial protein synthesis and reduced activities of respiratory chain complexes. In the present study, we have tested whether the mitochondrial targeting of recombinant tRNAs bearing the identity elements for human mitochondrial leucyl-tRNA synthetase can rescue the phenotype caused by MELAS mutation in human *trans*mitochondrial cybrid cells. We demonstrate that nuclear expression and mitochondrial targeting of specifically designed transgenic tRNAs results in an improvement of mitochondrial translation, increased levels of mitochondrial DNA-encoded respiratory complexes subunits, and significant rescue of respiration. These findings prove the possibility to direct tRNAs with changed aminoacylation specificities into mitochondria, thus extending the potential therapeutic strategy of allotopic expression to address mitochondrial disorders.

INTRODUCTION

The m.3243A>G mutation in the mitochondrial DNA (mtDNA) *MT-TL1* gene coding for mitochondrial $tRNA^{Leu(UUR)}$ (mt-$tRNA^{Leu(UUR)}$) was first identified as a genetic cause of mitochondrial encephalomyopathy with lactic acidosis and stroke-like episodes (MELAS, MIM 5400 000) (1). It is one of the most common mitochondrial pathogenic mutations with a carrier frequency estimated in the range between 0.95 and 18.4/100 000 in northern European populations (2–4). Like many mutations affecting mitochondrial respiratory chain, the m.3243A>G mutation is associated not only with MELAS, but also with other clinical phenotypes, including CPEO (Chronic Progressive External Ophthalmoplegia), DMDF (Diabetes Mellitus and DeaFness), etc. (5). In all cases, the m.3243A>G mutation was present in a heteroplasmic state, which means the co-existence of mutant and wild-type mtDNA molecules in one cell. The proportion of mutant mtDNA molecules that leads to the manifestation of the disease varied strongly in different tissues (6). Patients with m.3243A>G mutation often show severe respiratory chain deficiency with complexes I and IV affected in a first place (7,8), but the precise mechanism connecting the mutation with clinical phenotypes is still

*To whom correspondence should be addressed. Tel: +33 368851481; Fax: +33 388417087; Email: i.tarassov@unistra.fr
Present addresses:
Olga Z. Karicheva, Research Institute of the Biotechnology School of Strasbourg, UMR 7242, Ecole Supérieure de Biotechnologie de Strasbourg; 67412 Illkirch, France.
Olga A. Kolesnikova, Institut de Génétique et de Biologie Moléculaire et Cellulaire, CNRS/INSERM/ULP, 67404, Illkirch Cedex, France.

not fully understood. Accumulated data, mostly obtained on *trans*mitochondrial cybrid cells, suggest a deficiency of aminoacylation of mutant mt-tRNA$^{Leu(UUR)}$ (9–13) and hypomodification of its anti-codon wobble position affecting recognition of UUG codons (14–17) to be the origin of a mitochondrial translation defect. This leads to a decrease of respiratory chain complexes steady-state levels (7,18) and affected respiration rate (11,19,20). The mitochondrial translation defect observed varied from moderate in some cell lines to severe in others. Moreover, different groups reported qualitatively different patterns of mitochondrial translation in cells bearing the m.3243A>G mutation. In association with the mutation, it has been observed that there was a specific decrease of polypeptides rich in UUG codons (for instance, ND6) and appearance of abortive translation products (18,20). In other reports, no qualitative differences or specific correlation between number of leucine UUR codons and level of synthesis of particular mitochondrial proteins were found (11,21). The data on amino acid misincorporation at UUR codons are also somewhat controversial (18,22,23).

Up to now, no efficient therapy for MELAS and other mitochondrial diseases has been demonstrated. Antioxidants and vitamins have been used, but there have been no consistent successes reported (24). Spindle transfer, where the nuclear DNA is transferred to another healthy egg cell leaving the defective mtDNA behind, is a potential treatment procedure that has been successfully carried out on monkeys (25). Using a similar pronuclear transfer technique, healthy DNA in human eggs from women with mitochondrial disease was successfully transplanted into the eggs of women donors who were unaffected (26). Embryonic mitochondrial transplant and protofection have been proposed as a possible treatment for inherited mitochondrial disease. Allotopic expression of mitochondrial proteins (i.e. expression of mtDNA-encoded mitochondrial proteins in the nucleus) was also tested as a radical treatment for mtDNA mutation load. Promising results were obtained with MELAS cybrid cells overexpressing the mitochondrial leucyl-tRNA synthetase (mt-LeuRS) (27,28). Authors observed an increase in steady-state level of aminoacylated mt-tRNA$^{Leu(UUR)}$, partial restoration of COX1, COX2 and ND1 steady-state levels and increase of respiration rate. Interestingly, the rate of mitochondrial protein synthesis was almost the same as that in parental cells bearing MELAS mutation. Authors suggested that mutation suppression occurred via a mechanism that increased protein stability rather than translation rate. In an independent study, overexpression of mitochondrial translation factors EFTu and EFG2 in myoblasts derived from a MELAS patient partially restored mitochondrial translation, steady-state levels of certain respiratory chain subunits, assembly and activity of the OXPHOS complexes (18). A similar approach was also formerly and successfully modelled in yeast (29).

In addition to proteins, human mitochondria also import from the cytosol small RNAs such as 5S rRNA (30–32,34), tRNA^{Gln} (33), or RNase P and MRP RNA components (35,36). Moreover, we previously demonstrated that yeast importable tRNA^{Lys} derivatives and some other small artificial RNA substrates could be imported into mitochondria after their expression in human cells (37,38). We have shown that yeast tRNA^{Lys} derivatives targeted to mitochondria of cybrid cells or patient fibroblasts with the m.8344A>G mutation in the mtDNA *MT-TK* gene coding for mt-tRNA^{Lys} (commonly associated with the MERRF syndrome) partially restored their mitochondrial translation, activity of respiratory complexes, electrochemical potential across the mitochondrial inner membrane and respiration rate (39). In order to enlarge the spectrum of mtDNA mutations addressed we investigated here the possibility to rescue the MELAS mutation by allotopic expression of recombinant and importable tRNAs whose aminoacylation identity had been changed from lysine to leucine.

MATERIALS AND METHODS

Cell culture

The MELAS cybrid cell line used in this study was kindly provided by E. A. Shoubridge (Montreal Neurologic Institute, Quebec, Canada). It carried 90 ± 5% of m.3243A>G mutation and was functionally characterized previously (40). They were generated by fusing rho^0 cells from osteosarcoma cell line 143B.TK$^-$ with cytoplasts from clonal primary myoblasts established from a patient carrying the m.3243A>G point mutation in *MT-TL1* gene (MELAS mutation) as described elsewhere (41). Cybrid cells were cultivated in DMEM medium with high glucose (4.5 g/l), sodium pyruvate (110 mg/l) and L-glutamine (2 mM) from Sigma, supplemented with 10% (w:v) fetal calf serum (FCS), 50 mg/ml uridine, standard concentrations of antibiotics (penicillin, streptomycin and fungizone) and, for stable transfectants, 2 μg/ml of puromycin. 143Brho$^+$ cells were used as healthy cell control and were cultivated in the same conditions as MELAS cybrid cells. HEK-293T cells were used for production of lentiviral particles and were cultivated in standard DMEM medium with 1 g/l glucose. All cell lines were cultivated at 37°C and 5% of CO_2.

Cell transfection

Transfection of MELAS cybrid cells with tRNA transcripts was performed using Lipofectamine2000 (Invitrogen) as described previously (32) with minor modifications: 1 μg of transcript and 12.5 μl Lipofectamine2000 were used per 2×10^6 cells. Transient transfection was performed with a mix of 4 μg of pBK-CMV-tRK plasmid and 12 μl of Lipofectamine2000 per 600×10^3 cells according to manufacturer protocol. Efficiency of transfection was estimated by FACS analysis of GFP expression from pmax-GFP plasmid transfected in parallel. MELAS cybrid cells stably expressing recombinant tRNAs were obtained by lentiviral transfection. Production of lentiviral particles was performed in HEK-293T cells using FuGENE6 transfection reagent (Roche Applied Sciences), 3 μg of pLKO.1-tRK (Addgene), 1.5 μg of pLP1, 0.75 μg of pLP2 and 0.75 μg pLP-VSGV packaging plasmids (Invitrogen) according to manufacturer protocol. Infection of MELAS cybrid cells was performed with

virus-containing medium from HEK-293T cells during 2–3 days. Cells containing transgenes were selected in the presence of 2μg/ml of puromycin during 2–3 days.

Construction of recombinant tRNA genes and plasmids

The hmtLeuRS gene without mitochondria-targeting sequence (186–302 nucleotides coding for the first 39 amino acids), was PCR-amplified from cDNA purchased from the RIKEN collection and cloned in the expression pET3a (Amp^r) vector.

Cloning of yeast tRK1, tRK2 (G1-C72; G73; U34) and tRK3 genes was performed previously (42). tRNA genes coding sequences were placed under control of T7 promoter in pUC19 (Amp^r) (Invitrogen), *Bst*NI site was introduced at its 3′-terminus to further generate the CCA-3′ sequence in the T7 transcript. Mutations aimed to change tRNA aminoacylation identity (Lys > Leu) were introduced by several steps of PCR-mutagenesis. Discriminator base A73—using oligonucleotides: tRK1-T7 GGGATCCATAATACGACTCACTATA GCCTT GTTGGCG, tRK1-A73-BstNI GGGATCCTGGTGC CCTGTAGGGGGCTCG, tRK2-G1-T7 GGGATCCA TAATACGACTCACTATAGCCTTGTTAGCTCAG, tRK2-C72A73-BstNI GGGATCCTGGTGCCTCATAG GGGGCTCG. Anti-codon substitution was performed by Quick Change Site-Directed Mutagenesis Kit (Stratagene) according to manufacturer protocol. The following pairs of oligonucleotides were used ('As' for forward and 'Br' for reverse): tRK1UAAAs GACTTAA AATCATAAGG, tRK1UAABr TATGATTTTAAGTC ATACGC, tRK1CAAAs GACTCAAAATCATAAGG, tRK1CAABr TATGATTTTGAGTCATACGC, tRK2UAAAs GTTCGGCTTAAAACCG, tRK2UAABr CATTTCGGTTTTAAGCCG, tRK2CAAAs GTTCGG CTCAAAACCG, tRK2CAABr CATTTCGGTTTTG AGCCG, tRK3UAAAs GTCTTAAAAGCAACCC, tRK3UAABr GCTTTTAAGACAAC, tRK3CAAAs CA GTTGTCTCAAAAGCAACCC, tRK3CAABr GGGTT GCTTTTGAGACAACTG.

For transient expression in MELAS cybrid cells, tRK1UAA/CAA, tRK2UAA/CAA, tRK3UAA/CAA genes we cloned in pBK-CMV (Kan^r) vector (Stratagene) in *Bgl*II/*Bam*HI (*Bgl*II in the fragment and cohesive site *Bam*HI - in the vector) sites using oligonucleotides: TRK1/F1-Aviv GGCAAGATCTGGTCAGATTTCCA ATAACAGAATATCCTTGTTAGCCTTGTTGGCG, TRK1/F1-A73-Bviv GGCAAGATCTGTCATCGTGTT TTAAAAAAAAAAAGAATGCCCTGTAGGGGGCT C, TRK2/F1-G1-Aviv GGCAAGATCTGGTCAGATTT CCAATAACAGAATATCCTTGTTAGCCTTGTTAG CTCAG, TRK2/F1-C72A73-Bviv GGCAAGATCTGTC AT CGTGTTTTAAAAAAAAAAAGAATGCCTCATA GGGGGCTCG, TRK3/F1-Aviv CCCAAGAGATCTG GTCAGATTTCCAATAACAGAATAGAGAATATTG TTTAATG, TRK3/F1-Bviv CCCAAGAGATCTGTCA TCGTGTTTTAAAAAAAAAAAGAATGAGAATAG CTGGAGTTG. tRNA genes were flanked by non-coding flanking regions of one of the well expressed tRK1 copies and were cloned in an opposite direction with respect to the CMV promoter in order to favour their transcription from internal promoter by RNA polymerase III (RpoIII) and further correct maturation.

For stable transfection tRK1UAA/CAA, tRK2UAA/CAA genes were cloned in plKO.1 (Amp^r) lentiviral vector (Addgene) (43) in *Age*I/*Eco*RI sites under the control of external U6-promoter without any flanking regions using oligonucleotides: trk1plkoAs GGCAACCGGTGC CTTGTTGGCG, trk1plkoBr GGCAGAATTCAAAAA TGCCCTGTAGGG, trk2plkoAs GGCAACCGGTGCC TTGTTAGCTCAG, trk2plkoBr GGCAGAATTCAAA AATGCCTCATAGGGGG.

Purification of hmtLeuRS and *in vitro* aminoacylation assay

His-tagged hmtLeuRS and hmtLysRS were purified to homogeneity from BL21 CodonPlus (DE3)-RIL *Escherichia coli* strain through nickel affinity chromatography, followed by protein concentration through Nanosep 30 K (Pall) columns, and stored as 40% glycerol solution at −20°C. Activities of different enzyme fractions were tested on commercially available preparation of *E. coli* tRNA. Aminoacylation of tRNA T7-transcripts was done according to the described procedure (44). Final conditions were: 50 mM HEPES–NaOH (pH 7.6), 25 mM NaCl, 12 mM $MgCl_2$, 2.5 mM ATP, 0.2 mg/ml BSA, 0.8 μM [^{3}H]-Leu or 0.8 μM [^{3}H]-Lys (>400 Ci/mmole, NEC) and adapted concentrations of tRNA and enzyme. Aminoacylation rates and Km were measured as described elsewhere (45,46). Aminoacylation efficiencies of recombinant tRNA transcripts were compared to that of wild-type human mt-tRNA$^{Leu(UUR)}$ and mt-tRNA^{Lys} T7-transcripts.

Isolation and analysis of DNA

Total cellular DNA was isolated by standard procedures and the m.3243A>G mutation level was tested systematically by *Apa*I restriction analysis, as described elsewhere (47). Briefly, mutation containing mtDNA region was PCR-amplified using oligonucleotide primers: hp3081 G TAATCCAGGTCGGTTTCT and hp3380 CGTTCGGT AAGCATTAGG, PCR-products were digested by *Apa*I for 2 h and analyzed by gel-electrophoresis.

Isolation and analysis of total and mitochondrial RNAs

Total and mitochondrial RNAs were isolated by standard TRIzol-extraction (Invitrogen) from cells and purified mitochondria, respectively. Mitochondria were isolated from cells as described previously, using the differential centrifugation protocol (48). RNA preparations were analyzed by Northern-hybridization with [^{32}P]-5′-end-labelled oligonucleotide probes. To detect tRK1 versions we used oligonucleotide probe anti-tRK1 (1–34): GAGTC ATACGCGCTACCGATTGCGCCAACAAGGC, for tRK2 versions, the probe anti-tRK2 (2–32): GCCGAACG CTCTACCAACTCAGCTAACAAGG, for tRK3 versions, the probe anti-tRK3 (1–39): CTTAAAAGACAACTGTT TTACCATTAAACAAATATTCTC. The probes anti-mt-tRNA^{Leu}: GAACCTCTGACTCTAAAG and anti-mt-tRNA^{Thr}: CATCTCCGGTTTACAAG were used to control the quality of mitochondrial RNA. The probes anti-cy-tRNA^{Lys}: CTTGAACCCTGGACC and

anti-cy-5.8SrRNA: AAGTGACGCTCAGACAGGCA to control the absence of contamination of mitochondrial RNA by cytosolic RNA.

Analysis of aminoacylation *in vivo*

Analysis of aminoacylation levels of recombinant tRNAs *in vivo* was performed through PAGE in acid conditions and subsequent Northern hybridization analysis as described elsewhere (49). Briefly, RNAs from cells were isolated with TRIzol-reagent (Invitrogen), precipitated on ice with 50% isopropanol and dissolved in 10 mM Sodium acetate pH4.5, 1 mM EDTA. Deacylated controls were prepared by 30 min incubation at 37°C in 0.25 M Tris-HCl pH8.5, 0.25 M $MgCl_2$ followed by RNA precipitation. RNAs in a loading buffer with 0.1 M Sodium acetate pH5.0 were run in a cold room through 35 cm long denaturing acid 6.5% PAAG with 0.1 M Sodium acetate pH5.0 and analyzed by Northern hybridization with [^{32}P]-5′-end-labelled oligonucleotide probes.

Immunoblotting

For immunoblotting, whole cells were solubilized in a Laemmli's buffer (50) in the way to have SDS: protein ratio ~25–30 (w/w), sonicated for 5 s to break cellular DNA; incubated for 10 min at 60°C, and 30 µg of protein were run on a 12.5% SDS–PAGE, and subsequently transferred to a nitrocellulose membrane. When several cell lines were compared, we either used the same filter cut at the levels of different proteins of interest or separate runs of equal aliquots of the same protein extract with simultaneous electrotransfer, to ensure the comparability of the results. In all cases the amount of analyzed proteins was in the linear area of signal detection, as verified by in-gel titration with following scanning in the Typhoon-Trio. In no case the signal was saturated in the experiments presented. For immunodetection following antibodies were used: polyclonal antibodies against COX2, ND1 and commercially available monoclonal antibodies against porin (Calbiochem 529538), α-tubulin (Sigma T6074). Detection was done either using ECL^{TM} horseradish peroxidase linked secondary antibodies and 'ECL Plus Western Blotting Detection Reagent', or using ECL Plex^{TM} Cy3 and Cy5-conjugated secondary antibodies, on Typhoon-Trio (all from GE Healthcare). Signal quantification was performed in ImageQuantTL programme from the same manufacturer.

In vivo mitochondrial translation

The analysis of mitochondrial protein synthesis was performed as previously described (39) with minor modifications. Briefly, 600×10^3 cells were incubated for 10 min in DMEM w/o methionine (Sigma) in the presence of 100 µg/ml of emetine to inhibit cytoplasmic translation, followed by 30 min with 200 µCi/ml [^{35}S]-methionine (>1000 Ci/mmole, GE Healthcare), and, finally, 10 min chase in the normal growth medium. Cells were solubilized in a Laemmli's buffer (50), sonicated for 5 s to fragmentize chromosomal DNA; incubated for 10 min at 37°C, and 100 µg of protein were run on a 10–20% gradient SDS–PAGE. Protein amounts loaded were before normalized by anti-porin immunoblotting of the same preparations. Visualization and quantification were performed using Typhoon-Trio and ImageQuantTL software from GE Healthcare.

Measurement of oxygen consumption

The rates of oxygen consumption were measured using Hansatech Oxygraph. Respiration of intact (non-permeabilized) cells was measured using $1–2 \times 10^6$ cells/ml in PBS in the presence of 5 mM glucose. A 1 µg/ml of oligomycin, FCCP in the range of 10–500 nM and 1 mM of KCN were sequentially added to measure coupled, uncoupled and non-mitochondrial oxygen consumption, respectively.

The rates of substrate dependent oxygen consumption were measured on $1–2 \times 10^6$ cells/ml in a respiration buffer containing 20 mM HEPES–KOH (pH 7.4), 200 mM sucrose, 3 mM $MgCl_2$, 10 mM KH_2PO_4, 0.5 mM EGTA and 1 g/l of BSA. Cells were permeabilized by digitonin [100 µg of digitonin per 1 mg of total cell protein (~1×10^6 cells)]. Succinate was used to donate electrons at Complex II level, while Complex I was inhibited by 0.5 µM rotenone. Ascorbate was used to donate electrons at Complex IV level, while both Complex I and Complex II (by 5 mM malonic acid) were inhibited. Maximal possible respiration rates were measured in the presence of the uncoupler FCCP (50–500 nM) and oligomycin (1 µg/ml). Non-mitochondrial oxygen consumption was measured at the end of each experiment upon addition of 1 mM KCN.

RESULTS

Construction of importable tRNAs with leucine aminoacylation identity

The major identity elements required for recognition of tRNA$^{Leu(UUR)}$ by mitochondrial LeuRS are 'discriminator' base A73 and the A14 base (affected by m.3243A>G mutation) (Figure 1) (44,45). Among yeast tRNA derivatives mitochondrially importable *in vivo* in human cells we have previously characterized three lysine isoacceptor tRNAs (tRKs). Two of them are cytosolic type tRNAs: wild-type tRK1 and recombinant tRK2 (G1-C72; G73; U34). The third—a mitochondrial-type : tRK3, which can be nuclearly expressed and then targeted into mitochondria (Figure 1) (39). We introduced in these three tRNAs the discriminator base A73 and leucine anticodons, either UAA or CAA. The first one with the expectation that the U in the wobble position would be correctly modified, the last one with the purpose to decode UUG codons even if the anticodon will be not modified. Therefore, six different versions of potentially therapeutic tRNAs: tRK1UAA, tRK1CAA, tRK2UAA, tRK2CAA, tRK3UAA and tRK3CAA were designed and further used for *in vitro* and *in vivo* assays (Figure 1). All these versions were compared for their capacity to be aminoacylated by recombinant human mitochondrial leucyl-tRNA- and lysyl-tRNA synthetases (Table 1). As expected, all versions gained the capacity to be leucinylated with efficienies comparable with that of human mt-

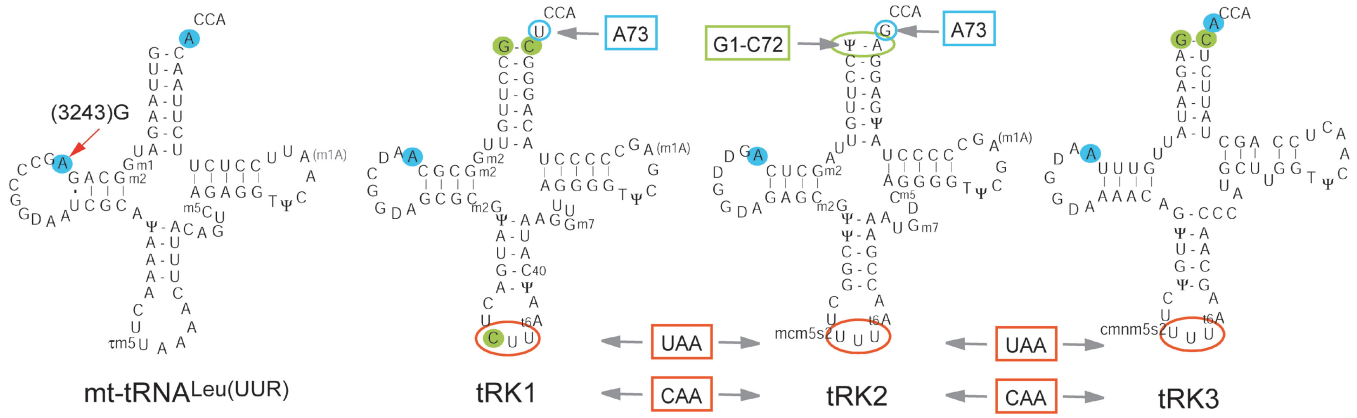

Figure 1. Cloverleaf structures of tRNAs used in this study. From left to right: native human mitochondrial $tRNA^{Leu(UUR)}$, major identity elements of recognition by mtLeuRS are in blue filled circles and MELAS m.3243A>G mutation is indicated by the red arrow; three yeast lysine tRNAs, tRK1, tRK2; tRK3 and their recombinant versions, tRK1UAA/CAA, tRK2UAA/CAA, tRK3UAA/CAA, with determinants of mitochondrial import indicated in green filled circles, identity elements for human mtLeuRS are in blue filled circles, mutations and regions where they were introduced are indicated by arrows and enclosed in blue for leucine aminoacylation identity elements, in green—for import determinants and in red—for leucine anticodons. Post-transcriptional modifications: 5-taurinomethyluridine (τm^5U), 5-methylcarboxymethyl-2-thiouridine (mcm^5s^2U), 5-carboxymethylaminomethyl-2-thiouridine ($cmnm^5s^2U$), 1-methylguanosine (m^1G), 2-methylguanosine (m^2G), 7-methylguanosine (m^7G), 1-methyladenosine (m^1A), 5-methylcytidine (m^5C), pseudouridine (Ψ), dihydrouridine (D), 5-methyluridine (T) and N6-threonylcarbamoyladenosine (t^6A).

$tRNA^{Leu}$ (the tRK2CAA version having a lowest efficiency, but still at the level of 37% in comparison with the cognate tRNA). On the other hand, we observed that most of the version also retained a low capacity to be lysinylated. The best version from the point of view of aminoacylation properties was tRK1CAA, which was as well leucinylated as the cognate mt-$tRNA^{Leu}$ and retained a lowest lysinylation capacity (6% of mt-$tRNA^{Lys}$).

We tested then whether new recombinant tRNAs preserved their ability to be imported into mitochondria of human cells. To this end, MELAS cybrid cells were transfected with corresponding T7-transcripts, total and mitochondrial RNAs from cells were isolated 24 h after transfection and analyzed by Northern hybridization with ^{32}P-5′-end labelled oligonucleotide probes (Figure 2A). The import capacity of different recombinant tRNAs was evaluated as a ratio of the hybridization signal corresponding to the recombinant RNA in purified mitochondrial RNA fraction to that of human mt-$tRNA^{Leu}$ in the same isolate. It was then expressed as relative value in comparison with the import of tRK1 or tRK3 transcripts taken as 1.0 in each series. All synthetic tRNAs tested were found to be imported into mitochondria of MELAS cybrid cells *in vivo* with various efficiencies (Figure 2B). Mutations introduced in the anti-codon region of tRK3UAA (U35:A35, U36:A36) and tRK3CAA (U34:C34, U35:A35, U36:A36) did not significantly reduce efficiency of their import, while substitutions made in tRK1UUA (U73:A73, C34:U34, U35:A35, U36:A36) and tRK1CAA (U73:A73, U35:A35, U36:A36) decreased their import 3- and 5-fold, respectively, compared to tRK1 without mutations. Import efficiency of tRK2CAA was estimated comparing to tRK1 transcript, since wild-type tRK2 is not imported into mitochondria (42,51–53), and its import was approximately seven times lower when compared to tRK1.

Table 1. Aminoacylation of tRK mutant versions by recombinant human mitochondrial LeuRS et LysRS

tRNA	Km (μM)	V (pmoles × 10^{-3}/min)	V/Km	Relative efficiency of aminoacylation (%)
LysRS				
mt-$tRNA^{Lys}$	1	50	50.0	100
tRK3	0.3	25	83.3	167
tRK2CAA	0.9	27.5	30.6	61
tRK2UAA	2.2	50	22.7	45
tRK3CAA	3.7	21	5.7	11
tRK3UAA	8	75	9.4	19
tRK1CAA	4.2	12.5	3.0	6
tRK1UAA	1.9	31	16.4	33
LeuRS				
mt-$tRNA^{Leu}$	0.5	62.5	125.0	100
tRK2CAA	0.8	37	46.3	37
tRK2UAA	0.6	80	133.3	107
tRK3CAA	0.65	59	90.8	73
tRK3UAA	0.6	60	100.0	80
tRK1CAA	0.7	81	115.5	93
tRK1UAA	0.55	58	105.5	84

T7-transcripts were used as substrates. The mean values presented are the result of several ($n > 3$) independent measures with the error <10%.

Using the same approach, we found that T7-transcripts were stable in transfected cells at least 48 h after transfection. Despite efficient targeting into mitochondria of all synthetic recombinant tRNAs, we were not able to observe any effect on mitochondrial translation (data not shown). Moreover, the analysis of aminoacylation state of these transcripts using the acid gel method (49) showed that they were mostly present in deacylated form, a finding which could be explained by the absence of posttranscriptional modifications in T7-transcripts. To overcome this problem, the experiments were axed at *in vivo* expression of the recombinant tRNAs.

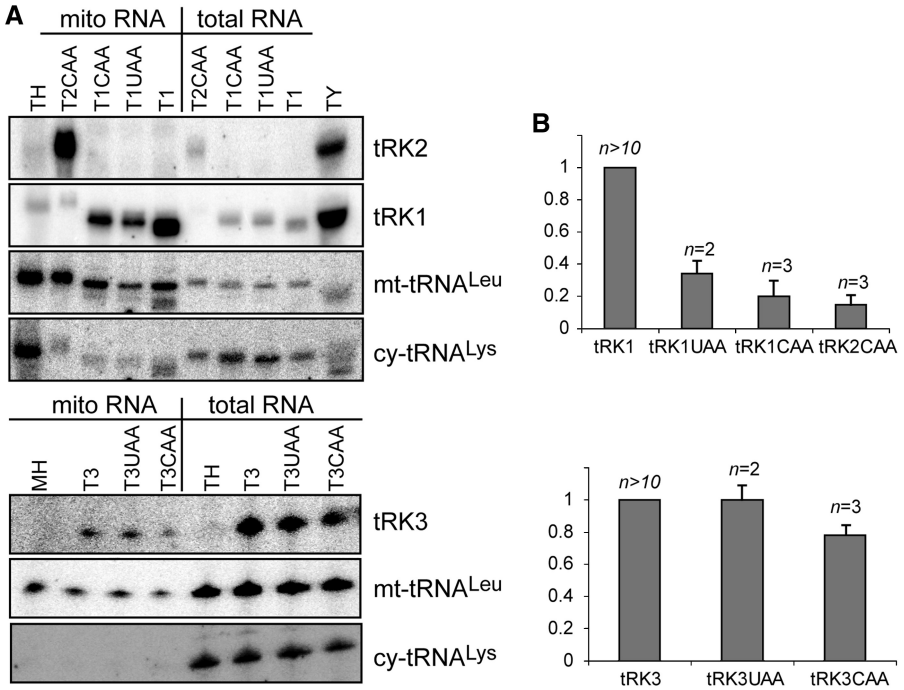

Figure 2. Analysis of *in vivo* import of synthetic recombinant tRNAs in mitochondria of MELAS cybrid cells. (**A**) Northern hybridization of total and mitochondrial RNA isolated from MELAS cybrid cells transfected with T7-transcripts. Specific [^{32}P]-oligonucleotide probes to tRK1, tRK2 and tRK3 were used to check for mitochondrial import, mt-tRNA-Leu probe—to control the absence of degradation of mitochondrial tRNAs and cy-tRNA-Lys probe to control the absence of its contamination by cytosolic tRNAs (the probes are indicated at the right of the panels). Minor bands visible with tRK1 probe in tRK2-transfectants and with cy-tRNA-Lys probe in tRK1 and tRK2 ones represent the unwashed traces of previous hybridizations of the same membrane and are unspecific (they do not migrate as the cognate tRNAs and therefore do not alter any interpretation of the specific signals). TH and MH are total and mitochondrial RNAs from non-transfected MELAS cells, TY stands for total yeast RNA used as the control of hybridization specificity. T1 and T3 are the transcripts of yeast tRK1 and tRK3 without mutations used to estimate the import efficiency of recombinant tRNAs (**B**) Relative amount of imported recombinant tRNAs calculated as a ratio of hybridization signals for recombinant tRNAs in mitochondrial RNA fraction to that of mt-tRNA^{Leu} in the same preparation. The import efficiencies presented on the graph represent relative values in comparison to these of tRK1 or tRK3 taken as 1.0 in each series. The presented error bars are issued from several independent experiments, as indicated above the diagrams.

Analysis of transient expression of recombinant tRNAs in MELAS cybrid cells

In order to express functional recombinant tRNAs in cybrid cells, we performed transfection with DNA constructs containing corresponding mutated genes. To this end, we first used mammalian expression vector pBK-CMV and cloned recombinant tRNA genes in an opposite direction with respect to the CMV promoter in order to favour their transcription from their internal promoter for RNA polymerase III (RpoIII) and their further correct maturation. MELAS cybrid cells were transiently transfected with pBK-CMV-tRK plasmids with the efficiency close to 90% (as revealed by FACS analysis of the transfection control with a GFP-expressing plasmid). Total cellular RNA was then analyzed by Northern hybridization 24 h, 48 h and 72 h after transfection to check expression and stability of recombinant tRNAs. tRK1 and tRK2-based versions were stable for 24 h, while their amount strongly decreased at day 2 (Figure 3A). Expression of tRK3 versions was not detected, which can be explained by non-optimal sequence of internal promoter for RpoIII in these transgenes as compared to tRK1/tRK2 versions. In order to increase the period during which transgenic tRNAs are present in transfected cells, we performed successive transfections, with a second transfection on the 3rd day after the first one. MELAS cybrid cell line used has defective steady-state level of the mtDNA-encoded COX2 subunit and decreased cytochrome *c* oxidase (COX) enzymatic activity, which is in agreement with previously published data (40). We analyzed steady-state level of COX2 protein during 6 days after transfection by immunoblotting of total cell protein extracts (Figure 3B). For several tRNA versions, reproducible increase of COX2 was observed with the most pronounced effect detected after transfection with tRK2CAA, where COX2 level was increased approximately three times as compared to non-transfected cybrid cells with its maximum being at the fourth day (1 day after the second transfection). tRK1UAA version also caused a two-fold increase of COX2 on the fifth day (2 days after second transfection), while tRK1CAA induced only a slight increase (1.5 times) 1 day after first transfection. The increase of COX2 level was however temporary in all assays, which is in agreement with the transient presence of recombinant RNAs in transfected cells.

The presence of recombinant tRNA versions in mitochondria of transfected cells was checked by Northern hybridisation (Figure 3C, left panel). All three

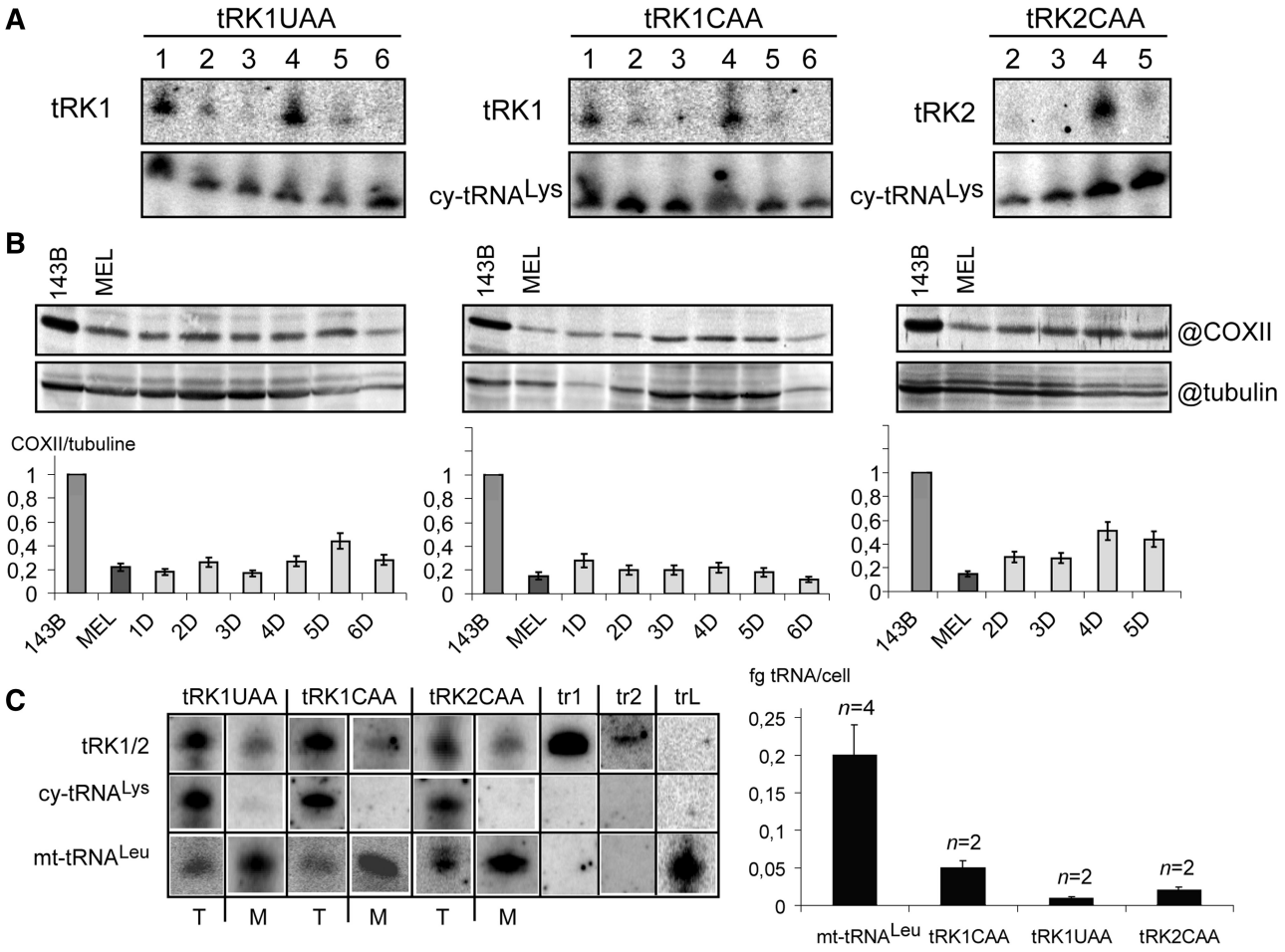

Figure 3. Effect of transient expression of recombinant tRNAs on COXII level in MELAS cybrid cells. (**A**) Northern hybridization analysis of total RNAs isolated from pBK-CMV-tRK transfected MELAS cybrid cells. Cells were transfected twice, second transfection was performed on the third day after the first one, and RNAs were isolated 1–6 days after the first transfection. Specific [^{32}P]-oligonucleotide probes are indicated on the left of the autoradiographs (tRK1, tRK2 or cy-tRNA^{Lys}—for the control cytoplasmic tRNA^{Lys} used as the quantification reference). (**B**) Western analysis of protein extracts from the transfected cells with anti-COX2 antibodies. Anti-tubulin antibodies were used as the quantification reference. Two different MW zones of the same blot were analyzed for COX2 and tubulin. The steady-state levels of COX2 before and after transfection, normalized to tubulin, are shown as diagrams for each tRNA-version in the lower panel of the figure. Values are presented relative to COX2 level in 143B parental cells, taken as 1. Error bars correspond to the results of 3–5 independent assays. (**C**) Northern hybridization of total (T) and mitochondrial (M) RNA isolated from MELAS cybrid cells 24 h after transient transfection with recombinant tRNAs. Hybridisation probes are indicated at the left. Transfected RNAs (tRK1UAA; tRK1CAA, tRK2CAA) and quantitative controls (2 ng of T7-transcritpts of tRK1, tr1, tRK2, tr2 and mt-tRNA^{Leu}, trL) are indicated at the top. The diagram at the right is a result of at least two independent experiments, as indicated.

recombinant versions were present in mitochondria which did not contain any detectable cytosolic contamination. tRK1 versions were analysed along with T7 transcripts of tRK1, tRK2 and mt-tRNA^{Leu}, which permitted quantification of the import (Figure 3C, right panel). The amount of all three versions was significantly lower than that of the reference host mt-tRNA^{Leu}, which can explain the limited effect of their expression on COX2 level, so far this recovery effect was observed in all the cases in a reproducible manner.

Generation of MELAS cybrid cells stably expressing leucine recombinant tRNA genes

In an attempt to stabilize the curative effect of mitochondrial import of recombinant tRNAs, we used the lentiviral transfection system. tRNA genes were cloned in the vector pLKO.1 under the control of an external U6 RpoIII promoter. Before infection, pLKO.1-tRK constructs were first verified in the transient transfection system, in which expression of tRK1UAA/CAA and tRK2UAA/CAA was observed. For stable lentiviral transfection, MELAS cybrid cells were analyzed 72 h or 96 h after infection for transgene expression, and tRK1CAA was found to be the only one stably and efficiently expressed (Figure 4A). Other constructs, giving no sufficient levels of expression (although the presence of the transgene was confirmed by PCR) were not analyzed further. The MELAS-pLKO.1-tRK1CAA cell line was therefore analyzed in depth. Furthermore, this very version proved to be the most prospective one, taking into account its best aminoacylation properties (Table 1) and import capacity comparable with other versions.

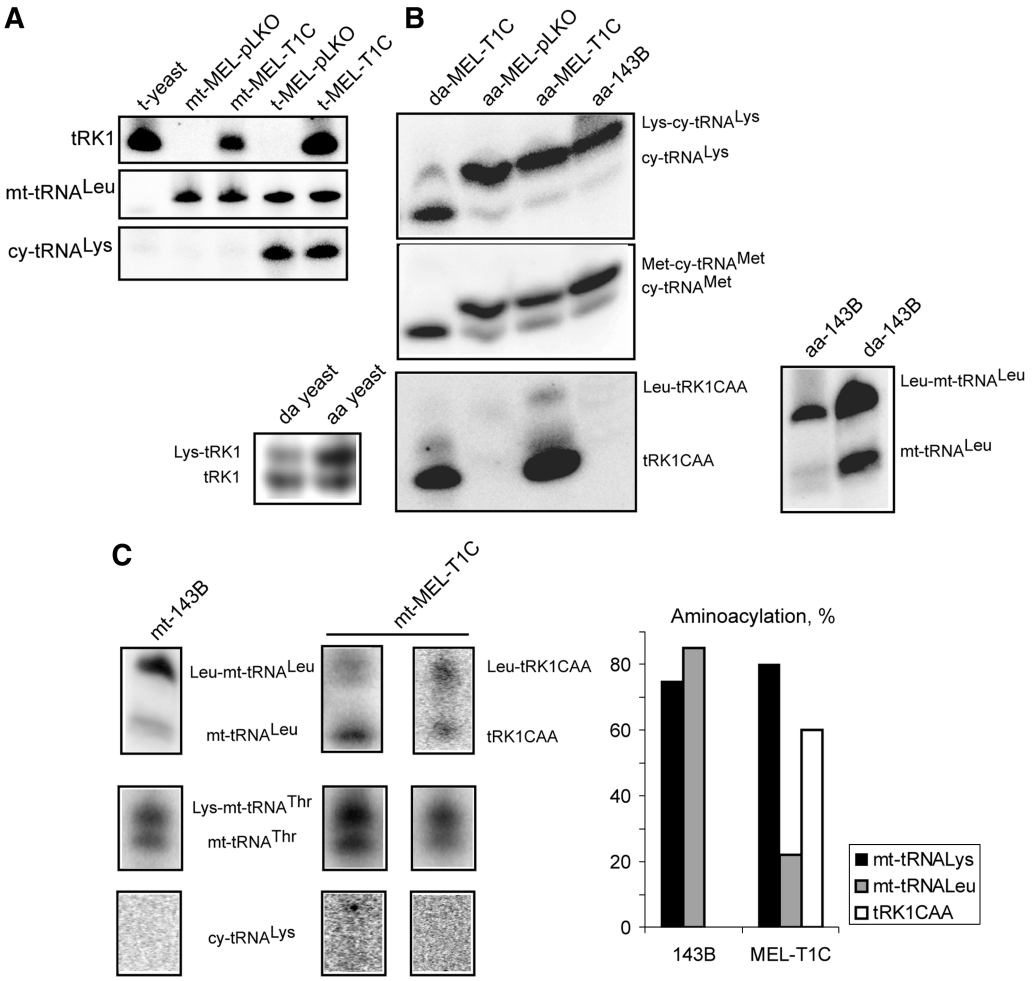

Figure 4. Import and aminoacylation of tRK1CAA stably expressed in MELAS cells. (**A**) Northern hybridization of total (t) and mitochondrial RNA (mt) from MEL-pLKO.1-T1CAA (MEL-T1C), MEL-pLKO.1 (MEL-pLKO) human cells and yeast with tRK1 and cy-tRNALys-specific [^{32}P]-labelled oligonucleotide probes. (**B**) Acid gel and northern analysis of total RNAs isolated from MEL-T1C, MEL-pLKO, 143B human cells and yeast with tRK1, mt-tRNA^{Leu}, cy-tRNA^{Lys} and cy-RNA^{Met}-specific [^{32}P]-labelled oligonucleotide probes (aa, aminoacylated RNA; da, RNA partially deacylated in basic conditions before loading). (**C**) Acid gel and northern analysis of mitochondrial RNA isolated from parental 143B and MEL-T1C cells. Aminoacylated and deacylted forms of mt-tRNA^{Leu}, mt-tRNA^{Thr} and tRK1CAA are indicated. The diagram at the right shows the quantification of aminoacylation levels for all these tRNAs (tRK1CAA was not analysed in the parental line since this RNA is absent therein).

By Northern hybridization analysis of purified mitochondrial RNA, we have shown that fraction of tRK1CAA was imported into mitochondria of MELAS-pLKO.1-tRK1CAA cells (Figure 4A), which confirmed our results obtained with T7-transcripts. RNA acid gel analysis demonstrated that at least a part of recombinant tRK1CAA in MELAS cells was aminoacylated (Figure 4B). Comparing the distance between aminoacylated and not aminoacylated forms of tRK1CAA and of other cellular tRNAs, we concluded, that the upper band corresponded to tRK1CAA aminoacylated with leucine. The middle band could correspond to tRK1CAA aminoacylated with lysine, so far, taking into account its low lysinylation level *in vitro* (Table 1) and the fact that the same band is detectable in both native and deacylated preparations, we suggest rather a non-specific signal. Furthermore, a possible unspecific aminoacylation is most likely done by cytoplasmic LysRS rather than by its mitochondrial counterpart taken into account that in mitochondria the amount of tRK1CAA is lower and mitochondrial LeuRS is present as a competitor. Therefore we hope that the minor portion of tRK1CAA possibly charged with lysine, if any, would have no considerable effects either on mitochondrial translation, or on cytosolic protein synthesis. Since leucine identity elements for human mitochondrial LeuRS we introduced in tRK1CAA were distinct from those for cytosolic LeuRS (44), and taking into account the possibility to leucinylate the recombinant tRNA *in vitro*, we conclude that tRK1CAA was aminoacylated with the leucine by mitochondrial LeuRS after its mitochondrial import. The portion of leucinylated tRK1CAA is modest probably because of non-optimal aminoacylation efficiency of recombinant tRNAs *in vivo*, but also because of naturally low amounts of tRNAs imported into mitochondria.

The above conclusions were verified by measuring the extent of tRK1CAA leucinylation in mitochondrial RNA preparations (Figure 4C). We compared the stable

tRK1CAA expressor with the MELAS cybrid line and observed, as expected, a very low aminoacyaltion level for the host mt-tRNA^{Leu} affected by the mutation (10–20%). At the same time the overall level of tRNA aminoacylation (as judged by the reference mt-tRNA^{Thr}) was high (>70%). The recombinant tRK1CAA was found partially aminoacylated (50–60%), which is significantly more pronounced than in the total RNA. This result is in agreement with the speculations above, and is likely to be explained by the efficient aminoacylation by the LeuRS in the mitochondria, while the major portion of deacylated tRK1CAA resides in the cytosol of the transfectant. Therefore, one can consider that if the level of import may be low (if comparable with the transient expression experiment), the aminoacylation by the mitochondrial enzyme was rather efficient and therefore one could expect to detect the curative effect.

Improvement of mitochondrial functions in MELAS-pLKO.1-tRK1CAA cells

In agreement with previous reports (11,21), the original MELAS cybrid cells showed strongly decreased mitochondrial protein synthesis, with large polypeptides ND2, COX1, COX2 and COX3 being particularly affected, but the qualitative pattern of mitochondrial translation products was unchanged. In MELAS-pLKO.1-tRK1CAA cells amounts of mitochondrial translation products were found to be increased to 30–50% in a generalized manner, compared to control cells transfected with an empty vector (MELAS-pLKO.1) (Figure 5). Further western analysis of mitochondrial DNA-encoded respiratory subunits revealed a reproducible increase of COX2 (+22%) and ND1 (+10%) proteins in MELAS cells stably expressing tRK1CAA transgene (Figure 6).

Oxygen consumption levels in MELAS-pLKO.1-tRK1CAA and MELAS cells transfected with the empty plasmid were then compared (Figure 7A and B). The reference MELAS-pLKO.1 cells demonstrated strongly decreased respiration with the ratio of uncoupled to coupled respiration (respiratory control) approximately two times lower than for 143B cells, which was in agreement with previously reported data (19). In MELAS-pLKO.1-tRK1CAA cells the rates of coupled and uncoupled oxygen consumption were increased about two times in comparison with the respective rates in MELAS-pLKO.1 cells, while respiration control was also improved.

To decipher this positive effect on cellular respiration, substrate-dependent oxygen consumption on digitonin permeabilized cells was analyzed. MELAS and 143B cells revealed similar succinate-supported respiration rates through complex II entirely encoded by nuclear DNA (Figure 7C). This succinate-supported respiration was not affected by tRK1CAA expression, as expected. In contrast, there was a substantial decrease in respiration rate through complex IV in MELAS-pLKO.1 cells comparing to 143B cells (Figure 7D). Importantly, this ascorbate-supported respiration was strongly increased in the MELAS cells with tRK1CAA, which confirmed previously observed rise of COX2 steady-state level and general improvement of mitochondrial translation.

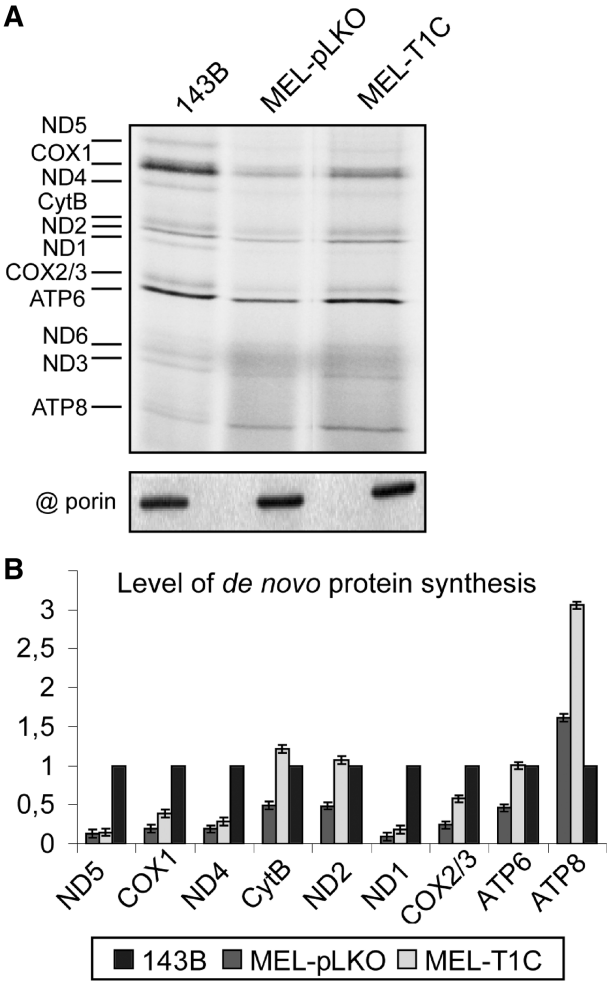

Figure 5. Mitochondrial translation in MELAS-pLKO-tRK1CAA cybrid cells. (**A**) Pulse-chase analysis of mitochondrial translation. Radioautograph of [^{35}S]-labelled mitochondrial translation products separated by SDS–PAGE is presented. The lines used are indicated at the top: 143B, MEL-pLKO and MEL-T1C. The bands corresponding to individual translation products are indicated according to standard pattern (56). Equal amounts of proteins were loaded in each case, which was controlled by Western analysis of porin in the same samples performed in parallel (below the main panel). (**B**) The diagram shows the levels of individual translation products in each cell line relative to those in 143B cells (taken as 1).

Since the high heteroplasmy level in MELAS-pLKO.1-tRK1CAA was unchanged upon transfection (~90%), one can conclude that the observed functional improvement of mitochondrial functions was due to expression and mitochondrial import of the recombinant tRNA.

DISCUSSION

The results of this study clearly demonstrate that one can alter aminoacylation identity of a tRNA preserving its ability to be imported *in vivo* into human mitochondria and to participate in the organellar translation. Indeed, we

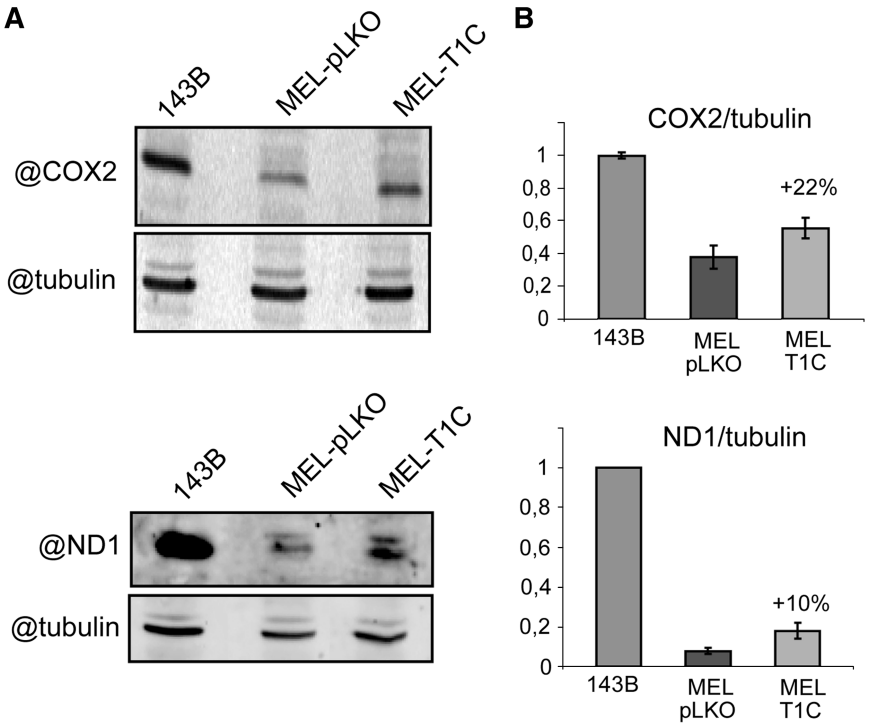

Figure 6. Steady-state level of mitochondrial proteins in MELAS-pLKO-tRK1CAA cybrid cells. (**A**) Western analysis of protein extracts from 143B, MEL-pLKO and MEL-T1C cell lines with antibodies against mitochondrial proteins COX2, ND1 and tubulin. (**B**) COX2 and ND1 steady-state levels in each cell line, normalized to tubulin and relative to the steady-state level of the corresponding protein in parental 143B cells (taken as 1).

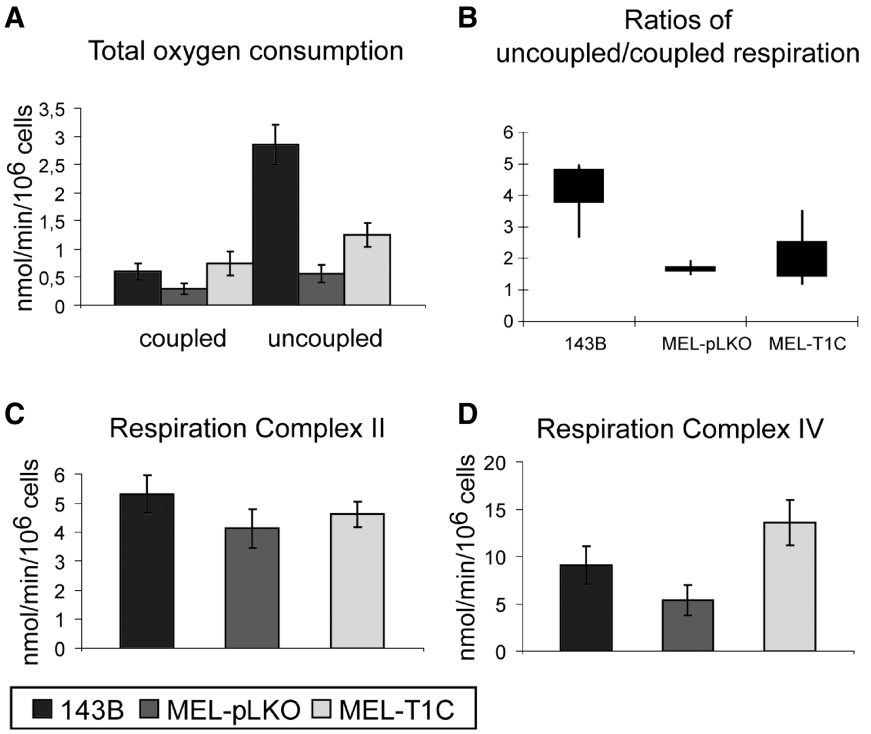

Figure 7. Oxygen consumption in MELAS-pLKO-tRK1CAA cybrid cells. (**A**) The rates of coupled and uncoupled oxygen consumption (the mean values ± SD, $n = 3$) in 143B, MEL-pLKO and MEL-T1C cell lines in nmol $O_2/10^6$ cell*min. (**B**) Box and whisker plots (57) represent the ratios of uncoupled to coupled respiration rates in 143B, MEL-pLKO and MEL-T1C cell lines. The overall data range is represented as a vertical line, while boxes represent the interquartile range containing central 50% data. (**C**) The rates of the respiration on succinate in permeabilized 143B, MEL-pLKO and MEL-T1C cells. (**D**) The rates of the respiration on ascorbate in permeabilized 143B, MEL-pLKO and MEL-T1C cells.

show that nuclear expression and subsequent mitochondrial import of specifically designed tRNAs of yeast origin with artificially changed identity (cytoplasmic lysine to mitochondrial leucine) partially rescues various negative effects of the mutation m.3243A>G in the mitochondrial $tRNA^{Leu}$ gene underlying the MELAS syndrome in cultured human cells. This rescue was observed at the levels of mitochondrial translation, steady state of mitochondrial DNA-encoded subunits of the respiratory chain and cellular respiration.

The increase of COX2 steady-state level that we observed in MELAS cells in transient transfection system varied in strength and duration depending on tRNA version expressed (Figure 3). This could indicate on possible differences in behaviour and action of different recombinant tRNAs in the cell. Thus, lower import efficiency of tRK1CAA comparing to tRK1UAA (Figure 2) can partially explain its moderate effect on COX2 level. On the other hand, the less efficient import substrate tRK2CAA lead to the best improvement of COX2 level, probably taking advantage of its CAA anti-codon, which did not need post-transcriptional modification to decode leucine UUG codons. This experimental fact is in frame of a suggestion that the MELAS mutation might affect essentially decoding UUG, but not UUA. On the other hand, it is to be outlined that the improvement of mitochondrial function depended not only on the efficiency of a particular tRNA to participate in mitochondrial translation, but also on the time it was present in cell. For example, the effect of tRK1CAA on COX2 steady-state level was more pronounced once it has been expressed in cybrid cells in a stable manner. The importance of the effect depends on a multitude of linked or non-linked factors influencing each step of the experiment: efficiency of transfection, efficiency of expression of the tRNA gene, efficiency of import, mitochondrial activity state that may vary significantly even in continuously cultivated line, modification and aminoacylation of the transgenic tRNAs, the stability of the given transgenic tRNA in the cell and in the mitochondria, misaminoacylation of the tRNA, which can give negative effects on mitochondrial or cytoplasmic translation, etc. On the other hand, if the efficiency of different versions varies, all of them provided a detectable and reproducible curative effect, thus validating the strategy, whose efficiency certainly needs to be improved to make it applicable in therapy.

Meanwhile, MELAS-pLKO.1-tRK1CAA cells clearly demonstrated a significant rescue of mitochondrial functions at all levels analyzed (Figures 5–7). Thus, synthesis of certain polypeptides reached or even exceeded (for ND2, CytB and ATP6) its level in 143B wild type cells, while synthesis of others was improved up to 30% (for COX1)—50% (for COX2/3) of its wild-type level, indicating that tRK1CAA participated in mitochondrial translation. However, no clear correlation between number of leucine codons (neither UUG, nor UUR) and translation level of particular mitochondrial proteins was observed in MELAS cybrid cell before or after transfection, which is corroborated by previously reported data (11,21). The partial nature of the effect could be explained by insufficient level of expression of the recombinant tRNA gene(s), defective post-transcriptional modifications of recombinant tRNAs, ineffective export of tRNAs from nucleus and targeting into mitochondria or, finally, low efficiency of re-aminoacylation inside the organelle. Furthermore, one could also imagine that the growth conditions used (high glucose and pyruvate) do not favour the switch from glycolysis to oxidative phosphorylation in transfected cybrid cells energy production. In any case, the observed increase of mitochondrial translation level and subsequent augmentation of COX2 and ND1 steady states was sufficient to improve the rate of oxygen consumption in MELAS-pLKO.1-tRK1CAA cells about 2-fold. Such an increase may prove to be sufficient for further therapeutic application. The question that might emerge, is the validity of the strategy described here for various cell/tissue types. The efficiency of the approach relies to the RNA import mechanism, which is far to be understood in details. Indeed, our studies of the human RNA import (both natural, for 5S rRNA, and artificial, for tRNA derivatives) indicate on the importance of the membrane charge and ATP hydrolysis for import (31,54). It was reported that isolated and discharged mitochondria from cybrid cells bearing a pathogenic mutation fail to incorporate tRNAs (33). So far, these data are in contradiction with our previously published report of the *in vivo* import of $tRNA^{Lys}$ derivatives which, in spite of the lower energized state of mitochondria in MERRF cybrids can import tRNAs enough to complement mitochondrial deficiency (39). So, we believe that, since no mtDNA mutation described led to a complete discharging of the mitochondrial membrane potential, one could expect the possibility to target RNAs into mitochondria. As a confirmation of our former study, the results obtained in the current work show that in the strongly affected cybrid cell line tRNA import may be achieved and the phenotypic effect is measurable, if even the cells were affected by another mutation (MELAS versus MERRF) and the phenotypic alteration caused by the mutation were different. On the other hand, it is evident that the efficiency of the approach will not only depend on the efficiency of import *per se*, but also on the amount of the 'therapeutic' RNA in a given type of cell, which will depend on the delivery procedure, as well as on the functionality of the tRNA itself, in terms of aminoacylation and decoding properties.

In conclusion, the recombinant leucine tRNAs validated in the present work could be tested in modelling therapeutic approaches to a number of other disorders caused by dysfunction of $mt\text{-}tRNA^{Leu(UUR)}$. As an important issue of the study, it clearly appears that the mitochondrial translation system in human cells possesses a significant extent of flexibility, accepting not only cytosolic-type tRNAs, but also tRNAs of yeast origin, which are evolutionary very distinct from the human ones. This makes us believe that the strategy developed in this study can be applied to all tRNA mutations which are not affecting the overall expression of mtDNA, however for each case the importable and functionally active molecule must be designed. Construction of these new importable versions may be helped by a

comprehensive view of the mechanisms governing the selectivity of tRNA import, taking into account the identified import determinants (42,51,55) and the possibility of their structural rearrangements (52). The new observations, together with previously published data (38,39), strongly support the approach of allotopic expression of mitochondrially targeted RNAs as a powerful tool for different kinds of disorders caused by mutations in mitochondrial tRNA-coding genes.

ACKNOWLEDGEMENTS

We thank Dr E. A. Shoubridge (Montreal Neurological Institute and Hospital) for providing the MELAS cell line; Dr M. Sissler (IBMC, Strasbourg) for providing the hmLysRS expressing construct; Dr H. Puccio and Dr. Irwin Davidson (IGBMC, Strasbourg) for the help with lentiviral transfections, Dr F. Monneaux and Dr. F. Gros (IBMC, Strasbourg) for the help with FACS analysis.

FUNDING

Centre National de la Recherche Scientifique (CNRS), Université de Strasbourg (UdS); Agence Nationale de la Recherche (ANR); Fondation pour la Recherche Médicale (FRM); the ARCUS grant (collaboration Alsace Region – Russie–Ukraine); Association Française contre les Myopathies (AFM). Funding for open access charge: ANR.

Conflict of interest statement. None declared.

REFERENCES

1. Goto,Y., Nonaka,I. and Horai,S. (1990) A mutation in the tRNA(Leu)(UUR) gene associated with the MELAS subgroup of mitochondrial encephalomyopathies. *Nature*, **348**, 651–653.
2. Chinnery,P.F., Johnson,M.A., Wardell,T.M., Singh-Kler,R., Hayes,C., Brown,D.T., Taylor,R.W., Bindoff,L.A. and Turnbull,D.M. (2000) The epidemiology of pathogenic mitochondrial DNA mutations. *Ann. Neurol.*, **48**, 188–193.
3. Majamaa,K., Moilanen,J.S., Uimonen,S., Remes,A.M., Salmela,P.I., Karppa,M., Majamaa-Voltti,K.A., Rusanen,H., Sorri,M., Peuhkurinen,K.J. *et al.* (1998) Epidemiology of A3243G, the mutation for mitochondrial encephalomyopathy, lactic acidosis, and strokelike episodes: prevalence of the mutation in an adult population. *Ma. J. Hum. Genet.*, **63**, 447–454.
4. Uusimaa,J., Moilanen,J.S., Vainionpaa,L., Tapanainen,P., Lindholm,P., Nuutinen,M., Lopponen,T., Maki-Torkko,E., Rantala,H. and Majamaa,K. (2007) Prevalence, segregation, and phenotype of the mitochondrial DNA 3243A>G mutation in children. *Ann. Neurol.*, **62**, 278–287.
5. Ruiz-Pesini,E., Lott,M.T., Procaccio,V., Poole,J.C., Brandon,M.C., Mishmar,D., Yi,C., Kreuziger,J., Baldi,P. and Wallace,D.C. (2007) An enhanced MITOMAP with a global mtDNA mutational phylogeny. *Nucleic Acids Res.*, **35**, D823–D828.
6. Shanske,S., Pancrudo,J., Kaufmann,P., Engelstad,K., Jhung,S., Lu,J., Naini,A., DiMauro,S. and De Vivo,D.C. (2004) Varying loads of the mitochondrial DNA A3243G mutation in different tissues: implications for diagnosis. *Am. J. Med. Genet.*, **130A**, 134–137.
7. Fornuskova,D., Brantova,O., Tesarova,M., Stiburek,L., Honzik,T., Wenchich,L., Tietzeova,E., Hansikova,H. and Zeman,J. (2008) The impact of mitochondrial tRNA mutations on the amount of ATP synthase differs in the brain compared to other tissues. *Biochim. Biophys. Acta*, **1782**, 317–325.
8. Dubeau,F., De Stefano,N., Zifkin,B.G., Arnold,D.L. and Shoubridge,E.A. (2000) Oxidative phosphorylation defect in the brains of carriers of the tRNAleu(UUR) A3243G mutation in a MELAS pedigree. *Ann. Neurol.*, **47**, 179–185.
9. Borner,G.V., Zeviani,M., Tiranti,V., Carrara,F., Hoffmann,S., Gerbitz,K.D., Lochmuller,H., Pongratz,D., Klopstock,T., Melberg,A. *et al.* (2000) Decreased aminoacylation of mutant tRNAs in MELAS but not in MERRF patients. *Hum. Mol. Genet.*, **9**, 467–475.
10. Chomyn,A., Enriquez,J.A., Micol,V., Fernandez-Silva,P. and Attardi,G. (2000) The mitochondrial myopathy, encephalopathy, lactic acidosis, and stroke-like episode syndrome-associated human mitochondrial tRNALeu(UUR) mutation causes aminoacylation deficiency and concomitant reduced association of mRNA with ribosomes. *J. Biol. Chem.*, **275**, 19198–19209.
11. King,M.P., Koga,Y., Davidson,M. and Schon,E.A. (1992) Defects in mitochondrial protein synthesis and respiratory chain activity segregate with the tRNA(Leu(UUR)) mutation associated with mitochondrial myopathy, encephalopathy, lactic acidosis, and stroke like episodes. *Mol. Cell Biol.*, **12**, 480–490.
12. El Meziane,A., Lehtinen,S.K., Hance,N., Nijtmans,L.G., Dunbar,D., Holt,I.J. and Jacobs,H.T. (1998) A tRNA suppressor mutation in human mitochondria. *Nature Genet.*, **18**, 350–353.
13. Park,H., Davidson,E. and King,M.P. (2003) The pathogenic A3243G mutation in human mitochondrial tRNALeu(UUR) decreases the efficiency of aminoacylation. *Biochemistry*, **42**, 958–964.
14. Helm,M., Florentz,C., Chomyn,A. and Attardi,G. (1999) Search for differences in post-transcriptional modification patterns of mitochondrial DNA-encoded wild-type and mutant human tRNALys and tRNALeu(UUR). *Nucleic Acids Res.*, **27**, 756–763.
15. Kirino,Y., Yasukawa,T., Ohta,S., Akira,S., Ishihara,K., Watanabe,K. and Suzuki,T. (2004) Codon-specific translational defect caused by a wobble modification deficiency in mutant tRNA from a human mitochondrial disease. *Proc. Natl Acad. Sci. USA*, **101**, 15070–15075.
16. Yasukawa,T., Kirino,Y., Ishii,N., Holt,I.J., Jacobs,H.T., Makifuchi,T., Fukuhara,N., Ohta,S., Suzuki,T. and Watanabe,K. (2005) Wobble modification deficiency in mutant tRNAs in patients with mitochondrial diseases. *FEBS Lett.*, **579**, 2948–2952.
17. Yasukawa,T., Suzuki,T., Ueda,T., Ohta,S. and Watanabe,K. (2000) Modification defect at anticodon wobble nucleotide of mitochondrial tRNAs(Leu)(UUR) with pathogenic mutations of mitochondrial myopathy, encephalopathy, lactic acidosis, and stroke-like episodes. *J. Biol. Chem.*, **275**, 4251–4257.
18. Sasarman,F., Antonicka,H. and Shoubridge,E.A. (2008) The A3243G tRNALeu(UUR) MELAS mutation causes amino acid misincorporation and a combined respiratory chain assembly defect partially suppressed by overexpression of EFTu and EFG2. *Hum. Mol. Genet.*, **17**, 3697–3707.
19. James,A.M., Wei,Y.H., Pang,C.Y. and Murphy,M.P. (1996) Altered mitochondrial function in fibroblasts containing MELAS or MERRF mitochondrial DNA mutations. *Biochem. J.*, **318 (Pt 2)**, 401–407.
20. Dunbar,D.R., Moonie,P.A., Zeviani,M. and Holt,I.J. (1996) Complex I deficiency is associated with 3243G:C mitochondrial DNA in osteosarcoma cell cybrids. *Hum. Mol. Genet.*, **5**, 123–129.
21. Chomyn,A., Martinuzzi,A., Yoneda,M., Daga,A., Hurko,O., Johns,D., Lai,S.T., Nonaka,I., Angelini,C. and Attardi,G. (1992) MELAS mutation in mtDNA binding site for transcription termination factor causes defects in protein synthesis and in respiration but no change in levels of upstream and

downstream mature transcripts. *Proc. Natl Acad. Sci. USA*, **89**, 4221–4225.
22. Flierl,A., Reichmann,H. and Seibel,P. (1997) Pathophysiology of the MELAS 3243 transition mutation. *J. Biol. Chem.*, **272**, 27189–27196.
23. Janssen,G.M., Hensbergen,P.J., van Bussel,F.J., Balog,C.I., Maassen,J.A., Deelder,A.M. and Raap,A.K. (2007) The A3243G tRNALeu(UUR) mutation induces mitochondrial dysfunction and variable disease expression without dominant negative acting translational defects in complex IV subunits at UUR codons. *Hum. Mol. Genet.*, **16**, 2472–2481.
24. Marriage,B., Clandinin,M.T. and Glerum,D.M. (2003) Nutritional cofactor treatment in mitochondrial disorders. *J. Am. Dietetic Assoc.*, **103**, 1029–1038.
25. Tachibana,M., Sparman,M., Sritanaudomchai,H., Ma,H., Clepper,L., Woodward,J., Li,Y., Ramsey,C., Kolotushkina,O. and Mitalipov,S. (2009) Mitochondrial gene replacement in primate offspring and embryonic stem cells. *Nature*, **461**, 367–372.
26. Craven,L., Tuppen,H.A., Greggains,G.D., Harbottle,S.J., Murphy,J.L., Cree,L.M., Murdoch,A.P., Chinnery,P.F., Taylor,R.W., Lightowlers,R.N. *et al.* (2010) Pronuclear transfer in human embryos to prevent transmission of mitochondrial DNA disease. *Nature*, **465**, 82–85.
27. Park,H., Davidson,E. and King,M.P. (2008) Overexpressed mitochondrial leucyl-tRNA synthetase suppresses the A3243G mutation in the mitochondrial tRNA(Leu(UUR)) gene. *RNA*, **14**, 2407–2416.
28. Li,R. and Guan,M.X. (2010) Human mitochondrial leucyl-tRNA synthetase corrects mitochondrial dysfunctions due to the tRNALeu(UUR) A3243G mutation, associated with mitochondrial encephalomyopathy, lactic acidosis, and stroke-like symptoms and diabetes. *Mol. Cell Biol.*, **30**, 2147–2154.
29. Feuermann,M., Francisci,S., Rinaldi,T., De Luca,C., Rohou,H., Frontali,L. and Bolotin-Fukuhara,M. (2003) The yeast counterparts of human 'MELAS' mutations cause mitochondrial dysfunction that can be rescued by overexpression of the mitochondrial translation factor EF-Tu. *EMBO Rep.*, **4**, 53–58.
30. Magalhaes,P.J., Andreu,A.L. and Schon,E.A. (1998) Evidence for the presence of 5S rRNA in mammalian mitochondria. *Mol. Biol. Cell*, **9**, 2375–2382.
31. Entelis,N.S., Kolesnikova,O.A., Dogan,S., Martin,R.P. and Tarassov,I.A. (2001) 5 S rRNA and tRNA import into human mitochondria. Comparison of in vitro requirements. *J. Biol. Chem.*, **276**, 45642–45653.
32. Smirnov,A., Tarassov,I., Mager-Heckel,A.M., Letzelter,M., Martin,R.P., Krasheninnikov,I.A. and Entelis,N. (2008) Two distinct structural elements of 5S rRNA are needed for its import into human mitochondria. *RNA*, **14**, 749–759.
33. Rubio,M.A., Rinehart,J.J., Krett,B., Duvezin-Caubet,S., Reichert,A.S., Soll,D. and Alfonzo,J.D. (2008) Mammalian mitochondria have the innate ability to import tRNAs by a mechanism distinct from protein import. *Proc. Natl Acad. Sci. USA*, **105**, 9186–9191.
34. Smirnov,A., Comte,C., Mager-Heckel,A.M., Addis,V., Krasheninnikov,I.A., Martin,R.P., Entelis,N. and Tarassov,I. (2010) Mitochondrial enzyme rhodanese is essential for 5 S ribosomal RNA import into human mitochondria. *J. Biol. Chem.*, **285**, 30792–30803.
35. Puranam,R.S. and Attardi,G. (2001) The RNase P associated with HeLa cell mitochondria contains an essential RNA component identical in sequence to that of the nuclear RNase P. *Mol. Cell Biol.*, **21**, 548–561.
36. Wang,G., Chen,H.W., Oktay,Y., Zhang,J., Allen,E.L., Smith,G.M., Fan,K.C., Hong,J.S., French,S.W., McCaffery,J.M. *et al.* (2010) PNPASE Regulates RNA Import into Mitochondria. *Cell*, **142**, 456–467.
37. Kolesnikova,O., Kazakova,H., Comte,C., Steinberg,S., Kamenski,P., Martin,R.P., Tarassov,I. and Entelis,N. (2010) Selection of RNA aptamers imported into yeast and human mitochondria. *RNA*, **16**, 926–941.
38. Kolesnikova,O.A., Entelis,N.S., Mireau,H., Fox,T.D., Martin,R.P. and Tarassov,I.A. (2000) Suppression of mutations in mitochondrial DNA by tRNAs imported from the cytoplasm. *Science*, **289**, 1931–1933.
39. Kolesnikova,O.A., Entelis,N.S., Jacquin-Becker,C., Goltzene,F., Chrzanowska-Lightowlers,Z.M., Lightowlers,R.N., Martin,R.P. and Tarassov,I. (2004) Nuclear DNA-encoded tRNAs targeted into mitochondria can rescue a mitochondrial DNA mutation associated with the MERRF syndrome in cultured human cells. *Hum. Mol. Genet.*, **13**, 2519–2534.
40. Bakker,A., Barthelemy,C., Frachon,P., Chateau,D., Sternberg,D., Mazat,J.P. and Lombes,A. (2000) Functional mitochondrial heterogeneity in heteroplasmic cells carrying the mitochondrial DNA mutation associated with the MELAS syndrome (mitochondrial encephalopathy, lactic acidosis, and strokelike episodes). *Pediatr. Res.*, **48**, 143–150.
41. King,M.P. and Attardi,G. (1989) Human cells lacking mtDNA: repopulation with exogenous mitochondria by complementation. *Science*, **246**, 500–503.
42. Entelis,N.S., Kieffer,S., Kolesnikova,O.A., Martin,R.P. and Tarassov,I.A. (1998) Structural requirements of tRNALys for its import into yeast mitochondria. *Proc. Natl Acad. Sci. USA*, **95**, 2838–2843.
43. Moffat,J., Grueneberg,D.A., Yang,X., Kim,S.Y., Kloepfer,A.M., Hinkle,G., Piqani,B., Eisenhaure,T.M., Luo,B., Grenier,J.K. *et al.* (2006) A lentiviral RNAi library for human and mouse genes applied to an arrayed viral high-content screen. *Cell*, **124**, 1283–1298.
44. Sohm,B., Frugier,M., Brule,H., Olszak,K., Przykorska,A. and Florentz,C. (2003) Towards understanding human mitochondrial leucine aminoacylation identity. *J. Mol. Biol.*, **328**, 995–1010.
45. Sohm,B., Sissler,M., Park,H., King,M.P. and Florentz,C. (2004) Recognition of human mitochondrial tRNALeu(UUR) by its cognate leucyl-tRNA synthetase. *J. Mol. Biol.*, **339**, 17–29.
46. Tolkunova,E., Park,H., Xia,J., King,M.P. and Davidson,E. (2000) The human lysyl-tRNA synthetase gene encodes both the cytoplasmic and mitochondrial enzymes by means of an unusual alternative splicing of the primary transcript. *J. Biol. Chem.*, **275**, 35063–35069.
47. Moraes,C.T., Ricci,E., Bonilla,E., DiMauro,S. and Schon,E.A. (1992) The mitochondrial tRNA(Leu(UUR)) mutation in mitochondrial encephalomyopathy, lactic acidosis, and strokelike episodes (MELAS): genetic, biochemical, and morphological correlations in skeletal muscle. *Am. J. Hum. Genet.*, **50**, 934–949.
48. Entelis,N., Kolesnikova,O., Kazakova,H., Brandina,I., Kamenski,P., Martin,R.P. and Tarassov,I. (2002) Import of nuclear encoded RNAs into yeast and human mitochondria: experimental approaches and possible biomedical applications. *Genet. Eng.*, **24**, 191–213.
49. Varshney,U., Lee,C.P. and RajBhandary,U.L. (1991) Direct analysis of aminoacylation levels of tRNAs in vivo. Application to studying recognition of Escherichia coli initiator tRNA mutants by glutaminyl-tRNA synthetase. *J. Biol. Chem.*, **266**, 24712–24718.
50. Laemmli,U.K. (1970) Cleavage of structural proteins during the assembly of the head of bacteriophage T4. *Nature*, **227**, 680–685.
51. Kolesnikova,O., Entelis,N., Kazakova,H., Brandina,I., Martin,R.P. and Tarassov,I. (2002) Targeting of tRNA into yeast and human mitochondria: the role of anticodon nucleotides. *Mitochondrion*, **2**, 95–107.
52. Kolesnikova,O., Kazakova,H., Comte,C., Steinberg,S., Kamenski,P., Martin,R.P., Tarassov,I. and Entelis,N. (2010) Selection of RNA aptamers imported into yeast and human mitochondria. *RNA*, **16**, 926–941.
53. Tarassov,I., Entelis,N. and Martin,R. (1995) Mitochondrial import of a cytoplasmic lysine-tRNA in yeast is mediated by cooperation of cytoplasmic and mitochondrial lysyl-tRNA synthetases. *EMBO J.*, **14**, 3461–3471.
54. Entelis,N.S., Kolesnikova,O.A., Martin,R.P. and Tarassov,I.A. (2001) RNA delivery into mitochondria. *Adv. Drug Deliv. Rev.*, **49**, 199–215.

55. Entelis,N.S., Krasheninnikov,I.A., Martin,R.P. and Tarassov,I.A. (1996) Mitochondrial import of a yeast cytoplasmic tRNA (Lys): possible roles of aminoacylation and modified nucleosides in subcellular partitioning. *FEBS Lett.*, **384**, 38–42.
56. Enriquez,J.A., Cabezas-Herrera,J., Bayona-Bafaluy,M.P. and Attardi,G. (2000) Very rare complementation between mitochondria carrying different mitochondrial DNA mutations points to intrinsic genetic autonomy of the organelles in cultured human cells. *J. Biol. Chem.*, **275**, 11207–11215.
57. Tukey,J.W. (1977) *Exploratory Data Analysis*. Addison-Wesley, Reading, MA.

MATERIAL AND METHODS

MATERIAL AND METHODS

1. Strains and Growth Conditions

Wild type *Saccharomyces cerevisiae* strains W303 (*MAT*a {*leu2-3,112; trp1-1; can1-100; ura3-1; ade2-1; his3-11,15*}) and BY4742 (*MATα* {*his3Δ1; leu2Δ0; lys2Δ0; ura3Δ0*}) were used for isolation of mitochondria. Deletion mutant strains *por1*Δ, *por2*Δ, *tom5*Δ, *tom6*Δ and *tom7*Δ, based on the genetic background of BY4742, were purchased from Euroscarf (http://web.uni-frankfurt.de/fb15/mikro/euroscarf/). The deletion strain *tom20*Δ_{112} (*MAT*α {ρ^-, *tom20*-Δ112::URA3, *ade2-101*^{ochre}, *his3-Δ200*, *leu2-Δ1*, *ura3-52*, *trp1-Δ63*, *lys2Δ-801*^{amber}}) was as described in (Moczko et al., 1994). For mitochondria isolation purposes, yeast cells were grown on the YPGlyGlu media (yeast extract 1%, peptone 2%, glycerol 4% and glucose 0,5%) to reach an OD_{600nm} = 3,5 - 4.

Escherichia coli BMH 71-18 {*thi*, *supE*, Δ(*lac-pro*AB), [*mutS*::Tn10], [F', *pro*AB, *lac*$I^qZ\Delta M15$]} and BL21-CodonPlus(DE3)-RIL {F^-, *omp*T, *hsd*S(r^-_B m^-_B), dcm^+, Tet^r, *gal*, *end*A, Hte [*arg*U, *ile*Y, *leu*W, Cam^r] strains, used for expression of recombinant proteins, were grown overnight in LB (yeast extract 0,5%, peptone 1%, NaCl 0,5%) in presence of selective antibiotics. Prior to IPTG induction, cells were diluted in LB and grown to an OD_{600nm} = 0,8.

2. Isolation of Mitochondria

The method used for the isolation of mitochondria was based on a published procedure by (Daum et al., 1982) with slight modifications.

- Grown yeast cells were harvested (2000xg 15' 20°C) then washed twice with sterile water.
- Spheroplasting was achieved by incubating cells at 37°C for 10'-20' under slight shaking (Infors incubator 80rpm) in spheroplasting buffer (1,35M sorbitol; 1mM EDTA; 1mM EGTA; 0,2M Na-phosphate pH7,4) (1g wet weight/10ml) containing 10-15mg Zymolyase 20T/g wet cells. Spheroplasting was checked by measuring the OD_{600nm} drop (~60%) in water.

- Spheroplasts were then harvested (1000xg 10' 4°C) and washed once in spheroplast washing buffer (0,75M sorbitol; 0,4M mannitol; 0,1% bovine serum albumin; 10mM HEPES-NaOH pH7).
- Total cell lysate was obtained by lysing spheroplasts in breakage buffer (BB) (0,6M sorbitol; 0,5mM EDTA; 0,1% bovine serum albumin; 10mM HEPES-NaOH pH7) (0,2g wet weight/ml), containing a protease inhibitor cocktail (Roche), with 10-15 strokes in a Dounce homogenizer (Wheaton) using the "loose" pestle.
- Cell debris were removed by differential centrifugation (3000xg 10' 4°C) and crude mitochondria were obtained by centrifugation of the clarified lysate (10000xg 20' 4°C). Mitochondria were washed again in BB without bovine serum albumin (10000xg 20' 4°C).
- If needed, crude mitochondria were further purified by centrifugation (45000xg 60' 4°C) through a discontinuous sucrose gradient (60%-32%-23%-15% in BB), where pure mitochondria were recovered from the 60%-32% interphase and washed again in buffer BB (10000xg 20' 4°C).

Mitochondrial protein concentration was calculated by standard Bradford assay:

- Isolated mitochondria were suspended in a minimal volume of BB. For protein determination a part of this suspension was diluted 10x in BB.
- 5µl, 10µl and 20µl of this diluted suspension were mixed with 50µl of NaOH 6% (prepared from tablets) and incubated at room temperature for 2'.
- Then H_2O was added up to 800µl and this mixture was supplied by 200µl of Bradford reagent. Samples were incubated during 5' at 30°C.
- Protein concentration was measured by taking OD_{595nm}. The blank was the same mixture as described above without mitochondria.
- The calibration curve was done for bovine serum albumin (1 to 10µg).

Complete mitochondrial integrity was checked by the citrate synthase assay (Matlib et al., 1979). The assay consisted in a preparation of the following mixture:

- 20-200µg of mitochondria (mitochondrial protein) = 10µl
- 810µl 1M sorbitol
- 100µl DTNB solution [100mM]
- 30µl acetyl-CoA solution [12mM]

This mixture was used immediately as a blank at 412nm in a 1ml cuvette. Kinetic recording was started for ~2' until a constant OD_{412nm} was reached. Then:

- 50µl sodium oxaloacetate [85mM] were added

Recording at OD_{412nm} was continued until saturation was reached.

The control reaction consisted in dissolving mitochondria in 50µl of 0,5% Triton-X100 and H2O *qsp*. 820µl. The remaining order of addition events was as described above. Percentage of intact mitochondria was calculated by: $\% = 1 - (\Delta OD_{412nm}\ dt_a / \Delta OD_{412nm}\ dt_c) \times 100$, where $\Delta OD_{412nm}\ dt_a$ is the difference of OD_{412nm} during a time laps at the linear recording phase of the assay reaction after addition of oxaloacetate and $\Delta OD_{412nm}\ dt_c$ the difference of OD_{412nm} during a time laps at the linear recording phase of the control reaction after addition of oxaloacetate.

Integrity of the mitochondrial outer membrane was assessed by accessibility of externally added cytochrome *c* (cyt *c*) to the respiratory chain during respiration measurements (Oxygraph, Hansatech). The percentage reflecting the integrity of the mitochondrial outer membrane was determined by taking the ratio : $I = \rho_{IV}/\rho_{IV+cyt\ c} \times 100$, where ρ_{IV} is the respiration rate at state IV and $\rho_{IV+cyt\ c}$ the respiration rate at state IV in presence of 2,5µM cyt *c*. This value was normally in between 85%-95%. Respiratory control of isolated mitochondria was calculated according (Chance and Williams, 1955) as a ratio of respiration rates at metabolic states III and IV. Respiratory controls were in a range from 2 to 4.

3. Purification of recombinant Proteins

The recombinant enolase-2 and the precursor form of mitochondrial lysyl-tRNA-synthetase (preMSK) from *Saccharomyces cerevisiae* were purified according to the procedures described in (Entelis et al., 2006).

- To this aim the *E.coli* strain BL21-CodonPlus(DE3)-RIL was transformed with the pET3a plasmid expressing the cloned gene of enolase-2 or preMSK under *lacZ* promoter. Both proteins were expressing a C-terminal 6-His tag.
- Transformants were repicted and cultivated in presence of appropriate antibiotics until an $OD_{600nm} = 0,8$.
- Cells were induced with 1mM IPTG for 1h at 37°C for cells expressing enolase-2 and for 15h at 18°C for cells expressing preMSK.

- After induction cells were harvested, washed and lysed with lysozyme (1mg/ml cell solution) at 0°C for 30'. The lysate was treated with 15-20 strokes in a Dounce homogenizer (Wheaton) using the "tight" pestle.
- The lysate was clarified (35000xg 4°C 30') and the clear lysate containing the native recombinant proteins was subjected to affinity purification using Ni-NTA agarose beads (Qiagen).

The recombinant fusion protein cyt*b*2-DHFR consisted of the first 167 amino acids of the *Saccharomyces cerevisiae* cytochrome *b*2 (cyt*b2*) with a deletion of residues 47-65 that was fused to the entire mouse dihydrofolate reductase (DHFR), was purified according (Koll et al., 1992).

- *E.coli* BMH 71-18 strain was transformed with the pUHE73-1 plasmid expressing the cloned gene of the fusion protein cyt*b*2-DHFR under *lacZ* promoter.
- Transformants were repicted and cultivated in presence of appropriate antibiotics until an OD_{600nm} = 0,8.
- Cells were induced with 1mM IPTG for 1h at 37°C.
- After induction cells were harvested, washed and lysed with lysozyme (1mg/ml cell solution) at 0°C for 30'. The lysate was treated with 15-20 strokes in a Dounce homogenizer (Wheaton) using the "tight" pestle.
- Inclusion bodies containing cyt*b*2-DHFR were purified according to (Koll et al., 1992).
- The crude fraction of cyt*b*2-DHFR was further purified by passage through a PD10 desalting column (GE Healthcare) to exchange the buffer to 20mM MES-KOH pH6 followed by subsequent cation exchange chromatography on a Resource-S column (Pharmacia Biotech) using the AKTÄ-FPLC system (Amersham Pharmacia Biotech).
- A single protein peak corresponding to cyt*b*2-DHFR was detected at OD_{280nm} and eluted between 300-350mM KCl on a linear gradient (0-500mM).
- Peak fractions of 0.5ml size were collected, verified for their purity on SDS-PAGE, aliquoted and stored at –80˚C.

4. Synthesis of $tRNA^{Lys(CUU)}$ (tRK1), radioactive Labelling and Aminoacylation

The plasmid used for *in vitro* transcription of the $tRNA^{Lys(CUU)}$ (tRK1) gene was constructed by cloning the corresponding PCR product of the tRK1 gene in a pUC119 vector under the control of a T7 promoter. The gene was cloned in order to have a *BstNI* restriction site at its 5'-end that after digestion and T7 transcription yielded a 3'CCA-OH terminus in the T7 transcript required for aminoacylation of tRK1. T7 transcription was carried out using the T7 RiboMAX™ Large Scale RNA production system (Promega) according to manufacturer instructions and the corresponding T7 transcript (tRK1) was gel purified on a denaturing 10% 8M Urea PAGE. The band corresponding to the tRK1 transcript was localized under UV light and tRK1 was eluted in RNA elution buffer (0,5M ammonium acetate; 10mM magnesium acetate; 1mM EDTA; 1% SDS) supplemented with 1/10V acid phenol pH5. Eluted tRK1 was ethanol precipitated and purified tRK1 transcript meant to be radioactively labelled was dephosphorylated using calf intestinal phosphatase (Roche) (1U/µg tRK1 1h 37°C).

tRK1 was 5'-end labelled with γ^{32}P-ATP using T4 polynucleotide kinase (10U/0,5µg tRK1 1h 37°C) and gel purified on a denaturing 10% 8M Urea PAGE. Labelled tRK1 was eluted and ethanol precipitated. *Prior* to aminoacylation tRK1 was refolded in presence of 1V of 10mM $MgCl_2$ by heating at 90°C during 1' and cooling down at room temperature during 15'. Subsequent aminoacylation was carried out (15' 37°C) by adding 1V of aminoacylation buffer (100mM Tris-HCl pH7,5; 30mM KCl; 10mM $MgCl_2$; 2mM ATP; 1mM DTT; 0,05mM lysine) and 1nM recombinant lysyl-tRNA-synthetase (KRS). Aminoacylated tRK1 was extracted by acid phenol pH5, ethanol precipitated and dissolved in 10mM sodium acetate pH5.

5. Synthesis of ^{35}S-Met labelled preMSK

The synthesis of ^{35}S-Met labelled preMSK was done in a rabbit reticulocyte lysate as described by the manufacturer (TnT® T7 Quick for PCR DNA, Promega). The template consisted in a PCR product of the preMSK gene put under the T7 promoter.

6. Import of tRK1 and preMSK into Mitochondria

In vitro import assays of tRK1 were carried out in a final volume of 100µl using 50µg of mitochondria (mitochondrial protein) *per* import assay.

- Mitochondria (Yx50µg) corresponding to Y assays were incubated during 5' at 0°C in presence of *E.coli* ribosomal RNAs (12µg/mg mitochondrial protein) (Roche) to avoid unspecific binding of tRK1 during the import reaction. Mitochondria were centrifuged (13000xg 5' 4°C).
- The mitochondrial pellet was resuspended in Yx50µl of import mixture (10mM HEPES-NaOH pH7; 0,6M sorbitol; 10mM succinate; 2mM NADH; 1mM $MgCl_2$; 30mM KCl; 5mM ATP). In parallel Yx50µl import mixture was supplied with radiolabelled aminoacylated tRK1 transcript (100cps final).
- 50µl of radioactive import mixture was distributed in each Eppendorf tube and 50µl of mitochondria solution was added.
- This suspension was supplied with recombinant enolase-2 (Eno-2) (0,21µM) and recombinant precursor form of mitochondrial lysyl-tRNA-synthetase (preMSK) (44nM).
- Samples were subsequently incubated at 30°C for indicated times to permit tRK1 import.
- Non-imported tRK1 was degraded by adding 1V (100µl) of 2x RNaseA solution (12,5-25µg/ml RNaseA; 0,6M sorbitol; 8mM $MgCl_2$; 10mM HEPES-NaOH pH7) for 10' at 0°C. The reaction was stopped with 5V of BB containing 5mM EDTA.
- Mitochondria were pelleted (13000xg 5' 4°C), resuspended in 500µl BB, transferred into fresh Eppendorf tubes and pelleted again (13000xg 5' 4°C).
- The mitochondrial pellet was then lysed in 100µl lysis buffer (0,1M sodium acetate pH5; 1% SDS; 0,1% DEPC) at 100°C during 1', mitochondrial RNA's were extracted by hot acid phenol pH5 (55°C) and ethanol precipitated in presence of 10µg *E.coli* carrier tRNAs.
- Extracted mitochondrial RNAs were separated by electrophoresis on a denaturing 10% 8M Urea PAGE, the gel was fixed (10% EtOH/10% acetic acid), dried and exposed to a PhophoImager plate (Fuji).
- Autoradiograms were revealed using a TyphoonTrio scanner. The treatment of images and subsequent calculations of import efficiencies were done with the help of the ImageQuant™TL program. For representation of relative imports on the plots, error

bars were calculated according to standard deviation for parallel experiments, if applicable.

In case if DIDS (4,4'-Diisothiocyano-2,2'-stilbenedisulfonic acid) (Thinnes et al., 1994) was used, mitochondria were resuspended in BB (1mg/ml) and pre-incubated in presence of indicated DIDS concentrations during 5' at 0°C. Excess of DIDS was removed by pelleting mitochondria *prior* to resuspension in import mixture.

In vitro import assays of preMSK were carried out in a final volume of 100µl using 50µg of mitochondria (mitochondrial protein) *per* import assay.

- Mitochondria (Yx50µg) corresponding to Y assays were pelleted (13000xg 5' 4°C).
- Mitochondria were resuspended in Yx100µl of import mixture (10mM HEPES-NaOH pH7; 0,6M sorbitol; 10mM succinate; 2mM NADH; 1mM $MgCl_2$; 30mM KCl; 5mM ATP).
- 100µl aliquots were distributed in Eppendorf tubes and supplied with ^{35}S-Met labelled preMSK.
- Samples were subsequently incubated at 25°C for indicated times to allow preMSK import.
- Non-imported preMSK was degraded by proteinase K treatment (100µg/ml) during 2' at 25°C. The reaction was stopped by adding 9V of ice-cold BB containing 1mM PMSF.
- Mitochondria were pelleted, dissolved in Laemmli buffer and heated at 60°C during 5'. Proteins were separated on a 12% SDS-PAGE, the gel was fixed, dried and exposed to a PhosphoImager plate.

To block the TOM40 channel of the preprotein import machinery, the recombinant cyt*b*2-DHFR (26pmol/50µg mitochondrial protein) was imported in presence of 5µM methotrexate in the same conditions as described above. After import, non-imported cyt*b*2-DHFR was removed by pelleting mitochondria *prior* to resuspension in import mixture. Blocking was checked by inhibition of *in vitro* import of preMSK. To investigate the effect of TOM40 channel blocking on tRK1 import, cyt*b*2-DHFR treated mitochondria were used for *in vitro* tRK1 import assays.

7. Northern Blot Hybridization

- Total RNAs of different *S.cerevisiae* strains were extracted from spheroplasts (obtained from 1ml cell culture OD_{600} = 1) by suspending them in 1V lysis buffer (0,1M sodium acetate pH5; 1% SDS; DEPC 0,1%) followed by heating at 100°C during 1'. 1V of hot acid phenol pH5 (55°C) was added and samples were subsequently vortexed, centrifuged (16000xg 10' 4°C) and total RNAs were ethanol precipitated from the aqueous phase.
- For isolation of mitochondrial RNAs, mitochondria (1mg/ml) were treated with a 2x RNaseA solution (100µg/ml RNaseA; 0,6M sorbitol; 8mM $MgCl_2$; 10mM HEPES-NaOH pH7) for 15' at 0°C and the reaction was stopped by addition of 5V of BB containing 5mM EDTA. The mitochondrial RNA extraction procedure was done as for total RNAs.
- Total and mitochondrial RNAs were separated on a 10% 8M Urea PAGE and electroblotted (15h 10V 200mA 4°C) on a Hybond-N membrane (Amersham) in transfer buffer (17mM NaH_2PO_4/8mM Na_2HPO_4 pH 6,5).
- Blotted RNAs were covalently bound to the Hybond-N membrane by UV irradiation during 3' (254nm; E = $150x10^3 \mu J/cm^2$) (Stratalinker).
- Membranes were prehybridized in prehybridization solution (6x SSC; 10x Denhardt solution; 0,2%SDS) (1x SSC: 150mM NaCl; 15mM trisodium citrate; NaOH *qsp*. pH7) (100x Denhardt solution: 2% Ficoll; 2% Polyvinyl-pyrrolidone; 2% bovine serum albumin).
- Subsequent hybridizations were carried out using γ^{32}P-ATP 5'-end radiolabelled DNA probes directed against tRK1 (5'-TGG-AGC-CCT-GTA-GGG-GG-3') ($T°_M$ = 54°C), mitochondrial $tRNA^{Gly}$ (5'-ATT-CAA-TGT-TTG-GAA-GAC-3') ($T°_M$ = 48°C) and cytoplasmic tRK2 (5'-TGG-CTC-CTC-ATA-GGG-GG-3') ($T°_M$ = 52°C). Annealing temperatures were chosen 5°C below melting temperatures ($T°_M$).
- After hybridization the membrane was washed in washing buffer (1xSSC; 0,1%SDS) (3x10', 25°C) before exposition to a PhosphoImager plate and quantification with the ImageQuant™TL program.
- Before a new hybridization was done the membrane was stripped in stripping buffer (0,02xSSC; 0,1%SDS) (3x10', 80°C).

8. Isolation of VDAC1 and VDAC2

Saccharomyces cerevisiae mitochondria from wild type or *por2*Δ strains were used to prepare mitochondrial outer membranes (*cf.* section 12) that were used to purify VDAC1.

- The pellet of mitochondrial outer membranes was suspended in solubilisation buffer (20mM Tris-HCl pH7; 1mM EDTA; 2% Triton X-100) and protein extraction was performed for 30' at 4°C.
- One-step hydroxyapatite/celite column chromatography was applied to purify VDAC1 (de Pinto et al., 1987; Ludwig et al., 1988). Triton-X100 extract was applied on a well-packed dry hydroxyapatite (Biorad) - celite 535 (Sigma) column (2:1 w/w) and VDAC1 was eluted with solubilisation buffer. The first 8 fractions with a size of 0.4ml were collected.
- The protein concentration was determined using the calculated extinction coefficient of 24050 $(mol/L)^{-1}*cm^{-1}$ at 280nm (Bay and Court, 2009).
- Protein purity was monitored by SDS-PAGE and was estimated to be at least 95%, based on silver staining of gels or by Western blot with monoclonal antibodies against VDAC1. Additional identification of VDAC1 was provided by mass spectrometry analysis. The final yield of VDAC1 was ~0,5mg/l yeast culture.

Saccharomyces cerevisiae mitochondria from a *por1*Δ strains were used to prepare mitochondrial outer membranes (*cf.* section 12) that were used to purify VDAC2.

- The pellet of mitochondrial outer membranes was suspended in solubilisation buffer (20mM Tris-HCl pH7; 1mM EDTA; 2% Triton X-100) and protein extraction was performed for 30' at 4°C.
- The Triton X-100 extract was loaded on a hydroxyapatite/celite (2:1 w/w) column, the resin was washed with 5 column volumes of solubilisation buffer and bound proteins were eluted with 0.5M NaCl (0,5ml fractions).
- Fractions were analysed by 12.5% SDS-PAGE and desalted on a PD10 column (Pharmacia) equilibrated with 20mM MOPS pH6, 100mM NaCl and 0.5% Triton X-100 at 4°C.
- Peak fractions collected from the PD-10 desalting column were loaded on a cation exchange column (Resourse S) equilibrated with the same buffer. The column was washed with 5 volumes of loading buffer and VDAC2 was eluted with a NaCl gradient from 100mM to 1M. VDAC2 was eluted between 150mM and 200mM NaCl and

combined peak fractions were concentrated on 30kDa cut off Nanosep membranes (16000xg 30' 4°C).

- Purity of isolated VDAC2 was checked by silver stained SDS-PAGE and by mass spectrometry analysis.

The native state of isolated VDAC2 was confirmed by measuring its channel-forming activity in a bilayer system according to (Rostovtseva and Bezrukov, 1998; Rostovtseva et al., 2006). Mixtures of diphytanoyl-phosphatidylcholine (DPhPC) (Avanti Polar Lipids, Inc.) and ergosterol (Sigma Aldrich) were prepared from stock solutions of 100mg/ml and 10 mg/ml in chloroform respectively with a ratio of 50/1 (w/w). Lipid mixtures were dried under nitrogen on a rotary evaporator and then dissolved in n-hexane to a total lipid concentration of 5 mg/ml. Bilayer membranes were formed from lipid drops applied on a 100µm diameter hole in a 20µm-thick Teflon film that separated two chambers with volumes of 1ml. Chamber cleaning was done by sonication in a Folch solution (chloroform/methanol (2:1)) for 30 min. Applied potential was established with Ag^0/AgCl electrodes in 3M KCl connected by agarose bridges. For recording of channel activity 1M KCl buffered by 10mM Tris-HCl pH7 was used. VDAC2 channel insertion was achieved by adding 1-10µl of a 0.5% Triton X-100 solution of purified VDAC2 to the 1-ml aqueous phase in the *cis*-compartment under stirring. Potential was defined as positive when it is greater at the side of the VDAC addition (*cis*-side) according to (Rostovtseva et al., 2004). The voltage-dependent properties of VDAC2-containing bilayer membranes were studied according to a protocol described in (Zizi et al., 1998). Record of single channel or multiple channels was acquired with the help of a L-CARD 1210 and a digital amplifier (Axon Instruments, Inc.) at a sampling frequency of 1Hz. Recording was analysed using the pClamp 10 software (Axon Instruments).

9. Reconstitution of VDAC1 and VDAC2 into Vesicles

Mitochondrial VDAC1 and VDAC2 were reconstituted into small unilamellar vesicles (SUVs) in the presence of ergosterol using modifications of the procedure described by (Shao et al., 1996).

- A 46:33:10:1:4:6 mixture of egg yolk L-a-phosphatidyl choline, L-a-phosphatidyl ethanolamine, L-a-phosphatidyl inositol, L-a-phosphatidyl serine, egg lecithin L-a-phosphatidic acid and cardiolipin (Sigma) was dissolved in chloroform and dried in a rotary evaporator at room temperature under argon during 1 hour.

- The dried lipid mixture (between 10 and 11mg) was resuspended in 500µl ice-cold 10 mM Tris-HCl buffer pH7, containing 1mM EDTA (TE buffer). The resulting cloudy suspension was diluted and sonicated on ice (Fisher Scientific Sonifier 300) to yield the stock suspension of SUVs (4 mg/mL).
- For VDAC1 and VDAC2 preincubation with ergosterol (Sigma), 50µL of protein solution (20µg/mL) diluted in TE was mixed with 50 µL of ergosterol (1mg/ml) resuspended in TE and the mixture was gently shaken on ice for 10min.
- Thereafter, this mixture was added to 0,6mL of 1% Triton X-100 and 50µL of SUV stock solution.
- Resulting 0,75 mL were mixed with 150 µL of SUV stock solution giving a final SUV concentration of ~1mg/ml, with a lipid/ergosterol ratio of 20 and a lipid/protein ratio of 1000.
- This SUV solution was subjected to 3 freeze-thaw cycles (liquid N_2, room temperature).
- Resulting vesicles were then dialysed over-night against TE buffer.
- Presence of reconstituted protein was checked by Western blot, vesicles were aliquoted and stored at -80°C.

Obtained vesicles with reconstituted VDACs were called VDAC-SUV, versus control SUV, where VDACs were absent. These liposomes lacking VDACs were prepared by the same method with an adequate amount of a 2% Triton X-100 solution in TE instead of VDAC protein solutions.

10. Determination of the functional State of VDAC1 reconstituted in SUVs

To test the functional state of reconstituted VDAC1 in VDAC1-SUVs, its ability to form channels for metabolites was studied. For this test hexokinase (HK) (ATP:D-hexose 6-phosphotransferase) (Sigma) from *Saccharomyces cerevisiae* was used assuming that this glycolytic enzyme, with a molecular weight of 54 kDa, cannot pass the VDAC1 channel (cut-off is about 6 kD) after inclusion into VDAC1-SUVs.

- HK (approximately 10U) was included by sonication (3x10s) (45% of maximal power, Fisher Scientific Sonifier 300) in VDAC1-SUVs containing 10 µg of VDAC1.
- Loaded vesicles were washed from non-included enzyme (100000xg 4˚C 60').

Absence of non-included enzyme and specific activity of HK loaded into vesicles were checked spectrophotometrically according to (Bücher et al., 1964) with a coupled enzymatic reaction using the bacterial glucose 6-phosphate dehydrogenase (GPD) as coupling enzyme with an excess of NAD+ as a second substrate.

- HK substrates glucose (2 mM) and ATP (5 mM) were added to 100 µL of VDAC1-SUVs and entered the vesicles *via* VDAC1.
- The enzymatic activity of HK was detected indirectly by GPD generation of NADH measured at 340 nm (Beckman Coulter DU730 spectrophotometer).
- To monitor the inhibition of VDAC1, the specific blocker DIDS was used in concentrations from 50 to 500µM to prevent transport of ATP and glucose into hexokinase-loaded vesicles.
- Full activity of loaded HK was calculated for digitonin (50 µg) treated SUVs after complete solubilisation.

11. Import of tRK1 into VDAC-SUVs

Assays of tRK1 import into VDAC-SUVs (100 µL of vesicles/assay) were carried out as described above for isolated mitochondria with the exception that no recombinant import directing proteins were added to the import mixture. In control experiments SUVs or VDAC-SUVs prepared without ergosterol were used. *Prior* to import, all types of vesicles were dialysed overnight at 4˚C against import mixture (10mM HEPES-NaOH pH7; 0.6M sorbitol; 10mM succinate; 2mM NADH; 5mM ATP; 30mM KCl; 2.5mM $MgCl_2$). After completion of tRK1 import, vesicles were treated with 100µl RNaseA (25µg/ml) during 10' at 0°C and sedimented (100000xg 60’ 4˚C) (Beckman TL100 bench top ultracentrifuge). tRK1 was extracted from the pellet of VDAC-SUVs by hot acid phenol pH5, precipitated with ethanol in presence of 10µg *E.coli* carrier tRNAs and analysed as described above for tRK1 import into isolated mitochondria.

12. Subfractionation of Mitochondria and Preparation of outer mitochondrial Membrane Vesicles (OMV)

Wild type, *por1*Δ and *por2*Δ deletion strains were grown and mitochondria were isolated as described above including the supplemental purification step on discontinuous sucrose gradients. Outer mitochondrial membrane (OM) isolation and preparation of outside-out sealed vesicles was performed essentially as described by (Riezman et al., 1983).

- To this purpose mitochondria were incubated for 20' at 0°C in hypotonic buffer (HB) (20mM Tris-HCl pH 7,4; 1mM PMSF) and occasionally homogenized in a Potter homogenizer using the "tight" pestle.
- Then the mitochondrial suspension was diluted with 1/3 volume of 1,8M sucrose prepared on HB containing 2mM ATP and 2mM $MgCl_2$. Shrunk mitochondria were sonicated (Fisher Scientific Sonifier 300) and the mixture centrifuged (30000xg 15' 4°C).
- The supernatant was collected and centrifuged (100000xg 60' 4°C) to obtain the crude OM fraction.
- Membranes were resuspended in HB supplemented by 1mM PMSF and this fraction was further purified on a sucrose density gradient from 30,5-53% buffered with 20mM Tris-HCl pH7,4/1mM PMSF by overnight centrifugation (120000xg 16h 4°C).
- The tube content was fractionated into 1ml fractions from the top to the bottom and OM fractions were identified by monitoring VDAC1 by Western blot using rabbit polyclonal antibodies against *Saccharomyces cerevisiae* VDAC1.
- OM purity was estimated by the absence of succinate dehydrogenase activity (inner membrane marker) (Sottocasa et al., 1967), myokinase (intermembrane space marker) (Ernster and Luylenstierna, 1970) and citrate synthase (matrix marker) (Matlib et al., 1979).
- Pure OM fractions were combined and centrifuged (100000xg 60' 4°C). The OM pellet was resuspended in 10mM Tris-HCl pH7,5. The protein concentration was measured and adjusted to achieve a final protein concentration of 1mg/ml.
- Prepared OMV aliquots (100µl) were stored at -80°C.
- Orientation of prepared OMVs was checked by treatment with trypsin (20µg/ml) followed by immunodecoration against the cytosolic part of *Saccharomyces cerevisiae* mitochondrial outer membrane protein Tom70. The major degradation of Tom70

compared to trypsine untreated OMVs was in favour with an outside-out orientation of prepared OMVs.

- Intactness of OMVs was checked as described above for SUVs (hexokinase activity accessibility test). tRK1 import assays into OMVs were carried out as described above for isolated mitochondria.

13. Formation of Protein Oligomers on the mitochondrial Surface upon tRK1 *in vitro* Import

- Isolated mitochondria (100µg mitochondrial protein/assay) from a BY4742 wild type strain were suspended in 100µl import mixture (10mM HEPES-NaOH pH7; 0,6M sorbitol; 10mM succinate; 2mM NADH; 1mM $MgCl_2$; 30mM KCl).
- Import reactions were carried out in presence of 3pmol aminoacylated tRK1 as a standard control import (*cf.* section 6) (+ tRK1), in presence of tRK1 and 0,5mM DIDS (+ tRK1; + DIDS) and in presence of tRK1 without external ATP source (+ tRK1; -ATP) or import directing proteins Eno-2/preMSK (+ tRK1; -Eno-2/-preMSK).
- Samples were incubated for 2' at 30°C.
- Then 1mM of the chemical protein-protein crosslinker 3-maleimidobenzoyl-N-hydroxysuccinimide ester (MBS) (Sigma) was added where indicated and incubation was continued for further 5' at 30°C.
- Mitochondria were reisolated, mitochondrial proteins separated on a gradient 4%-20% SDS-PAGE and electroblotted on a nitrocellulose membrane.
- VDAC1 oligomers were identified by Western blot using a monoclonal mouse antibody directed against *S.cerevisiae* VDAC1.

14. North-Western Hybridization

- Sucrose gradient purified mitochondria (200µg mitochondrial protein) were used to prepare a total mitochondrial lysate by dissolving mitochondria in Laemmli buffer and by heating the suspension at 60°C during 5'.
- Mitochondrial proteins were separated on 2 gradient 4%-12% SDS-PAGE (2x100µg mitochondrial protein).
- One gel was colored by Coomassie blue (Fermentas) and the other identical gel was electroblotted on a nitrocellulose membrane (Invitrogen) (100V 200mA 1h 4°C).

- This membrane was incubated in renaturation buffer (0,1% v/v Nonidet NP-40; 0,1M Tris-HCl pH7,5) at 4°C during 6h and then washed (3x10', 4°C) in hybridization buffer (10mM Tris-HCl pH7,5; 5mM $MgCl_2$; 1% bovine serum albumine).
- 5'-end labelled aminoacylated tRK1 transcript was added on the prepared membrane (100cps, 15h, 4°C).
- The membrane was washed again in hybridization buffer (3x10', 4°C) and exposed to a PhophoImager plate (Fuji). Autoradiograms were revealed using TyphoonTrio scanner and images were treated in ImageQuant™TL program.
- Bands on the Coomassie colored gel were localized according to the signal obtained by North-Western and cut for mass spectrometry analysis.

15. Crosslinking and Immunoprecipitation (CLIP)

- Mitochondria were isolated as described above and used in standard tRK1 *in vitro* import conditions (*cf*. section 6).
- The T7 BrU-tRK1 transcript was synthesised as described in section 4 with the exception that uridine was replaced by the photoactivable base 5-bromouridine (5-BrU) (Sigma).
- Mitochondria (10mg mitochondrial protein) were diluted (1mg/ml) in import mixture without ATP (10mM HEPES-NaOH pH7; 0,6M sorbitol; 10mM succinate; 2mM NADH; 1mM $MgCl_2$; 30mM KCl) and spread on a glass petri dish (9 cm diameter) in order to have a solution depth of ~1mm.
- Aminoacylated BrU-tRK1 (30nM), Eno-2 (0,21µM) and preMSK (44nM) were added and the import reaction was allowed to proceed for 2' at room temperature under gentle stirring.
- Crosslinking between tRK1 and proteins was induced by UV irradiation (312nm, 12W). The distance between the UV source and the solution was ~2cm. In order to prevent evaporation of the sample, the petri dish was placed in a recipient containing water up to the same level as the solution inside the petri dish. The import reaction was continued for another 30' under UV at room temperature.
- After crosslinking mitochondria were washed in buffer BB (10000xg 20' 4°C).
- The mitochondrial pellet was dissolved under slight shaking during 15h in immunoprecipitation buffer (IP) (50mM HEPES-NaOH pH7; 150mM NaCl) containing 0,5% Triton X-100.

- Non-dissolved membranes were removed by ultracentrifugation (100000xg 60' 4°C).
- The supernatant was subjected to immunoprecipitation that was performed by adding a biotinylated monoclonal mouse anti-5-bromouridine antibody (1:100 dilution) (Millipore). Immunoprecipitation was allowed to proceed during 15h at 4°C.
- After immunoprecipitation the mixture was applied on 100µl streptavidin-sepharose beads (GE Healthcare) previously equilibrated with IP buffer. The sample was incubated during 4h at 4°C under slight shaking.
- Beads were centrifuged (3000xg 2' 4°C) and flow-through was collected.
- Beads were subjected to 5 further washing steps with 100µl of IP buffer.
- Elution (50µl fractions) of bound tRK1/protein complexes was done in elution buffer (0,1M glycine-HCl pH3). Before separation of proteins on SDS-PAGE, samples were neutralized by addition of 0,5M Tris base until the indicator in Laemmli buffer turned to blue (±1µl/50µl eluate) and heated at 60°C during 5'.
- Eluted samples were separated on a gradient 4%-12% SDS-PAGE.
- After migration, the gel was colored by Coomassie, bands of interest were cut and proteins were identified by mass spectrometry.

16. Mass Spectrometry Analysis

Proteins were identified by mass spectrometry analysis using MALDI-TOF/TOFIII Smartbeam (Bruker), TripleTOF® 5600 (AB SCIEX) and nanoLC-MS/MS (nanoU3000 (Dionex)-ESI-MicroTOFQII) (Bruker). Mass spectrometry data were analysed with the help of Mascot software (Matrix science). Mass spectrometry identification of proteins for North-Western studies was done in collaboration with Professor Laurence SABATIER (ECPM, Strasbourg). Mass spectrometry identification of proteins for CLIP studies was done in collaboration with Philippe HAMMANN and Lauriane KUHN at the proteomic platform of the University of Strasbourg (Strasbourg Esplanade).

17. Measurement of Oxygen Consumption

Oxygen consumption of isolated mitochondria was measured in liquid phase using the oxygraph system (Hansatech). To this aim mitochondria (50-200µg mitochondrial protein) were suspended in preheated BB (30°C) in order to have a final volume of 1ml. Rates of oxygen consumption were measured in the recording chamber thermostated at 30°C in

presence of substrates, uncouplers and inhibitors. Used substrates were succinate (10mM), NADH (1mM) and ethanol (1mM). Carbonyl cyanide-4-(trifluoromethoxy)phenylhydrazone (FCCP) was used as uncoupler in 10nM steps. Inhibitors were 4,4'-Diisothiocyano-2,2'-stilbenedisulfonic acid (DIDS) (0,5mM) and potassium cyanide (2,5mM).

BIBLIOGRAPHY

BIBLIOGRAPHY

Abe, Y., Shodai, T., Muto, T., Mihara, K., Torii, H., Nishikawa, S., Endo, T., and Kohda, D. (2000). **Structural basis of presequence recognition by the mitochondrial protein import receptor Tom20.** Cell *100*, 551–560.

Adhya, S. (2008). **Leishmania mitochondrial tRNA importers**. Int J Biochem Cell Biol *40*, 2681–2685.

Adhya, S., Ghosh, T., Das, A., Bera, S. K., and Mahapatra, S. (1997). **Role of an RNA-binding protein in import of tRNA into Leishmania mitochondria.** J Biol Chem *272*, 21396–21402.

Ahting, U., Thieffry, M., Engelhardt, H., Hegerl, R., Neupert, W., and Nussberger, S. (2001). **Tom40, the pore-forming component of the protein-conducting TOM channel in the outer membrane of mitochondria.** The Journal of cell biology *153*, 1151–1160.

Ahting, U., Thun, C., Hegerl, R., Typke, D., Nargang, F. E., Neupert, W., and Nussberger, S. (1999). **The TOM core complex: the general protein import pore of the outer membrane of mitochondria.** J Cell Biol *147*, 959–968.

Alconada, A., Kübrich, M., Moczko, M., Hönlinger, A., and Pfanner, N. (1995). **The mitochondrial receptor complex: the small subunit Mom8b/Isp6 supports association of receptors with the general insertion pore and transfer of preproteins.** Molecular and cellular biology *15*, 6196–6205.

Alfonzo, J. D., Blanc, V., Estevez, A. M., Rubio, M. A., and Simpson, L. (1999). **C to U editing of the anticodon of imported mitochondrial tRNA(Trp) allows decoding of the UGA stop codon in Leishmania tarentolae.** Embo J *18*, 7056–7062.

Andersson, S. G., Zomorodipour, A., Andersson, J. O., Sicheritz-Pontén, T., Alsmark, U. C., Podowski, R. M., Näslund, A. K., Eriksson, A. S., Winkler, H. H., and Kurland, C. G. (1998). **The genome sequence of Rickettsia prowazekii and the origin of mitochondria.** Nature *396*, 133–140.

Antos, N., Stobienia, O., Budzińska, M., and Kmita, H. (2001). **Under conditions of insufficient permeability of VDAC1, external NADH may use the TOM complex channel to cross the outer membrane of Saccharomyces cerevisiae mitochondria.** Journal of bioenergetics and biomembranes *33*, 119–126.

Azoulay-Zohar, H., Israelson, A., Abu-Hamad, S., and Shoshan-Barmatz, V. (2004). **In self-defence: hexokinase promotes voltage-dependent anion channel closure and prevents mitochondria-mediated apoptotic cell death.** The Biochemical journal *377*, 347–355.

Baker, K. P., Schaniel, A., Vestweber, D., and Schatz, G. (1990). **A yeast mitochondrial outer membrane protein essential for protein import and cell viability.** Nature *348*, 605–609.

Banci, L., Bertini, I., Cefaro, C., Ciofi-Baffoni, S., Gallo, A., Martinelli, M., Sideris, D. P., Katrakili, N., and Tokatlidis, K. (2009). **MIA40 is an oxidoreductase that catalyzes oxidative protein folding in mitochondria.** Nature structural & molecular biology *16*, 198–206.

Bay, D. C., and Court, D. A. (2009). **Effects of ergosterol on the structure and activity of Neurospora mitochondrial porin in liposomes.** Canadian journal of microbiology *55*, 1275–1283.

Bayrhuber, M., Meins, T., Habeck, M., Becker, S., Giller, K., Villinger, S., Vonrhein, C., Griesinger, C., Zweckstetter, M., and Zeth, K. (2008). **Structure of the human voltage-dependent anion channel.** Proceedings of the National Academy of Sciences of the United States of America *105*, 15370–15375.

Becker, T., Guiard, B., Thornton, N., Zufall, N., Stroud, D. A., Wiedemann, N., and Pfanner, N. (2010). **Assembly of the mitochondrial protein import channel: role of Tom5 in two-stage interaction of Tom40 with the SAM complex.** Molecular biology of the cell *21*, 3106–3113.

Becker, T., Wenz, L.-S., Krüger, V., Lehmann, W., Müller, J. M., Goroncy, L., Zufall, N., Lithgow, T., Guiard, B., Chacinska, A., et al. (2011a). **The mitochondrial import protein Mim1 promotes biogenesis of multispanning outer membrane proteins.** The Journal of cell biology *194*, 387–395.

Becker, T., Wenz, L.-S., Thornton, N., Stroud, D., Meisinger, C., Wiedemann, N., and Pfanner, N. (2011b). **Biogenesis of mitochondria: dual role of Tom7 in modulating assembly of the preprotein translocase of the outer membrane.** Journal of molecular biology *405*, 113–124.

Beilharz, T., Egan, B., Silver, P. A., Hofmann, K., and Lithgow, T. (2003). **Bipartite signals mediate subcellular targeting of tail-anchored membrane proteins in Saccharomyces cerevisiae.** The Journal of biological chemistry *278*, 8219–8223.

Benz, R. (1994). **Permeation of hydrophilic solutes through mitochondrial outer membranes: review on mitochondrial porins.** Biochimica et biophysica acta *1197*, 167–196.

Bhattacharyya, S. N., Chatterjee, S., and Adhya, S. (2002). **Mitochondrial RNA import in Leishmania tropica: aptamers homologous to multiple tRNA domains that interact cooperatively or antagonistically at the inner membrane.** Mol Cell Biol *22*, 4372–4382.

Bhattacharyya, S. N., Chatterjee, S., Goswami, S., Tripathi, G., Dey, S. N., and Adhya, S. (2003). **"Ping-pong" interactions between mitochondrial tRNA import receptors within a multiprotein complex.** Mol Cell Biol *23*, 5217–5224.

Blachly-Dyson, E., and Forte, M. (2001). **VDAC channels.** IUBMB life *52*, 113–118.

Blachly-Dyson, E., Song, J., Wolfgang, W. J., Colombini, M., and Forte, M. (1997). **Multicopy suppressors of phenotypes resulting from the absence of yeast VDAC encode a VDAC-like protein.** Molecular and cellular biology *17*, 5727–5738.

Blachly-Dyson, E., Zambronicz, E. B., Yu, W. H., Adams, V., McCabe, E. R., Adelman, J., Colombini, M., and Forte, M. (1993). **Cloning and functional expression in yeast of two human isoforms of the outer mitochondrial membrane channel, the voltage-dependent anion channel.** The Journal of biological chemistry *268*, 1835–1841.

Bouzaidi-Tiali, N., Aeby, E., Charriere, F., Pusnik, M., and Schneider, A. (2007). **Elongation factor 1a mediates the specificity of mitochondrial tRNA import in T. brucei.** Embo J *26*, 4302–4312.

Brubacher-Kauffmann, S., Marechal-Drouard, L., Cosset, A., Dietrich, A., and Duchene, A. M. (1999). **Differential import of nuclear-encoded tRNAGly isoacceptors into solanum Tuberosum mitochondria.** Nucleic Acids Res *27*, 2037–2042.

Bücher, T., Luh, E., and Pette, D. (1964). **Einfache und zusammengestzte optische Tests mit Pyridininucleotiden.** ,in: K. Lang, E. Lehnartz (Eds.), Hoppe-Seyler/Thierfelder, Handbuch der physiologisch-und pathologisch-chemischen Analyse, vol VI/ASpringer, Berlin, 292–339.

Chacinska, A., Koehler, C. M., Milenkovic, D., Lithgow, T., and Pfanner, N. (2009). **Importing mitochondrial proteins: machineries and mechanisms.** Cell *138*, 628–644.

Chacinska, A., Lind, M., Frazier, A. E., Dudek, J., Meisinger, C., Geissler, A., Sickmann, A., Meyer, H. E., Truscott, K. N., Guiard, B., et al. (2005). **Mitochondrial presequence translocase: switching between TOM tethering and motor recruitment involves Tim21 and Tim17.** Cell *120*, 817–829.

Chan, D. C. (2006). **Mitochondrial fusion and fission in mammals.** Annual review of cell and developmental biology *22*, 79–99.

Chan, N. C., Likić, V. A., Waller, R. F., Mulhern, T. D., and Lithgow, T. (2006). **The C-terminal TPR domain of Tom70 defines a family of mitochondrial protein import receptors found only in animals and fungi.** Journal of molecular biology *358*, 1010–1022.

Chan, N. C., and Lithgow, T. (2008). **The peripheral membrane subunits of the SAM complex function codependently in mitochondrial outer membrane biogenesis.** Molecular biology of the cell *19*, 126–136.

Chance, B., and Williams, G. R. (1955). **A simple and rapid assay of oxidative phosphorylation.** Nature *175*, 1120–1121.

Charrière, F., Helgadóttir, S., Horn, E. K., Söll, D., and Schneider, A. (2006). **Dual targeting of a single tRNA(Trp) requires two different tryptophanyl-tRNA synthetases in Trypanosoma brucei.** Proceedings of the National Academy of Sciences of the United States of America *103*, 6847–6852.

Chatterjee, S., Home, P., Mukherjee, S., Mahata, B., Goswami, S., Dhar, G., and Adhya, S. (2006). **An RNA-binding respiratory component mediates import of type II tRNAs into Leishmania mitochondria.** J Biol Chem *281*, 25270–25277.

Chauwin, J. F., Oster, G., and Glick, B. S. (1998). **Strong precursor-pore interactions constrain models for mitochondrial protein import.** Biophysical journal *74*, 1732–1743.

Chen, H.-W., Rainey, R. N., Balatoni, C. E., Dawson, D. W., Troke, J. J., Wasiak, S., Hong, J. S., McBride, H. M., Koehler, C. M., Teitell, M. A., et al. (2006). **Mammalian polynucleotide phosphorylase is an intermembrane space RNase that maintains mitochondrial homeostasis.** Molecular and cellular biology *26*, 8475–8487.

Choudhary, O. P., Ujwal, R., Kowallis, W., Coalson, R., Abramson, J., and Grabe, M. (2010). **The electrostatics of VDAC: implications for selectivity and gating.** Journal of molecular biology *396*, 580–592.

Cipollone, R., Ascenzi, P., and Visca, P. (2007). **Common themes and variations in the rhodanese superfamily.** IUBMB Life *59*, 51–59.

Curran, S. P., Leuenberger, D., Oppliger, W., and Koehler, C. M. (2002). **The Tim9p-Tim10p complex binds to the transmembrane domains of the ADP/ATP carrier.** The EMBO journal *21*, 942–953.

Daum, G., Bohni, P. C., and Schatz, G. (1982). **Import of proteins into mitochondria. Cytochrome b2 and cytochrome c peroxidase are located in the intermembrane space of yeast mitochondria.** J Biol Chem *257*, 13028–13033.

Davis, A. J., Alder, N. N., Jensen, R. E., and Johnson, A. E. (2007). **The Tim9p/10p and Tim8p/13p complexes bind to specific sites on Tim23p during mitochondrial protein import.** Molecular biology of the cell *18*, 475–486.

Dekker, P. J., Martin, F., Maarse, A. C., Bömer, U., Müller, H., Guiard, B., Meijer, M., Rassow, J., and Pfanner, N. (1997). **The Tim core complex defines the number of mitochondrial translocation contact sites and can hold arrested preproteins in the absence of matrix Hsp70-Tim44.** The EMBO journal *16*, 5408–5419.

Delage, L., Dietrich, A., Cosset, A., and Marechal-Drouard, L. (2003a). **In vitro import of a nuclearly encoded tRNA into mitochondria of Solanum tuberosum.** Mol Cell Biol *23*, 4000–4012.

Delage, L., Duchene, A. M., Zaepfel, M., and Marechal-Drouard, L. (2003b). **The anticodon and the D-domain sequences are essential determinants for plant cytosolic tRNAVal import into mitochondria.** Plant J *34*, 623–633.

Dietmeier, K., Hönlinger, A., Bömer, U., Dekker, P. J., Eckerskorn, C., Lottspeich, F., Kübrich, M., and Pfanner, N. (1997). **Tom5 functionally links mitochondrial preprotein receptors to the general import pore.** Nature *388*, 195–200.

Dietrich, A., Marechal-Drouard, L., Carneiro, V., Cosset, A., and Small, I. (1996). **A single base change prevents import of cytosolic tRNA(Ala) into mitochondria in transgenic plants.** Plant J *10*, 913–918.

Dimmer, K. S., Papic, D., Schumann, B., Sperl, D., Krumpe, K., Walther, D. M., and Rapaport, D. (2012). **A crucial role of Mim2 in the biogenesis of mitochondrial outer membrane proteins.** Journal of cell science.

Duchêne, A.-M., Pujol, C., and Maréchal-Drouard, L. (2009). **Import of tRNAs and aminoacyl-tRNA synthetases into mitochondria.** Current genetics *55*, 1–18.

Duy, D., Soll, J., and Philippar, K. (2007). **Solute channels of the outer membrane: from bacteria to chloroplasts.** Biological chemistry *388*, 879–889.

Dörner, M., Altmann, M., Pääbo, S., and Mörl, M. (2001). **Evidence for import of a lysyl-tRNA into marsupial mitochondria.** Molecular biology of the cell *12*, 2688–2698.

D'Silva, P. R., Schilke, B., Hayashi, M., and Craig, E. A. (2008). **Interaction of the J-protein heterodimer Pam18/Pam16 of the mitochondrial import motor with the translocon of the inner membrane.** Molecular biology of the cell *19*, 424–432.

Eilers, M., Oppliger, W., and Schatz, G. (1987). **Both ATP and an energized inner membrane are required to import a purified precursor protein into mitochondria.** The EMBO journal *6*, 1073–1077.

Entelis, N., Brandina, I., Kamenski, P., Krasheninnikov, I. A., Martin, R. P., and Tarassov, I. (2006). **A glycolytic enzyme, enolase, is recruited as a cofactor of tRNA targeting toward mitochondria in Saccharomyces cerevisiae.** Genes Dev *20*, 1609–1620.

Entelis, N. S., Kieffer, S., Kolesnikova, O. A., Martin, R. P., and Tarassov, I. A. (1998). **Structural requirements of tRNALys for its import into yeast mitochondria.** Proc Natl Acad Sci U S A *95*, 2838–2843.

Entelis, N. S., Kolesnikova, O. A., Dogan, S., Martin, R. P., and Tarassov, I. A. (2001**). 5 S rRNA and tRNA Import into Human Mitochondria. Comparison of in vitro requirements.** J Biol Chem *276*, 45642–53.

Ernster, L., and Luylenstierna, B. (1970). **in Membranes of Mitochondria and Chloroplasts.** Racker E., ed., van Nostrand Reinhold, New York, 172.

Español, Y., Thut, D., Schneider, A., and Ribas de Pouplana, L. (2009). **A mechanism for functional segregation of mitochondrial and cytosolic genetic codes.** Proceedings of the National Academy of Sciences of the United States of America *106*, 19420–19425.

Esseiva, A. C., Naguleswaran, A., Hemphill, A., and Schneider, A. (2004). **Mitochondrial tRNA import in Toxoplasma gondii.** The Journal of biological chemistry *279*, 42363–42368.

Fass, D. (2008). **The Erv family of sulfhydryl oxidases.** Biochimica et biophysica acta *1783*, 557–566.

Florentz, C., Sohm, B., Tryoen-Toth, P., Putz, J., and Sissler, M. (2003). **Human mitochondrial tRNAs in health and disease.** Cell Mol Life Sci *60*, 1356–1375.

Foury, F., Roganti, T., Lecrenier, N., and Purnelle, B. (1998). **The complete sequence of the mitochondrial genome of Saccharomyces cerevisiae.** FEBS Lett *440*, 325–31.

Frazier, A. E., Dudek, J., Guiard, B., Voos, W., Li, Y., Lind, M., Meisinger, C., Geissler, A., Sickmann, A., Meyer, H. E., et al. (2004). **Pam16 has an essential role in the mitochondrial protein import motor.** Nature Structural & Molecular Biology *11*, 226–233.

Frechin, M., Senger, B., Braye, M., Kern, D., Martin, R. P., and Becker, H. D. (2009). **Yeast mitochondrial Gln-tRNA(Gln) is generated by a GatFAB-mediated transamidation pathway involving Arc1p-controlled subcellular sorting of cytosolic GluRS.** Genes Dev *23*, 1119–1130.

Gao, Y., and Wang, H. (2006). **Casein kinase 2 Is activated and essential for Wnt/beta-catenin signaling.** The Journal of biological chemistry *281*, 18394–18400.

Gebert, M., Schrempp, S. G., Mehnert, C. S., Heißwolf, A. K., Oeljeklaus, S., Ieva, R., Bohnert, M., von der Malsburg, K., Wiese, S., Kleinschroth, T., et al. (2012). **Mgr2 promotes coupling of the mitochondrial presequence translocase to partner complexes.** The Journal of cell biology *197*, 595–604.

Geslain, R., Aeby, E., Guitart, T., Jones, T. E., Castro de Moura, M., Charrière, F., Schneider, A., and Ribas de Pouplana, L. (2006). **Trypanosoma seryl-tRNA synthetase is a metazoan-like enzyme with high affinity for tRNASec.** The Journal of biological chemistry *281*, 38217–38225.

Giegé, R., Jühling, F., Pütz, J., Stadler, P., Sauter, C., and Florentz, C. (2012). **Structure of transfer RNAs: similarity and variability.** Wiley interdisciplinary reviews. RNA *3*, 37–61.

Gincel, D., Zaid, H., and Shoshan-Barmatz, V. (2001). **Calcium binding and translocation by the voltage-dependent anion channel: a possible regulatory mechanism in mitochondrial function.** The Biochemical journal *358*, 147–155.

Glick, B. S., Brandt, A., Cunningham, K., Müller, S., Hallberg, R. L., and Schatz, G. (1992). **Cytochromes c1 and b2 are sorted to the intermembrane space of yeast mitochondria by a stop-transfer mechanism.** Cell *69*, 809–822.

Gonçalves, R. P., Buzhynskyy, N., Prima, V., Sturgis, J. N., and Scheuring, S. (2007). **Supramolecular assembly of VDAC in native mitochondrial outer membranes.** Journal of molecular biology *369*, 413–418.

Goswami, S., Chatterjee, S., Bhattacharyya, S. N., Basu, S., and Adhya, S. (2003). **Allosteric regulation of tRNA import: interactions between tRNA domains at the inner membrane of Leishmania mitochondria.** Nucleic Acids Res *31*, 5552–5559.

Goswami, S., Dhar, G., Mukherjee, S., Mahata, B., Chatterjee, S., Home, P., and Adhya, S. (2006). **A bifunctional tRNA import receptor from Leishmania mitochondria.** Proc Natl Acad Sci U S A *103*, 8354–8359.

Goto, Y., Nonaka, I., and Horai, S. (1990). **A mutation in the tRNA(Leu)(UUR) gene associated with the MELAS subgroup of mitochondrial encephalomyopathies.** Nature *348*, 651–3.

Gray, M. W. (1999). **Evolution of organellar genomes.** Curr Opin Genet Dev *9*, 678–687.

Guerrier-Takada, C., Gardiner, K., Marsh, T., Pace, N., and Altman, S. (1983). **The RNA moiety of ribonuclease P is the catalytic subunit of the enzyme.** Cell *35*, 849–857.

Guo, X. W., Smith, P. R., Cognon, B., D'Arcangelis, D., Dolginova, E., and Mannella, C. A. (1995). **Molecular design of the voltage-dependent, anion-selective channel in the mitochondrial outer membrane.** Journal of structural biology *114*, 41–59.

Gutmann, B., Gobert, A., and Giege, P. (2012). **PRORP proteins support RNase P activity in both organelles and the nucleus in Arabidopsis**. Genes & Development *26*, 1022–1027.

Guzun, R., Timohhina, N., Tepp, K., Gonzalez-Granillo, M., Shevchuk, I., Chekulayev, V., Kuznetsov, A. V., Kaambre, T., and Saks, V. A. (2011). **Systems bioenergetics of creatine kinase networks: physiological roles of creatine and phosphocreatine in regulation of cardiac cell function.** Amino acids *40*, 1333–1348.

Hancock, K., and Hajduk, S. L. (1990a). **The mitochondrial tRNAs of Trypanosoma brucei are nuclear encoded.** J Biol Chem *265*, 19208–19215.

Hancock, K., and Hajduk, S. L. (1990b). **The mitochondrial tRNAs of Trypanosoma brucei are nuclear encoded.** The Journal of biological chemistry *265*, 19208–19215.

Harner, M., Körner, C., Walther, D., Mokranjac, D., Kaesmacher, J., Welsch, U., Griffith, J., Mann, M., Reggiori, F., and Neupert, W. (2011). **The mitochondrial contact site complex, a determinant of mitochondrial architecture.** The EMBO journal *30*, 4356–4370.

He, L., and Lemasters, J. J. (2002). **Regulated and unregulated mitochondrial permeability transition pores: a new paradigm of pore structure and function?** FEBS letters *512*, 1–7.

Hermann, G. J., and Shaw, J. M. (1998). **Mitochondrial dynamics in yeast.** Annual review of cell and developmental biology *14*, 265–303.

Herrmann, J. M., and Riemer, J. (2012). **Mitochondrial Disulfide Relay: Redox-regulated Protein Import into the Intermembrane Space.** The Journal of biological chemistry *287*, 4426–4433.

Hiller, S., Garces, R. G., Malia, T. J., Orekhov, V. Y., Colombini, M., and Wagner, G. (2008). **Solution structure of the integral human membrane protein VDAC-1 in detergent micelles.** Science (New York, N.Y.) *321*, 1206–1210.

Hofhaus, G., Lee, J.-E., Tews, I., Rosenberg, B., and Lisowsky, T. (2003). **The N-terminal cysteine pair of yeast sulfhydryl oxidase Erv1p is essential for in vivo activity and**

interacts with the primary redox centre. European journal of biochemistry / FEBS *270*, 1528–1535.

Holzmann, J., Frank, P., Löffler, E., Bennett, K. L., Gerner, C., and Rossmanith, W. (2008). **RNase P without RNA: identification and functional reconstitution of the human mitochondrial tRNA processing enzyme.** Cell *135*, 462–474.

Hoogenboom, B. W., Suda, K., Engel, A., and Fotiadis, D. (2007). **The supramolecular assemblies of voltage-dependent anion channels in the native membrane.** Journal of molecular biology *370*, 246–255.

Hoppins, S., Collins, S. R., Cassidy-Stone, A., Hummel, E., Devay, R. M., Lackner, L. L., Westermann, B., Schuldiner, M., Weissman, J. S., and Nunnari, J. (2011). **A mitochondrial-focused genetic interaction map reveals a scaffold-like complex required for inner membrane organization in mitochondria.** The Journal of cell biology *195*, 323–340.

Huber, P. W., and Wool, I. G. (1984). **Nuclease protection analysis of ribonucleoprotein complexes: use of the cytotoxic ribonuclease alpha-sarcin to determine the binding sites for Escherichia coli ribosomal proteins L5, L18, and L25 on 5S rRNA.** Proceedings of the National Academy of Sciences of the United States of America *81*, 322–326.

Ibrahim, N., Handa, H., Cosset, A., Koulintchenko, M., Konstantinov, Y., Lightowlers, R. N., Dietrich, A., and Weber-Lotfi, F. (2011). **DNA Delivery to Mitochondria: Sequence Specificity and Energy Enhancement.** Pharm Res.

Kamenski, P., Kolesnikova, O., Jubenot, V., Entelis, N., Krasheninnikov, I. A., Martin, R. P., and Tarassov, I. (2007). **Evidence for an Adaptation Mechanism of Mitochondrial Translation via tRNA Import from the Cytosol.** Mol Cell *26*, 625–637.

Kamenski, P., Smirnova, E., Kolesnikova, O., Krasheninnikov, I. A., Martin, R. P., Entelis, N., and Tarassov, I. (2010). **tRNA mitochondrial import in yeast: Mapping of the import determinants in the carrier protein, the precursor of mitochondrial lysyl-tRNA synthetase.** Mitochondrion *10*, 284–293.

Kaneko, T., Suzuki, T., Kapushoc, S. T., Rubio, M. A., Ghazvini, J., Watanabe, K., and Simpson, L. (2003). **Wobble modification differences and subcellular localization of tRNAs in Leishmania tarentolae: implication for tRNA sorting mechanism.** Embo J *22*, 657–667.

Kaufman, B. A., Newman, S. M., Hallberg, R. L., Slaughter, C. A., Perlman, P. S., and Butow, R. A. (2000). **In organello formaldehyde crosslinking of proteins to mtDNA: identification of bifunctional proteins.** Proceedings of the National Academy of Sciences of the United States of America *97*, 7772–7777.

Kawano, S., Yamano, K., Naoé, M., Momose, T., Terao, K., Nishikawa, S., Watanabe, N., and Endo, T. (2009). **Structural basis of yeast Tim40/Mia40 as an oxidative translocator in the mitochondrial intermembrane space.** Proceedings of the National Academy of Sciences of the United States of America *106*, 14403–14407.

Kazakova, H. A., Entelis, N. S., Martin, R. P., and Tarassov, I. A. (1999). **The aminoacceptor stem of the yeast tRNA(Lys) contains determinants of mitochondrial import selectivity.** FEBS Lett *442*, 193–197.

Keinan, N., Tyomkin, D., and Shoshan-Barmatz, V. (2010). **Oligomerization of the mitochondrial protein voltage-dependent anion channel is coupled to the induction of apoptosis.** Molecular and cellular biology *30*, 5698–5709.

Kiparisov, S., Petrov, A., Meskauskas, A., Sergiev, P. V., Dontsova, O. A., and Dinman, J. D. (2005). **Structural and functional analysis of 5S rRNA in Saccharomyces cerevisiae.** Molecular genetics and genomics : MGG *274*, 235–247.

Kmita, H., Antos, N., Wojtkowska, M., and Hryniewiecka, L. (2004). **Processes underlying the upregulation of Tom proteins in S. cerevisiae mitochondria depleted of the VDAC channel.** Journal of bioenergetics and biomembranes *36*, 187–193.

Kmita, H., and Budzińska, M. (2000). **Involvement of the TOM complex in external NADH transport into yeast mitochondria depleted of mitochondrial porin1.** Biochimica et biophysica acta *1509*, 86–94.

Kokoszka, J. E., Waymire, K. G., Levy, S. E., Sligh, J. E., Cai, J., Jones, D. P., MacGregor, G. R., and Wallace, D. C. (2004). **The ADP/ATP translocator is not essential for the mitochondrial permeability transition pore.** Nature *427*, 461–465.

Kolesnikova, O. A., Entelis, N. S., Jacquin-Becker, C., Goltzene, F., Chrzanowska-Lightowlers, Z. M., Lightowlers, R. N., Martin, R. P., and Tarassov, I. (2004). **Nuclear DNA-encoded tRNAs targeted into mitochondria can rescue a mitochondrial DNA mutation associated with the MERRF syndrome in cultured human cells.** Hum Mol Genet *13*, 2519–2534.

Kolesnikova, O. A., Entelis, N. S., Mireau, H., Fox, T. D., Martin, R. P., and Tarassov, I. A. (2000). **Suppression of mutations in mitochondrial DNA by tRNAs imported from the cytoplasm.** Science *289*, 1931–1933.

Kolesnikova, O., Entelis, N., Kazakova, H., Brandina, I., Martin, R. P., and Tarassov, I. (2002). **Targeting of tRNA into yeast and human mitochondria : the role of anticodon nucleotides.** Mitochondrion *2*, 95–107.

Kolesnikova, O., Kazakova, H., Comte, C., Steinberg, S., Kamenski, P., Martin, R. P., Tarassov, I., and Entelis, N. (2010). **Selection of RNA aptamers imported into yeast and human mitochondria.** Rna *16*, 926–941.

Koll, H., Guiard, B., Rassow, J., Ostermann, J., Horwich, A. L., Neupert, W., and Hartl, F. U. (1992). **Antifolding activity of hsp60 couples protein import into the mitochondrial matrix with export to the intermembrane space.** Cell *68*, 1163–1175.

Koulintchenko, M., Konstantinov, Y., and Dietrich, A. (2003). **Plant mitochondria actively import DNA via the permeability transition pore complex.** Embo J *22*, 1245–1254.

Kozany, C., Mokranjac, D., Sichting, M., Neupert, W., and Hell, K. (2004). **The J domain–related cochaperone Tim16 is a constituent of the mitochondrial TIM23 preprotein translocase.** Nature Structural & Molecular Biology *11*, 234–241.

Krayl, M., Lim, J. H., Martin, F., Guiard, B., and Voos, W. (2007). **A cooperative action of the ATP-dependent import motor complex and the inner membrane potential drives mitochondrial preprotein import.** Molecular and cellular biology *27*, 411–425.

Krimmer, T., Rapaport, D., Ryan, M. T., Meisinger, C., Kassenbrock, C. K., Blachly-Dyson, E., Forte, M., Douglas, M. G., Neupert, W., Nargang, F. E., et al. (2001). **Biogenesis of porin of the outer mitochondrial membrane involves an import pathway via receptors and the general import pore of the TOM complex.** The Journal of cell biology *152*, 289–300.

Kroemer, G., Galluzzi, L., and Brenner, C. (2007). **Mitochondrial membrane permeabilization in cell death.** Physiological reviews *87*, 99–163.

Kumar, R., Marechal-Drouard, L., Akama, K., and Small, I. (1996). **Striking differences in mitochondrial tRNA import between different plant species.** Mol Gen Genet *252*, 404–411.

Kutik, S., Stojanovski, D., Becker, L., Becker, T., Meinecke, M., Krüger, V., Prinz, C., Meisinger, C., Guiard, B., Wagner, R., et al. (2008). **Dissecting membrane insertion of mitochondrial beta-barrel proteins.** Cell *132*, 1011–1024.

van der Laan, M., Bohnert, M., Wiedemann, N., and Pfanner, N. (2012). **Role of MINOS in mitochondrial membrane architecture and biogenesis.** Trends in cell biology *22*, 185–192.

van der Laan, M., Meinecke, M., Dudek, J., Hutu, D. P., Lind, M., Perschil, I., Guiard, B., Wagner, R., Pfanner, N., and Rehling, P. (2007). **Motor-free mitochondrial presequence translocase drives membrane integration of preproteins.** Nature Cell Biology *9*, 1152–1159.

van der Laan, M., Wiedemann, N., Mick, D. U., Guiard, B., Rehling, P., and Pfanner, N. (2006). **A role for Tim21 in membrane-potential-dependent preprotein sorting in mitochondria.** Current biology : CB *16*, 2271–2276.

Laforest, M. J., Delage, L., and Marechal-Drouard, L. (2005). **The T-domain of cytosolic tRNAVal, an essential determinant for mitochondrial import.** FEBS Lett *579*, 1072–1078.

Lauffer, S., Mäbert, K., Czupalla, C., Pursche, T., Hoflack, B., Rödel, G., and Krause-Buchholz, U. (2012). **Saccharomyces cerevisiae porin pore forms complexes with the mitochondrial outer membrane proteins Om14p and Om45p.** The Journal of biological chemistry *287*, 17447–17458.

Lee, C. P., Mandal, N., Dyson, M. R., and RajBhandary, U. L. (1993). **The discriminator base influences tRNA structure at the end of the acceptor stem and possibly its interaction with proteins.** Proceedings of the National Academy of Sciences of the United States of America *90*, 7149–7152.

Lemeshko, S. V., and Lemeshko, V. V. (2000). **Metabolically derived potential on the outer membrane of mitochondria: a computational model.** Biophysical journal *79*, 2785–2800.

Li, J., Qian, X., Hu, J., and Sha, B. (2009). **Molecular chaperone Hsp70/Hsp90 prepares the mitochondrial outer membrane translocon receptor Tom71 for preprotein loading.** The Journal of biological chemistry *284*, 23852–23859.

Li, K., Smagula, C. S., Parsons, W. J., Richardson, J. A., Gonzalez, M., Hagler, H. K., and Williams, R. S. (1994). **Subcellular partitioning of MRP RNA assessed by ultrastructural and biochemical analysis.** J Cell Biol *124*, 871–882.

Lill, R. (2009). **Function and biogenesis of iron-sulphur proteins.** Nature *460*, 831–838.

Liu, M. Y., and Colombini, M. (1992). **A soluble mitochondrial protein increases the voltage dependence of the mitochondrial channel, VDAC**. Journal of bioenergetics and biomembranes *24*, 41–46.

Ludwig, O., Krause, J., Hay, R., and Benz, R. (1988). **Purification and characterization of the pore forming protein of yeast mitochondrial outer membrane.** European biophysics journal : EBJ *15*, 269–276.

Lund, E., and Dahlberg, J. E. (1998). **Proofreading and aminoacylation of tRNAs before export from the nucleus.** Science *282*, 2082–2085.

Lutz, T., Neupert, W., and Herrmann, J. M. (2003). **Import of small Tim proteins into the mitochondrial intermembrane space.** The EMBO journal *22*, 4400–4408.

Magalhaes, P. J., Andreu, A. L., and Schon, E. A. (1998). **Evidence for the presence of 5S rRNA in mammalian mitochondria.** Mol Biol Cell *9*, 2375–2382.

Mahapatra, S., and Adhya, S. (1996). **Import of RNA into Leishmania mitochondria occurs through direct interaction with membrane-bound receptors.** J Biol Chem *271*, 20432–20437.

Mahapatra, S., Ghosh, S., Bera, S. K., Ghosh, T., Das, A., and Adhya, S. (1998). **The D arm of tRNATyr is necessary and sufficient for import into Leishmania mitochondria in vitro.** Nucleic Acids Res *26*, 2037–2041.

Mannella, C. A., Colombini, M., and Frank, J. (1983). **Structural and functional evidence for multiple channel complexes in the outer membrane of Neurospora crassa mitochondria.** Proceedings of the National Academy of Sciences of the United States of America *80*, 2243–2247.

Martin, R. P., Schneller, J. M., Stahl, A. J., and Dirheimer, G. (1979). **Import of nuclear deoxyribonucleic acid coded lysine-accepting transfer ribonucleic acid (anticodon C-U-U) into yeast mitochondria.** Biochemistry *18*, 4600–4605.

Martin, R. P., Schneller, J. M., Stahl, A. J., and Dirheimer, G. (1977). **Study of yeast mitochondrial tRNAs by two-dimensional polyacrylamide gel electrophoresis:**

characterization of isoaccepting species and search for imported cytoplasmic tRNAs. Nucleic acids research *4*, 3497–3510.

Martin, R. P., Sibler, A. P., Gehrke, C. W., Kuo, K., Edmonds, C. G., McCloskey, J. A., and Dirheimer, G. (1990). **5-[[(carboxymethyl)amino]methyl]uridine is found in the anticodon of yeast mitochondrial tRNAs recognizing two-codon families ending in a purine.** Biochemistry *29*, 956–959.

Maréchal-Drouard, L., Weil, J. H., and Guillemaut, P. (1988). **Import of several tRNAs from the cytoplasm into the mitochondria in bean Phaseolus vulgaris.** Nucleic acids research *16*, 4777–4788.

Matlib, M. A., Shannon, W. A., and Srere, P. A. (1979). **Measurement of matrix enzyme activity in situ in isolated mitochondria made permeable with toluene.** Methods in enzymology *56*, 544–550.

Mayer, A., Nargang, F. E., Neupert, W., and Lill, R. (1995). **MOM22 is a receptor for mitochondrial targeting sequences and cooperates with MOM19.** The EMBO journal *14*, 4204–4211.

Meinecke, M., Wagner, R., Kovermann, P., Guiard, B., Mick, D. U., Hutu, D. P., Voos, W., Truscott, K. N., Chacinska, A., Pfanner, N., et al. (2006). **Tim50 maintains the permeability barrier of the mitochondrial inner membrane.** Science (New York, N.Y.) *312*, 1523–1526.

Meisinger, C., Rissler, M., Chacinska, A., Szklarz, L. K. S., Milenkovic, D., Kozjak, V., Schönfisch, B., Lohaus, C., Meyer, H. E., Yaffe, M. P., et al. (2004). **The mitochondrial morphology protein Mdm10 functions in assembly of the preprotein translocase of the outer membrane.** Developmental cell *7*, 61–71.

Milenkovic, D., Gabriel, K., Guiard, B., Schulze-Specking, A., Pfanner, N., and Chacinska, A. (2007). **Biogenesis of the Essential Tim9 Tim10 Chaperone Complex of Mitochondria: Site-specific recognition of cysteine residues by the intermembrane space receptor Mia40.** Journal of Biological Chemistry *282*, 22472–22480.

Milenkovic, D., Ramming, T., Müller, J. M., Wenz, L.-S., Gebert, N., Schulze-Specking, A., Stojanovski, D., Rospert, S., and Chacinska, A. (2009). **Identification of the signal directing Tim9 and Tim10 into the intermembrane space of mitochondria.** Molecular biology of the cell *20*, 2530–2539.

Mireau, H., Cosset, A., Marechal-Drouard, L., Fox, T. D., Small, I. D., and Dietrich, A. (2000). **Expression of Arabidopsis thaliana mitochondrial alanyl-tRNA synthetase is not sufficient to trigger mitochondrial import of tRNAAla in yeast.** J Biol Chem *275*, 13291–13296.

Moczko, M., Ehmann, B., Gartner, F., Honlinger, A., Schafer, E., and Pfanner, N. (1994). **Deletion of the receptor MOM19 strongly impairs import of cleavable preproteins into Saccharomyces cerevisiae mitochondria**. J Biol Chem *269*, 9045–9051.

Mokranjac, D., Bourenkov, G., Hell, K., Neupert, W., and Groll, M. (2006). **Structure and function of Tim14 and Tim16, the J and J-like components of the mitochondrial protein import motor.** The EMBO journal *25*, 4675–4685.

Mokranjac, D., and Neupert, W. (2009). **Thirty years of protein translocation into mitochondria: unexpectedly complex and still puzzling.** Biochimica et biophysica acta *1793*, 33–41.

Mukherjee, S., Basu, S., Home, P., Dhar, G., and Adhya, S. (2007). **Necessary and sufficient factors for the import of transfer RNA into the kinetoplast mitochondrion.** EMBO rep *8*, 589–595.

Neupert, W., and Herrmann, J. M. (2007). **Translocation of proteins into mitochondria.** Annual review of biochemistry *76*, 723–749.

Okada, S. F., O'Neal, W. K., Huang, P., Nicholas, R. A., Ostrowski, L. E., Craigen, W. J., Lazarowski, E. R., and Boucher, R. C. (2004). **Voltage-dependent anion channel-1 (VDAC-1) contributes to ATP release and cell volume regulation in murine cells.** The Journal of general physiology *124*, 513–526.

Osman, C., Merkwirth, C., and Langer, T. (2009). **Prohibitins and the functional compartmentalization of mitochondrial membranes.** Journal of cell science *122*, 3823–3830.

Otera, H., Taira, Y., Horie, C., Suzuki, Y., Suzuki, H., Setoguchi, K., Kato, H., Oka, T., and Mihara, K. (2007**). A novel insertion pathway of mitochondrial outer membrane proteins with multiple transmembrane segments.** The Journal of cell biology *179*, 1355–1363.

O'Brien, E. A., Zhang, Y., Wang, E., Marie, V., Badejoko, W., Lang, B. F., and Burger, G. (2009). **GOBASE: an organelle genome database.** Nucleic acids research *37*, D946–50.

Palmieri, F., Pierri, C. L., De Grassi, A., Nunes-Nesi, A., and Fernie, A. R. (2011). **Evolution, structure and function of mitochondrial carriers: a review with new insights.** The Plant journal : for cell and molecular biology *66*, 161–181.

Paschen, S. A., Waizenegger, T., Stan, T., Preuss, M., Cyrklaff, M., Hell, K., Rapaport, D., and Neupert, W. (2003). **Evolutionary conservation of biogenesis of beta-barrel membrane proteins.** Nature *426*, 862–866.

Pastorino, J. G., and Hoek, J. B. (2008). **Regulation of hexokinase binding to VDAC.** Journal of bioenergetics and biomembranes *40*, 171–182.

Pavlov, E., Grigoriev, S. M., Dejean, L. M., Zweihorn, C. L., Mannella, C. A., and Kinnally, K. W. (2005). **The mitochondrial channel VDAC has a cation-selective open state.** Biochimica et biophysica acta *1710*, 96–102.

Payne, A. H., and Hales, D. B. (2004). **Overview of steroidogenic enzymes in the pathway from cholesterol to active steroid hormones.** Endocrine reviews *25*, 947–970.

Perkins, G., Renken, C., Martone, M. E., Young, S. J., Ellisman, M., and Frey, T. (1997). **Electron tomography of neuronal mitochondria: three-dimensional structure and organization of cristae and membrane contacts.** Journal of structural biology *119*, 260–272.

De Pinto, V., al Jamal, J. A., Benz, R., and Palmieri, F. (1990). **Positive residues involved in the voltage-gating of the mitochondrial porin-channel are localized in the external moiety of the pore.** FEBS letters *274*, 122–126.

De Pinto, V., Prezioso, G., Thinnes, F., Link, T. A., and Palmieri, F. (1991). **Peptide-specific antibodies and proteases as probes of the transmembrane topology of the bovine heart mitochondrial porin.** Biochemistry *30*, 10191–10200.

de Pinto, V., Prezioso, G., and Palmieri, F. (1987). **A simple and rapid method for the purification of the mitochondrial porin from mammalian tissues.** Biochimica et biophysica acta *905*, 499–502.

Pinton, P., Giorgi, C., Siviero, R., Zecchini, E., and Rizzuto, R. (2008). **Calcium and apoptosis: ER-mitochondria Ca2+ transfer in the control of apoptosis.** Oncogene *27*, 6407–6418.

Popov-Celeketić, J., Waizenegger, T., and Rapaport, D. (2008). **Mim1 functions in an oligomeric form to facilitate the integration of Tom20 into the mitochondrial outer membrane.** Journal of molecular biology *376*, 671–680.

Preuss, M., Ott, M., Funes, S., Luirink, J., and Herrmann, J. M. (2005). **Evolution of mitochondrial oxa proteins from bacterial YidC. Inherited and acquired functions of a conserved protein insertion machinery.** The Journal of biological chemistry *280*, 13004–13011.

Puranam, R. S., and Attardi, G. (2001). **The RNase P associated with HeLa cell mitochondria contains an essential RNA component identical in sequence to that of the nuclear RNase P.** Mol Cell Biol *21*, 548–61.

Pusnik, M., Charrière, F., Mäser, P., Waller, R. F., Dagley, M. J., Lithgow, T., and Schneider, A. (2009). **The single mitochondrial porin of Trypanosoma brucei is the main metabolite transporter in the outer mitochondrial membrane.** Molecular biology and evolution *26*, 671–680.

Pusnik, M., Schmidt, O., Perry, A. J., Oeljeklaus, S., Niemann, M., Warscheid, B., Lithgow, T., Meisinger, C., and Schneider, A. (2011). **Mitochondrial preprotein translocase of trypanosomatids has a bacterial origin.** Current biology : CB *21*, 1738–1743.

Raghavan, A., Sheiko, T., Graham, B. H., and Craigen, W. J. (2011). **Voltage-dependant anion channels: Novel insights into isoform function through genetic models.** Biochimica et biophysica acta *1818*, 1477–1485.

Rao, S., Gerbeth, C., Harbauer, A., Mikropoulou, D., Meisinger, C., and Schmidt, O. (2011). **Signaling at the gate: phosphorylation of the mitochondrial protein import machinery.** Cell cycle (Georgetown, Tex.) *10*, 2083–2090.

Rao, S., Schmidt, O., Harbauer, A. B., Schönfisch, B., Guiard, B., Pfanner, N., and Meisinger, C. (2012). **Biogenesis of the preprotein translocase of the outer mitochondrial membrane: protein kinase A phosphorylates the precursor of Tom40 and impairs its import.** Molecular biology of the cell *23*, 1618–1627.

Rehling, P., Model, K., Brandner, K., Kovermann, P., Sickmann, A., Meyer, H. E., Kühlbrandt, W., Wagner, R., Truscott, K. N., and Pfanner, N. (2003). **Protein insertion into the mitochondrial inner membrane by a twin-pore translocase.** Science (New York, N.Y.) *299*, 1747–1751.

Reichert, A. S., and Neupert, W. (2002). **Contact sites between the outer and inner membrane of mitochondria-role in protein transport.** Biochimica et biophysica acta *1592*, 41–49.

Riezman, H., Hay, R., Gasser, S., Daum, G., Schneider, G., Witte, C., and Schatz, G. (1983). **The outer membrane of yeast mitochondria: isolation of outside-out sealed vesicles.** The EMBO journal *2*, 1105–1111.

Rinehart, J., Krett, B., Rubio, M. A., Alfonzo, J. D., and Soll, D. (2005). **Saccharomyces cerevisiae imports the cytosolic pathway for Gln-tRNA synthesis into the mitochondrion.** Genes Dev *19*, 583–592.

Robert, N., d' Erfurth, I., Marmagne, A., Erhardt, M., Allot, M., Boivin, K., Gissot, L., Monachello, D., Michaud, M., Duchêne, A.-M., et al. (2012). **Voltage-dependent-anion-channels (VDACs) in Arabidopsis have a dual localization in the cell but show a distinct role in mitochondria.** Plant molecular biology *78*, 431–446.

Rosenfeld, E., and Beauvoit, B. (2003). **Role of the non-respiratory pathways in the utilization of molecular oxygen by Saccharomyces cerevisiae.** Yeast (Chichester, England) *20*, 1115–1144.

Rostovtseva, T., and Colombini, M. (1997). **VDAC channels mediate and gate the flow of ATP: implications for the regulation of mitochondrial function.** Biophysical journal *72*, 1954–1962.

Rostovtseva, T. K., Antonsson, B., Suzuki, M., Youle, R. J., Colombini, M., and Bezrukov, S. M. (2004). **Bid, but not Bax, regulates VDAC channels.** The Journal of biological chemistry *279*, 13575–13583.

Rostovtseva, T. K., and Bezrukov, S. M. (1998). **ATP transport through a single mitochondrial channel, VDAC, studied by current fluctuation analysis.** Biophysical journal *74*, 2365–2373.

Rostovtseva, T. K., Kazemi, N., Weinrich, M., and Bezrukov, S. M. (2006). **Voltage gating of VDAC is regulated by nonlamellar lipids of mitochondrial membranes.** The Journal of biological chemistry *281*, 37496–37506.

Rostovtseva, T. K., Tan, W., and Colombini, M. (2005). **On the role of VDAC in apoptosis: fact and fiction.** Journal of bioenergetics and biomembranes *37*, 129–142.

Rubio, M. A., Liu, X., Yuzawa, H., Alfonzo, J. D., and Simpson, L. (2000). **Selective importation of RNA into isolated mitochondria from Leishmania tarentolae.** Rna *6*, 988–1003.

Rubio, M. A., Rinehart, J. J., Krett, B., Duvezin-Caubet, S., Reichert, A. S., Soll, D., and Alfonzo, J. D. (2008). **Mammalian mitochondria have the innate ability to import tRNAs by a mechanism distinct from protein import.** Proc Natl Acad Sci U S A *105*, 9186–9191.

Rubio, M. A. T., and Hopper, A. K. (2011). **Transfer RNA travels from the cytoplasm to organelles.** Wiley interdisciplinary reviews. RNA *2*, 802–817.

Rusconi, C. P., and Cech, T. R. (1996a). **Mitochondrial import of only one of three nuclear-encoded glutamine tRNAs in Tetrahymena thermophila.** Embo J *15*, 3286–3295.

Rusconi, C. P., and Cech, T. R. (1996b). **The anticodon is the signal sequence for mitochondrial import of glutamine tRNA in Tetrahymena.** Genes Dev *10*, 2870–2880.

Sabirov, R. Z., Sheiko, T., Liu, H., Deng, D., Okada, Y., and Craigen, W. J. (2006). **Genetic demonstration that the plasma membrane maxianion channel and voltage-dependent anion channels are unrelated proteins.** The Journal of biological chemistry *281*, 1897–1904.

Saitoh, T., Igura, M., Obita, T., Ose, T., Kojima, R., Maenaka, K., Endo, T., and Kohda, D. (2007). **Tom20 recognizes mitochondrial presequences through dynamic equilibrium among multiple bound states.** The EMBO Journal *26*, 4777–4787.

Salinas, T., Duchene, A. M., Delage, L., Nilsson, S., Glaser, E., Zaepfel, M., and Marechal-Drouard, L. (2006). **The voltage-dependent anion channel, a major component of the tRNA import machinery in plant mitochondria.** Proc Natl Acad Sci U S A *103*, 18362–18367.

Salinas, T., Duchene, A. M., and Marechal-Drouard, L. (2008). **Recent advances in tRNA mitochondrial import.** Trends Biochem Sci *33*, 320–329.

Salinas, T., Schaeffer, C., Marechal-Drouard, L., and Duchene, A. M. (2005). **Sequence dependence of tRNA(Gly) import into tobacco mitochondria.** Biochimie *87*, 863–872.

Sampson, M. J., Lovell, R. S., and Craigen, W. J. (1997). **The murine voltage-dependent anion channel gene family. Conserved structure and function.** The Journal of biological chemistry *272*, 18966–18973.

Scheffler, I. E. (2001a). **A century of mitochondrial research: achievements and perspectives.** Mitochondrion *1*, 3–31.

Scheffler, I. E. (2001b). **Mitochondria make a come back.** Adv Drug Deliv Rev *49*, 3–26.

Schein, S. J., Colombini, M., and Finkelstein, A. (1976). **Reconstitution in planar lipid bilayers of a voltage-dependent anion-selective channel obtained from paramecium mitochondria.** The Journal of membrane biology *30*, 99–120.

Schekman, R. (2010). **Editorial Expression of Concern: A bifunctional tRNA import receptor from Leishmania mitochondria.** Proceedings of the National Academy of Sciences *107*, 9476–9476.

Schleyer, M., Schmidt, B., and Neupert, W. (1982). **Requirement of a membrane potential for the posttranslational transfer of proteins into mitochondria.** European journal of biochemistry / FEBS *125*, 109–116.

Schmidt, O., Harbauer, A. B., Rao, S., Eyrich, B., Zahedi, R. P., Stojanovski, D., Schönfisch, B., Guiard, B., Sickmann, A., Pfanner, N., et al. (2011). **Regulation of mitochondrial protein import by cytosolic kinases.** Cell *144*, 227–239.

Schmidt, O., Pfanner, N., and Meisinger, C. (2010). **Mitochondrial protein import: from proteomics to functional mechanisms.** Nature reviews. Molecular cell biology *11*, 655–667.

Schneider, A. (2011). **Mitochondrial tRNA import and its consequences for mitochondrial translation.** Annual review of biochemistry *80*, 1033–1053.

Schneider, A., and Marechal-Drouard, L. (2000). **Mitochondrial tRNA import: are there distinct mechanisms?** Trends Cell Biol *10*, 509–513.

Sepuri, N. B. V., Gorla, M., and King, M. P. (2012). **Mitochondrial lysyl-tRNA synthetase independent import of tRNA lysine into yeast mitochondria.** PloS one *7*, e35321.

Shao, L., Kinnally, K. W., and Mannella, C. A. (1996). **Circular dichroism studies of the mitochondrial channel, VDAC, from Neurospora crassa.** Biophysical journal *71*, 778–786.

Shariff, K., Ghosal, S., and Matouschek, A. (2004). **The force exerted by the membrane potential during protein import into the mitochondrial matrix.** Biophysical journal *86*, 3647–3652.

Sharma, S., Singha, U. K., and Chaudhuri, M. (2010). **Role of Tob55 on mitochondrial protein biogenesis in Trypanosoma brucei.** Molecular and biochemical parasitology *174*, 89–100.

Sherrer, R. L., Yermovsky-Kammerer, A. E., and Hajduk, S. L. (2003). **A sequence motif within trypanosome precursor tRNAs influences abundance and mitochondrial localization.** Molecular and cellular biology *23*, 9061–9072.

Shimizu, S., Konishi, A., Kodama, T., and Tsujimoto, Y. (2000). **BH4 domain of antiapoptotic Bcl-2 family members closes voltage-dependent anion channel and inhibits apoptotic mitochondrial changes and cell death.** Proceedings of the National Academy of Sciences of the United States of America *97*, 3100–3105.

Shimizu, S., Narita, M., and Tsujimoto, Y. (1999). **Bcl-2 family proteins regulate the release of apoptogenic cytochrome c by the mitochondrial channel VDAC.** Nature *399*, 483–487.

Shimizu, S., and Tsujimoto, Y. (2000). **Proapoptotic BH3-only Bcl-2 family members induce cytochrome c release, but not mitochondrial membrane potential loss, and do not directly modulate voltage-dependent anion channel activity.** Proceedings of the National Academy of Sciences of the United States of America *97*, 577–582.

Sideris, D. P., and Tokatlidis, K. (2007). **Oxidative folding of small Tims is mediated by site-specific docking onto Mia40 in the mitochondrial intermembrane space.** Molecular microbiology *65*, 1360–1373.

Simpson, A. M., Suyama, Y., Dewes, H., Campbell, D. A., and Simpson, L. (1989). **Kinetoplastid mitochondria contain functional tRNAs which are encoded in nuclear DNA and also contain small minicircle and maxicircle transcripts of unknown function.** Nucleic Acids Res *17*, 5427–5445.

Singha, U. K., Peprah, E., Williams, S., Walker, R., Saha, L., and Chaudhuri, M. (2008). **Characterization of the mitochondrial inner membrane protein translocator Tim17 from Trypanosoma brucei.** Molecular and biochemical parasitology *159*, 30–43.

Small, I., Marechal-Drouard, L., Masson, J., Pelletier, G., Cosset, A., Weil, J. H., and Dietrich, A. (1992). **In vivo import of a normal or mutagenized heterologous transfer RNA into the mitochondria of transgenic plants: towards novel ways of influencing mitochondrial gene expression?** Embo J *11*, 1291–1296.

Smirnov, A., Comte, C., Mager-Heckel, A. M., Addis, V., Krasheninnikov, I. A., Martin, R. P., Entelis, N., and Tarassov, I. (2010). **Mitochondrial enzyme rhodanese is essential for 5 S ribosomal RNA import into human mitochondria.** J Biol Chem *285*, 30792–30803.

Smirnov, A., Entelis, N., Martin, R. P., and Tarassov, I. (2011). **Biological significance of 5S rRNA import into human mitochondria: role of ribosomal protein MRP-L18.** Genes Dev *25*, 1289–1305.

Smirnov, A., Tarassov, I., Mager-Heckel, A. M., Letzelter, M., Martin, R. P., Krasheninnikov, I. A., and Entelis, N. (2008). **Two distinct structural elements of 5S rRNA are needed for its import into human mitochondria.** Rna *14*, 749–759.

Sottocasa, G. L., Kuylenstierna, B., Ernster, L., and Bergstrand, A. (1967). Methods Enzymol *10*, 448.

Stojanovski, D., Bragoszewski, P., and Chacinska, A. (2012). **The MIA pathway: A tight bond between protein transport and oxidative folding in mitochondria.** Biochimica et biophysica acta *1823*, 1142–1150.

Stojanovski, D., Guiard, B., Kozjak-Pavlovic, V., Pfanner, N., and Meisinger, C. (2007). **Alternative function for the mitochondrial SAM complex in biogenesis of alpha-helical TOM proteins.** The Journal of cell biology *179*, 881–893.

Sugiyama, T., Shimizu, S., Matsuoka, Y., Yoneda, Y., and Tsujimoto, Y. (2002). **Activation of mitochondrial voltage-dependent anion channel by apro-apoptotic BH3-only protein Bim.** Oncogene *21*, 4944–4956.

Summers, W. A. T., and Court, D. A. (2010). **Origami in outer membrane mimetics: correlating the first detailed images of refolded VDAC with over 20 years of biochemical data.** Biochemistry and cell biology = Biochimie et biologie cellulaire *88*, 425–438.

Suyama, Y. (1967). **The origins of mitochondrial ribonucleic acids in Tetrahymena pyriformis.** Biochemistry *6*, 2829–2839.

Suyama, Y., Wong, S., and Campbell, D. A. (1998). **Regulated tRNA import in Leishmania mitochondria.** Biochim Biophys Acta *1396*, 138–142.

Tan, T. H., Bochud-Allemann, N., Horn, E. K., and Schneider, A. (2002a). **Eukaryotic-type elongator tRNAMet of Trypanosoma brucei becomes formylated after import into mitochondria.** Proc Natl Acad Sci U S A *99*, 1152–1157.

Tan, T. H., Pach, R., Crausaz, A., Ivens, A., and Schneider, A. (2002b). **tRNAs in Trypanosoma brucei: genomic organization, expression, and mitochondrial import.** Mol Cell Biol *22*, 3707–3717.

Tarassov, I., Entelis, N., and Martin, R. (1995a). **Mitochondrial import of a cytoplasmic lysine-tRNA in yeast is mediated by cooperation of cytoplasmic and mitochondrial lysyl-tRNA synthetases.** EMBO J. *14*, 3461–3471.

Tarassov, I., Entelis, N., and Martin, R. P. (1995b). **An intact protein translocating machinery is required for mitochondrial import of a yeast cytoplasmic tRNA.** J Mol Biol *245*, 315–323.

Tarassov, I., Kamenski, P., Kolesnikova, O., Karicheva, O., Martin, R. P., Krasheninnikov, I. A., and Entelis, N. (2007). **Import of nuclear DNA-encoded RNAs into mitochondria and mitochondrial translation.** Cell Cycle *6*, 2473–2477.

Taylor, A. B., Smith, B. S., Kitada, S., Kojima, K., Miyaura, H., Otwinowski, Z., Ito, A., and Deisenhofer, J. (2001). **Crystal structures of mitochondrial processing peptidase reveal the mode for specific cleavage of import signal sequences.** Structure (London, England : 1993) *9*, 615–625.

Terziyska, N., Grumbt, B., Kozany, C., and Hell, K. (2009). **Structural and functional roles of the conserved cysteine residues of the redox-regulated import receptor Mia40 in the intermembrane space of mitochondria.** The Journal of biological chemistry *284*, 1353–1363.

Thinnes, F. P., Flörke, H., Winkelbach, H., Stadtmüller, U., Heiden, M., Karabinos, A., Hesse, D., Kratzin, H. D., Fleer, E., and Hilschmann, N. (1994). **Channel active mammalian porin, purified from crude membrane fractions of human B lymphocytes or bovine skeletal muscle, reversibly binds the stilbene-disulfonate group of the chloride channel blocker DIDS.** Biological chemistry Hoppe-Seyler *375*, 315–322.

Thomas, L., Blachly-Dyson, E., Colombini, M., and Forte, M. (1993). **Mapping of residues forming the voltage sensor of the voltage-dependent anion-selective channel.** Proceedings of the National Academy of Sciences of the United States of America *90*, 5446–5449.

Thornton, N., Stroud, D. A., Milenkovic, D., Guiard, B., Pfanner, N., and Becker, T. (2010). **Two modular forms of the mitochondrial sorting and assembly machinery are involved in biogenesis of alpha-helical outer membrane proteins.** Journal of molecular biology *396*, 540–549.

Tschopp, F., Charriere, F., and Schneider, A. (2011). **In vivo study in Trypanosoma brucei links mitochondrial transfer RNA import to mitochondrial protein import.** EMBO reports *12*, 825–832.

Ujwal, R., Cascio, D., Colletier, J.-P., Faham, S., Zhang, J., Toro, L., Ping, P., and Abramson, J. (2008). **The crystal structure of mouse VDAC1 at 2.3 A resolution reveals mechanistic insights into metabolite gating.** Proceedings of the National Academy of Sciences of the United States of America *105*, 17742–17747.

Vandamme, J., Castermans, D., and Thevelein, J. M. (2012). **Molecular mechanisms of feedback inhibition of protein kinase A on intracellular cAMP accumulation.** Cellular signalling *24*, 1610–1618.

Vinogradova, E., Salinas, T., Cognat, V., Remacle, C., and Marechal-Drouard, L. (2009). **Steady-state levels of imported tRNAs in Chlamydomonas mitochondria are correlated with both cytosolic and mitochondrial codon usages.** Nucleic Acids Res.

Vyssokikh, M. Y., and Brdiczka, D. (2003). **The function of complexes between the outer mitochondrial membrane pore (VDAC) and the adenine nucleotide translocase in regulation of energy metabolism and apoptosis.** Acta biochimica Polonica *50*, 389–404.

Vyssokikh, M. Y., Katz, A., Rueck, A., Wuensch, C., Dörner, A., Zorov, D. B., and Brdiczka, D. (2001). **Adenine nucleotide translocator isoforms 1 and 2 are differently distributed in the mitochondrial inner membrane and have distinct affinities to cyclophilin D.** The Biochemical journal *358*, 349–358.

Wagner, K., Gebert, N., Guiard, B., Brandner, K., Truscott, K. N., Wiedemann, N., Pfanner, N., and Rehling, P. (2008). **The assembly pathway of the mitochondrial carrier translocase involves four preprotein translocases.** Molecular and cellular biology *28*, 4251–4260.

Wang, G., Chen, H. W., Oktay, Y., Zhang, J., Allen, E. L., Smith, G. M., Fan, K. C., Hong, J. S., French, S. W., McCaffery, J. M., et al. (2010). **PNPASE Regulates RNA Import into Mitochondria.** Cell *142*, 456–467.

Webb, C. T., Gorman, M. A., Lazarou, M., Ryan, M. T., and Gulbis, J. M. (2006). **Crystal Structure of the Mitochondrial Chaperone TIM9•10 Reveals a Six-Bladed α-Propeller.** Molecular Cell *21*, 123–133.

Wiedemann, N., Kozjak, V., Chacinska, A., Schönfisch, B., Rospert, S., Ryan, M. T., Pfanner, N., and Meisinger, C. (2003). **Machinery for protein sorting and assembly in the mitochondrial outer membrane.** Nature *424*, 565–571.

Wiedemann, N., Pfanner, N., and Ryan, M. T. (2001). **The three modules of ADP/ATP carrier cooperate in receptor recruitment and translocation into mitochondria.** Embo J *20*, 951–60.

Wiedemann, N., Truscott, K. N., Pfannschmidt, S., Guiard, B., Meisinger, C., and Pfanner, N. (2004). **Biogenesis of the protein import channel Tom40 of the mitochondrial outer membrane: intermembrane space components are involved in an early stage of the assembly pathway.** The Journal of biological chemistry *279*, 18188–18194.

van Wilpe, S., Ryan, M. T., Hill, K., Maarse, A. C., Meisinger, C., Brix, J., Dekker, P. J., Moczko, M., Wagner, R., Meijer, M., et al. (1999). **Tom22 is a multifunctional organizer of the mitochondrial preprotein translocase.** Nature *401*, 485–489.

Wilson, J. E., and Chung, V. (1989). **Rat brain hexokinase: further studies on the specificity of the hexose and hexose 6-phosphate binding sites.** Archives of biochemistry and biophysics *269*, 517–525.

Wu, Y., and Sha, B. (2006). **Crystal structure of yeast mitochondrial outer membrane translocon member Tom70p.** Nature Structural & Molecular Biology *13*, 589–593.

Xu, X., Decker, W., Sampson, M. J., Craigen, W. J., and Colombini, M. (1999). **Mouse VDAC isoforms expressed in yeast: channel properties and their roles in mitochondrial outer membrane permeability.** The Journal of membrane biology *170*, 89–102.

Yamano, K., Tanaka-Yamano, S., and Endo, T. (2010). **Mdm10 as a dynamic constituent of the TOB/SAM complex directs coordinated assembly of Tom40.** EMBO reports *11*, 187–193.

Yamano, K., Yatsukawa, Y. -i., Esaki, M., Hobbs, A. E. A., Jensen, R. E., and Endo, T. (2007). **Tom20 and Tom22 Share the Common Signal Recognition Pathway in Mitochondrial Protein Import.** Journal of Biological Chemistry *283*, 3799–3807.

Yang, D., Oyaizu, Y., Oyaizu, H., Olsen, G. J., and Woese, C. R. (1985). **Mitochondrial origins.** Proceedings of the National Academy of Sciences of the United States of America *82*, 4443–4447.

Yermovsky-Kammerer, A. E., and Hajduk, S. L. (1999). **In vitro import of a nuclearly encoded tRNA into the mitochondrion of Trypanosoma brucei.** Mol Cell Biol *19*, 6253–9.

Yoshionari, S., Koike, T., Yokogawa, T., Nishikawa, K., Ueda, T., Miura, K., and Watanabe, K. (1994). **Existence of nuclear-encoded 5S-rRNA in bovine mitochondria.** FEBS Lett *338*, 137–142.

Young, J. C., Hoogenraad, N. J., and Hartl, F. U. (2003). **Molecular chaperones Hsp90 and Hsp70 deliver preproteins to the mitochondrial import receptor Tom70.** Cell *112*, 41–50.

Zara, V., Ferramosca, A., Robitaille-Foucher, P., Palmieri, F., and Young, J. C. (2009). **Mitochondrial carrier protein biogenesis: role of the chaperones Hsc70 and Hsp90.** The Biochemical journal *419*, 369–375.

Zeth, K. (2010). **Structure and evolution of mitochondrial outer membrane proteins of beta-barrel topology.** Biochimica et biophysica acta *1797*, 1292–1299.

Zizi, M., Byrd, C., Boxus, R., and Colombini, M. (1998). **The voltage-gating process of the voltage-dependent anion channel is sensitive to ion flow.** Biophysical journal *75*, 704–713.

Zizi, M., Forte, M., Blachly-Dyson, E., and Colombini, M. (1994). **NADH regulates the gating of VDAC, the mitochondrial outer membrane channel.** The Journal of biological chemistry *269*, 1614–1616.

Zoratti, M., Szabò, I., and De Marchi, U. (2005). **Mitochondrial permeability transitions: how many doors to the house?** Biochimica et biophysica acta *1706*, 40–52.

ANNEX

ANNEX

A) Measurements of oxygen consumption of *Saccharomyces cerevisiae* strains

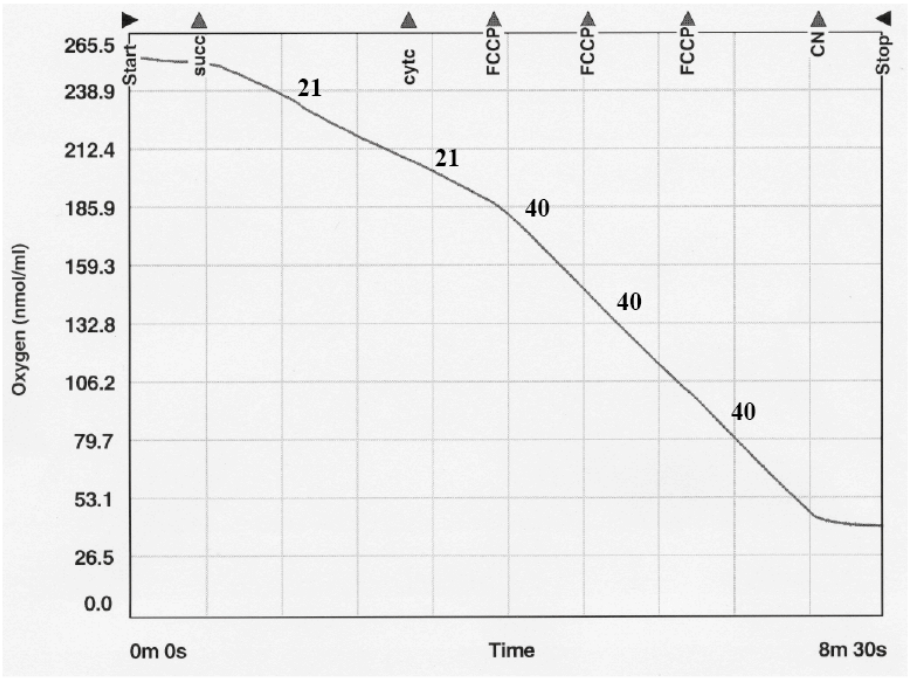

A.1 : Oxygen consumption of mitochondria isolated from a wild type strain. Representative plot illustrating oxygen consumption corresponding to 200µg of wild type mitochondria. Respiration rates are indicated in bold numbers for added chemical compounds. succ : succinate (10mM); cytc : cytochrome *c* (20µM); FCCP : carbonyl cyanide-4-(trifluoromethoxy)phenylhydrazone (5nM/addition); CN : potassium cyanide (2.5mM).

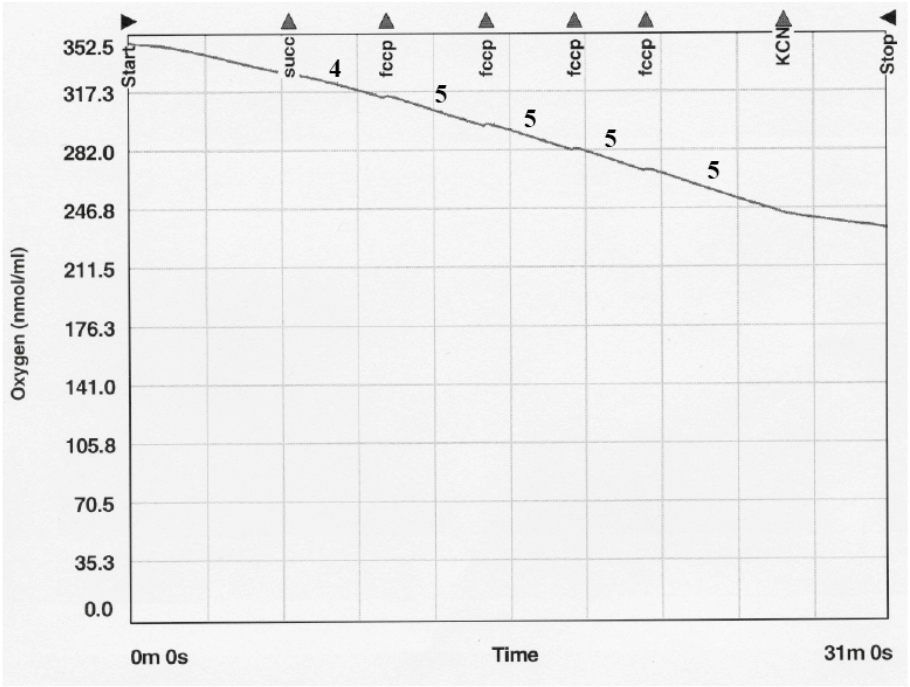

A.2 : Oxygen consumption of mitochondria isolated from a *por1*Δ strain. Representative plot illustrating oxygen consumption corresponding to 500µg of *por1*Δ mitochondria. Respiration rates are indicated in bold numbers for added chemical compounds. succ : succinate (10mM); FCCP : carbonyl cyanide-4-(trifluoromethoxy)phenylhydrazone (10nM/addition); CN : potassium cyanide (2mM).

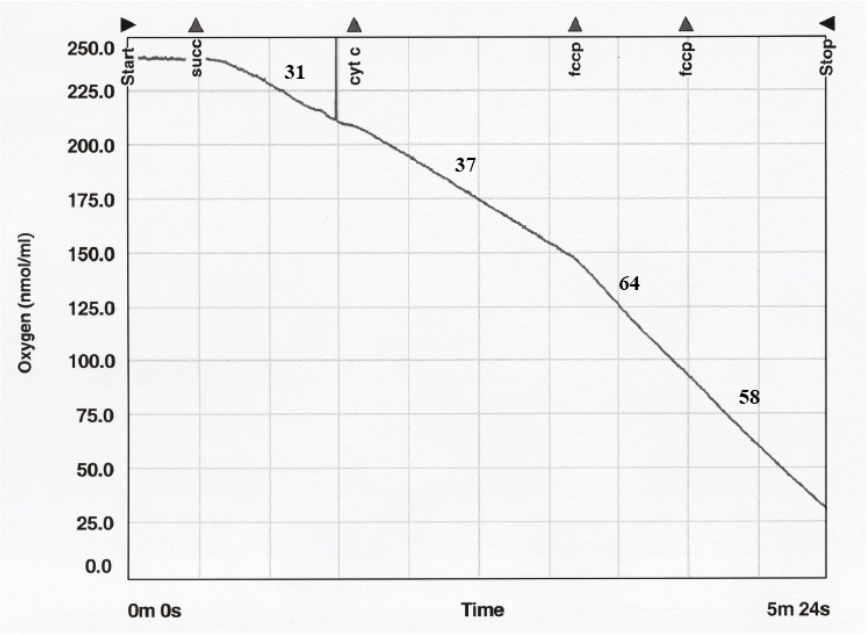

A.3 : Oxygen consumption of mitochondria isolated from a *por2*Δ strain. Representative plot illustrating oxygen consumption corresponding to 200µg of *por2*Δ mitochondria. Respiration rates are indicated in bold numbers for added chemical compounds. succ : succinate (10mM); cytc : cytochrome *c* (12,5µM); FCCP : carbonyl cyanide-4-(trifluoromethoxy)phenylhydrazone (0,2nM/addition).

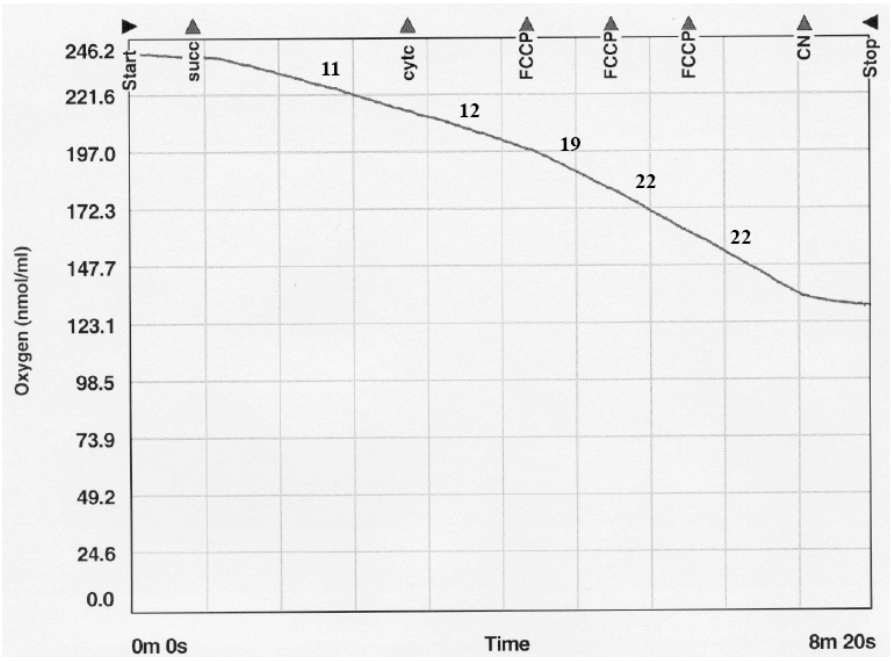

A.4 : Oxygen consumption of mitochondria isolated from a *tom5*Δ strain. Representative plot illustrating oxygen consumption corresponding to 200µg of *tom5*Δ mitochondria. Respiration rates are indicated in bold numbers for added chemical compounds. succ : succinate (10mM); cytc : cytochrome *c* (20µM); FCCP : carbonyl cyanide-4-(trifluoromethoxy)phenylhydrazone (5nM/addition); CN : potassium cyanide (2.5mM).

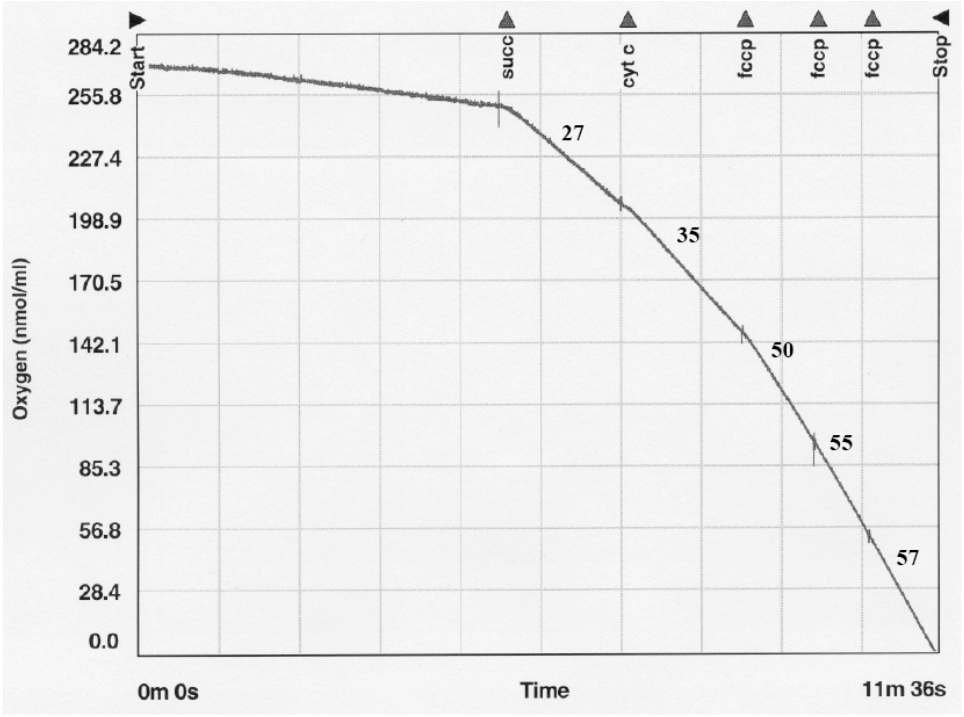

A.5 : Oxygen consumption of mitochondria isolated from a *tom6*Δ strain. Representative plot illustrating oxygen consumption corresponding to 200µg of *tom6*Δ mitochondria. Respiration rates are indicated in bold numbers for added chemical compounds. succ : succinate (5mM); cytc : cytochrome *c* (12.5µM); FCCP : carbonyl cyanide-4-(trifluoromethoxy)phenylhydrazone (5nM/addition).

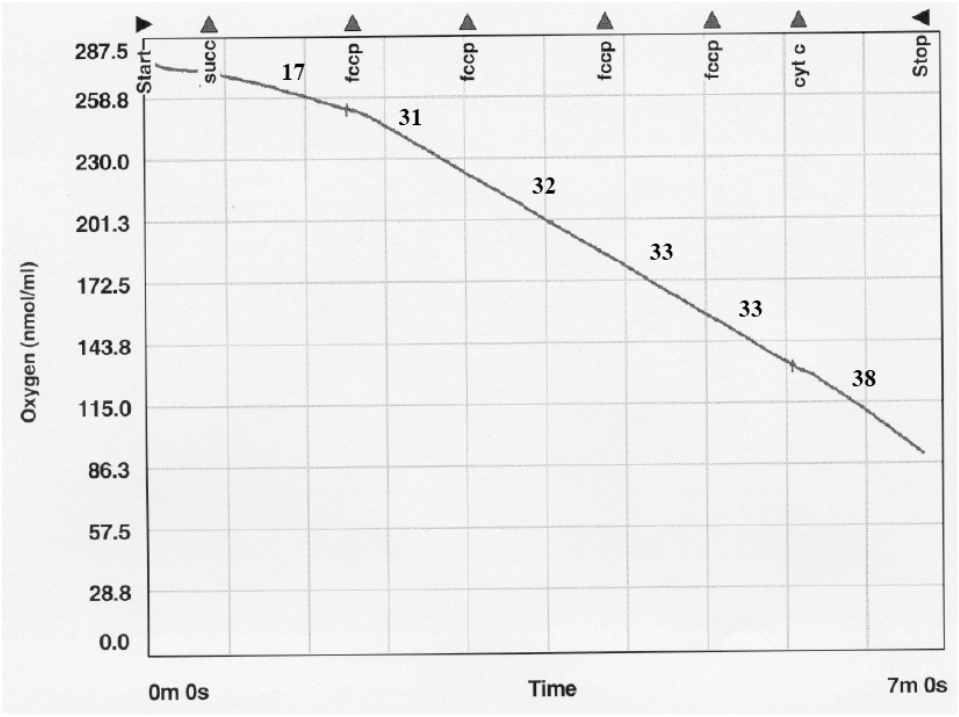

A.6 : Oxygen consumption of mitochondria isolated from a *tom7*Δ strain. Representative plot illustrating oxygen consumption corresponding to 200µg of *tom7*Δ mitochondria. Respiration rates are indicated in bold numbers for added chemical compounds. succ : succinate (5mM); cytc : cytochrome *c* (6µM); FCCP : carbonyl cyanide-4-(trifluoromethoxy)phenylhydrazone (5nM/addition).

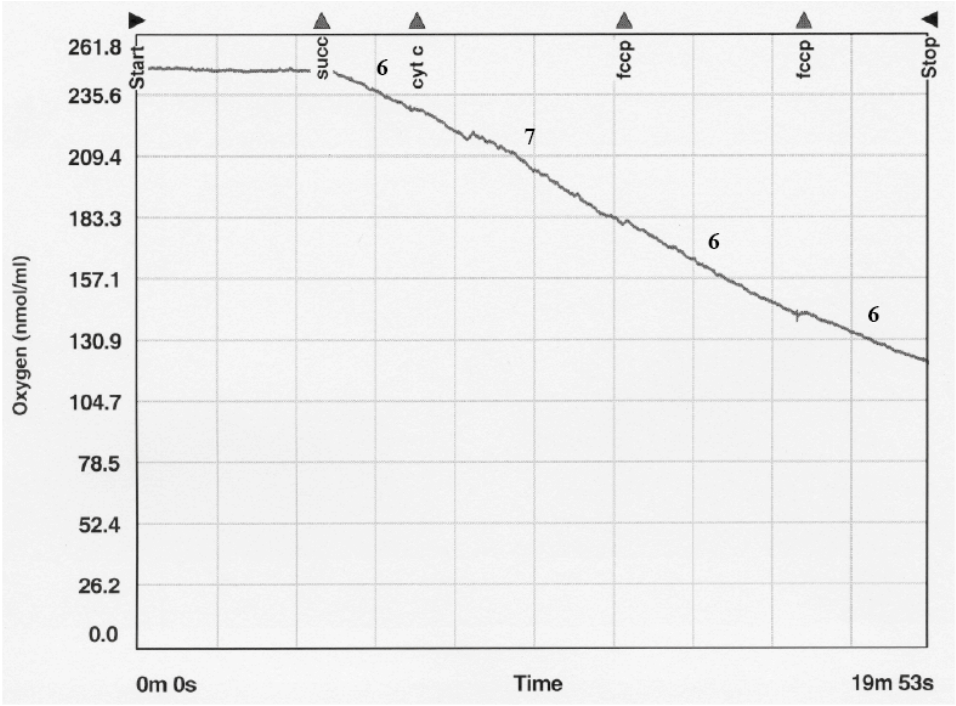

A.7 : Oxygen consumption of mitochondria isolated from a *tom20*Δ_{112} strain. Representative plot illustrating oxygen consumption corresponding to 200µg of *tom20*Δ_{112} mitochondria. Respiration rates are indicated in bold numbers for added chemical compounds. succ : succinate (10mM); cytc : cytochrome *c* (12.5µM); FCCP : carbonyl cyanide-4-(trifluoromethoxy)phenylhydrazone (5nM/addition).

B) Mass spectrometry parameters of proteins indentified by North-Western and CLIP analysis

Strain	Protein name (mass)	Identification probability	Number of unique peptides	Percentage of sequence coverage	Peptides sequence(s)
Wild type	TOM 5 (5,97kDa)	93,7%	1	30%	MFGLPQQEVSEEEKR
	VDAC 1 (30,41kDa)	100%	15	59,4%	AKQPVKDGPLSTNVEAK - DFYHATPAAFDVQTTTANGIK - DGPLSTNVEAK - GAFDLCLK - LEFANLTPGLK - LEFANLTPGLKNELITSLTPGVAK - LPNSNVNIEFATR - NELITSLTPGVAK - NINDLLNK - QLLRPGVTLGVGSSFDALK - SAVLNTTFTQPFFTAR - SPPVYSDISR - VSDSGIVTLAYK - YAMALSYFAK - YLPDASSQVK
	AIM 37 (26,96kDa)	99,5%	2	56,6%	DAEILAK - LGNDDEVILFR - LNQAEVVAVGPGFTDANGNKVVPQVK - VGDQVLIPQFGGSTIK
	PHB 2 (34,4kDa)	66,2%	1	11,6%	TLGQDYDER
	HSP 10 (11,37kDa)	99,5%	2	56,6%	DAEILAK - LGNDDEVILFR - LNQAEVVAVGPGFTDANGNKVVPQVK - VGDQVLIPQFGGSTIK
	PET 9 (34,43kDa)	80,5%	1	2,83%	SDGVAGLYR
	MIR 1 (32,8kDa)	100%	6	26%	APGQSTVGLLAQLAK - ASEFYYGFAGPK - EEGIGSFYSGFTPILFK - FFIDNLGYDTASR - IQLEPTVYNK - QLGFFGSFAGLPTR
*por1*Δ	TOM 20 (20,3kDa)	99,8%	2	16,4%	ALTVYPQPADLLGIYQR - EATFTTNVENGER
	TOM 22 (20,3kDa)	99,9%	3	24,3%	IVALK - QTISNFFGFTSSFVR - TFDLQSDANNILAQGEK
	TOM 40 (42kDa)	99,1%	2	10,3%	SAPTPLAEASQIPTIPALSPLTAK - TDGSAPGDAGVSYLTR
	PHB 1 (31,43kDa)	77,9%	2	7,67%	AIIYDVR - SIVAQFDAAELITQR
	TIM 50 (55,1kDa)		1	2,52%	
	MIR 1 (32,8kDa)	100%	14	59,5%	APGQSTVGLLAQLAK - ASEFYYGFAGPK - EEGIGSFYSGFTPILFK - FALAGAIGCGSTHSSMVPIDVVK - FFIDNLGYDTASR - FGGYEVFK - FGGYEVFKK - FLVFER - GMVGSFK - IQLEPTVYNK - LVSQPQFANGLVGGFSR - QIPYNIAK - QLGFFGSFAGLPTR - STLGCPPTIEIGGGGH - SVSAAPAIPQYSVSDYMK
	PET 9 (34,43kDa)	99,8%	3	11,3%	GFLPSVVGIVVYR - LLIQNQDEMLK - YFPTQALNFAFK

B.1 :Table illustrating mass spectrometry parameters of proteins identified by North-Western analysis.

B.2 : Table illustrating mass spectrometry parameters of proteins identified by CLIP analysis.

peptide number	Identification	Mw (kDa)	pI	N°Access	Score Mascot	Erreur (ppm)
12	**Lysyl-tRNA synthetase, mitochondrial OS=Saccharomyces cerevisiae (strain ATCC 204508 / S288c) GN=MSK1 PE=1 SV=3**	66.1	9.7	**SYKM_YEAST**	332.9	3.10
2	ATP-dependent RNA helicase DED1 OS=Saccharomyces cerevisiae (strain ATCC 204508 / S288c) GN=DED1 PE=1 SV=2	65.5	8.6	DED1_YEAST	60.7	5.99
10	**ATP synthase subunit alpha, mitochondrial OS=Saccharomyces cerevisiae (strain ATCC 204508 / S288c) GN=ATP1 PE=1 SV=5**	58.6	9.5	**ATPA_YEAST**	290.8	4.25
8	Phosphatidylinositol 4,5-bisphosphate-binding protein SLM1 OS=Saccharomyces cerevisiae (strain ATCC 204508 / S288c) GN=SLM1 PE=1 SV=1	77.9	8.5	SLM1_YEAST	245.2	3.22
5	**External NADH-ubiquinone oxidoreductase 1, mitochondrial OS=Saccharomyces cerevisiae (strain ATCC 204508 / S288c) GN=NDE1 PE=1 SV=1**	62.7	9.7	**NDH1_YEAST**	127.8	2.15
2	ATP-dependent RNA helicase DED1 OS=Saccharomyces cerevisiae (strain ATCC 204508 / S288c) GN=DED1 PE=1 SV=2	65.5	8.6	DED1_YEAST	63.0	4.49
41	**ADP,ATP carrier protein 2 OS=Saccharomyces cerevisiae (strain ATCC 204508 / S288c) GN=PET9 PE=1 SV=2**	34.4	10.3	**ADT2_YEAST**	957.6	3.59
22	Phosphomannomutase OS=Saccharomyces cerevisiae (strain ATCC 204508 / S288c) GN=SEC53 PE=1 SV=1	29.0	5.0	PMM_YEAST	615.5	3.78
17	Dihydrolipoyllysine-residue succinyltransferase component of 2-oxoglutarate dehydrogenase complex, mitochondrial OS=Saccharomyces cerevisiae (strain A	50.4	9.4	ODO2_YEAST	468.8	3.38
16	**Mitochondrial outer membrane protein porin 1 OS=Saccharomyces cerevisiae (strain ATCC 204508 / S288c) GN=POR1 PE=1 SV=4**	30.4	8.8	**VDAC1_YEAST**	496.6	4.21
13	40S ribosomal protein S3 OS=Saccharomyces cerevisiae (strain ATCC 204508 / S288c) GN=RPS3 PE=1 SV=5	26.5	9.9	RS3_YEAST	357.7	6.40
12	**Mitochondrial homologous recombination protein 1 OS=Saccharomyces cerevisiae (strain ATCC 204508 / S288c) GN=MHR1 PE=1 SV=1**	26.9	10.1	**MHR1_YEAST**	329.1	3.53
10	**Prohibitin-1 OS=Saccharomyces cerevisiae (strain ATCC 204508 / S288c) GN=PHB1 PE=1 SV=2**	31.4	8.9	**PHB1_YEAST**	259.3	3.34
9	60S ribosomal protein L2-A OS=Saccharomyces cerevisiae (strain ATCC 204508 / S288c) GN=RPL2A PE=1 SV=1	27.4	11.6	RL2A_YEAST	210.6	2.38
8	**Mitochondrial genome maintenance protein MGM101 OS=Saccharomyces cerevisiae (strain ATCC 204508 / S288c) GN=MGM101 PE=1 SV=1**	30.1	10.1	**MG101_YEAST**	256.0	4.05
7	**Protein SCO1, mitochondrial OS=Saccharomyces cerevisiae (strain ATCC 204508 / S288c) GN=SCO1 PE=1 SV=1**	33.1	9.7	**SCO1_YEAST**	120.5	4.26
7	**Mitochondrial DNA replication protein YHM2 OS=Saccharomyces cerevisiae (strain ATCC 204508 / S288c) GN=YHM2 PE=1 SV=1**	34.2	10.4	**YHM2_YEAST**	124.5	8.68
6	**Uncharacterized mitochondrial membrane protein FMP10 OS=Saccharomyces cerevisiae (strain ATCC 204508 / S288c) GN=FMP10 PE=1 SV=1**	27.7	10.1	**FMP10_YEAST**	176.8	2.73
6	60S ribosomal protein L8-B OS=Saccharomyces cerevisiae (strain ATCC 204508 / S288c) GN=RPL8B PE=1 SV=3	28.1	10.5	RL8B_YEAST	174.3	2.20
6	60S ribosomal protein L15-B OS=Saccharomyces cerevisiae (strain ATCC 204508 / S288c) GN=RPL15B PE=1 SV=2	24.4	11.9	RL15B_YEAST	145.6	2.29
6	54S ribosomal protein L1, mitochondrial OS=Saccharomyces cerevisiae (strain ATCC 204508 / S288c) GN=MRPL1 PE=1 SV=1	31.0	10.5	RM01_YEAST	166.9	4.46
5	**Succinate dehydrogenase [ubiquinone] iron-sulfur subunit, mitochondrial OS=Saccharomyces cerevisiae (strain ATCC 204508 / S288c) GN=SDH2**	30.2	10.1	**DHSB_YEAST**	129.4	3.81
5	**Mitochondrial phosphate carrier protein OS=Saccharomyces cerevisiae (strain ATCC 204508 / S288c) GN=MIR1 PE=1 SV=1**	32.8	0.0	**MPCP_YEAST**	137.4	4.37
5	Elongation factor 2 OS=Saccharomyces cerevisiae (strain ATCC 204508 / S288c) GN=EFT1 PE=1 SV=1	93.2	5.9	EF2_YEAST	83.1	4.18
5	40S ribosomal protein S5 OS=Saccharomyces cerevisiae (strain ATCC 204508 / S288c) GN=RPS5 PE=1 SV=3	25.0	9.4	RS5_YEAST	186.0	4.61
4	**Succinate/fumarate mitochondrial transporter OS=Saccharomyces cerevisiae (strain ATCC 204508 / S288c) GN=SFC1 PE=1 SV=2**	35.3	10.3	**SFC1_YEAST**	129.9	4.02
4	**Mitochondrial import receptor subunit TOM40 OS=Saccharomyces cerevisiae (strain ATCC 204508 / S288c) GN=TOM40 PE=1 SV=1**	42.0	5.2	**TOM40_YEAST**	126.9	5.50
4	**Lysyl-tRNA synthetase, mitochondrial OS=Saccharomyces cerevisiae (strain ATCC 204508 / S288c) GN=MSK1 PE=1 SV=3**	66.1	9.7	**SYKM_YEAST**	101.0	4.55
4	**37S ribosomal protein S9, mitochondrial OS=Saccharomyces cerevisiae (strain ATCC 204508 / S288c) GN=MRPS9 PE=1 SV=1**	31.9	10.6	**RT09_YEAST**	112.9	3.15
3	**Uncharacterized protein YNR040W OS=Saccharomyces cerevisiae (strain ATCC 204508 / S288c) GN=YNR040W PE=1 SV=1**	28.6	10.7	**YN8O_YEAST**	87.0	5.47
3	GTP-binding protein RHO3 OS=Saccharomyces cerevisiae (strain ATCC 204508 / S288c) GN=RHO3 PE=1 SV=2	25.3	4.7	RHO3_YEAST	90.0	2.12
2	**Pyruvate dehydrogenase E1 component subunit beta, mitochondrial OS=Saccharomyces cerevisiae (strain ATCC 204508 / S288c) GN=PDB1 PE=1**	40.0	5.1	**ODPB_YEAST**	72.8	2.48
2	N-terminal acetyltransferase 2 OS=Saccharomyces cerevisiae (strain ATCC 204508 / S288c) GN=NAT2 PE=1 SV=2	32.8	10.5	NAT2_YEAST	93.8	7.75
2	**Ketol-acid reductoisomerase, mitochondrial OS=Saccharomyces cerevisiae (strain ATCC 204508 / S288c) GN=ILV5 PE=1 SV=1**	44.3	9.6	**ILV5_YEAST**	58.8	2.61
2	GTP-binding nuclear protein GSP1/CNR1 OS=Saccharomyces cerevisiae (strain ATCC 204508 / S288c) GN=GSP1 PE=1 SV=1	24.8	6.1	GSP1_YEAST	64.2	1.84
2	**Carrier protein YMC1, mitochondrial OS=Saccharomyces cerevisiae (strain ATCC 204508 / S288c) GN=YMC1 PE=1 SV=2**	33.4	10.2	**YMC1_YEAST**	64.6	4.41
2	**ATP synthase subunit beta, mitochondrial OS=Saccharomyces cerevisiae (strain ATCC 204508 / S288c) GN=ATP2 PE=1 SV=2**	54.8	5.4	**ATPB_YEAST**	52.0	3.05
2	**2-oxoglutarate dehydrogenase, mitochondrial OS=Saccharomyces cerevisiae (strain ATCC 204508 / S288c) GN=KGD1 PE=1 SV=2**	114.3	6.8	**ODO1_YEAST**	42.6	1.16
1	**Glyceraldehyde-3-phosphate dehydrogenase 3 OS=Saccharomyces cerevisiae (strain ATCC 204508 / S288c) GN=TDH3 PE=1 SV=3**	35.7	6.5	**G3P3_YEAST**	51.0	6.11
1	60S ribosomal protein L9-A OS=Saccharomyces cerevisiae (strain ATCC 204508 / S288c) GN=RPL9A PE=1 SV=2	21.6	10.2	RL9A_YEAST	50.3	10.16
11	60S ribosomal protein L36-B OS=Saccharomyces cerevisiae (strain ATCC 204508 / S288c) GN=RPL36B PE=1 SV=3	11.1	12.1	RL36B_YEAST	391.5	4.37
9	60S ribosomal protein L25 OS=Saccharomyces cerevisiae (strain ATCC 204508 / S288c) GN=RPL25 PE=1 SV=4	15.7	10.5	RL25_YEAST	250.9	5.44
6	Pyruvate kinase 1 OS=Saccharomyces cerevisiae (strain ATCC 204508 / S288c) GN=CDC19 PE=1 SV=2	54.5	8.6	KPYK1_YEAST	163.8	3.45
6	60S ribosomal protein L43-A OS=Saccharomyces cerevisiae (strain ATCC 204508 / S288c) GN=RPL43A PE=1 SV=1	10.1	11.8	RL43A_YEAST	128.4	2.59
6	**54S ribosomal protein IMG2, mitochondrial OS=Saccharomyces cerevisiae (strain ATCC 204508 / S288c) GN=IMG2 PE=1 SV=2**	16.4	10.6	**IMG2_YEAST**	157.8	2.26
5	**Mitochondrial outer membrane protein porin 1 OS=Saccharomyces cerevisiae (strain ATCC 204508 / S288c) GN=POR1 PE=1 SV=4**	30.4	8.8	**VDAC1_YEAST**	170.5	3.91
5	40S ribosomal protein S16-A OS=Saccharomyces cerevisiae (strain ATCC 204508 / S288c) GN=RPS16A PE=1 SV=1	15.8	10.7	RS16A_YEAST	100.3	1.29
4	**Mitochondrial organizing structure protein 1 OS=Saccharomyces cerevisiae (strain ATCC 204508 / S288c) GN=MOS1 PE=1 SV=1**	10.4	10.7	**MOS1_YEAST**	165.8	3.19
4	**Altered inheritance of mitochondria protein 5, mitochondrial OS=Saccharomyces cerevisiae (strain RM11-1a) GN=AIM5 PE=3 SV=1**	12.4	9.0	**AIM5_YEAS1**	83.5	3.88

B.2 : Table illustrating mass spectrometry parameters of proteins identified by CLIP analysis.

4	**ADP,ATP carrier protein 2 OS=Saccharomyces cerevisiae (strain ATCC 204508 / S288c) GN=PET9 PE=1 SV=2**	34.4	10.3	ADT2_YEAST	143.2	4.78
3	Histone H4 OS=Saccharomyces cerevisiae (strain ATCC 204508 / S288c) GN=HHF1 PE=1 SV=2	11.4	11.8	H4_YEAST	124.6	2.50
2	**Succinate/fumarate mitochondrial transporter OS=Saccharomyces cerevisiae (strain ATCC 204508 / S288c) GN=SFC1 PE=1 SV=2**	35.3	10.3	**SFC1_YEAST**	39.7	5.78
2	60S ribosomal protein L26-A OS=Saccharomyces cerevisiae (strain ATCC 204508 / S288c) GN=RPL26A PE=1 SV=3	14.2	11.0	RL26A_YEAST	59.7	1.77
2	60S ribosomal protein L20-A OS=Saccharomyces cerevisiae (strain ATCC 204508 / S288c) GN=RPL20A PE=1 SV=1	20.4	10.7	RL20A_YEAST	46.5	3.05
1	**Cytochrome c oxidase subunit 6, mitochondrial OS=Saccharomyces cerevisiae (strain ATCC 204508 / S288c) GN=COX6 PE=1 SV=1**	17.3	5.7	**COX6_YEAST**	30.4	0.70
1	60S ribosomal protein L13-B OS=Saccharomyces cerevisiae (strain ATCC 204508 / S288c) GN=RPL13B PE=1 SV=1	22.5	11.6	RL13B_YEAST	35.4	1.48
70	**Dihydrolipoyl dehydrogenase, mitochondrial OS=Saccharomyces cerevisiae (strain ATCC 204508 / S288c) GN=LPD1 PE=1 SV=1**	54.0	8.9	**DLDH_YEAST**	2046.0	4.73
24	**External NADH-ubiquinone oxidoreductase 1, mitochondrial OS=Saccharomyces cerevisiae (strain ATCC 204508 / S288c) GN=NDE1 PE=1 SV=1**	62.7	9.7	**NDH1_YEAST**	567.7	3.64
16	**ATP synthase subunit alpha, mitochondrial OS=Saccharomyces cerevisiae (strain ATCC 204508 / S288c) GN=ATP1 PE=1 SV=5**	58.6	9.5	**ATPA_YEAST**	500.5	4.66
12	**Rotenone-insensitive NADH-ubiquinone oxidoreductase, mitochondrial OS=Saccharomyces cerevisiae (strain ATCC 204508 / S288c) GN=NDI1 PE=**	57.2	9.8	**NDI1_YEAST**	313.6	6.21
10	Phosphatidylinositol 4,5-bisphosphate-binding protein SLM1 OS=Saccharomyces cerevisiae (strain ATCC 204508 / S288c) GN=SLM1 PE=1 SV=1	77.9	8.5	SLM1_YEAST	247.3	5.88
8	Elongation factor 2 OS=Saccharomyces cerevisiae (strain ATCC 204508 / S288c) GN=EFT1 PE=1 SV=1	93.2	5.9	EF2_YEAST	182.6	3.38
7	Plasma membrane ATPase 1 OS=Saccharomyces cerevisiae (strain ATCC 204508 / S288c) GN=PMA1 PE=1 SV=2	99.6	4.8	PMA1_YEAST	144.8	6.76
7	ATP-dependent RNA helicase DED1 OS=Saccharomyces cerevisiae (strain ATCC 204508 / S288c) GN=DED1 PE=1 SV=2	65.5	8.6	DED1_YEAST	250.0	5.67
7	**ADP,ATP carrier protein 2 OS=Saccharomyces cerevisiae (strain ATCC 204508 / S288c) GN=PET9 PE=1 SV=2**	34.4	10.3	**ADT2_YEAST**	172.2	5.24
6	**Asparaginyl-tRNA synthetase, mitochondrial OS=Saccharomyces cerevisiae (strain ATCC 204508 / S288c) GN=SLM5 PE=1 SV=1**	56.7	9.4	**SYNM_YEAST**	197.6	5.17
5	**Lysyl-tRNA synthetase, mitochondrial OS=Saccharomyces cerevisiae (strain ATCC 204508 / S288c) GN=MSK1 PE=1 SV=3**	66.1	9.7	**SYKM_YEAST**	94.4	4.45
5	**ATPase expression protein 2, mitochondrial OS=Saccharomyces cerevisiae (strain ATCC 204508 / S288c) GN=AEP2 PE=1 SV=3**	67.5	10.2	**AEP2_YEAST**	122.1	5.38
4	Protoporphyrinogen oxidase OS=Saccharomyces cerevisiae (strain ATCC 204508 / S288c) GN=HEM14 PE=1 SV=1	59.7	9.9	PPOX_YEAST	58.7	0.34
4	**Mitochondrial outer membrane protein porin 1 OS=Saccharomyces cerevisiae (strain ATCC 204508 / S288c) GN=POR1 PE=1 SV=4**	30.4	8.8	**VDAC1_YEAST**	121.2	4.61
4	**37S ribosomal protein NAM9, mitochondrial OS=Saccharomyces cerevisiae (strain ATCC 204508 / S288c) GN=NAM9 PE=1 SV=2**	56.3	10.1	**NAM9_YEAST**	137.0	7.28
3	**Dihydroxy-acid dehydratase, mitochondrial OS=Saccharomyces cerevisiae (strain ATCC 204508 / S288c) GN=ILV3 PE=1 SV=2**	62.8	8.8	**ILV3_YEAST**	90.6	4.33
2	V-type proton ATPase subunit B OS=Saccharomyces cerevisiae (strain ATCC 204508 / S288c) GN=VMA2 PE=1 SV=2	57.7	4.8	VATB_YEAST	39.6	1.53
2	Serine/threonine-protein kinase RIO2 OS=Saccharomyces cerevisiae (strain ATCC 204508 / S288c) GN=RIO2 PE=1 SV=1	49.1	5.0	RIO2_YEAST	66.0	5.81
2	Pyruvate decarboxylase isozyme 1 OS=Saccharomyces cerevisiae (strain ATCC 204508 / S288c) GN=PDC1 PE=1 SV=7	61.5	5.8	PDC1_YEAST	34.4	2.35
2	**Protein TOM71 OS=Saccharomyces cerevisiae (strain ATCC 204508 / S288c) GN=TOM71 PE=1 SV=1**	71.8	5.8	**TOM71_YEAST**	59.5	1.97
2	Protein STB2 OS=Saccharomyces cerevisiae (strain ATCC 204508 / S288c) GN=STB2 PE=1 SV=2	97.8	6.2	STB2_YEAST	33.4	11.90
2	Histone H2A.Z OS=Saccharomyces cerevisiae (strain ATCC 204508 / S288c) GN=HTZ1 PE=1 SV=3	14.3	11.1	H2AZ_YEAST	49.7	2.16
2	Hexokinase-1 OS=Saccharomyces cerevisiae (strain ATCC 204508 / S288c) GN=HXK1 PE=1 SV=2	53.7	5.2	HXKA_YEAST	42.5	3.86
1	**Aconitate hydratase, mitochondrial OS=Saccharomyces cerevisiae (strain ATCC 204508 / S288c) GN=ACO1 PE=1 SV=2**	85.3	8.9	**ACON_YEAST**	47.7	13.79
1	**ATP synthase subunit beta, mitochondrial OS=Saccharomyces cerevisiae (strain ATCC 204508 / S288c) GN=ATP2 PE=1 SV=2**	54.8	5.4	**ATPB_YEAST**	69.4	9.19
22	**Serine hydroxymethyltransferase, mitochondrial OS=Saccharomyces cerevisiae (strain ATCC 204508 / S288c) GN=SHM1 PE=1 SV=2**	53.7	9.4	**GLYM_YEAST**	606.6	5.01
14	**ATP synthase subunit alpha, mitochondrial OS=Saccharomyces cerevisiae (strain ATCC 204508 / S288c) GN=ATP1 PE=1 SV=5**	58.6	9.5	**ATPA_YEAST**	519.4	6.92
8	**Aconitate hydratase, mitochondrial OS=Saccharomyces cerevisiae (strain ATCC 204508 / S288c) GN=ACO1 PE=1 SV=2**	85.3	8.9	**ACON_YEAST**	224.7	7.75
7	Phosphatidylinositol 4,5-bisphosphate-binding protein SLM1 OS=Saccharomyces cerevisiae (strain ATCC 204508 / S288c) GN=SLM1 PE=1 SV=1	77.9	8.5	SLM1_YEAST	252.2	5.32
5	**Threonyl-tRNA synthetase, mitochondrial OS=Saccharomyces cerevisiae (strain ATCC 204508 / S288c) GN=MST1 PE=1 SV=2**	54.1	9.3	**SYTM_YEAST**	103.7	4.64
4	Plasma membrane ATPase 1 OS=Saccharomyces cerevisiae (strain ATCC 204508 / S288c) GN=PMA1 PE=1 SV=2	99.6	4.8	PMA1_YEAST	142.1	7.37
4	**Aldehyde dehydrogenase 5, mitochondrial OS=Saccharomyces cerevisiae (strain YJM789) GN=ALD5 PE=3 SV=1**	56.7	9.1	**ALDH5_YEAS7**	78.7	5.09
3	RuvB-like protein 1 OS=Saccharomyces cerevisiae (strain ATCC 204508 / S288c) GN=RVB1 PE=1 SV=1	50.4	5.6	RUVB1_YEAST	88.4	8.28
3	**Mitochondrial outer membrane protein porin 1 OS=Saccharomyces cerevisiae (strain ATCC 204508 / S288c) GN=POR1 PE=1 SV=4**	30.4	8.8	**VDAC1_YEAST**	54.5	7.70
3	Dihydrolipoyl dehydrogenase, mitochondrial OS=Saccharomyces cerevisiae (strain ATCC 204508 / S288c) GN=LPD1 PE=1 SV=1	54.0	8.9	DLDH_YEAST	125.0	9.15
3	**ATPase expression protein 1, mitochondrial OS=Saccharomyces cerevisiae (strain AWRI1631) GN=AEP1 PE=3 SV=1**	59.5	9.9	**AEP1_YEAS6**	88.1	5.31
3	ATP-dependent RNA helicase DED1 OS=Saccharomyces cerevisiae (strain ATCC 204508 / S288c) GN=DED1 PE=1 SV=2	65.5	8.6	DED1_YEAST	85.3	5.66
2	**Mitochondrial respiratory chain complexes assembly protein AFG3 OS=Saccharomyces cerevisiae (strain ATCC 204508 / S288c) GN=AFG3 PE=1 S**	84.5	9.7	**AFG3_YEAST**	33.0	5.03
2	Elongation factor 1-alpha 1 OS=Trypanosoma brucei brucei (strain 927/4 GUTat10.1) GN=TEF1 PE=1 SV=1	49.1	9.7	EF1A1_TRYB2	58.9	2.87
2	**ATP synthase subunit beta, mitochondrial OS=Saccharomyces cerevisiae (strain ATCC 204508 / S288c) GN=ATP2 PE=1 SV=2**	54.8	5.4	**ATPB_YEAST**	64.8	6.09
1	**Potassium-activated aldehyde dehydrogenase, mitochondrial OS=Saccharomyces cerevisiae (strain ATCC 204508 / S288c) GN=ALD4 PE=1 SV=2**	56.7	6.3	**ALDH4_YEAST**	58.8	10.50
11	**ADP,ATP carrier protein 2 OS=Saccharomyces cerevisiae (strain ATCC 204508 / S288c) GN=PET9 PE=1 SV=2**	34.4	10.3	**ADT2_YEAST**	256.1	7.97
9	**Dihydrolipoyllysine-residue succinyltransferase component of 2-oxoglutarate dehydrogenase complex, mitochondrial OS=Saccharomyces cerevis**	50.4	9.4	**ODO2_YEAST**	141.8	3.38
4	**Uncharacterized mitochondrial membrane protein FMP10 OS=Saccharomyces cerevisiae (strain ATCC 204508 / S288c) GN=FMP10 PE=1 SV=1**	27.7	10.1	**FMP10_YEAST**	145.6	8.83
4	**Mitochondrial homologous recombination protein 1 OS=Saccharomyces cerevisiae (strain ATCC 204508 / S288c) GN=MHR1 PE=1 SV=1**	26.9	10.1	**MHR1_YEAST**	98.3	5.36

B.2 : Table illustrating mass spectrometry parameters of proteins identified by CLIP analysis.

4	**Mitochondrial genome maintenance protein MGM101 OS=Saccharomyces cerevisiae (strain ATCC 204508 / S288c) GN=MGM101 PE=1 SV=1**	30.1	10.1	**MG101_YEAST**	114.7	5.56
4	**37S ribosomal protein S9, mitochondrial OS=Saccharomyces cerevisiae (strain ATCC 204508 / S288c) GN=MRPS9 PE=1 SV=1**	31.9	10.6	**RT09_YEAST**	116.5	6.68
2	**Mitochondrial outer membrane protein porin 1 OS=Saccharomyces cerevisiae (strain ATCC 204508 / S288c) GN=POR1 PE=1 SV=4**	30.4	8.8	**VDAC1_YEAST**	33.7	6.60
2	**Mitochondrial DNA replication protein YHM2 OS=Saccharomyces cerevisiae (strain ATCC 204508 / S288c) GN=YHM2 PE=1 SV=1**	34.2	10.4	**YHM2_YEAST**	40.6	4.35
2	40S ribosomal protein S5 OS=Saccharomyces cerevisiae (strain ATCC 204508 / S288c) GN=RPS5 PE=1 SV=3	25.0	9.4	RS5_YEAST	38.1	1.39
1	Transposon Ty1-ER1 Gag polyprotein OS=Saccharomyces cerevisiae (strain ATCC 204508 / S288c) GN=TY1A-ER1 PE=2 SV=1	48.9	8.6	YE11A_YEAST	47.1	1.56
1	Actin OS=Saccharomyces cerevisiae (strain ATCC 204508 / S288c) GN=ACT1 PE=1 SV=1	41.7	5.4	ACT_YEAST	69.2	4.18
1	**54S ribosomal protein L1, mitochondrial OS=Saccharomyces cerevisiae (strain ATCC 204508 / S288c) GN=MRPL1 PE=1 SV=1**	31.0	10.5	**RM01_YEAST**	44.3	2.08
42	**Dihydrolipoyl dehydrogenase, mitochondrial OS=Saccharomyces cerevisiae (strain ATCC 204508 / S288c) GN=LPD1 PE=1 SV=1**	54.0	8.9	**DLDH_YEAST**	1072.4	8.06
22	**37S ribosomal protein NAM9, mitochondrial OS=Saccharomyces cerevisiae (strain ATCC 204508 / S288c) GN=NAM9 PE=1 SV=2**	56.3	10.1	**NAM9_YEAST**	579.6	8.04
21	Phosphatidylinositol 4,5-bisphosphate-binding protein SLM1 OS=Saccharomyces cerevisiae (strain ATCC 204508 / S288c) GN=SLM1 PE=1 SV=1	77.9	8.5	SLM1_YEAST	490.1	7.96
16	**External NADH-ubiquinone oxidoreductase 1, mitochondrial OS=Saccharomyces cerevisiae (strain ATCC 204508 / S288c) GN=NDE1 PE=1 SV=1**	62.7	9.7	**NDH1_YEAST**	414.8	8.26
16	**ATP synthase subunit alpha, mitochondrial OS=Saccharomyces cerevisiae (strain ATCC 204508 / S288c) GN=ATP1 PE=1 SV=5**	58.6	9.5	**ATPA_YEAST**	560.8	9.03
10	Plasma membrane ATPase 1 OS=Saccharomyces cerevisiae (strain ATCC 204508 / S288c) GN=PMA1 PE=1 SV=2	99.6	4.8	PMA1_YEAST	295.6	9.89
9	ATP-dependent RNA helicase DED1 OS=Saccharomyces cerevisiae (strain ATCC 204508 / S288c) GN=DED1 PE=1 SV=2	65.5	8.6	DED1_YEAST	232.3	9.47
7	**Rotenone-insensitive NADH-ubiquinone oxidoreductase, mitochondrial OS=Saccharomyces cerevisiae (strain ATCC 204508 / S288c) GN=NDI1 PE=**	57.2	9.8	**NDI1_YEAST**	149.0	5.57
7	**Dihydrolipoyllysine-residue succinyltransferase component of 2-oxoglutarate dehydrogenase complex, mitochondrial OS=Saccharomyces cerevis**	50.4	9.4	**ODO2_YEAST**	195.9	9.85
5	High-affinity hexose transporter HXT6 OS=Saccharomyces cerevisiae (strain ATCC 204508 / S288c) GN=HXT7 PE=1 SV=1	62.7	8.8	HXT7_YEAST	123.9	5.61
5	**Dihydroxy-acid dehydratase, mitochondrial OS=Saccharomyces cerevisiae (strain ATCC 204508 / S288c) GN=ILV3 PE=1 SV=2**	62.8	8.8	**ILV3_YEAST**	104.3	7.88
4	ATPase expression protein 2, mitochondrial OS=Saccharomyces cerevisiae (strain ATCC 204508 / S288c) GN=AEP2 PE=1 SV=3	67.5	10.2	AEP2_YEAST	76.3	3.38
4	ATP-dependent molecular chaperone HSC82 OS=Saccharomyces cerevisiae (strain ATCC 204508 / S288c) GN=HSC82 PE=1 SV=4	80.8	4.6	HSC82_YEAST	70.0	7.45
3	Ribosome biogenesis protein NSA1 OS=Saccharomyces cerevisiae (strain ATCC 204508 / S288c) GN=NSA1 PE=1 SV=1	51.9	8.5	NSA1_YEAST	116.7	3.16
3	Intermediate cleaving peptidase of 55 kDa OS=Saccharomyces cerevisiae (strain ATCC 204508 / S288c) GN=ICP55 PE=1 SV=1	58.0	6.1	ICP55_YEAST	78.0	9.06
3	Elongation factor 1-alpha OS=Saccharomyces cerevisiae (strain ATCC 204508 / S288c) GN=TEF1 PE=1 SV=1	50.0	9.8	EF1A_YEAST	84.0	6.28
2	Phosphatidylinositol 4,5-bisphosphate-binding protein SLM2 OS=Saccharomyces cerevisiae (strain ATCC 204508 / S288c) GN=SLM2 PE=1 SV=1	74.7	9.3	SLM2_YEAST	43.6	4.82
2	**Aconitate hydratase, mitochondrial OS=Saccharomyces cerevisiae (strain ATCC 204508 / S288c) GN=ACO1 PE=1 SV=2**	85.3	8.9	**ACON_YEAST**	59.8	10.29
2	ATP-dependent RNA helicase MSS116, mitochondrial OS=Saccharomyces cerevisiae (strain ATCC 204508 / S288c) GN=MSS116 PE=1 SV=1	76.2	9.6	MS116_YEAST	60.7	12.16
1	**Asparaginyl-tRNA synthetase, mitochondrial OS=Saccharomyces cerevisiae (strain ATCC 204508 / S288c) GN=SLM5 PE=1 SV=1**	56.7	9.4	**SYNM_YEAST**	51.9	10.25
1	**2-isopropylmalate synthase 2, mitochondrial OS=Saccharomyces cerevisiae (strain ATCC 204508 / S288c) GN=LEU9 PE=1 SV=1**	67.2	6.3	**LEU9_YEAST**	69.7	5.70
3	**Ribosomal protein VAR1, mitochondrial OS=Saccharomyces cerevisiae (strain ATCC 204508 / S288c) GN=VAR1 PE=1 SV=3**	47.1	10.3	**RMAR_YEAST**	96.9	7.22
2	Alcohol dehydrogenase 2 OS=Saccharomyces cerevisiae (strain ATCC 204508 / S288c) GN=ADH2 PE=1 SV=3	36.7	6.3	ADH2_YEAST	31.9	3.46
25	**54S ribosomal protein L35, mitochondrial OS=Saccharomyces cerevisiae (strain ATCC 204508 / S288c) GN=MRPL35 PE=1 SV=1**	42.8	9.9	**RM35_YEAST**	485.5	8.60
7	**Cytochrome b-c1 complex subunit 2, mitochondrial OS=Saccharomyces cerevisiae (strain ATCC 204508 / S288c) GN=QCR2 PE=1 SV=1**	40.5	8.6	**QCR2_YEAST**	164.1	7.39
7	**54S ribosomal protein L2, mitochondrial OS=Saccharomyces cerevisiae (strain ATCC 204508 / S288c) GN=MRP7 PE=1 SV=1**	43.2	10.3	**RM02_YEAST**	142.4	8.07
6	**37S ribosomal protein MRP51, mitochondrial OS=Saccharomyces cerevisiae (strain ATCC 204508 / S288c) GN=MRP51 PE=1 SV=1**	39.4	10.4	**RT51_YEAST**	117.5	4.84
4	**Branched-chain-amino-acid aminotransferase, mitochondrial OS=Saccharomyces cerevisiae (strain ATCC 204508 / S288c) GN=BAT1 PE=1 SV=1**	43.6	9.6	**BCA1_YEAST**	75.4	7.55
2	Transposon Ty1-ER1 Gag polyprotein OS=Saccharomyces cerevisiae (strain ATCC 204508 / S288c) GN=TY1A-ER1 PE=2 SV=1	48.9	8.6	YE11A_YEAST	41.3	2.29
2	**Mitochondrial nuclease OS=Saccharomyces cerevisiae (strain ATCC 204508 / S288c) GN=NUC1 PE=1 SV=1**	37.2	9.6	**NUC1_YEAST**	39.6	5.27
2	**Mitochondrial distribution and morphology protein 38 OS=Saccharomyces cerevisiae (strain ATCC 204508 / S288c) GN=MDM38 PE=1 SV=1**	65.0	8.4	**MDM38_YEAST**	31.6	0.03
2	Actin OS=Saccharomyces cerevisiae (strain ATCC 204508 / S288c) GN=ACT1 PE=1 SV=1	41.7	5.4	ACT_YEAST	71.0	6.02
1	Sphingolipid long chain base-responsive protein LSP1 OS=Saccharomyces cerevisiae (strain ATCC 204508 / S288c) GN=LSP1 PE=1 SV=1	38.0	4.5	LSP1_YEAST	35.3	12.91
1	Chaperone protein DnaJ OS=Salmonella paratyphi B (strain ATCC BAA-1250 / SPB7) GN=dnaJ PE=3 SV=1	41.3	9.3	DNAJ_SALPB	49.8	4.19
8	**37S ribosomal protein MRP51, mitochondrial OS=Saccharomyces cerevisiae (strain ATCC 204508 / S288c) GN=MRP51 PE=1 SV=1**	39.4	10.4	**RT51_YEAST**	190.8	4.90
13	**Prohibitin-2 OS=Saccharomyces cerevisiae (strain ATCC 204508 / S288c) GN=PHB2 PE=1 SV=2**	34.4	10.4	**PHB2_YEAST**	292.8	6.88
1	Sphingolipid long chain base-responsive protein PIL1 OS=Saccharomyces cerevisiae (strain ATCC 204508 / S288c) GN=PIL1 PE=1 SV=1	38.3	4.4	PIL1_YEAST	41.7	9.75
20	**Prohibitin-1 OS=Saccharomyces cerevisiae (strain ATCC 204508 / S288c) GN=PHB1 PE=1 SV=2**	31.4	8.9	**PHB1_YEAST**	473.7	7.08
6	**37S ribosomal protein S24, mitochondrial OS=Saccharomyces cerevisiae (strain ATCC 204508 / S288c) GN=RSM24 PE=1 SV=1**	37.4	9.6	**RT24_YEAST**	140.3	5.55
5	**Prohibitin-2 OS=Saccharomyces cerevisiae (strain ATCC 204508 / S288c) GN=PHB2 PE=1 SV=2**	34.4	10.4	**PHB2_YEAST**	140.3	8.27
5	**Heat shock protein 60, mitochondrial OS=Saccharomyces cerevisiae (strain ATCC 204508 / S288c) GN=HSP60 PE=1 SV=1**	60.7	5.1	**HSP60_YEAST**	126.1	0.36
5	**Dihydrolipoyllysine-residue succinyltransferase component of 2-oxoglutarate dehydrogenase complex, mitochondrial OS=Saccharomyces cerevis**	50.4	9.4	**ODO2_YEAST**	183.0	7.47
2	**ATPase synthesis protein 25, mitochondrial OS=Saccharomyces cerevisiae (strain RM11-1a) GN=ATP25 PE=3 SV=1**	70.3	9.9	**ATP25_YEAS1**	95.6	6.24
2	**54S ribosomal protein YmL6, mitochondrial OS=Saccharomyces cerevisiae (strain ATCC 204508 / S288c) GN=YML6 PE=1 SV=1**	31.9	10.0	**RL4P_YEAST**	53.4	11.24

B.2 : Table illustrating mass spectrometry parameters of proteins identified by CLIP analysis.

1	**Potassium-activated aldehyde dehydrogenase, mitochondrial OS=Saccharomyces cerevisiae (strain ATCC 204508 / S288c) GN=ALD4 PE=1 SV=2**	56.7	6.3	**ALDH4_YEAST**	62.8	11.13
15	**54S ribosomal protein YmL6, mitochondrial OS=Saccharomyces cerevisiae (strain ATCC 204508 / S288c) GN=YML6 PE=1 SV=1**	31.9	10.0	**RL4P_YEAST**	374.0	8.94
12	**Dihydrolipoyllysine-residue succinyltransferase component of 2-oxoglutarate dehydrogenase complex, mitochondrial OS=Saccharomyces cerevis**	50.4	9.4	**ODO2_YEAST**	270.7	8.88
11	**54S ribosomal protein L17, mitochondrial OS=Saccharomyces cerevisiae (strain ATCC 204508 / S288c) GN=MRPL17 PE=1 SV=2**	32.2	9.5	**RM17_YEAST**	163.3	5.70
9	**Uncharacterized protein YDL027C OS=Saccharomyces cerevisiae (strain ATCC 204508 / S288c) GN=YDL027C PE=1 SV=1**	48.3	10.4	**YD027_YEAST**	178.3	6.03
8	Sphingolipid long chain base-responsive protein PIL1 OS=Saccharomyces cerevisiae (strain ATCC 204508 / S288c) GN=PIL1 PE=1 SV=1	38.3	4.4	PIL1_YEAST	215.2	11.02
8	Sphingolipid long chain base-responsive protein LSP1 OS=Saccharomyces cerevisiae (strain ATCC 204508 / S288c) GN=LSP1 PE=1 SV=1	38.0	4.5	LSP1_YEAST	225.8	10.67
8	**Heat shock protein 60, mitochondrial OS=Saccharomyces cerevisiae (strain ATCC 204508 / S288c) GN=HSP60 PE=1 SV=1**	60.7	5.1	**HSP60_YEAST**	207.2	4.10
7	**Prohibitin-1 OS=Saccharomyces cerevisiae (strain ATCC 204508 / S288c) GN=PHB1 PE=1 SV=2**	31.4	8.9	**PHB1_YEAST**	155.7	6.62
6	**Prohibitin-2 OS=Saccharomyces cerevisiae (strain ATCC 204508 / S288c) GN=PHB2 PE=1 SV=2**	34.4	10.4	**PHB2_YEAST**	134.5	7.11
6	**37S ribosomal protein S24, mitochondrial OS=Saccharomyces cerevisiae (strain ATCC 204508 / S288c) GN=RSM24 PE=1 SV=1**	37.4	9.6	**RT24_YEAST**	146.5	5.63
5	**ADP,ATP carrier protein 2 OS=Saccharomyces cerevisiae (strain ATCC 204508 / S288c) GN=PET9 PE=1 SV=2**	34.4	10.3	**ADT2_YEAST**	156.9	2.65
4	**37S ribosomal protein S5, mitochondrial OS=Saccharomyces cerevisiae (strain ATCC 204508 / S288c) GN=MRPS5 PE=1 SV=1**	34.9	10.0	**RT05_YEAST**	92.0	4.57
3	Myosin tail region-interacting protein MTI1 OS=Saccharomyces cerevisiae (strain ATCC 204508 / S288c) GN=BBC1 PE=1 SV=2	128.2	5.0	BBC1_YEAST	88.2	7.65
2	Peroxisomal biogenesis factor 3 OS=Pichia angusta GN=PEX3 PE=3 SV=1	52.0	4.9	PEX3_PICAN	38.6	4.68
2	**54S ribosomal protein L41, mitochondrial OS=Saccharomyces cerevisiae (strain ATCC 204508 / S288c) GN=MRP20 PE=1 SV=1**	30.5	9.9	**RM41_YEAST**	45.7	1.77
1	Actin OS=Saccharomyces cerevisiae (strain ATCC 204508 / S288c) GN=ACT1 PE=1 SV=1	41.7	5.4	ACT_YEAST	38.4	4.79
1	**2-oxoglutarate dehydrogenase, mitochondrial OS=Saccharomyces cerevisiae (strain ATCC 204508 / S288c) GN=KGD1 PE=1 SV=2**	114.3	6.8	**ODO1_YEAST**	43.9	9.81
30	Dihydrolipoyllysine-residue succinyltransferase component of 2-oxoglutarate dehydrogenase complex, mitochondrial OS=Saccharomyces cerevisiae (strain A	50.4	9.4	ODO2_YEAST	414.5	7.07
10	**Mitochondrial outer membrane protein porin 1 OS=Saccharomyces cerevisiae (strain ATCC 204508 / S288c) GN=POR1 PE=1 SV=4**	30.4	8.8	**VDAC1_YEAST**	253.3	10.70
10	60S ribosomal protein L8-B OS=Saccharomyces cerevisiae (strain ATCC 204508 / S288c) GN=RPL8B PE=1 SV=3	28.1	10.5	RL8B_YEAST	176.7	7.54
9	**54S ribosomal protein L22, mitochondrial OS=Saccharomyces cerevisiae (strain ATCC 204508 / S288c) GN=MRPL22 PE=1 SV=2**	34.9	10.5	**RM22_YEAST**	160.6	5.74
8	Sphingolipid long chain base-responsive protein PIL1 OS=Saccharomyces cerevisiae (strain ATCC 204508 / S288c) GN=PIL1 PE=1 SV=1	38.3	4.4	PIL1_YEAST	188.2	10.95
7	**54S ribosomal protein L9, mitochondrial OS=Saccharomyces cerevisiae (strain ATCC 204508 / S288c) GN=MRPL9 PE=1 SV=3**	29.8	10.7	**RM09_YEAST**	169.5	4.51
6	60S acidic ribosomal protein P0 OS=Saccharomyces cerevisiae (strain ATCC 204508 / S288c) GN=RPP0 PE=1 SV=2	33.7	4.6	RLA0_YEAST	134.7	8.27
4	Protein MRH1 OS=Saccharomyces cerevisiae (strain ATCC 204508 / S288c) GN=MRH1 PE=1 SV=1	36.2	10.1	MRH1_YEAST	62.1	6.38
4	Dihydrolipoyllysine-residue acetyltransferase component of pyruvate dehydrogenase complex, mitochondrial OS=Saccharomyces cerevisiae (strain ATCC 20	51.8	8.6	ODP2_YEAST	85.9	4.94
4	**54S ribosomal protein L28, mitochondrial OS=Saccharomyces cerevisiae (strain ATCC 204508 / S288c) GN=MRPL28 PE=1 SV=2**	17.3	11.1	**RM28_YEAST**	116.8	10.32
4	40S ribosomal protein S2 OS=Saccharomyces cerevisiae (strain ATCC 204508 / S288c) GN=RPS2 PE=1 SV=3	27.4	11.0	RS2_YEAST	75.3	5.57
4	**37S ribosomal protein S9, mitochondrial OS=Saccharomyces cerevisiae (strain ATCC 204508 / S288c) GN=MRPS9 PE=1 SV=1**	31.9	10.6	**RT09_YEAST**	59.8	7.30
3	**54S ribosomal protein L8, mitochondrial OS=Saccharomyces cerevisiae (strain ATCC 204508 / S288c) GN=MRPL8 PE=1 SV=4**	26.9	10.4	**RM08_YEAST**	80.0	4.26
2	Transposon Ty1-ER1 Gag polyprotein OS=Saccharomyces cerevisiae (strain ATCC 204508 / S288c) GN=TY1A-ER1 PE=2 SV=1	48.9	8.6	YE11A_YEAST	57.2	4.74
2	**Mitochondrial respiratory chain complexes assembly protein AFG3 OS=Saccharomyces cerevisiae (strain ATCC 204508 / S288c) GN=AFG3 PE=1 S**	84.5	9.7	**AFG3_YEAST**	44.6	8.39
2	**Mitochondrial genome maintenance protein MGM101 OS=Saccharomyces cerevisiae (strain ATCC 204508 / S288c) GN=MGM101 PE=1 SV=1**	30.1	10.1	**MG101_YEAST**	45.2	2.81
2	Actin OS=Saccharomyces cerevisiae (strain ATCC 204508 / S288c) GN=ACT1 PE=1 SV=1	41.7	5.4	ACT_YEAST	81.1	4.73
2	**54S ribosomal protein L11, mitochondrial OS=Saccharomyces cerevisiae (strain ATCC 204508 / S288c) GN=MRPL11 PE=1 SV=2**	28.5	10.2	**RM11_YEAST**	58.3	14.33
1	**54S ribosomal protein L7, mitochondrial OS=Saccharomyces cerevisiae (strain ATCC 204508 / S288c) GN=MRPL7 PE=1 SV=2**	33.1	10.3	**RM07_YEAST**	38.9	4.44
11	**54S ribosomal protein L20, mitochondrial OS=Saccharomyces cerevisiae (strain ATCC 204508 / S288c) GN=MRPL20 PE=1 SV=2**	22.4	10.8	**RM20_YEAST**	266.7	9.86
3	Dihydrolipoyllysine-residue succinyltransferase component of 2-oxoglutarate dehydrogenase complex, mitochondrial OS=Saccharomyces cerevisiae (strain A	50.4	9.4	ODO2_YEAST	62.4	3.74
2	60S ribosomal protein L6-A OS=Saccharomyces cerevisiae (strain ATCC 204508 / S288c) GN=RPL6A PE=1 SV=2	19.9	10.5	RL6A_YEAST	42.7	1.00
2	**54S ribosomal protein L12, mitochondrial OS=Saccharomyces cerevisiae (strain ATCC 204508 / S288c) GN=MNP1 PE=1 SV=1**	20.6	9.7	**MNP1_YEAST**	36.3	1.72
22	**ATP-dependent RNA helicase MSS116, mitochondrial OS=Saccharomyces cerevisiae (strain ATCC 204508 / S288c) GN=MSS116 PE=1 SV=1**	76.2	9.6	**MS116_YEAST**	424.6	7.02
14	**ATP-dependent RNA helicase DED1 OS=Saccharomyces cerevisiae (strain ATCC 204508 / S288c) GN=DED1 PE=1 SV=2**	65.5	8.6	**DED1_YEAST**	352.6	9.53
10	**Protein TOM71 OS=Saccharomyces cerevisiae (strain ATCC 204508 / S288c) GN=TOM71 PE=1 SV=1**	71.8	5.8	**TOM71_YEAST**	248.2	5.24
9	**Succinate dehydrogenase [ubiquinone] flavoprotein subunit, mitochondrial OS=Saccharomyces cerevisiae (strain ATCC 204508 / S288c) GN=SDH**	70.2	7.4	**DHSA_YEAST**	211.4	6.24
6	Heat shock protein SSB2 OS=Saccharomyces cerevisiae (strain ATCC 204508 / S288c) GN=SSB2 PE=1 SV=2	66.6	5.2	HSP76_YEAST	162.0	5.94
4	**NAD-dependent malic enzyme, mitochondrial OS=Saccharomyces cerevisiae (strain ATCC 204508 / S288c) GN=MAE1 PE=1 SV=1**	74.3	9.2	**MAOM_YEAST**	81.3	7.93
4	**C-1-tetrahydrofolate synthase, mitochondrial OS=Saccharomyces cerevisiae (strain ATCC 204508 / S288c) GN=MIS1 PE=1 SV=1**	106.2	9.4	**C1TM_YEAST**	73.6	7.01
4	**Altered inheritance of mitochondria protein 9, mitochondrial OS=Saccharomyces cerevisiae (strain YJM789) GN=AIM9 PE=3 SV=1**	72.3	9.3	**AIM9_YEAS7**	102.5	9.30
2	**Uncharacterized protein YER077C OS=Saccharomyces cerevisiae (strain ATCC 204508 / S288c) GN=YER077C PE=1 SV=1**	79.5	10.1	**YEQ7_YEAST**	60.7	12.95
2	**Lysyl-tRNA synthetase, mitochondrial OS=Saccharomyces cerevisiae (strain ATCC 204508 / S288c) GN=MSK1 PE=1 SV=3**	66.1	9.7	**SYKM_YEAST**	38.4	8.41
2	**Heat shock protein 60, mitochondrial OS=Saccharomyces cerevisiae (strain ATCC 204508 / S288c) GN=HSP60 PE=1 SV=1**	60.7	5.1	**HSP60_YEAST**	39.1	0.49

B.2 : Table illustrating mass spectrometry parameters of proteins identified by CLIP analysis.

2	CTP synthase 1 OS=Saccharomyces cerevisiae (strain ATCC 204508 / S288c) GN=URA7 PE=1 SV=2	64.7	5.6	URA7_YEAST	62.5	7.67
2	**2-isopropylmalate synthase 2, mitochondrial OS=Saccharomyces cerevisiae (strain ATCC 204508 / S288c) GN=LEU9 PE=1 SV=1**	67.2	6.3	**LEU9_YEAST**	52.7	1.68
2	**Altered inheritance of mitochondria protein 5, mitochondrial OS=Saccharomyces cerevisiae (strain RM11-1a) GN=AIM5 PE=3 SV=1**	12.4	9.0	**AIM5_YEAS1**	52.5	2.56
2	60S ribosomal protein L36-B OS=Saccharomyces cerevisiae (strain ATCC 204508 / S288c) GN=RPL36B PE=1 SV=3	11.1	12.1	RL36B_YEAST	51.6	6.15
2	**54S ribosomal protein IMG2, mitochondrial OS=Saccharomyces cerevisiae (strain ATCC 204508 / S288c) GN=IMG2 PE=1 SV=2**	16.4	10.6	**IMG2_YEAST**	35.4	3.58
1	**Mitochondrial outer membrane protein porin 1 OS=Saccharomyces cerevisiae (strain ATCC 204508 / S288c) GN=POR1 PE=1 SV=4**	30.4	8.8	**VDAC1_YEAST**	43.3	12.67

soluble mitochondrial proteins
mitochondrial outer membrane proteins
mitochondrial inner membrane proteins
respiratory chain complexe proteins
unidentified proteins
proteins not highlightened by bold letters correspond to cytosolic proteins or proteins of other cellular compartments

RESUME DE THESE

UNIVERSITÉ DE STRASBOURG

Résumé de la thèse de doctorat

Discipline : Aspects Moléculaires et Cellulaires de la Biologie

Présentée par : **SCHIRTZ Tom**

Titre : Etude du mécanisme de translocation de l'ARNt^{Lys} dans les mitochondries de *Saccharomyces cerevisiae*

Unité de Recherche : UMR 7156 CNRS-Université de Strasbourg
« Génétique Moléculaire, Génomique, Microbiologie »

Directeur de Thèse : TARASSOV Ivan – Directeur de Recherche

Localisation : Doctorat
de l'Université de Strasbourg (Strasbourg, France)

ECOLES DOCTORALES :

☐ ED - Sciences de l'Homme et des sociétés ☐ ED 99 – Humanités ☐ ED 101 – Droit, sciences politique et histoire ☐ ED 182 – Physique et chimie physique ☐ ED 221 – Augustin Cournot ☐ ED 222 - Sciences chimiques	☐ ED 269 - Mathématiques, sciences de l'information et de l'ingénieur ☐ ED 270 – Théologie et sciences religieuses ☐ ED 413 – Sciences de la terre, de l'univers et de l'environnement ☒ ED 414 – Sciences de la vie et de la santé

INTRODUCTION ET OBJECTIFS

L'import d'ARN dans les mitochondries de cellules eucaryotes est un phénomène largement répandu, observé chez les protozoaires, les champignons, les plantes ainsi que chez les mammifères. Les molécules importées sont majoritairement des ARN de transfert (ARNt), tandis qu'il y a aussi des rapports sur l'import de l'ARN ribosomique 5S et des parties ARN d'enzymes ribonucléoprotéiques. Malgré le caractère quasi-ubiquitaire du phénomène d'import, le nombre d'ARNt importés et le besoin en facteurs d'adressage varient considérablement d'une espèce à l'autre. Chez la levure *Saccharomyces cerevisiae* un seul ARNt cytoplasmique est importé dans les mitochondries, l'ARNt$^{Lys(CUU)}$ (tRK1). Il a été démontré que l'import de tRK1 nécessite de l'énergie fournie par l'hydrolyse d'ATP et éventuellement le potentiel électrochimique membranaire $\Delta\Psi$. Un prérequis pour que tRK1 soit adressé vers les mitochondries, est une aminoacylation par la lysyl-ARNt-synthétase cytoplasmique. L'ARNt aminoacylé est ensuite reconnu par l'enolase-2, une des enzymes glycolytiques, qui joue le rôle de facteur d'adressage et d'ARN-chaperonne en adressant tRK1 à la surface mitochondriale et en favorisant sa prise en charge par le deuxième facteur d'import, le précurseur de la lysyl-ARNt-synthétase mitochondriale (preMSK). Il a aussi été démontré que les sous-unités de la machinerie d'import des pré-protéines (TOM/TIM) Tom20 et Tim44 sont nécessaires pour que tRK1 rentre dans l'organite, mais le mécanisme de leur implication ainsi que les autres protéines membranaires nécessaires à la translocation de tRK1 à travers les deux membranes mitochondriales ne sont pas élucidés.

Dans la suite logique de ces pré-acquis, le projet principal de mon travail de thèse était la caractérisation de ces protéines membranaires et la vérification de leur rôle dans la translocation de tRK1 dans les mitochondries de la levure *Saccharomyces cerevisiae*. Les objectifs spécifiques pour répondre à ces questions étaient les suivants :

1. Identification de protéines interagissant avec tRK1

2. Implication des principaux canaux de la membrane externe dans la translocation de tRK1

3. Impact de la stabilité du complexe TOM sur l'import de tRK1 à travers la membrane externe

TRAVAUX EFFECTUÉS

1. Identification de protéines interagissant avec tRK1

L'import d'ARNt dans les mitochondries nécessite des interactions avec les protéines mitochondriales jouant les rôles de récepteurs et/ou translocateurs à travers les membranes des mitochondries. Une première approche utilisée pour mettre en évidence les protéines interagissant par affinité avec tRK1 était la technique du North-Western, appliquée sur une souche sauvage et une souche délétante pour le canal porine (*por1*Δ). La raison de ce choix a reposé sur le fait que la protéine porine 1/VDAC1 (Voltage-Dependant Anion Channel 1) a été démontré comme nécessaire pour l'import d'ARNt chez les plantes. Dans un premier temps nous nous sommes confinés à la caractérisation des protéines localisées dans la membrane mitochondriale externe. L'analyse des résultats a ainsi montré que dans la souche sauvage les protéines VDAC1 et Tom5 ont été identifiées tandis que dans le mutant *por1*Δ plusieurs composantes du complexe TOM (Translocase of the Outer Membrane) de la machinerie d'import des pré-protéines ont été trouvées, notamment Tom40, Tom20 et Tom22.

Une deuxième approche en vue d'identifier les protéines interagissant de manière physique avec tRK1 était le CLIP (CrossLinking and ImmunoPrecipitation), effectué sur la souche sauvage. Suite à l'irradiation aux UV, le transcrit de tRK1, comprenant le nucléotide photoactivable 5-bromouridine, forme des complexes covalents avec des protéines durant la réaction d'import *in vitro*. Ces complexes protéines/tRK1 ont été immunoprécipités et analysés par spectrométrie de masse. Par cette méthode il a été possible d'identifier les protéines majeures de la membrane externe : VDAC1 et Tom40.

2. Implication des principaux canaux de la membrane externe dans la translocation de tRK1

Les protéines VDAC1 et Tom40, trouvées par les approches de criblage, sont les protéines les plus abondantes de la membrane externe et y forment les deux canaux principaux permettant le passage de métabolites et l'import des pré-protéines respectivement.

Dans la souche *por1*Δ le taux d'import de tRK1, *in vitro* et *in vivo*, était diminué de ~80% par rapport à la souche sauvage, tandis que l'import dans le mutant de la deuxième isoforme de porine (*por2*Δ) n'était pas affecté. Puisque la protéine Tom40 est essentielle, l'étude dans la souche délétante n'était pas possible. Pour cette raison nous avons utilisé la protéine chimérique cyt*b2*-DHFR, une fusion de la partie N-terminale du cytochrome *b2* de

S.cerevisiae avec la dihydrofolate réductase (DHFR) de la souris, qui, en présence de la méthotrexate, a la particularité de bloquer les canaux Tom40/Tim23 de la machinerie d'import des pré-protéines. Le composé chimique DIDS (acide 4-4'-diisothiocyano-2,2'-stilbenedisulfonique), un inhibiteur spécifique des canaux anions sélectifs, nous a fourni un autre outil pour étudier, cette fois, le rôle de VDAC1 dans l'import de tRK1. Les essais d'import *in vitro* ont montré que, dans la souche sauvage, DIDS diminue le taux d'import de ~80% ce qui est comparable au résultat obtenu pour la souche *por1*Δ. Dans la souche *por2*Δ l'effet de DIDS est encore plus prononcé avec une diminution de ~90% par rapport au sauvage. La protéine cyt*b2*-DHFR toute seule n'a eu qu'un faible effet dans *por1*Δ, tandis que cyt*b2*-DHFR et DIDS ensemble ont bloqué complètement la translocation de tRK1 à travers la membrane externe dans les souches étudiées. Les études d'import *in vitro* ont aussi été effectuées dans des vésicules de membranes externes mitochondriales des souches sauvage, *por1*Δ et *por2*Δ. Ces résultats ont confirmé les observations faites dans les mitochondries isolées. Une preuve supplémentaire que VDAC1 est impliqué dans la translocation de tRK1 a été fournie par des essais d'import dans des vésicules lipidiques reconstituées avec la protéine VDAC1, qui a confirmé un import DIDS sensible.

L'ensemble de ces résultats montre que la translocation de tRK1 à travers la membrane externe suit en grande partie une voie VDAC1 dépendante. Mais en absence de cette protéine ou en conditions bloquant son canal, la protéine Tom40 est capable de complémenter en partie les fonctions de translocation de VDAC1. La présence de ces deux voies alternatives est en parfaite conformité avec les résultats obtenus lors de l'identification de protéines par les méthodes de criblage.

3. Impact de la stabilité du complexe TOM sur l'import de tRK1

La participation du complexe TOM dans l'import de tRK1 a déjà été proposée et, dans le but de compléter l'image, l'import *in vitro* a été analysé pour une série de mutants portant des délétions pour des protéines non-essentielles du complexe TOM. La protéine Tom7 a un rôle déstabilisant et empêche la maturation du complexe TOM, tandis que les protéines Tom5 et Tom6 présentent des caractéristiques antagonistes en conférant à ce complexe une plus grande stabilité. La protéine Tom20 agit comme récepteur principal dirigeant l'import des pré-protéines destinées à la matrice mitochondriale et son rôle crucial dans l'import de tRK1 a déjà été montré préalablement, où une délétion de Tom20 a conduit à une abrogation de l'import de tRK1.

L'import de tRK1 dans les souches *tom6*Δ et *tom7*Δ a été comparable à celui dans la souche sauvage, mais dans la souche *tom6*Δ l'import de tRK1 s'est montré quatre fois plus sensible à la drogue DIDS, indiquant un emprunt préféré de la voie d'import VDAC1 dépendante dans des conditions déstabilisant le complexe TOM. D'une manière intéressante, l'import s'est avéré deux à quatre fois plus important dans les souches *tom5*Δ et *tom20*Δ respectivement, tout en restant sensibles à la drogue DIDS, suggérant la possibilité d'un rôle régulateur de ces protéines. Un autre résultat, plutôt surprenant, a montré que dans la souche *tom20*Δ l'import de tRK1 a été possible en absence du facteur d'import preMSK, jusque là considéré comme essentiel, bien qu'il fût réduit d'un facteur deux. Le résultat obtenu semble en contradiction avec le résultat précédent où la délétion de la protéine Tom20 a conduit à une absence de l'import de tRK1 et a dépendu de facteurs protéiques d'import. Cette contradiction pourrait s'expliquer de la manière suivante : les expériences initiales ont été menées en utilisant des extraits totaux de protéines cytoplasmiques solubles comme facteurs d'import. Ces conditions, plutôt physiologiques, pourraient favoriser l'utilisation préférentielle de la voie d'import Tom40 dépendante ayant besoin de facteurs protéiques d'import. Les expériences d'import *in vitro*, menées au cours de mon travail, se sont limitées à un système minimal utilisant comme facteur d'import uniquement la preMSK recombinante, représentant des conditions plus artificielles dans lesquelles l'import de tRK1 se ferait majoritairement par la voie VDAC1 dépendante qui n'a pas montré une stricte dépendance aux facteurs d'import.

4. Conclusions et perspectives

Les travaux menés au cours de mon travail de thèse ont donc permis d'obtenir les résultats suivants :

- les approches de criblage ont identifié les protéines VDAC1, Tom5, Tom40, Tom20 et Tom22, probablement impliquées dans des voies d'import de tRK1 alternatives.

- les études d'import *in vitro* ont permis de discerner deux voies d'import potentielles suivant lesquelles tRK1 peut être transloqué à travers la membrane mitochondriale externe, une voie VDAC1 dépendante et une voie Tom40 dépendante.

- une déstabilisation du complexe TOM, et ainsi de la voie Tom40 dépendante, renforce l'import de tRK1 suivant la voie VDAC1 dépendante.

- les deux chemins d'import alternatifs à travers la membrane mitochondriale externe démontrent une demande différente en facteurs protéiques supplémentaires.

Perspectives

A court terme, l'import de tRK1 devra encore être étudié dans des conditions *in vivo* permettant de valider les résultats obtenus dans les études *in vitro*. Il serait aussi très intéressant de comparer l'abondance de la protéine VDAC1 dans certains mutants, notamment *tom5*Δ et *tom20*Δ, ce qui pourrait fournir des explications à propos de l'import augmenté dans ces souches. Aussi, en vue d'étudier le rôle régulateur potentiel des protéines Tom5 et Tom20 sur la protéine VDAC1, leur reconstitution dans des vésicules lipidiques sera indispensable. Néanmoins, la tâche principale restera la caractérisation des protéines de la membrane interne responsables de la translocation de tRK1 dans la matrice mitochondriale. Des expériences de CLIP préliminaires ont déjà été réalisées, mais les résultats devront encore être reproduits et les protéines candidates être étudiées pour leur implication dans l'import de tRK1.

Autre projet

A côté des travaux décrits ci-dessus, j'étais également impliqué dans un autre projet qui a visé à exploiter la voie d'adressage d'ARN dans les mitochondries afin de complémenter les effets de la mutation A3243G dans le gène de l'ARNt$^{Leu(UUR)}$ mitochondrial responsable du syndrome MELAS (Mitochondrial Encephalomyopathy , Lactic Acidosis, and Stroke-like episodes). Le travail a consisté à la modélisation et à la construction de versions d'ARNt recombinants pouvant être misaminoacylées par la leucine et être importées dans les mitochondries de cellules humaines portant la mutation MELAS A3243G. Il a été démontré que l'import mitochondrial d'ARNt recombinants menait à une amélioration des fonctions mitochondriales touchées par la mutation, telles que la traduction et, consécutivement, l'activité de complexes respiratoires I et IV.

PUBLICATIONS ET COMMUNICATIONS

Publications

1. Karicheva OZ, Kolesnikova OA, Schirtz T, Vysokikh MY, Mager-Heckel AM, Lombès A, Boucheham A, Krasheninnikov IA, Martin RP, Entelis N, Tarassov I. **Correction of the consequences of mitochondrial 3243A>G mutation in the MT-TL1 gene causing the MELAS syndrome by tRNA import into mitochondria**. ***Nucleic Acids Res***. 2011 Oct ;39(18) :8173-86.

2. Schirtz T, Geng W, Shimada E, Vysokikh MY, Entelis N, Teitell MA, Tarassov I, Koehler CM. **RNA translocation across the outer mitochondrial membrane is mediated by alternative channels** (submitted)

Communications

1. Schirtz T, Kolesnikova OA, Entelis N, Tarassov I. Studying the translocation mechanism of tRK1 into mitochondria of the yeast *Saccharomyces cerevisiae*. Congrès Mito@Strass, Strasbourg, France (2009).
2. Schirtz T, Vysokikh MY, Kolesnikova OA, Entelis N, Tarassov I. Studying the translocation mechanism of tRK1 into mitochondria of the yeast *Saccharomyces cerevisiae*. Congrès Mito@Strass, Strasbourg, France (2010).
3. Schirtz T, Vysokikh MY, Entelis N, Tarassov I. Studying the translocation mechanism of tRK1 into mitochondria of the yeast *Saccharomyces cerevisiae*. EBEC conference, Warsaw, Poland (2010). Abstract selected for oral presentation.
4. Schirtz T, Vysokikh MY, Entelis N, Tarassov I. Studying the translocation mechanism of tRK1 into mitochondria of the yeast *Saccharomyces cerevisiae*. Yeast LMO meeting, Strasbourg, France (2010).
5. Schirtz T, Vysokikh MY, Entelis N, Tarassov I. Studying the translocation mechanism of tRK1 into mitochondria of the yeast *Saccharomyces cerevisiae*. 3rd international summer school « Supramolecular Systems in Chemistry and Biology », Lviv, Ukraine (2010). Abstract selected for oral presentation.
6. Schirtz T, Vysokikh MY, Entelis N, Tarassov I. Studying the translocation mechanism of tRK1 into mitochondria of the yeast *Saccharomyces cerevisiae*. Colloque MeetOchondrie, La Colle-sur-Loup, France (2011).

7. Schirtz T, Vysokikh MY, Entelis N, Tarassov I. Studying the translocation mechanism of tRK1 into mitochondria of the yeast *Saccharomyces cerevisiae*. 25th international conference on yeast genetics and molecular biology, Olsztyn-Kortowo, Poland (2011). Abstract selected for oral presentation.
8. Schirtz T, Vysokikh MY, Entelis N, Tarassov I. Studying the translocation mechanism of tRK1 into mitochondria of the yeast *Saccharomyces cerevisiae*. Mitochondria in Life, Death and Disease (FEBS/EMBO Course), Crete, Greece (2012).